



Hydrogeologic Properties of Earth Materials and Principles of Groundwater Flow

William W. Woessner and Eileen P. Poeter



*Hydrogeologic Properties of Earth Materials
and Principles of Groundwater Flow*

The Groundwater Project

William W. Woessner

*Emeritus Regents' Professor of Hydrogeology,
University of Montana,
Missoula, Montana, USA*

Eileen P. Poeter

*Emeritus Professor of Geological Engineering,
Colorado School of Mines,
Golden, Colorado, USA*

Hydrogeologic Properties of Earth Materials and Principles of Groundwater Flow

*The Groundwater Project
Guelph, Ontario, Canada
Version 4, December, 2024,*

The Groundwater Project relies on private funding for book production
and management of the Project.

Please consider making a donation to the Groundwater Project ↗
so books will continue to be freely available.

Thank you.

All rights reserved. This publication is protected by copyright. No part of this book may be reproduced in any form or by any means without permission in writing from the authors (to request permission contact: permissions@gw-project.org). Commercial distribution and reproduction are strictly prohibited.

Groundwater-Project (The GW-Project) works are copyrighted and can be downloaded for free from gw-project.org. Anyone may use and share gw-project.org links to download GW-Project's work. It is not permissible to make GW-Project documents available on other websites nor to send copies of the documents directly to others. Kindly honor this source of free knowledge that benefits you and all those who want to learn about groundwater.

Copyright © 2020 William W. Woessner, Eileen P. Poeter (The Authors)

Published by the Groundwater Project, Guelph, Ontario, Canada, 2020.

Woessner, William W.

Hydrogeologic properties of earth materials and principles of groundwater flow /
William W. Woessner, Eileen P. Poeter - Guelph, Ontario, Canada, 2020.

212 p.

ISBN: 978-1-7770541-2-0

DOI: <https://doi.org/10.21083/978-1-7770541-2-0>

Please consider signing up to the Groundwater Project mailing list and stay informed about new book releases, events and ways to participate in the Groundwater Project. When you sign up to our email list it helps us build a global groundwater community. [Sign-up](#).

APA (7th ed.) Citation:

Woessner, W.W. & Poeter, E.P., (2020). [Hydrogeologic Properties of Earth Materials and Principles of Groundwater Flow](#). The Groundwater Project,
<https://doi.org/10.21083/978-1-7770541-2-0>.



Domain Editors: John Cherry and Eileen Poeter

Board: John Cherry, Stephen Moran, Everton de Oliveira and Eileen Poeter

Steering Committee: John Cherry, Allan Freeze, Paul Hsieh, Ineke Kalwij, Douglas Mackay, Stephen Moran, Everton de Oliveira, Beth Parker, Eileen Poeter, Ying Fan, Warren Wood, and Yan Zheng.

Cover Image: Woessner

Dedication

We dedicate this book to all who want to learn about and freely spread their knowledge of groundwater.

Table of Contents

DEDICATION.....	V
TABLE OF CONTENTS	VI
THE GROUNDWATER PROJECT FOREWORDX
FOREWORD.....	XI
PREFACE.....	XII
ACKNOWLEDGEMENTS	XII
1 INTRODUCTION.....	1
2 DEFINING GROUNDWATER	3
3 GROUNDWATER OCCURRENCE IN EARTH MATERIALS	7
<i>Porous Media.....</i>	7
<i>Representative Sample Scales</i>	7
3.1 TOTAL POROSITY.....	10
<i>Measuring Porosity.....</i>	10
<i>Values of Total Porosity</i>	12
3.2 EFFECTIVE POROSITY.....	13
<i>Measuring Effective Porosity.....</i>	14
<i>Values of Effective Porosity</i>	16
3.3 PRIMARY AND SECONDARY POROSITY	16
<i>Primary Porosity</i>	16
<i>Secondary Porosity</i>	18
3.4 VOID RATIO	20
3.5 VOLUMETRIC MOISTURE CONTENT.....	21
3.6 SPECIFIC YIELD AND SPECIFIC RETENTION.....	22
3.7 INTERRELATIONSHIP OF EFFECTIVE POROSITY, SPECIFIC YIELD AND SPECIFIC RETENTION.....	25
3.8 EXERCISES.....	26
4 Darcy's Law, Head, Gradient and Hydraulic Conductivity	27
4.1 Darcy's Law.....	27
<i>Specific Discharge</i>	30
<i>Average Linear Velocity</i>	30
4.2 HYDRAULIC HEAD	32
<i>Representing Hydraulic Head Distributions</i>	35
4.3 HYDRAULIC GRADIENT	39
<i>Transient Changes in Gradients</i>	42
4.4 HYDRAULIC CONDUCTIVITY	43
<i>Intrinsic Permeability</i>	44
<i>Fluid Properties</i>	45
4.5 APPLICABILITY OF Darcy's Law.....	48
4.6 FURTHER INVESTIGATION OF Darcy's Law, Head, Gradient and Hydraulic Conductivity	50
5 HYDRAULIC CONDUCTIVITY VALUES	51
5.1 CONDITIONS EFFECTING HYDRAULIC CONDUCTIVITY VALUES	51

<i>Primary and Secondary Hydraulic Conductivity</i>	53
5.2 METHODS TO ESTIMATE HYDRAULIC CONDUCTIVITY	53
5.3 HYDRAULIC CONDUCTIVITY VALUES FOR EARTH MATERIALS	54
5.4 SPATIAL AND DIRECTIONAL VARIATION OF HYDRAULIC CONDUCTIVITY.....	55
5.5 HYDRAULIC CONDUCTIVITY OF HOMOGENEOUS AND HETEROGENEOUS MATERIALS	58
<i>Equivalent Hydraulic Conductivity</i>	59
5.6 HYDRAULIC CONDUCTIVITY IN FRACTURED ROCKS	62
5.7 EXERCISES.....	65
6 AQUIFERS AND AQUIFER PROPERTIES	66
6.1 PERCHED AQUIFERS.....	67
6.2 UNCONFINED AQUIFERS.....	68
6.3 CONFINED AQUIFERS	69
6.4 PROPERTIES OF AQUIFERS AND CONFINING UNITS	71
<i>Transmissivity</i>	71
<i>Storativity</i>	73
6.5 EXERCISES.....	78
7 EQUATIONS OF GROUNDWATER FLOW	79
7.1 BASIS FOR FLOW EQUATION DEVELOPMENT.....	79
7.2 GOVERNING EQUATIONS FOR CONFINED TRANSIENT GROUNDWATER FLOW	80
<i>One-dimensional Flow</i>	81
<i>Three-dimensional Flow</i>	84
7.3 GOVERNING EQUATIONS FOR UNCONFINED GROUNDWATER FLOW	86
7.4 STEADY STATE EQUATIONS DESCRIBING CONFINED AND UNCONFINED FLOW	87
7.5 APPLYING GOVERNING EQUATIONS	88
<i>The Role of a Water Budget in Formulating Models</i>	89
<i>Boundary Value Problems</i>	91
<i>Methods for Solving Groundwater Problems</i>	92
<i>Boundary Conditions</i>	93
<i>Application of Flow Equations (Unconfined Aquifer Flow Between Water Bodies)</i>	94
<i>Example Numerical Application of Flow Equations to a Dewatering Problem</i>	97
7.6 EXERCISES.....	99
8 INTERPRETING GROUNDWATER FLOW	100
8.1 MAPPING THE HEAD DISTRIBUTION	101
8.2 DETERMINING GROUNDWATER FLOW DIRECTIONS.....	104
<i>Gradient and Flow Directions in Isotropic Material</i>	106
<i>Flow Directions in Anisotropic Materials</i>	107
<i>Flow Directions at Interfaces of Differing Hydraulic Conductivity</i>	109
8.3 THE INFLUENCE OF BOUNDARY CONDITIONS	110
<i>Physical Boundaries</i>	110
<i>Boundaries at Subsurface Features</i>	112
<i>Hydraulic Boundaries</i>	113
<i>Flow Systems with Distant Boundaries</i>	114
8.4 ANALYSIS OF GROUNDWATER FLOW SYSTEMS	115
<i>Developing Potentiometric Maps and Cross Sections</i>	116
<i>Putting the Concepts Together</i>	123
8.5 EXAMPLES OF FLOW SYSTEMS	124
<i>High Plains Aquifer in Wyoming, USA</i>	124

<i>Memphis Sand Aquifer, Memphis Tennessee, USA.....</i>	125
<i>Unconfined Aquifer in East Helena, Montana, USA.....</i>	127
<i>Summary of Flow System Examples.....</i>	129
8.6 EXERCISES.....	129
9 CONCLUSION	130
10 EXERCISES	131
EXERCISE 1	131
EXERCISE 2	131
EXERCISE 3	132
EXERCISE 4	132
EXERCISE 5	133
EXERCISE 6	134
EXERCISE 7	134
EXERCISE 8	134
EXERCISE 9	135
EXERCISE 10	135
EXERCISE 11	135
EXERCISE 12	136
EXERCISE 13	136
EXERCISE 14	137
EXERCISE 15	138
EXERCISE 16	139
11 REFERENCES.....	140
12 BOXES.....	146
Box 1 Density of Common Minerals, Rock Types and Soils	146
Box 2 Analyzing Grain-size Distribution.....	147
Box 3 Foundation for Understanding Hydraulic Head and Force Potentials	150
Box 4 Methods for Estimating Hydraulic Conductivity	157
Box 5 Equation Derivation for Equivalent K and a 4-layer Application.....	169
Box 6 Adding Recharge to the Unconfined Aquifer System	173
Box 7 Axis Transformation for 2-D Flow in an Anisotropic Medium	178
Box 8 Deriving the Tangent Law of Refraction	180
13 EXERCISE SOLUTIONS.....	183
SOLUTION TO EXERCISE 1	183
SOLUTION TO EXERCISE 2	187
SOLUTION TO EXERCISE 3	188
SOLUTION TO EXERCISE 4	189
SOLUTION TO EXERCISE 5	190
SOLUTION TO EXERCISE 6	192
SOLUTION TO EXERCISE 7	198
SOLUTION TO EXERCISE 8	199
SOLUTION TO EXERCISE 9	200
SOLUTION TO EXERCISE 10	201
SOLUTION TO EXERCISE 11	202
SOLUTION TO EXERCISE 12	203
SOLUTION TO EXERCISE 13	204

SOLUTION TO EXERCISE 14	205
SOLUTION TO EXERCISE 15	207
SOLUTION TO EXERCISE 16	210
ABOUT THE AUTHORS	211
MODIFICATIONS FROM ORIGINAL RELEASE	A

The Groundwater Project Foreword

The United Nations Water Members and Partners establish their annual theme a few years in advance. The theme for World Water Day of March 22, 2022, is “Groundwater: making the invisible visible”. This is most appropriate for the debut of the first Groundwater Project (GW-Project) books in 2020, which have the goal of making groundwater visible.

The GW-Project, a non-profit organization registered in Canada in 2019, is committed to contribute to advancement in education and brings a new approach to the creation and dissemination of knowledge for understanding and problem solving. The GW-Project operates the website <https://gw-project.org/> as a global platform for the democratization of groundwater knowledge and is founded on the principle that:

“Knowledge should be free and the best knowledge should be free knowledge.” Anonymous

The mission of the GW-Project is to provide accessible, engaging, high-quality, educational materials, free-of-charge online in many languages, to all who want to learn about groundwater and understand how groundwater relates to and sustains ecological systems and humanity. This is a new type of global educational endeavor in that it is based on volunteerism of professionals from different disciplines and includes academics, consultants and retirees. The GW-Project involves many hundreds of volunteers associated with more than 200 hundred organizations from over 14 countries and six continents, with growing participation.

The GW-Project is an on-going endeavor and will continue with hundreds of books being published online over the coming years, first in English and then in other languages, for downloading wherever the Internet is available. The GW-Project publications also include supporting materials such as videos, lectures, laboratory demonstrations, and learning tools in addition to providing, or linking to, public domain software for various groundwater applications supporting the educational process.

The GW-Project is a living entity, so subsequent editions of the books will be published from time to time. Users are invited to propose revisions.

We thank you for being part of the GW-Project Community. We hope to hear from you about your experience with using the books and related material. We welcome ideas and volunteers!

The GW-Project Steering Committee

August 2020

x

Foreword

This book describes the properties of earth materials that are relevant to groundwater flow and delineates the principles governing the flow of water through the Earth's subsurface. As such, it provides the foundation for other GW-Project books by introducing basic concepts and terminology concerning groundwater occurrence and flow. It expands on Chapter 2 of the 1979 Freeze-Cherry book titled *GROUNDWATER* which provided the seed for the GW-Project. This book, like many of the GW-Project books, is layered by including locations where readers can link to boxes which provide deeper information such as equation derivations, analysis methods, and learning tools, among other items. However, the information in each book is complete without the supplemental links if the reader chooses not to pursue them. The materials presented here are supplemented by a GW-Project Learning Module titled: *Conceptual and Visual Understanding of Hydraulic Head and Groundwater Flow*. The Module is a stand-alone book that expands on the relationship between Darcy's law and hydraulic head.

For a broad introduction to groundwater occurrence and flow, we recommend reading the GW-Project book titled "[Groundwater in Our Water Cycle](#)" ↗ because it provides a qualitative background for the quantitative coverage of groundwater flow in this book. The 'water cycle' book explains groundwater in our environment and presents groundwater problems faced by humanity and ecosystems, while this 'physical principles' book provides the fundamentals needed for the task of assessing and solving those problems.

This book was written by a groundwater scientist and engineer who taught a variety of introductory and advanced hydrogeology classes at the university level. They are specialists in field investigations, groundwater problem analysis, groundwater model development and computer simulation. Nine experts, who taught courses related to the topics presented herein, provided thorough reviews of this book to ensure its accuracy and high quality. Thus, the material in this book provides information that the world urgently needs to support better groundwater management and protection.

John Cherry, The Groundwater Project Leader
Guelph, Ontario, Canada, July 2020

Preface

Groundwater scientists need to have a solid understanding of the occurrence and behavior of groundwater in a variety of conditions and settings. This requires knowledge of how porous media store, yield, and transmit water. Darcy's Law defines the discharge of groundwater as directly proportional to the area perpendicular to the direction of flow, hydraulic gradient and transmission capacity of the earth material. The forces on water within pore spaces and fractures control groundwater flow rates and directions, so we describe them in detail. Then, we explain mathematical representations of groundwater flow and provide examples of their application to large and small groundwater systems.

Acknowledgements

We thank the following individuals for their thorough and useful reviews of and contributions to this book:

- ❖ Jack Sharp, Professor Emeritus, Department of Geological Sciences, Jackson School of Geosciences, University of Texas;
- ❖ Kamini Singha, Professor, Department of Geology and Geological Engineering, Colorado School of Mines;
- ❖ Will Robertson, Emeritus Professor, Earth Sciences, University of Waterloo;
- ❖ Jean van Niekerk, PhD Candidate, Institute of Groundwater Studies, Univ Free State;
- ❖ Payton Gardner, Assistant Professor, Department of Geosciences, University of Montana;
- ❖ Guy Patrick, Director, Patrick Consulting Incorporated., British Columbia, Canada;
- ❖ Dave McWhorter, Emeritus Professor of Chemical and Biological Engineering, Colorado State University;
- ❖ Roger Diamond, Lecturer Hydrogeology and Geochemistry, University of Pretoria, South Africa; and,
- ❖ Jana Levison, Professor, Water Resources Engineering, University of Guelph, Canada.

We appreciate the contributions of David McWhorter (Colorado State University) and Paul Hsieh (Independent Groundwater Hydrologist) to the explanatory boxes; as well as the work of Andrew Cohen (New Jersey Institute of Technology) and John Cherry (G360 Institute for Groundwater Research) in developing a Learning Module designed to support hydraulic head and groundwater flow concepts. We are grateful for Amanda Sills' oversight and production of this book and to Elhana Dyck for copyediting, both of the Groundwater Project, Guelph, Ontario, Canada. We appreciate the guidance and contributions of Everton de Oliveira, Diego Nogueira and Bruna Solderra of the Groundwater Project, São Paulo, São Paulo, Brazil, as we fostered this book to completion.

William Woessner
Eileen Poeter

***HYDROGEOLOGIC PROPERTIES OF EARTH MATERIALS
AND PRINCIPLES OF GROUNDWATER FLOW***

The Groundwater Project

1 Introduction

The purpose of this Groundwater Project book is to introduce basic concepts in groundwater science including terminology and equations that will provide readers with the foundational knowledge upon which they can:

- characterize hydrogeologic properties of earth materials;
- compute groundwater flow rates, fluxes and velocities;
- understand the development of equations that represent groundwater flow; and,
- interpret and visualize groundwater flow patterns.

This book explains how the size, shape and interconnectedness of voids in Earth's subsurface materials provide the framework for the storage and transmission of water found in the saturated zone below Earth's surface. To describe this transmission, in the mid 1800's, Henry Darcy developed a formula to calculate the volumetric rate of water flowing through sand from easily made measurements of head, gradient and hydraulic conductivity.

This book also introduces hydraulic head and shows that hydraulic head gradients drive groundwater flow in a manner similar to the way temperature gradients drive heat flow. The ease of groundwater flow through the subsurface is controlled by the intrinsic permeability of the geologic material as well as by the density and viscosity of the groundwater. Together these properties of the geologic material and water define the hydraulic conductivity of the earth material. When hydraulic head gradients are combined with the groundwater flow equations and hydraulic conductivity, the volumetric flow rate and average linear velocity of the groundwater is defined.

Darcy's Law and the law of mass conservation underpin the mathematics used to quantitatively describe groundwater systems. The use of these two principles to develop equations representing groundwater flow under steady and transient conditions is described herein.

Geologic materials and formations that contain and yield groundwater for useful purposes are referred to as aquifers. Unconfined, confined, and perched aquifer systems are explained in this book. Aquifer properties such as transmissivity, specific storage and storativity are defined and their utility is illustrated.

Groundwater flow systems are examined, and the methods used to illustrate groundwater flow directions and patterns are presented. Controls resulting from physical and hydraulic boundaries are described as well as flow in isotropic, anisotropic, homogeneous, and heterogeneous settings.

The introductory material presented in this book provides a beginning for a reader's journey into the hydrogeological world. Other [Groundwater Project books](#) ↗ address many of the subjects presented here in additional detail and introduce new concepts and

materials. A number of hydrogeological terms are introduced and defined in this book. A general reference for groundwater terms is provided the groundwater project book “*A Glossary of Hydrogeology*” (Sharp, 2023).

2 Defining Groundwater

Groundwater is water that occurs below the ground surface in zones of porous materials where all the cracks (fractures) and pore spaces are filled with water and that water is at a pressure higher than the pressure of the atmosphere (Figure 1). This region or zone is referred to as the zone of saturation, saturated zone, zone of phreatic water, or groundwater zone.

The top of the groundwater zone is represented by the water table which is defined as the level or elevation where the water pressure is equal to atmospheric pressure. Above the water table, water pressure is less than atmospheric pressure, and below the water table, water pressure is greater than atmospheric pressure. Some literature refers to all water below the land surface as groundwater, however; in the scientific literature groundwater is clearly defined as the water occurring in the saturated zone and this is how it is used here.

Between the land surface and the water table the fractures and pore spaces contain both air and water. This region is called the zone of aeration, unsaturated zone, or vadose zone. This book uses both vadose zone and unsaturated zone to describe the region above the water table. The term unsaturated zone is commonly used even though as soil water moves downward through the vadose zone towards the water table, portions of the zone can become saturated temporarily and later return to unsaturated conditions. Just above the water table, fractures and pores are completely filled with water at a pressure that is less than atmospheric and so, by definition, it is part of the vadose zone. This part of the vadose zone is called the capillary fringe indicating its unique nature (full saturation at less than atmospheric pressure). The capillary force can “pull” water upward, against gravity, much like a dry sponge soaking up spilled water on a kitchen countertop. The capillary fringe extends a few millimeters above the water table in large pores such as occur in gravel deposits and large fractures, tenths of a meter to a half-meter in sands, and multiple meters in silts and clays (Todd and Mays, 2004).

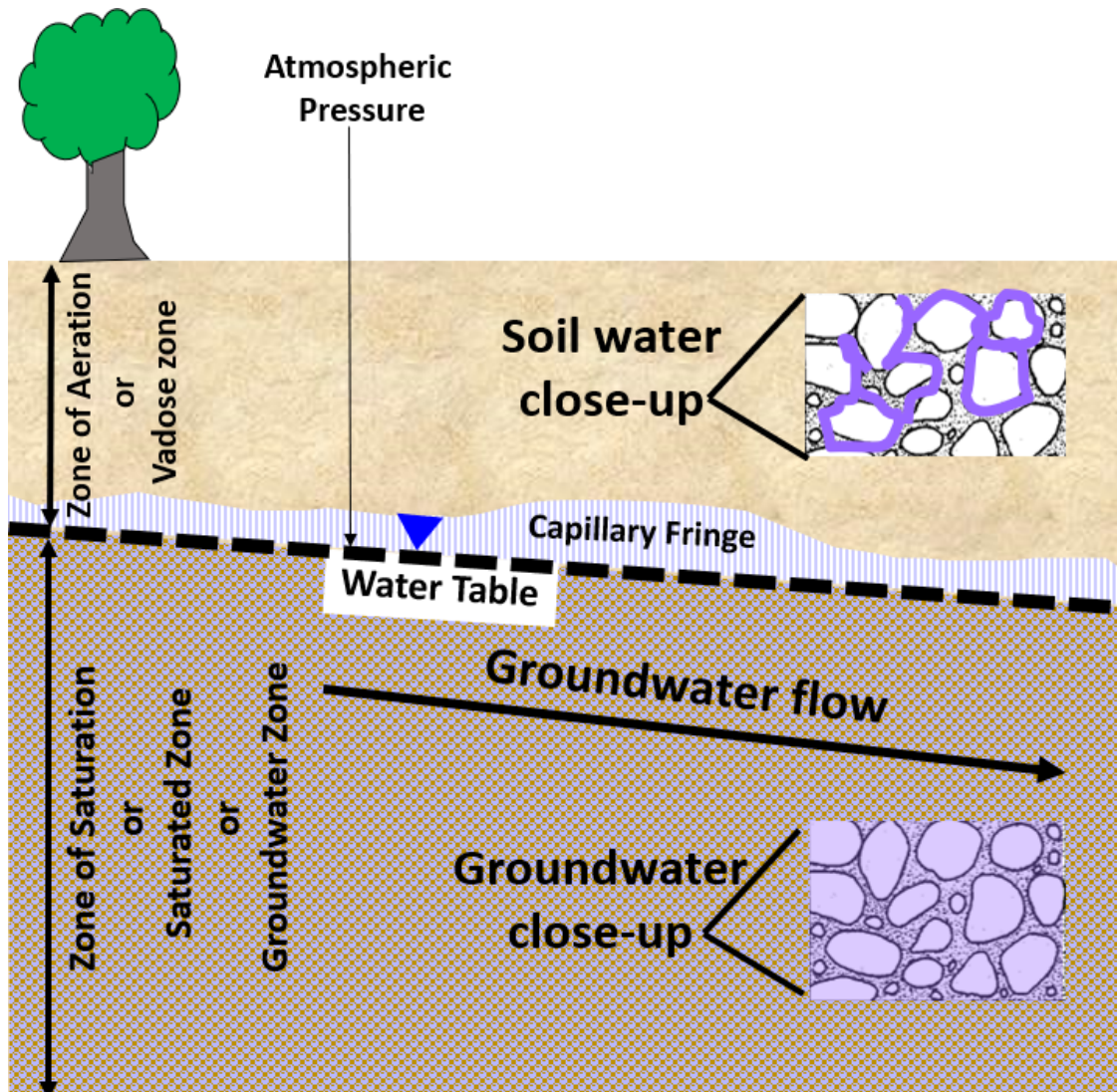


Figure 1 - Schematic of shallow water zones in the subsurface, including the Saturated Zone (violet brown stippled area) below the water table (heavy dashed line with inverted blue triangle) and the Vadose Zone (light tan) above, with the capillary fringe between them. Groundwater is defined as the water that occurs in the Zone of Saturation.

In contrast to the saturated zone, the water in the vadose zone is at less than atmospheric pressure as reflected by a negative pressure on a gauge that uses atmospheric pressure as the reference point. The negative pressures are due to capillary forces that result from the adhesion of water molecules to subsurface solids and the cohesion of water molecules to one another. The negative pressures vary depending on the amount of moisture in the soil (Figure 2). As the amount of water in the vadose zone increases the tensional forces decrease (pressure becomes less negative) enough for gravity to pull water downward to the water table and recharge the groundwater system.

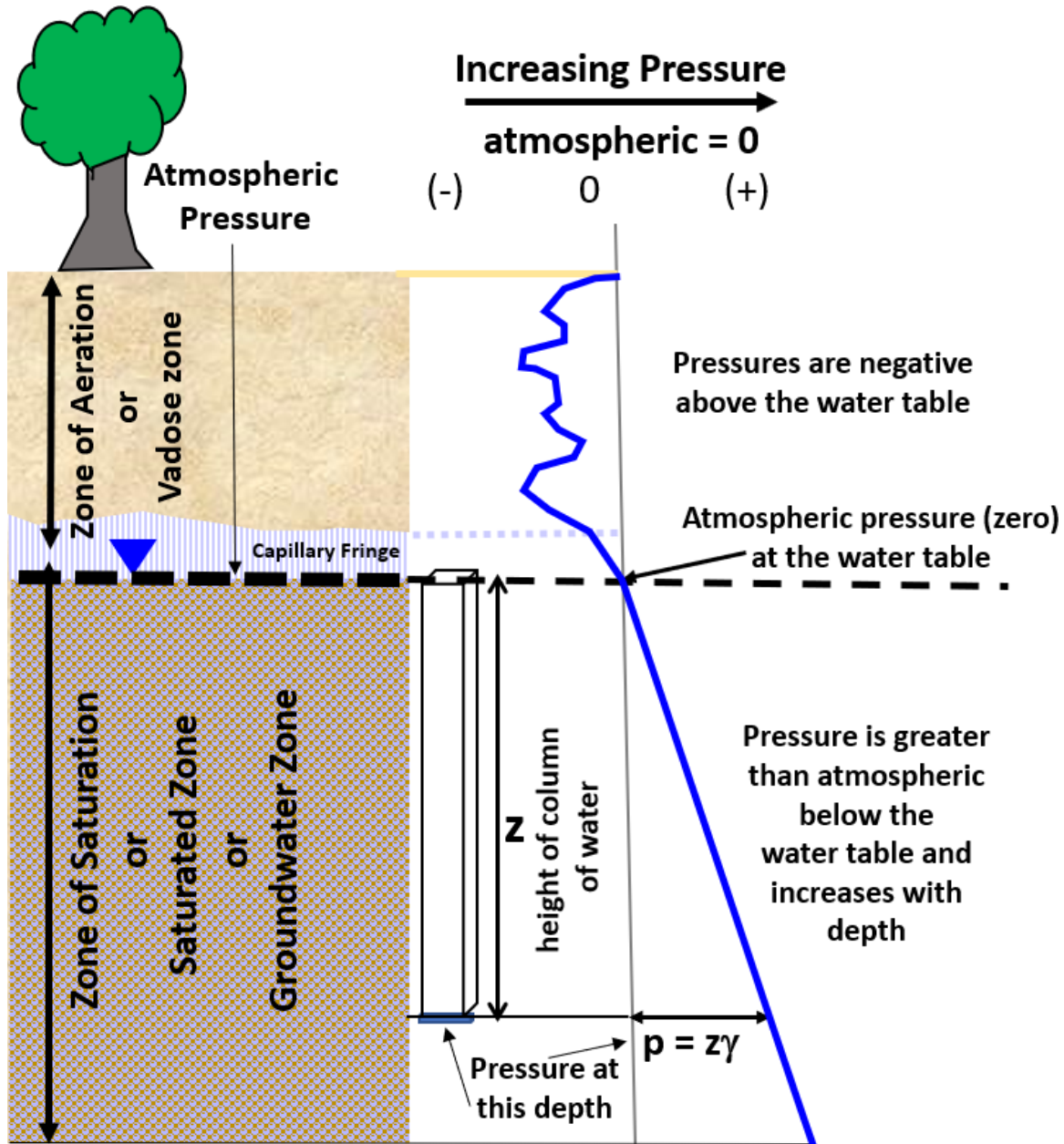


Figure 2 - Water pressure at a snapshot in time. In the vadose zone water pressure varies depending on the amount of moisture in the soil, but it is always less than atmospheric. The water table occurs at the elevation where the water pressure is equal to atmospheric pressure. In the saturated zone, water is at greater than atmospheric pressure.

The top of the zone of saturation is the water table. The water in the saturated zone at a particular depth below the water table is a combination of the atmosphere bearing down on the water table (zero on a gauge that uses atmospheric pressure as a reference pressure) and the pressure caused by the weight of water in the column between the water table and the depth of interest (pressure, p , in Equation 1 as shown in Figure 2). Specific weight, γ , is density of a substance times the gravitational constant, ρg .

$$p = z \gamma \quad (1)$$

where:

- p = pressure at the base of a column of water below the water table (F/L^2),
which is force (i.e., weight) per unit area
- z = height of the column of water (depth below water table) (L)
- γ = specific weight of the water (F/L^3)

In the saturated zone, groundwater movement is primarily lateral. Gravity drives flow through interconnected pores and fractures from areas of higher groundwater levels (elevations) to areas of lower water levels. Groundwater in the saturated zone can be extracted by wells, flow to surface water bodies such as lakes and rivers, transport contaminants, and provide water for cities, agriculture and industry.

3 Groundwater Occurrence in Earth Materials

Section 2 described the zones of subsurface water, defining groundwater as occurring in the zone of saturation where all openings are filled with water. This section defines terms hydrogeologists and engineers use to characterize how groundwater is stored and released from porous media.

Porous Media

Water occurs in the opening or spaces between solid particles of sediment and within fractures of rocks (Figure 3). These spaces are referred to as pore spaces, pores, openings, and voids as may occur in soil or sediments; fractures in sedimentary, igneous and metamorphic rocks; and caverns and cavities that are found in deposits of evaporates and carbonates (e.g., karst). These openings provide space to store water and, when the spaces are interconnected, pathways to transmit water through the vadose and saturated zones.

Earth materials containing pores are referred to as porous media. Hydrogeologists and engineers characterize porous media by quantifying the volumes occupied by pore space and solids, the degree and magnitude of pore space interconnections, and the response of the media to changes in loads and pressures.

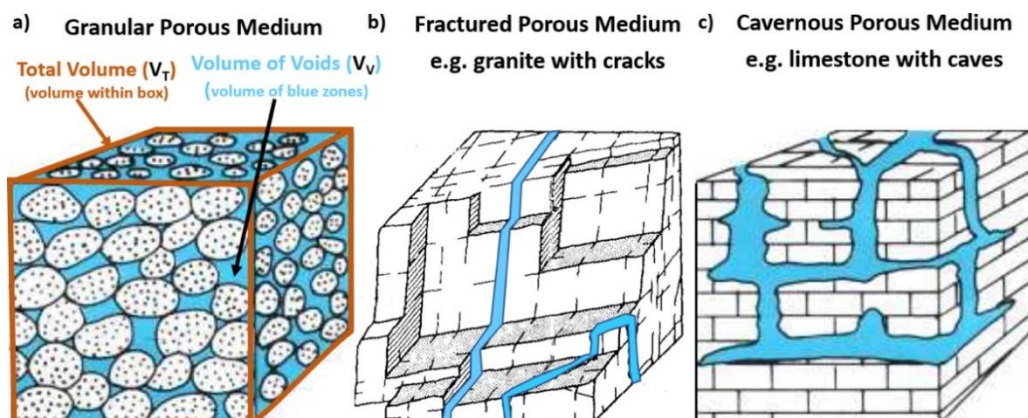


Figure 3 - Water fills the spaces of subsurface materials in: a) pores between particles of sediments (from Heath, 1983); b) fractures of rocks (after Gale, 1982); and c) caverns and cavities of carbonate rocks known as karst (from Heath, 1983). As indicated on (a), the volume of a sample is defined by all space within its exterior surface, the volume of voids is the non-solid space within that volume.

Representative Sample Scales

Hydrogeologic investigations are completed at various scales. For example: the exchange of groundwater with a small wetland; dewatering of a construction site; evaluation of the transport of contaminants from an industrial site to a municipal well field; and, regional investigations examining the sustainability of groundwater resources in large groundwater systems of arid basins require defining hydrogeologic properties of earth materials at a range of scales.

Hydrogeologic properties of earth material can be described at the microscopic scale where the behavior of water would be determined based on measurements of: the size and number of individual pore diameters, roughness of pore surfaces, pore channel shapes and the degree of pore interconnection. However, such small-scale measurements are neither practical nor useful because most hydrogeologic investigations focus on conditions encompassing volumes of earth material that are much larger than the pores. Thus, hydrogeologists use a macroscopic approach to represent properties of subsurface media.

The macroscopic approach uses a sample volume of porous media large enough so as to represent the average effects of pore character, sizes, and interconnectedness. "Sufficiently large" can be determined by thinking about how to establish a sample volume that reflects the average value of a hydrogeologic characteristic for the scale of the investigation (e.g., the storage or transmission capacity). One approach is to start with an extremely small sample volume, determine the characteristic value, and then progressively increase the sample volume until a stable characteristic value occurs. Bear (1972) described the minimum macroscopic volume where property characteristics stabilize as the representative elementary volume, REV (Figure 4). Any sample volume that provides these stable characteristic values can be used as a REV. Once a REV is identified, average hydrogeologic properties are assigned to the centroid of the REV. The minimum volume that yields Bear's (1972) REV can also be referred to as the Min REV. The upper boundary of REVs occurs when progressively larger sample volumes yield either a higher or lower characteristic value (Max REV).

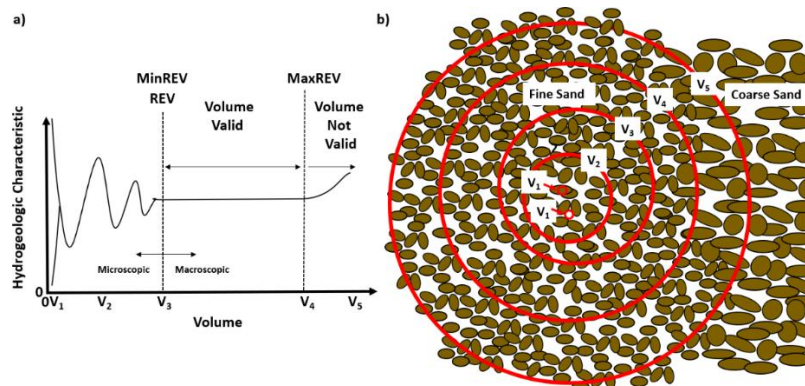


Figure 4 - Conceptualizing determination of a representative elementary volume, REV, of a porous medium. a) If a porous medium is sampled using extremely small volumes (V_1) and then progressively larger volumes (volumes from V_1 to V_5) the macroscopic representative hydrogeologic characteristic value can be identified. In this schematic, the sample volume V_3 establishes the REV. Measurement of larger sample volumes would yield the same average properties as V_3 . The Min REV corresponds to the definition of the REV (Bear, 1972). The Max REV marks the transition volume above which the average characteristics change (shown here as becoming higher). b) A sample dominated by zones of fine and coarse sand. The smallest circles (V_1) represent the results of sampling a single pore or a single solid grain. Other numbers and red circles represent progressively larger sample volumes. At the highest volume (V_5) additional material with characteristics that are different from the original sample material are included within the sample. The REV is defined at V_3 and characteristics remain constant until V_4 where samples of larger volumes begin to incorporate the coarse sand that, in this example, have a higher characteristic value.

The REV is not a standard volume (e.g., it is not always 1 cm^3 , 1 m^3 , 10 m^3 , 100 m^3 or 1 km^3), instead, it varies depending on the hydrogeologic character of the material and the proposed objectives of an investigation. The REV representing the groundwater storage properties of the sand at the site of the core shown in Figure 5 is most likely a smaller volume than the entire core, unless the formation includes multiple finer layers or cross bedding. In that case, the entire core or a larger sample may be required.

When conducting hydrogeological investigations, the properties of porous materials are used in equations and models for quantitative analyses. In some settings, using multiple laboratory scale measurements and then averaging them and assigning them to the entire site to represent the average field scale conditions is appropriate. However, often laboratory scale determinations are not sufficient to represent more complex geological conditions encountered at the field scale. As a consequence, field-scale hydrogeologic testing methods are used to provide average properties for larger volumes of earth material, because it is too expensive and time consuming to collect small sample volumes at thousands of locations, determine laboratory based hydrogeologic characteristics for each sample and then average the data to generate characteristics of volumes that represent many cubic kilometers of the subsurface. Instead, field testing methods designed to generate property values that incorporate field scale complexities are applied. At the field scale the REV may be conceptualized as being represented by much larger volumes than those used to represent laboratory scale samples (Figure 5).

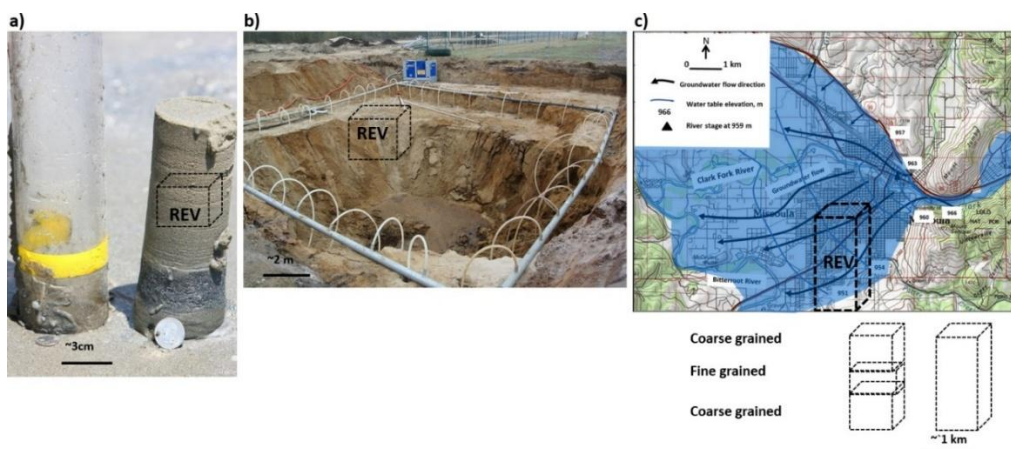


Figure 5 - Conceptual examples of the scale of REV's obtained from laboratory and field scale testing. a) A 10 cm diameter core of beach sand. The REV based on lab testing is most likely represented by a volume of a few cubic centimeters. If the sample contains layering and other structures, like cross bedding, the complete core may better represent the sand REV of the field site (Demcheck, 2010). b) A sand rich environment being dewatered (flexible piping serves as point dewatering wells). The more complex nature of the sand deposit would most likely have a REV on the order of cubic meters. Field scale testing of characteristics in a number of boreholes and by a multiple well pumping test would be appropriate for this investigation (photo from EVO, 2020). c) A regional study of a 30 m-thick sand and gravel water-bearing material (blue shaded area) where complexities of the geologic setting are represented by the average characteristics of large volumes of material. REV's may be defined using large-scale field-testing methods and assigning values of characteristics measured in each of three major layers to the individual layers (coarse-fine-coarse) or average the characteristics into a single value for all three layers (e.g., one square kilometer by 30 m thick) (modified from Weight, with permission, 2019).

Both field- and laboratory-scale characteristics are used to qualitatively and quantitatively describe natural groundwater flow conditions, the transport of contaminants in earth materials, the consequences of extracting or injecting groundwater, and the environmental links between surface water and groundwater systems.

This book describes the characteristics of porous media that hydrogeologists use to describe groundwater systems; compute groundwater discharge, flux and velocity; develop general groundwater flow equations; and determine groundwater flow directions. A number of other [Groundwater Project books](#) provide specific details addressing the theoretical foundation of methods needed to characterize hydrogeologic conditions at the field scale and approaches to using that information to investigate groundwater systems. This book defines terms associated with hydrogeologic characteristics and explains laboratory methodologies for their measurement.

3.1 Total Porosity

Water below the land surface occurs in the spaces between solid particles of sediment and within fractures of rocks (Figure 3). Total porosity (n) is the ratio of the volume of void space (V_V) in a sample of earth material to the total volume of the sample (V_T) including solids and void space. Total volume is enclosed within the entire box shown in Figure 3a, while void volume includes only the blue zones. In some texts total porosity is referred to as porosity and both terms are used in this book. Total porosity is preferred here because of the need to distinguish it from effective porosity defined in this section.

Porosity can be represented as a fraction of the total volume as shown in Equation 2, or as a percentage (if multiplied by 100%).

$$n = \frac{V_V}{V_T} \quad (2)$$

where:

n = total porosity (dimensionless)

V_V = volume of void space in a sample (L^3)

V_T = total volume of a sample (L^3)

Measuring Porosity

It is difficult to measure the volume of voids directly. However, the relationship between sample density and total porosity provides a means of calculating the void volume because the bulk density of a sample is controlled by the proportion of solids and voids. That is, the bulk density is equal to the fractional volume of solids ($1 - n$) times the particle density plus the fractional volume of voids (n) times the fluid density, as shown in Equation 3.

$$\rho_b = (1 - n) \rho_p + n \rho_f \quad (3)$$

where:

ρ_b = bulk density (M/L^3)

n = total porosity (dimensionless)

ρ_p = particle density (M/L^3)

ρ_f = fluid density (M/L^3)

Thus, the total porosity can be computed if the bulk density (ρ_b) of the sample is determined for either a fully saturated or a fully dried sample, and the fluid density (ρ_f) as well as the particle density (ρ_p) of the dominate mineral material making up the matrix (solid particles) of the sample are known, as shown in Equation 4. Typically, the fluid is air or water, so the fluid density is known.

$$n = \frac{\rho_b - \rho_p}{\rho_f - \rho_p} \quad (4)$$

To determine the total porosity of a sample, the sample volume can be measured by fully saturating the sample then immersing it in water and noting the volume of displaced fluid. Then, the wet bulk density is determined by weighing the saturated sample and dividing that weight by the volume. When water is the fluid, the density is assumed to be 1 gram per cubic centimeter (g/cm^3), because this is its density at $4^\circ C$ and the density does not noticeably change in the range of temperatures experienced in the field and lab. If the sample is dried and then weighed, the dry bulk density can be used to calculate porosity by assuming the air filling the pores to have a fluid density of $0 g/cm^3$.

For example, the porosity for a sample volume of one cubic centimeter of loose quartz sand can be computed knowing that the dry bulk density of the sand sample is $1.43 g/cm^3$ and the density of a corresponding cubic centimeter of solid quartz with no pore space (i.e., the composition of the sand grain) has a density of $2.65 g/cm^3$ as shown in Figure 6.

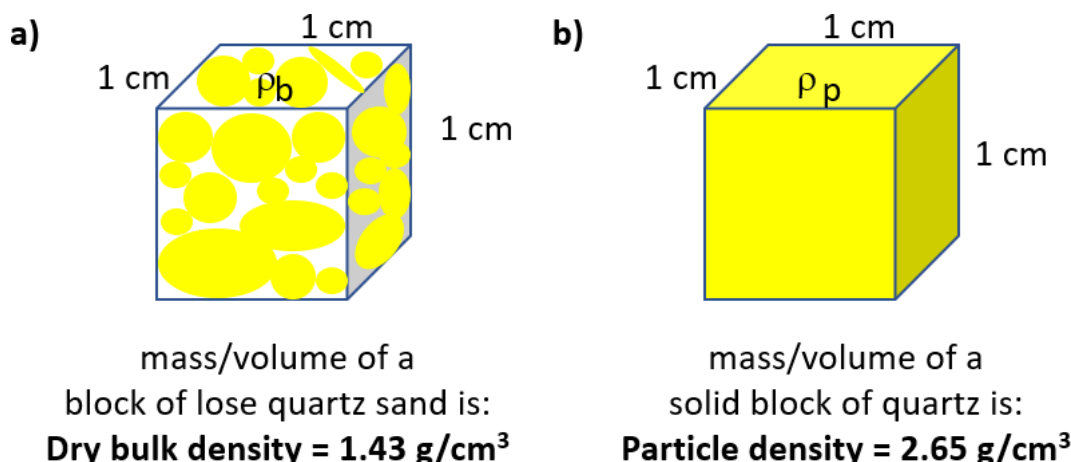


Figure 6 - Schematic of: a) dry bulk density of 1 cubic centimeter of loose quartz sand; and, b) density of 1 cubic centimeter of solid quartz, which provides the particle density of the quartz sand grains.

By using Equation 4, the total porosity can be calculated as 0.46 or 46%, as shown in Equation 5.

$$n = \frac{1.43 \frac{\text{g}}{\text{cm}^3} - 2.65 \frac{\text{g}}{\text{cm}^3}}{0 \frac{\text{g}}{\text{cm}^3} - 2.65 \frac{\text{g}}{\text{cm}^3}} = 0.46 \quad (5)$$

For additional information on the densities of earth materials, [Click here to link to Box 1](#).

Values of Total Porosity

Tables of total porosity values for earth materials are included in publications provided by government agencies and researchers, as well as in hydrogeology textbooks. Examples of total porosity values for earth materials are presented in Table 1.

Generally, unconsolidated materials have higher porosities (20 to 55%) than consolidated sediments and igneous and metamorphic rocks. Though, some consolidated sedimentary rocks; and weathered and/or fractured igneous and metamorphic rocks can also have high porosities. The porosity of vesicular basalt is a result of the degree of void creation during the solidification process.

Table 1 - Typical total porosity ranges of some common earth materials (after Rivera, 2014; with data from Freeze and Cherry, 1979 and Domenico and Schwartz, 1998).

Total Porosity Range of Some Common Earth Materials (Percent)	
Material	Range Total Porosity (%)
Unconsolidated Sediments	
Clay	45 - 55
Silt	35 - 50
Fine-sand	26 - 50
Coarse-sand	30 - 45
Gravel	25 - 35
Sand and gravel	20 - 30
Glacial till	20 - 30
Consolidated Sediments	
Shale	1 - 10
Siltstone	20 - 40
Sandstone	5 - 30
Limestone and dolomite	1 - 25
Karstic limestone	5 - 35
Igneous and Metamorphic Rocks	
Fresh granite and gneiss	0.01 - 3
Weathered granite and gneiss	5 - 25
Fractured basalt	5 - 30
Vesicular basalt	10 - 40
Tuff	10 - 55

3.2 Effective Porosity

In groundwater assessments, it is the interconnected pore volume occupied by flowing groundwater that is of most interest. Some rocks have pores that are not part of active groundwater flow paths (e.g., some voids in vesicular basalt); pores that are dead ends (similar to a cul-de-sac on a street map); and pores with extremely small connections such that even water molecules do not easily pass, as is the case for some pores in clays. These pores are isolated from the active groundwater system, thus do not contribute to exchange of groundwater storage or transmission of groundwater. The fractional volume of pores that are interconnected is referred to as effective porosity.

Effective porosity (n_e) is defined as the ratio of the volume of interconnected pore spaces (V_I) to the total volume (V_T) as defined in Equation 6 and illustrated in Figure 7. Interconnected void space allows groundwater to move into and out of porous material.

$$n_e = \frac{V_I}{V_T} \quad (6)$$

where:

n_e = effective porosity (dimensionless)

V_I = volume of interconnected pore space (L^3)

V_T = volume of sample (L^3)

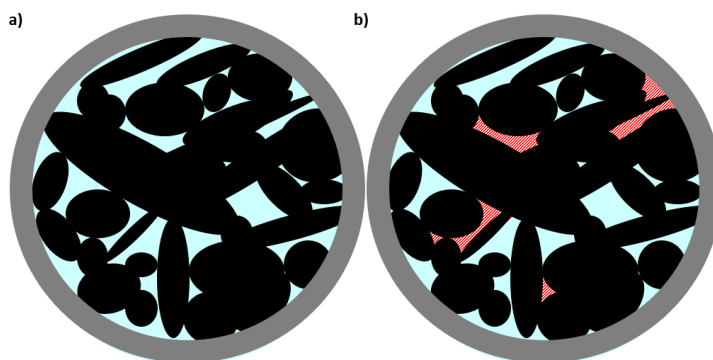


Figure 7 - Relationship between total porosity and effective porosity where the total sample volume, V_T , is represented by the area inside the gray circle. a) Water occupies all pore spaces (light blue spaces, V_I) and the total porosity is $n = V_V/V_T$; b) Some pore spaces are disconnected from other pores (red hatched spaces) and groundwater can only access the connected pore spaces (blue area, V_I), thus effective porosity is $n_e = V_I/V_T$.

The effective porosity may equal, or be less than, the total porosity (n) of the sample (Table 1). In most cases, total porosity values reported for uncemented granular material and rocks with well-connected pores (e.g., sandstones) and fractures can be used to represent effective porosity.

Measuring Effective Porosity

Effective porosity can be determined at the laboratory scale when sediment and rock samples of a given volume are dried and then the pore spaces are filled with water (Figure 8). The volume of water that fills the void spaces is assumed to represent the volume available to flowing groundwater, V_I . For example, to determine the effective porosity of a granular earth material, a sample volume is collected, allowed to dry completely, and then water is introduced slowly to the base of the sample (so that air can escape from the top). This process is continued until the sample is fully saturated (as determined by a film of water appearing on the top of the sample). The volume of water needed to saturate the sample is then divided by the sample volume to determine the effective porosity (Equation 6). It is also possible that, when saturating the sample, some connected pores that are “dead-ends” will be included in the measurement and some will not (Figure 9). Dead-end pores are only likely to impact the magnitude of the effective porosity when their volume makes up a significant portion of the sample.

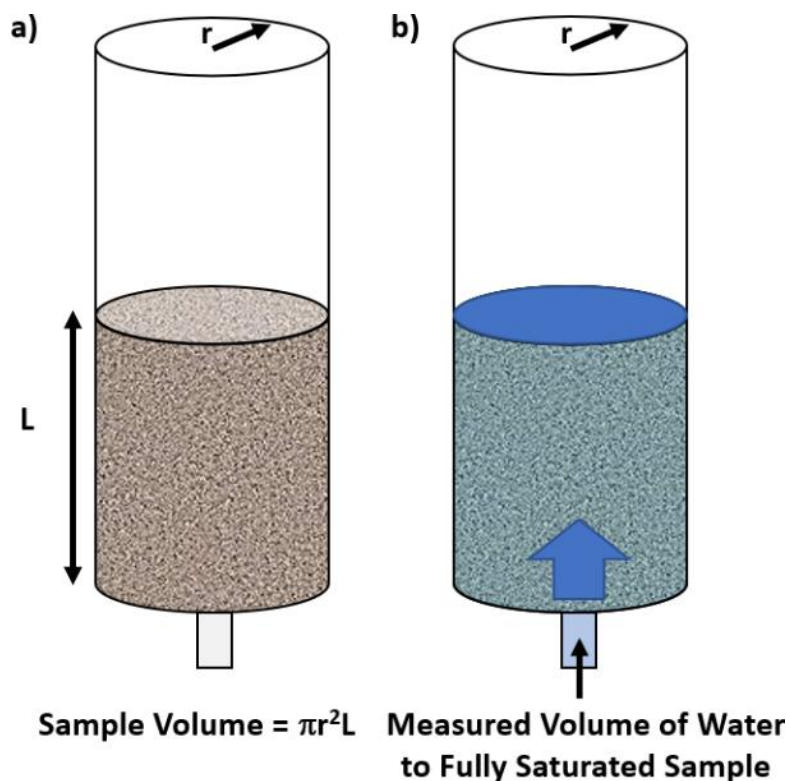
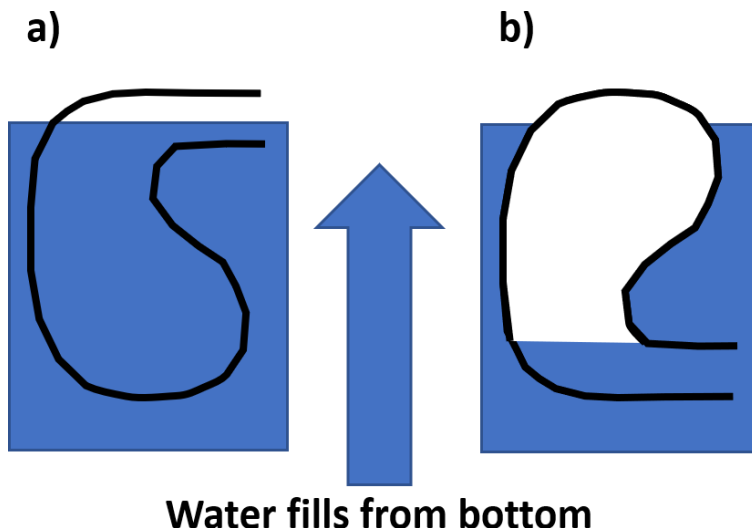


Figure 8 - A simple laboratory set up to measure effective porosity of a sample of earth material. a) Initially the sample volume (V_T) is determined using the length of the sample and inside radius of the cylinder, then the sample is dried such that no residual water is present in the pore space. b) Then, water is introduced slowly from the bottom of the sample to displace air in the pores and the volume of water required to saturate the sample, as indicated by the appearance of a thin film of water on the top of the sample, is determined. The volume of water required to fill the voids is the V_I and effective porosity is computed as $n_e = V_I/V_T$.



Water fills from bottom

Figure 9 - The geometry of dead-end pores may complicate an effective porosity measurement, but generally the infrequency of such situations will introduce only minor errors in the measurement: a) orientation of pore allows displacement of air; and b) pore orientation traps air and the air-filled pore space is not included in the effective porosity.

Effective porosity can also be determined by submerging a fully dried sample in a beaker filled with a measured quantity of water and applying suction to draw air out of the sample. The total volume of sample is determined by the initial increase volume read from the beaker markings immediately upon placing the sample in the water. Once the sample is fully saturated, the reduction in the volume of water is used to infer the volume of void space. For example, a 10 cm^3 cube ($10 \text{ milliliter (ml)}$ total volume) of sandstone is placed in a beaker filled with 100 ml of water such that the volume reading on the beaker is 110 ml . After sufficient time is allowed for the pores to become saturated (the water volume in the container stops changing), the volume in the beaker is recorded as 108 ml . The volume of void space is 2 ml (2 cm^3). The effective porosity can then be computed using Equation 6 as $2 \text{ cm}^3 / 10 \text{ cm}^3 = 0.20$. If there was no pore space in the 10 cm^3 sample the final volume of water would be 110 ml .

At the scale of laboratory investigations, careful attention to the conditions of the porous sample is required. Ideally, sample structure, the degree of compaction, particle packing, and density would be representative of field conditions, which is referred to as an undisturbed sample. However, in some cases, physical sampling methods may increase or decrease the sample porosity. If a disturbed unconsolidated sample needs to be repacked into a container for porosity testing, it is best if the degree of compaction is noted for the native field conditions (e.g., by using a cone penetrometer or a standard penetration test). This information allows the laboratory sample to be recompackaged to a similar consistency. Even so, the packing arrangement will differ, and thus laboratory measurements using recompackaged samples provide only approximations of the field effective porosity values.

Effective porosity values representing large volumes of earth materials can also be computed from field hydrogeological tracer testing where water containing a solute, dye,

or isotope is injected into a groundwater system and its spread is monitored. Ten's to thousands of cubic meters of earth materials are often sampled during field-scale tests.

Values of Effective Porosity

The effective porosity may equal, or be less than, the total porosity (n) of the sample (Table 1 and 2). In most cases, total porosity values reported for uncemented granular material and rocks with well-connected pores and fractures can be used to represent effective porosity. Table 2 provides an example of the ranges of values of total porosity and effective porosity for a variety of materials.

Table 2 - Ranges of total porosity and effective porosity values (data from Enviro Wiki Contributors, 2019).

Total and Effective Porosity		
	Total Porosity	Effective Porosity
Unconsolidated Material		
Gravel	0.25 - 0.44	0.13 - 0.44
Coarse Sand	0.31 - 0.46	0.18 - 0.43
Medium Sand		0.16 - 0.46
Fine Sand	0.25 - 0.53	0.01 - 0.46
Silt, loess	0.35 - 0.50	0.01 - 0.39
Clay	0.40 - 0.70	0.01 - 0.18
Sedimentary and Crystalline Rocks		
Karst and reef limestone	0.05 - 0.50	--
Limestone, dolomite	0.00 - 0.20	0.01 - 0.24
Sandstone	0.05 - 0.30	0.10 - 0.30
Siltstone	--	0.21 - 0.41
Basalt	0.05 - 0.50	--
Fractured crystalline rock	0.00 - 0.10	--
Weather granite	0.34 - 0.57	--
Unfractured crystalline rock	0.00 - 0.05	--

3.3 Primary and Secondary Porosity

The porosity of earth materials originates during two phases: 1) during the deposition of sediments, lithification or cooling of crystalline rock; and 2) after deposition as the earth material is exposed to other conditions such as compaction, weathering, fracturing and/or metamorphism. As a result, earth materials can have porosities dominated by primary conditions during initial formations, secondary events after formation, or both.

Primary Porosity

The porosity of an earth material during its original formation is referred to as primary porosity. A number of factors influence the porosity of earth materials. The primary porosity of granular material is affected by the shape and packing of grains, the distribution of grain sizes (sorting and uniformity) and the porosity of the particles themselves (Figure 10). The degree of cementation during lithification of sedimentary rocks will also affect the primary porosity.

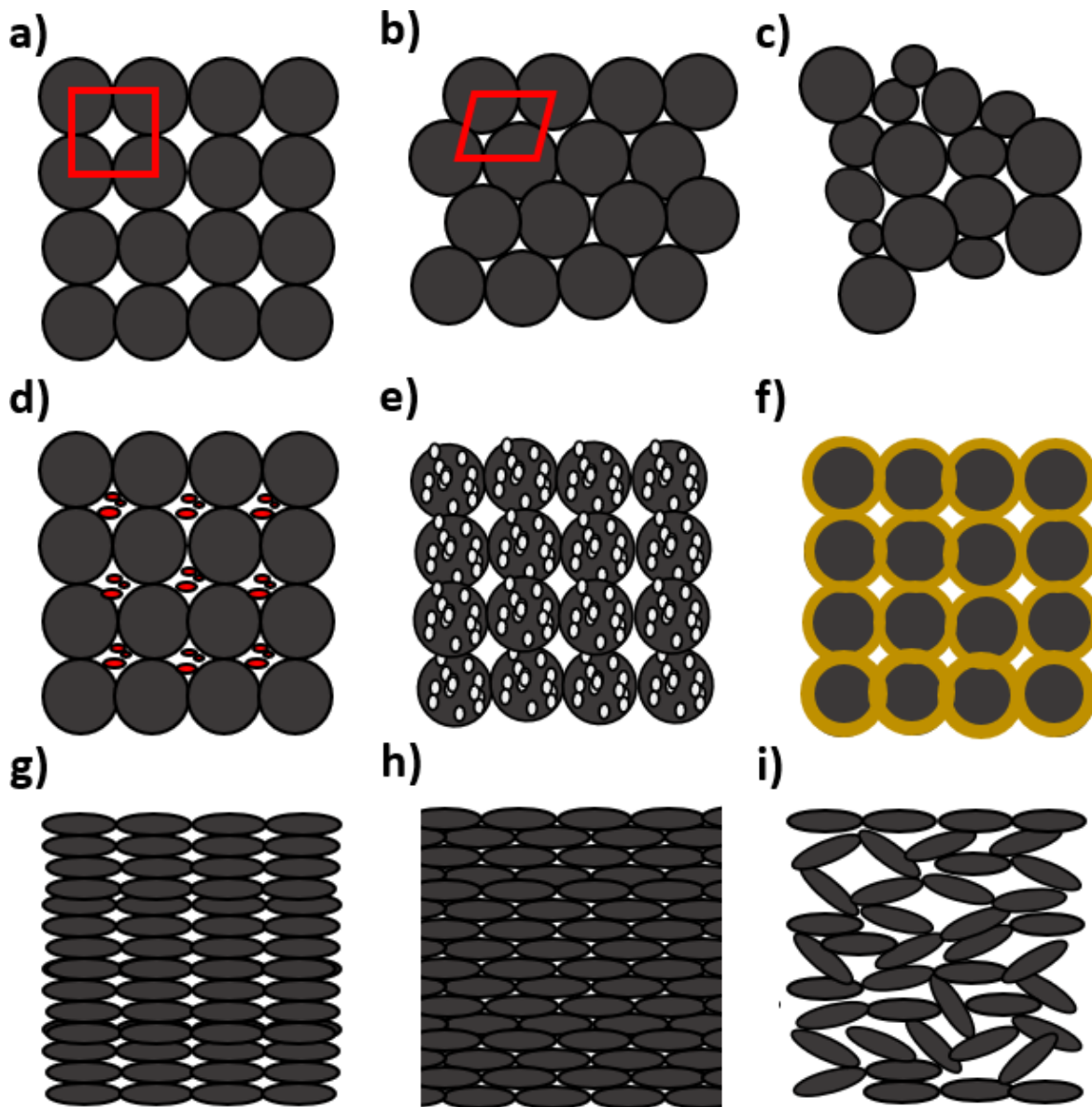


Figure 10 - The effect of particle shape, arrangement, packing density, grain size distribution, and porosity of the grains themselves on the number and size of pore spaces. As the volume of pore space is reduced, porosity will decrease:

- a) cubic packing (indicated by red square) of uniformly sized spherical particles;
- b) rhombohedral packing (indicated by red rhombohedron) of uniformly sized spherical particles decreases volume of pore space compared to (a);
- c) packing of non-uniformly sized spherical particles decreases the volume of pore space compared to (a);
- d) cubic packing of spherical particles where the pore space is partially filled with smaller solid particles (red grains) such that the smaller solid particles fill a portion of the void space between larger particles decreases the volume of pore space compared to (a);
- e) cubic packing of the same spheres as shown in (a) but the spheres themselves are porous (white dots on black spheres) increases the volume of pore space compared to (a);
- f) precipitation of minerals form coatings on sedimentary particle surfaces and cement particles together decreasing the volume of pore space compared to (a);
- g) cubic packing of elongated particles decreases the volume of pore space compared to (a);
- h) rhombohedral packing of elongated particles decreases the volume of pore space compared to (a and g); and,
- i) lose packing of bridged elongated particles increases the volume of pore space compared to (a, g, and h).

Porosity is highest when materials are loosely packed and grains are uniform in size and shape. As a thought experiment, consider two identical rooms (e.g., same total volume), one full of glass spheres the size of soccer balls and one full of 1-cm diameter spherical glass marbles. The spheres in each room are arranged to form cubes (cubic packing) as illustrated in Figure 10a. Based on this information, what would be the porosity of each room? The answer is that the porosity of both rooms would be exactly the same because the uniformly sized spheres in a cubic arrangement produce the same volume of voids in both rooms. The porosity of both rooms would be 48%. This can be confirmed by determining the number of spheres of any given size within the room, calculating their volume, then dividing by the volume of the room. If instead, two wheelbarrows full of marbles were dumped into the room full of soccer-ball-sized spheres the porosity would decrease as some of the large void space would be partially filled with solid marbles reducing the total pore space volume (Figure 10d). If the spheres of either size were packed in a rhombohedral arrangement, the porosity of both rooms would be 26%. A cubic packing is the loosest possible arrangement and rhombohedral packing is the tightest possible arrangement. Therefore, the minimum and maximum porosity for a material made of uniformly sized spheres is 26% and 48%, respectively.

When grains making up an earth material have an internal porosity, the material is said to have dual porosity (Figure 10e). In some cases, this internal porosity may or may not contribute to the value of effective porosity of the material.

After sediments are deposited, they often become lithified as time passes, that is, minerals precipitate from the groundwater, cementing the grains together. The cement fills some of the original pore volume, and so the cemented sediment will have less porosity than the sediment had before cementation occurred (Figure 10f).

If elongated particles such as the typical microscopic particles or platelets comprising clay are packed in cubic or rhombohedral arrangements, their shape would cause the porosity to be lower than for the spheres (Figure 10g, h). However, clay deposits often have high porosities because their microscopic mineral platelets are negatively charged, pushing the platelets apart and allowing water molecules to occupy the space between the grains. The small, uniformly sized, elongated particle shapes, coupled with their charged nature, results in a large volume of open space even though the spaces are small. As a consequence, porosities of clays can range from 40% to over 70% (Figure 10; Table 1 and Table 2).

Secondary Porosity

Many of Earth's rock materials have little to no primary porosity when formed. That is, there is little to no void space in the material when it is first formed. Examples of this include rocks formed: from cooling lava (igneous rocks); by precipitation of minerals during evaporation of water (e.g., salt and limestone); and those formed by the heating, folding and compression of any pre-existing rock (metamorphic rocks). However, porosity

of such rocks can increase because of weathering, fracturing, and/or dissolving (Tables 1 and 2).

Secondary porosity is the additional porosity acquired after the original rock formation process (Figure 11). A rock that is fractured or weathered (including solutioned) after its initial formation has secondary porosity. Whether the porosity is primary or secondary, the combined properties are included in the effective porosity. In most cases, the development of secondary porosity increases the effective porosity of a porous material.

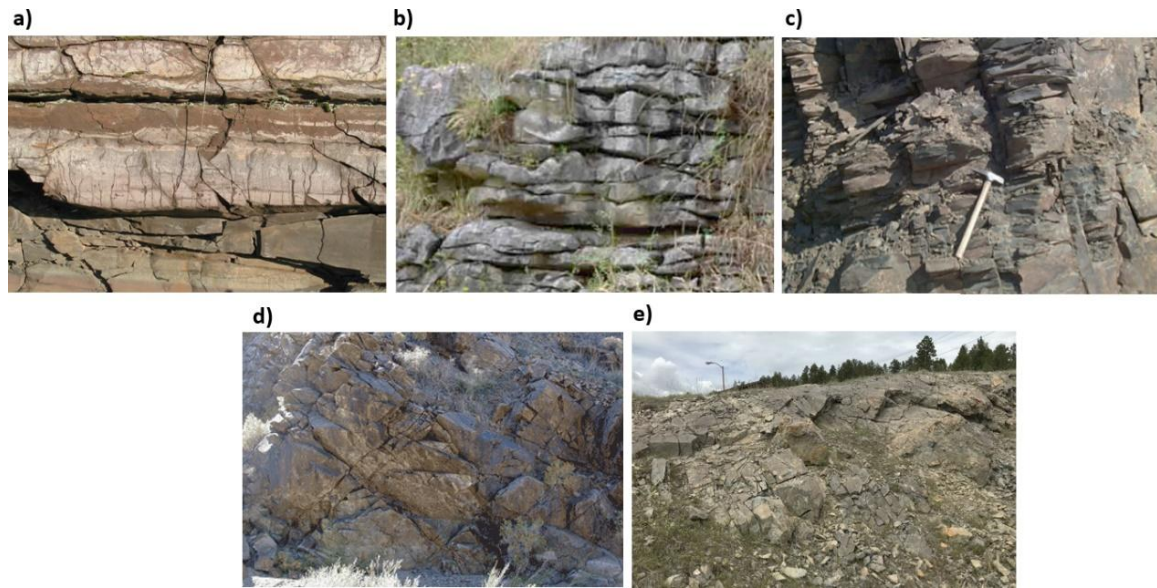


Figure 11 - Examples of secondary porosity developed in consolidated earth materials: a) fracturing of a sandstone (Goode, 2006); b) dissolution of a limestone (EPA, 2020); c) jointing of a shale (USGS, 2016); d) fracturing of granite (USGS, 2004); and, e) fracturing of a limestone.

As an example of the magnitude with which fracturing can enhance porosity of a rock, assume that a well cemented sandstone has an effective porosity of 0.13 (13%). Then, after deposition and lithification, the sandstone is uplifted by Earth's tectonic forces and eroded such that the upper 100 m is jointed. If a cube of the sandstone is 1 m^3 (total volume) with 10 fully penetrating vertical joints (1 m long by 1 m wide) and each joint aperture is 100 microns wide (1 micron = $1 \times 10^{-6} \text{ m}$), then the additional pore space provided by the fractures is 0.001 m^3 ($10 \text{ joints} \times (100 \times 10^{-6} \text{ m}) \times 1\text{m} \times 1\text{m}$). Dividing the fracture pore space by the total sample volume results in the addition of 0.001 to the total sample effective porosity, 0.131. If fractures were the only source of effective porosity in this 1 m^3 of rock, the effective porosity would be 0.001 (0.1%). Though fractures may not provide much water storage capacity, they may provide the only source of groundwater in some geologic environments. In addition to increasing porosity, fractures also act to enhance the transmission of water by creating fracture networks and joining pore spaces that were not originally connected.

The creation of secondary porosity by physical and chemical weathering of earth materials can also have a significant effect on limestones and dolostones as well as igneous

and metamorphic rocks. For example, granites are igneous rocks that form with almost no primary porosity, yet some have weathering induced porosity of 5% to 25%.

Just as secondary porosity enhances the overall void space in earth materials, the porosity of both unconsolidated and consolidated materials decreases with time as younger sediments are deposited on top of older layers, burying and compressing them. The weight of the overlying material compresses the older layers to varying degrees depending on the nature of the material and the initial arrangement of the sediment grains. Generally, porosity is less in formations with greater burial depths (Figure 12), but the variable character of material with similar names (e.g., silt, clay) and the differences in the weight of the overlying sediments makes it nearly impossible to predict the value of porosity given the type of material and depth of burial as indicated by the large scatter on the graphs of Figure 12.

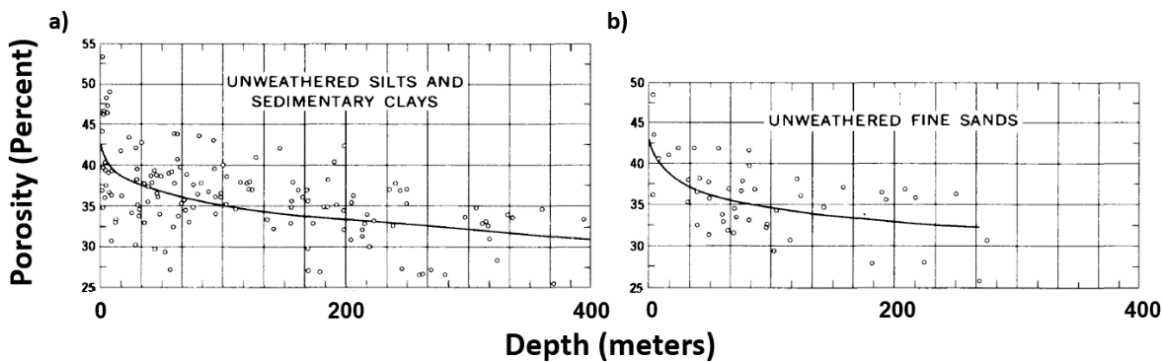


Figure 12 - Examples of decreasing porosity with depth for sedimentary deposits of the South Coastal Basin, CA, USA: a) unweathered silts and sedimentary clays; and, b) unweathered fine sands (after Eckis, 1934; Johnson, 1967).

The examples shown in Figure 12 are for unconsolidated sediments that were sampled to depths of 200 to 300 m. Additional loss of porosity occurs when sediments and rocks are overlain by thicker packages of earth materials. For example, Helm (1982) found porosities decreased by 25 to 50% within the first 1000 to 2000 m of burial and continued to decrease at greater depths (up to 75% at 3000 m depths). Porosity data for sandstones, carbonates and shales are frequently reported in the oil and gas literature as these types of formations are often associated with energy reservoirs.

3.4 Void Ratio

Engineering and soil mechanics professionals use the term void ratio, e , when describing the amount of void space in a soil or rock. The void ratio is the volume of voids divided by the volume of solids as shown in Equation 7.

$$e = \frac{V_V}{V_S} \quad (7)$$

where:

e = void ratio (dimensionless)

V_V = volume of voids (L^3)

V_S = volume of solids (L^3)

The void ratio, V_V/V_S , is always larger than the total porosity, V_V/V_T , because the value of V_S (the denominator of the void ratio) is always less than the total sample volume, V_T . Recognizing the total sample volume is equal to $V_V + V_S$, total porosity can be calculated from void ratio as shown in Equation 8.

$$n = \frac{e}{1+e} \quad (8)$$

Both porosity and void ratio are used to characterize the open space of soil, sediments and rocks. Groundwater professionals most commonly use total porosity or effective porosity to compare the open space of earth materials. They use effective porosity to determine the capacity of a material to store groundwater.

3.5 Volumetric Moisture Content

Another term used to describe the amount of water held in a porous material is the volumetric moisture content, θ . The volumetric moisture content is equal to the ratio of the volume of water, V_W , to the total volume, V_T , and is reported as either a decimal fraction or a percent. The moisture content of a sample will differ from the effective porosity if the pores are partially filled with water and partially filled with air as occurs in the vadose zone (Equation 9).

$$\theta = \frac{V_W}{V_T} \quad (9)$$

where:

θ = moisture content (dimensionless)

V_W = volume of water in the pore space (L^3)

When earth materials are not fully saturated then only some of the connected pores are filled with water and $\theta < n_e$. When the material is fully saturated, all connected pores are filled with water and $\theta = n_e$. The degree of saturation is described by the ratio of the moisture content to the interconnected porosity as shown in Equation 10.

$$\text{Degree of Saturation} = \frac{\theta}{n_e} \quad (10)$$

The volumetric moisture content is generally used when discussing water conditions in the vadose zone because, by definition, the vadose zone is not fully saturated and the ease with which water moves through a material varies with the degree of saturation.

3.6 Specific Yield and Specific Retention

If the water that fills the connected pores of a sample is allowed to drain under gravitational force, not all of the water occupying the voids is released. The volume of water that drains is less than the volume of water in the interconnected pore space because some of the water clings to the solids due to capillary forces. The term specific yield, S_y , is used to describe the ratio of the water that drains by gravity, V_D , to the total volume of sample, V_T , as shown by Equation 11.

$$S_y = \frac{V_D}{V_T} \quad (11)$$

where:

S_y = specific yield (dimensionless)

V_D = volume of water that drains by gravity (L^3)

V_T = volume of sample (L^3)

The water that does not drain remains as coatings on the surfaces of the solid material bordering the pore spaces or “hangs” in the pore spaces and is referred to as pendular water or residual water. The volume of retained water or pendular water depends on the number and size of the pore spaces, which essentially reflect the relative amount of surface area of the grains available to hold the water. The term specific retention, S_r , describes the fractional volume left behind after gravity drains a porous material and is the ratio of the volume retained, V_R , and the total sample volume, V_T (Equation 12). The volume retained, V_R , is the volume of water in the effective pore space minus the volume drained, ($V_I - V_D$). The specific retention can also be computed as the effective porosity minus the specific yield ($S_r = n_e - S_y$).

$$S_r = \frac{V_R}{V_T} \quad (12)$$

where:

S_r = specific retention (dimensionless)

V_R = volume of water retained against gravity after drainage ceases (L^3)

V_T = volume of sample (L^3)

Effective porosity, specific yield and specific retention each represent a ratio of a volume of water to the total volume of an earth material, and are related as indicated in Equation 13 and Figure 13. When any two of the parameters are known the third can be calculated.

$$n_e = S_y + S_r \quad (13)$$

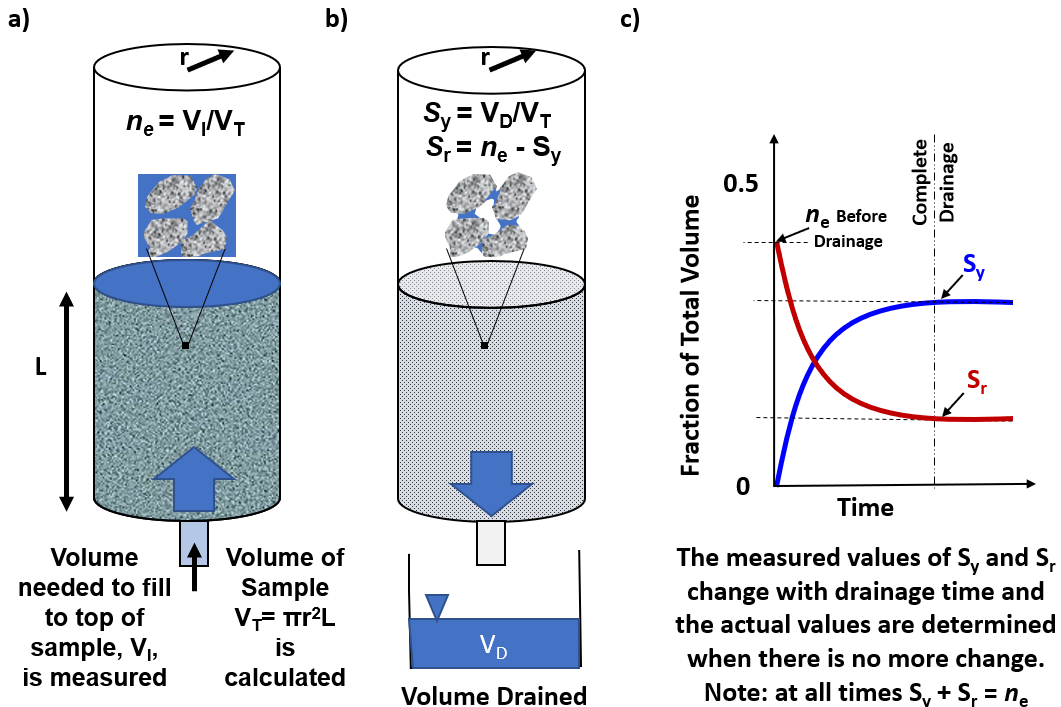


Figure 13 - Procedure for determining effective porosity, n_e , specific yield, S_y , and specific retention, S_r : a) by measuring the total volume, V_T , based on sample geometry, measuring the interconnected pore volume (V_I) by measuring the volume of water needed to saturate an initially completely dry sample from below, then calculating the effective porosity, n_e ; b) by draining the sample and measuring the volume of water drained (V_D), then computing the specific yield, S_y , and specific retention, S_r . c) The measured value of S_y will increase and S_r will decrease as drainage proceeds in (b). Neither value is accurate until drainage has ceased.

The specific yield of an earth material is of interest to the groundwater professional because it represents the volume of water that enters a groundwater system by recharge (a rise in the water table) or is drained from a system when a well is pumped. For example, consider an area that is 1000 m by 1000 m, in which the sand has an effective porosity of 25% and a specific yield of 15%. Now suppose the water table over that area is lowered by four meters. How much water would be drained from the sand? The total volume of drained sand is $4 \text{ m} \times 1000 \text{ m} \times 1000 \text{ m}$ or $4,000,000 \text{ m}^3$ and the volume of water in the sand is 25% of the total volume of drained sand ($n_e V_T = V_I = 1,000,000 \text{ m}^3$). However, the actual volume of groundwater that would drain from this area with a 4 m lowering of the water table is only 15% of the total volume ($S_y V_T = V_D = 600,000 \text{ m}^3$).

Next consider how much water is left clinging to the sand grains against the force of gravity by capillary tension after drainage. The sand contains 25% interconnected pore space, n_e , and 15% of the total volume drained, $S_y = 15\%$. It follows that that 10% of the total volume is retained water ($S_r = n_e - S_y$), so $400,000 \text{ m}^3$ of water remains on the grain surfaces in the drained pores.

To give some more thought to specific yield and specific retention, let's go back to the example of the two rooms, one filled with solid glass spheres the size of soccer balls and one filled with 1 cm diameter marbles. Both sets of balls are packed in the same cubic

arrangement, and thus the rooms have equal porosity (48%). Now let's examine the specific yield of each room. When the rooms are saturated with water and then allowed to drain, the room with the soccer-ball-sized glass spheres would produce a larger volume of drained water than the room full of marbles. This is because even though the pore volume is the same in both rooms, the pores in the marble room are smaller and there is substantially more surface area associated with the small, but numerous, solids than there is the room full of large glass spheres. Once again, the larger surface area of the marbles retains more water through capillary forces.

The water retained as a fraction of the total volume after drainage, S_r , is sometimes referred to as the field capacity. It is synonymous with the terms soil water holding capacity and water retention capacity and is used to describe the water available to plants once excess water has drained from the soil. Plants have the ability to lower porewater pressure (increase tension) in the vicinity of their roots so they can draw water from the surrounding soil. As time passes, if air is circulating in the partially saturated earth material (vadose zone), some water may evaporate and further decrease the moisture content. When the moisture content falls below the specific retention of the soil because of plant use or evaporation, the soil is below field capacity.

Specific yield measurements from several lab and field methods are compiled in Table 3 to provide insight on the range of specific yield of common earth materials. Specific yield can also be determined by measuring the response of the water table to pumping of wells and analyzing the changes of water levels with equations and models.

Table 3 - Summary of specific yield values of common earth materials compiled by Morris and Johnson (1967) with additional data from Rivera (2014), Freeze and Cherry (1979) and Domenico and Schwartz (1998). "NA" represents not available.

Measurements of Specific Yield for Some Common Earth Materials (Percent)		
Material	Number of Samples	Range of Specific Yield %
Unconsolidated Sediments		
Clay	27	1 - 18
Silt	299	1 - 40
Loess	5	14 - 22
Eolian sand	14	32 - 47
Sand (fine)	287	1 - 46
Sand (medium)	297	16 - 46
Sand (coarse)	143	18 - 43
Gravel (fine)	33	13 - 40
Gravel (medium)	13	17 - 44
Gravel (coarse)	9	13 - 25
Consolidated Sediments		
Shale	NA	0.5 - 5
Siltstone	13	1 - 33
Sandstone (fine-grained)	47	2 - 40
Sandstone (medium-grained)	10	12 - 41
Limestone and dolomite	32	0 - 36
Karstic limestone	NA	2 - 15
Igneous and Metamorphic Rocks		
Fresh granite and gneiss	NA	<0.1
Weathered granite/gneiss	NA	0.5 - 5
Fractured basalt	NA	2 - 10
Vesicular basalt	NA	5 - 15
Tuff	90	2 - 47

3.7 Interrelationship of Effective Porosity, Specific Yield and Specific Retention

As shown in Equation 13, effective porosity is equal to the sum of the specific yield and specific retention. These characteristics can be determined at the laboratory sample scale and at the broader field scale. Laboratory determination of two of the three properties allows for calculation of the third ($n_e - S_y = S_r; S_y + S_r = n_e; n_e - S_r = S_y$). Tables 1, 2 and 3, reveal that S_y is typically highest for granular materials with large diameter pore spaces and lowest in silts and clay even though their porosities may be high. It would be desirable to develop a relationship between some easily measured earth material property (like grain size) and effective porosity, specific yield and specific retention.

The relationship of effective porosity, specific yield and specific retention, to grain size of unconsolidated material has been described by experiment and observation. Unfortunately, the relationships are not simple linear functions, in part, because it is rare that a natural sediment is of a uniform grain size. Johnson (1967) compiled data from laboratory and field tests where porosity, specific yield and specific retention were estimated. Test results were reported based on grain-size distributions of unconsolidated samples collected under field conditions. Grain-size distributions are determined by passing the sediment through a series of screens with different mesh size and weighing the material remaining on each screen. [Click here to link to Box 2](#) for additional information about analyzing grain-size distribution.

Johnson plotted the values of n_e , S_y , and S_r , against the grain size (referred to as Grade Size on his figure) of the coarsest-10% of the grains (by weight) of each sample (Figure 14). The field samples did not have uniform grain size and, so, 90% of the sample (by weight) consisted of smaller grains. Johnson's graph shows that, for his data set, the highest porosity and specific yield values were associated with sands. This is likely because, even though the boulder to gravel grain sizes would have large pores, the presence of finer grained particles in the natural sample would fill a portion of the large pore spaces reducing the porosity. Coarse sand samples showed the largest porosity and specific yield. It may be that the coarse sands had more uniform grain sizes. For samples with smaller values of maximum 10% grain size, more water is retained after gravity drainage. This is consistent with more retention being associated with materials that have large solid surface areas. A similar reduction in specific yield and increase in specific retention would be expected for samples of silt and clay.

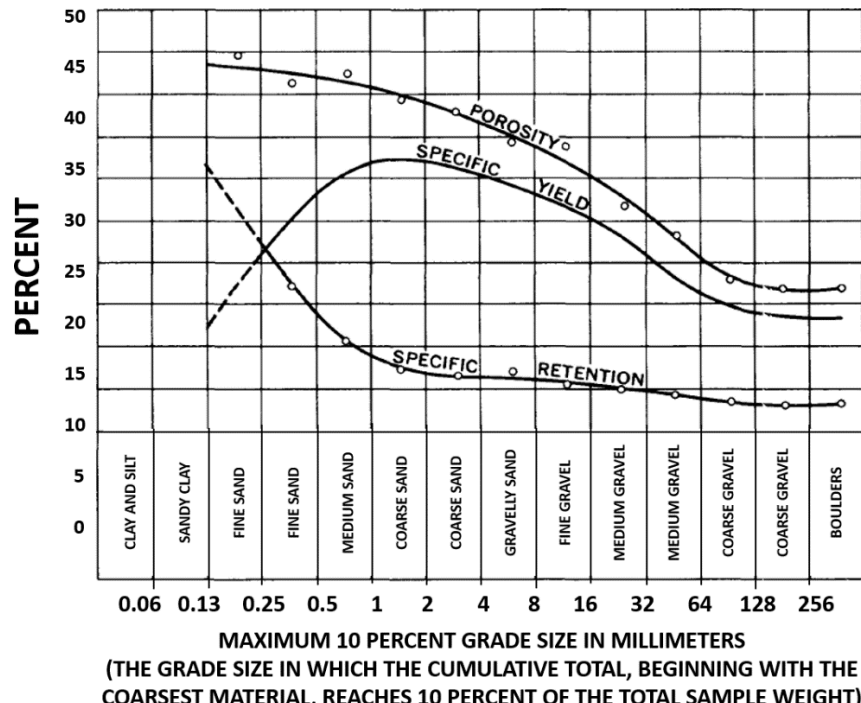


Figure 14 - Compilation of the results of testing 150 samples of South Coastal Basin sediments, California, USA. Determinations of porosity, specific yield and specific retention are plotted against the maximum 10% coarsest-grain size by weight (after Johnson, 1967).

3.8 Exercises

[Exercise 1](#) provides an opportunity to work with data for a sample to evaluate porosity, specific yield, specific retention, particle density, void ratio, moisture content, and degree of saturation. [Exercise 2](#) explores the relationship between porosity and void ratio.

4 Darcy's Law, Head, Gradient and Hydraulic Conductivity

Knowledge of the porosity, void ratio, moisture content, specific yield and specific retention of earth materials are needed to understand how soil water and groundwater are stored in earth materials and were discussed in Section 3. Properties that characterize the transmission of water through earth materials are presented in this section. To develop these concepts, Darcy's Law, which governs groundwater flow in porous media, is presented; and head, gradient and hydraulic conductivity components are defined and explained.

4.1 Darcy's Law

In 1856, Henry Darcy reported results of experiments used to enhance the water flow through sand filter beds used by the city of Dijon, France for water treatment (Darcy, 1856). As an engineer, he wanted to design sand beds that would efficiently and effectively filter the daily volume of water needed by the city. To evaluate the volume of water that could be filtered in a given period of time, Darcy experimented with changing: the type of sand; the area of the filter bed (diameter of the tube in his experiments); the thickness of the sand (length of the sample in his experiments); and, the force driving water through the filter bed (Figure 15).

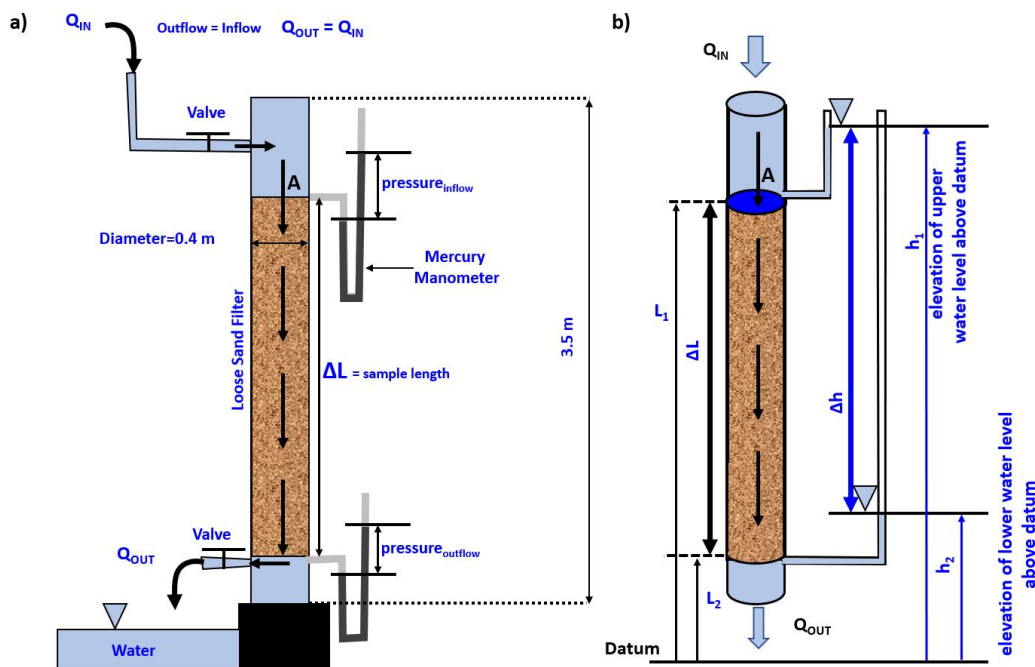


Figure 15 - Darcy's experiment. a) In the original apparatus using mercury manometers to measure water pressures, water flowed at a constant rate into the top of the column and exited at the bottom. b) Commonly, Darcy columns are equipped with water filled tubes referred to as piezometers to measure water pressures instead of mercury manometers. (after Darcy, 1856).

To determine the driving force, he used mercury manometers to measure pressure in the reservoir on each end of the sand filter because he knew that the combination of water pressure and elevation would describe the mechanical energy at each location.

By conducting a number of experiments under varying conditions, Darcy discovered a mathematical relationship that indicated the steady-state flow rate through the circular sand filter, Q , was: directly proportional to the cross sectional area of the filter, A ; directly proportional to the difference in hydraulic head (elevation of water in the piezometers measured from a datum) on each side of the filter, Δh ; and inversely proportional to the length of the filter material, ΔL (Equation 14 and Figure 15b). The elevation of the water level in the piezometers is referred to as hydraulic head.

$$Q \propto -\frac{\Delta h}{\Delta L} A \quad (14)$$

where:

Q = volumetric flow rate (L^3/T)

Δh = difference in hydraulic head between two measuring points, h_2-h_1 , where h_2 is head at a location beyond the location of h_1 in the direction of flow (L)

ΔL = length along flow path between locations where hydraulic heads are measured (L)

A = cross-sectional area perpendicular to the direction of flow (L^2)

The negative sign is included in Equation 14 because the volumetric flow rate, Q , is positive in the direction of flow under a negative change in head (i.e., head decreases in the direction of flow).

By experimenting with coarse- to fine-grained sands, Darcy found that the flow rate was also directly proportional to the character of the sand he placed in the column (Figure 15). The proportionality constant is referred to as the hydraulic conductivity or permeability and its use converts the proportionality to an equivalency. This mathematical relationship is referred to as Darcy's Law (Equation 15). Darcy's law is the fundamental equation used to describe the flow of fluid through porous media, including groundwater.

$$Q = -K \frac{\Delta h}{\Delta L} A \quad (15)$$

where:

Q = volumetric flow rate (L^3/T)

K = hydraulic conductivity, is the proportionality constant reflecting the ease with which water flows through a material (L/T)

Δh = difference in hydraulic head between two measuring points as defined for Equation 14 (L)

ΔL = length along the flow path between locations where hydraulic heads are measured (L)

$\frac{\Delta h}{\Delta L}$ = gradient of hydraulic head (dimensionless)

A = cross-sectional area of flow perpendicular to the direction of flow (L^2)

Consequently, if the area of the column is increased by a factor of two while the flow rate and length of saturated sediment are held constant, the difference in water elevations (Δh) in the piezometers will decrease by a factor of two (Figure 16). It also holds that if the cross-sectional area, flow rate and hydraulic conductivity were constant and the column length (ΔL) is reduced by one half the difference in head (Δh) will decrease by 2.

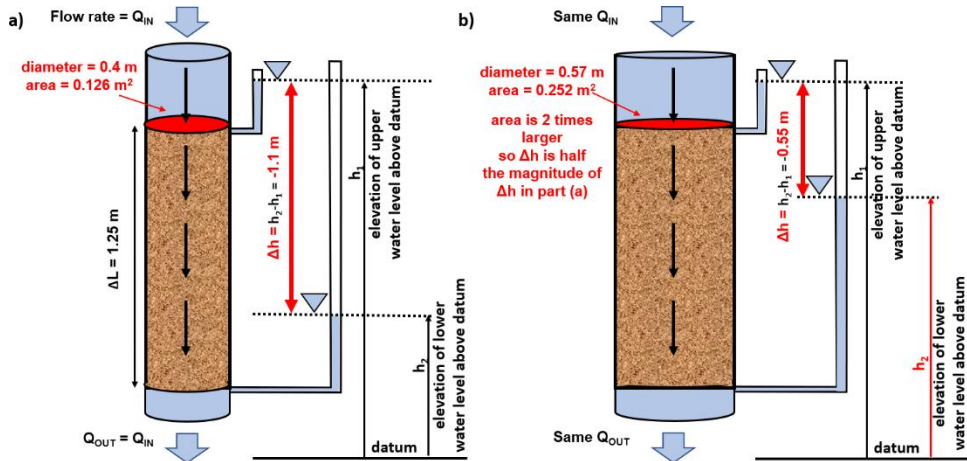


Figure 16 - Given Darcy's Law (Equation 15), if the flow rate ($Q_{IN} = Q_{OUT}$), sample length (ΔL), and sample material are equal in both a) and b), and the flow area is increased from that shown in (a) by a factor of two as shown in (b), the hydraulic head difference, $\Delta h = h_2 - h_1$, between the measurement locations will decrease by a factor of two because the larger area of flow offers less resistance to flow. Differences between a) and b) are indicated in red.

Darcy's Law in the most general form is presented as a differential where dh and dL are defined over an infinitesimally small interval, so Equation 15 becomes Equation 16.

$$Q = -K \frac{dh}{dL} A \quad (16)$$

where:

$$dh = \Delta h \text{ over an infinitesimal interval (L)}$$

$$dL = \Delta L \text{ over an infinitesimal interval (L)}$$

Darcy's Law describes how head, hydraulic gradients and hydraulic conductivity are linked to quantify and describe groundwater flow. For example, to compute the discharge of groundwater (Q) through a cross-sectional area of sand below the water table that is 100 m by 30 m (A) with a hydraulic conductivity of 15 m/d (K), and with a head change (Δh) of -2 m over a flow path length (ΔL) of 1000 m, Equation 15 is applied. The discharge is calculated as follows.

$$Q = -K \frac{\Delta h}{\Delta L} A = -\left(15 \frac{m}{d}\right) \frac{-2 m}{1000 m} (100 m) (30 m) = 90 \frac{m^3}{d}$$

Specific Discharge

Darcy's law can also be represented in terms of specific discharge, a flux, which is discharge per unit area (q) as shown in Equation 17.

$$q = \frac{Q}{A} = -K \frac{dh}{dl} \quad (17)$$

where:

q = specific discharge in the direction of flow (L^3/L^2T)

Specific discharge is also referred to as "groundwater flux" and has units of $L^3/(L^2T)$ which is discharge per unit area, or simply L/T (Figure 17a). It is also referred to as Darcy flux, Darcy velocity, and apparent velocity. It represents the volume of water that flows through a unit cross sectional area of porous media per unit time. The apparent velocity term is sometimes used because by cancelling L^2 of the flux units, the units become L/T , which are velocity units. However, this is not a true groundwater velocity, it is a flux. It is best to always use flux units ($L^3/(L^2T)$) when reporting specific discharge values, or at least to use the term flux or apparent velocity so the meaning will be clear.

To compute the flux of groundwater through the cross-sectional area under the conditions presented in groundwater discharge conditions described above it follows that:

$$q = \frac{Q}{A} = \frac{90 \frac{m^3}{d}}{(100 \text{ m}) (30 \text{ m})} = 0.03 \frac{m^3}{m^2 d}$$

Average Linear Velocity

In contrast to the apparent velocity portrayed by specific discharge (Figure 17a), Darcy's Law can also be used to derive the actual rate at which water is flowing through a cross sectional area of porous media, the groundwater velocity. The groundwater velocity, v , is higher than the specific discharge because the water can only pass through the portion of the cross-sectional area that is connected pore space, n_e . That cross-sectional area is the product of the area of porous medium and the effective porosity, n_e . This velocity is called the average linear velocity, seepage velocity or average interstitial velocity, and it is the flux, q , divided by the effective porosity, n_e , $q/n_e = v$ (Figure 17b).

$$\mathbf{a)} \quad q = \frac{Q}{A} = -K \frac{\Delta h}{\Delta L} \quad \mathbf{b)} \quad v = \frac{q}{n_e} = \frac{Q}{An_e} = -\frac{K\Delta h}{ne\Delta L}$$

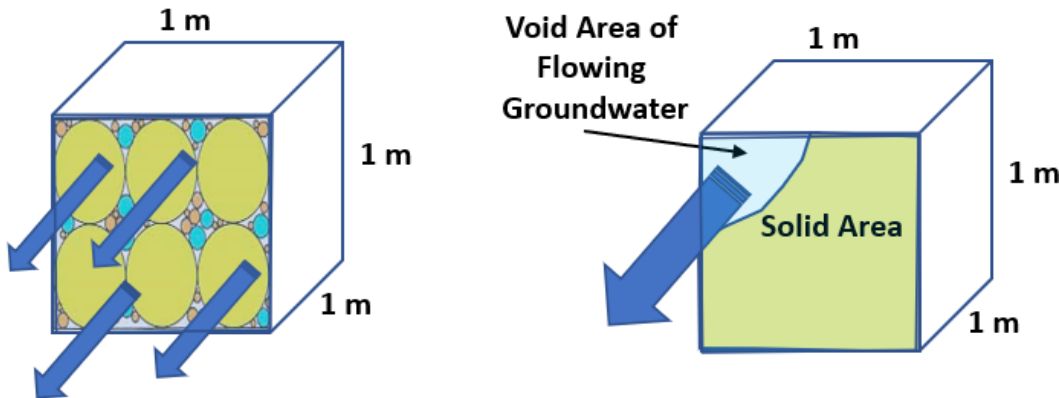


Figure 17 - Conceptualization of specific discharge, q , and average linear velocity, v . a) Specific discharge is the volume per time per unit area of water that leaves the face of the cube (area, including fluid and solids). b) In contrast, the actual rate at which water is flowing though the face is higher than the flux rate because water can only pass through the portion of cross-sectional area that is pore space, (area of pore space = An_e), where n_e is the effective porosity. The average linear velocity is the flux, q , divided by the porosity, n_e , $q/n_e = v$.

The concept of “actual” groundwater velocity, recognizes that microscopic velocities within the complex interconnected pore structure are variable and difficult to characterize (Figure 18a, b, and c). In addition to the variability of flow trajectory (Figure 18c), the microscopic velocities also vary because the pore throats and channels are variable (Figure 18a and b). Thus, the overall effect of groundwater flowing in a lattice work of varied pore channels is more easily represented by a composite groundwater velocity value, the average linear velocity for a representative elementary volume of porous material (Figure 18d and Figure 17b). The average linear velocity in the direction of flow is attained by considering the volumetric flow rate per unit area of porous medium divided by the effective porosity, n_e , using any of the forms of Equation 18.

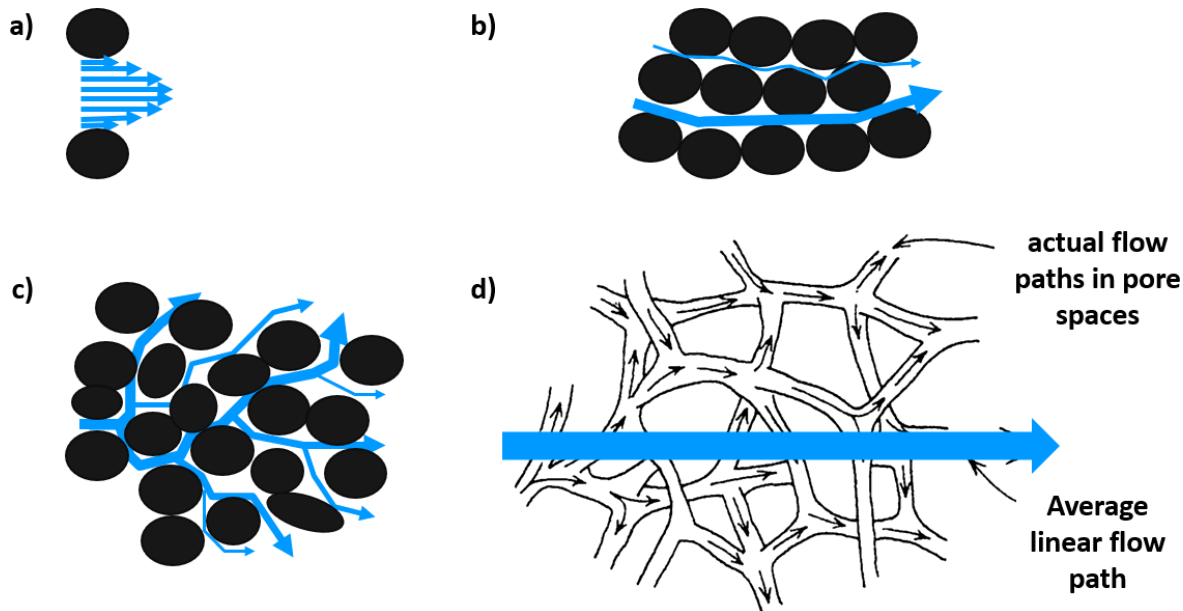


Figure 18 - Conceptual model of pore-scale micro-velocities (a, b, c) represented as an average linear velocity (d): a) velocity distribution as water passes through a single pore where drag along grain surfaces slows flow as compared with higher velocities near the center of the pore; b) velocity varies because pore openings have different cross-sectional areas; c) velocity distribution caused by pore channel branching; and, d) conceptual model of the average linear velocity (large straight arrow) (after Freeze and Cherry, 1979).

$$v = \frac{q}{n_e} = \frac{Q}{A n_e} = -\frac{K \Delta h}{n_e \Delta L} \quad (18)$$

The average linear velocity is a vector that represents the average direction and magnitude of the ensemble of water particles flowing through the porous medium as shown by the large arrow in Figure 18d. It does not represent the velocity in microscopic individual pore channels. Such velocities are highly variable and contribute to dispersion of dissolved constituents in groundwater systems.

When the volumetric flow rate is known, the average linear velocity can be computed using estimates of the flow area and effective porosity. If the effective porosity is 0.13 and the conditions as described in the specific discharge calculation above are applied, then the average linear velocity would be:

$$v = \frac{q}{n_e} = \frac{Q}{A n_e} = \frac{90 \frac{\text{m}^3}{\text{d}}}{(100 \text{ m})(30 \text{ m})(0.13)} = 0.23 \frac{\text{m}}{\text{d}}$$

Additional detail on the concept of groundwater velocity is provided in the groundwater project book “*Groundwater Velocity*” (Devlin, 2020).

4.2 Hydraulic Head

Water moves through a groundwater system because it is acted upon by forces. There are two forces that drive flow: 1) a pressure gradient and 2) the force of gravity. If the density of the groundwater is constant, the sum of these forces acting on a unit weight of water can be conveniently expressed as the gradient of hydraulic head. Hydraulic head

is a scalar quantity that has the potential for generating force. For this reason, it is sometimes called a force potential. A scalar quantity is one that can be represented by a single number describing magnitude. For example, temperature is a scalar. A gradient is a vector. A vector is described with two values: magnitude and direction. For example, velocity is a vector.

Both of the forces on groundwater are mechanical, so hydraulic head is thought of as mechanical energy and is defined as the mechanical energy per unit weight of water. It is composed of two components: potential energy from the water's elevation in the gravitational field and potential energy from the fluid pressure distribution as shown in Equation 19. These are often referred to as the elevation head and the pressure head as shown in Equation 20.

$$h = z + \frac{p}{\rho g} \quad (19)$$

where:

h = hydraulic head (L)

z = elevation of measurement point (L)

p = water pressure at measurement point (F/L^2 , force (weight) per unit area)

ρ = water density (M/L^3)

g = gravitational constant (acceleration of gravity) (L/T^2)

$$h = h_z + h_p \quad (20)$$

where:

h = hydraulic head (L)

h_z = elevation head (L)

h_p = pressure head (L)

The components of elevation head and pressure head are illustrated for a laboratory and a field setting in Figure 19. Hubbert (1940) recognized the head gradient drives groundwater flow and defined fluid potential (Φ) as the product of head and the gravitational constant (gh), yielding mechanical energy per unit mass. He stated that groundwater always moves from areas of high fluid potential to low fluid potential. Hydraulic head (mechanical energy per unit weight) is the most commonly used term to define the force potential that drives groundwater flow as it is easily represented by a water level elevation measured in a piezometer or well.

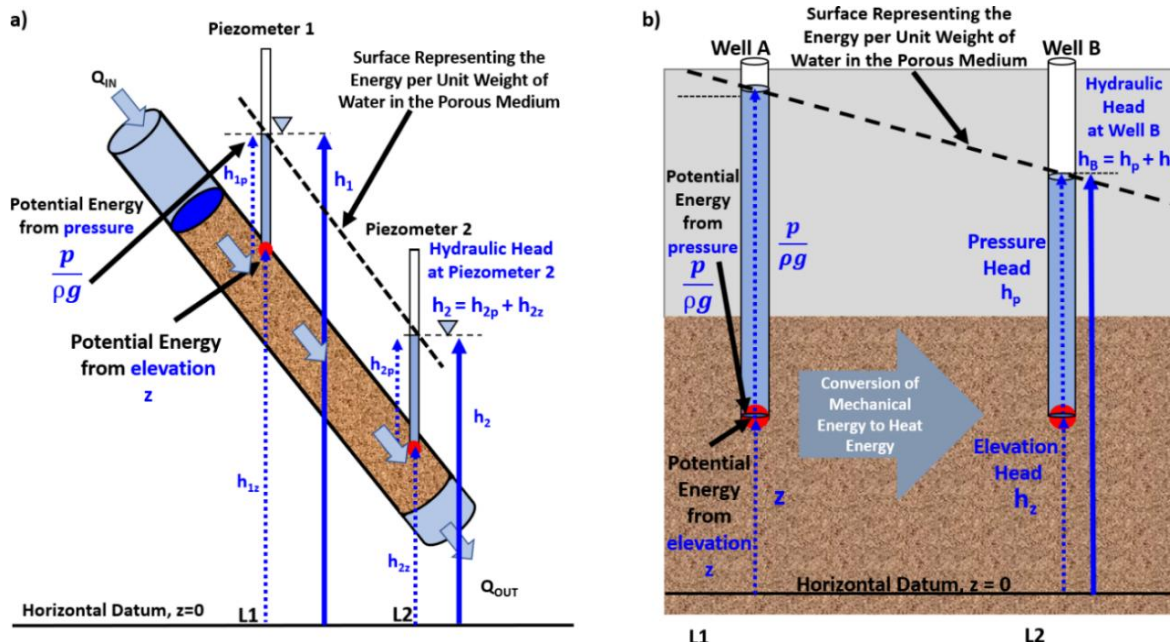


Figure 19 - Definition of hydraulic head in a Darcy column and a portion of a groundwater system. The location of the heads being measured are represented by red dots: a) components of head (blue dotted and solid arrows) and head distribution (dashed black line) in a saturated column of sand with water moving from upper left to lower right; and, b) components of head in a portion of a groundwater water system. Head decreases in the direction of flow as mechanical energy is converted to heat energy due to friction as water molecules flow by grain surfaces and other water molecules (large gray-blue arrow).

As water flows through porous media, the hydraulic head along a flow line gradually decreases as the fluid interacts with the pore walls resulting in conversion of a portion of the mechanical energy to thermal energy (Figure 17b). Physically, water warms in the direction of flow, however, changes in temperature are below detection in most settings.

The direction of flow is always from high to low hydraulic head regardless of the orientation or position of the porous medium in space. This is illustrated in Figure 20 where water flow is shown in a number of inclined, saturated, sand-filled cylinders. The hydraulic head is higher on the end of the cylinder where water is introduced and lower as water moves along the flow path. The white arrow shows the direction in which water is moving through the columns.

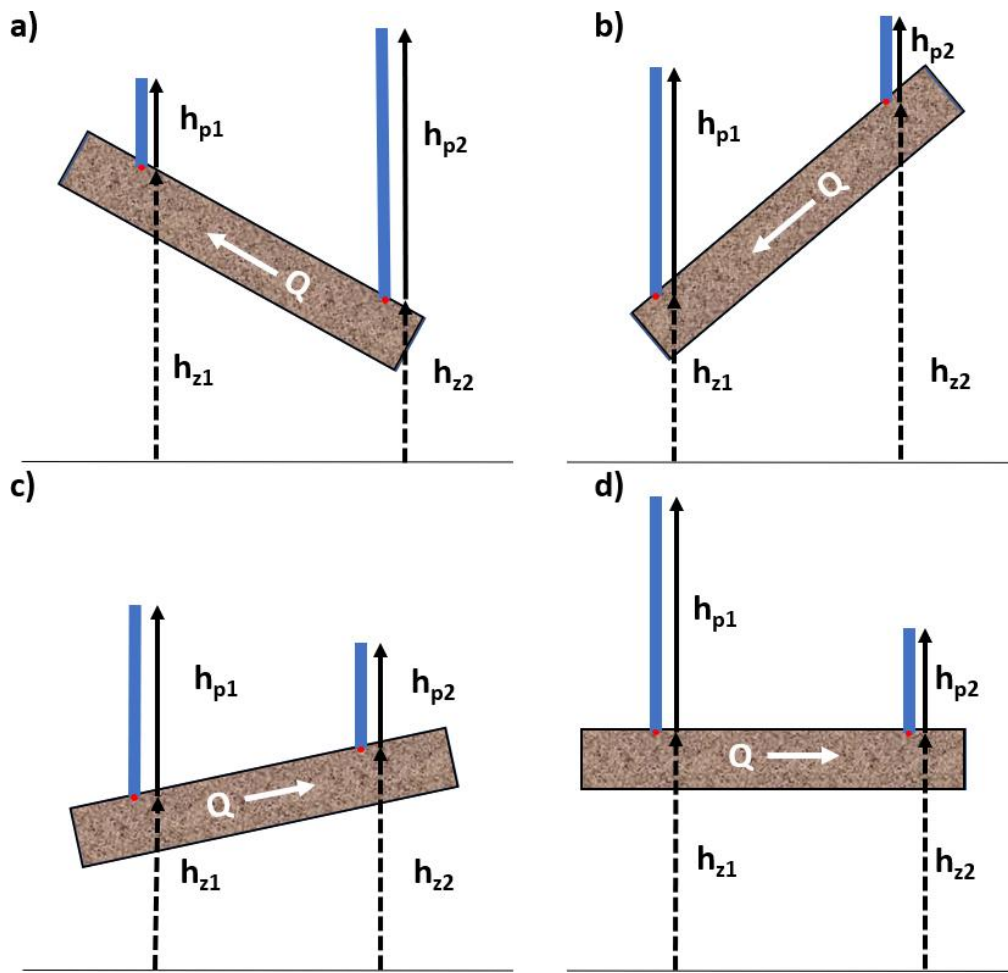


Figure 20 - The flow of water (Q and white arrow) in four saturated sand columns. The blue lines represent water in piezometers installed at the locations indicated by the red dots (the location where the hydraulic head is measured). The dashed arrows represent the elevation head (h_z) and the solid arrows represent the pressure head (h_p): a) flow is upward and to the left; b) flow is downward and to the left; c) flow is upward and to the right; and, d) flow is to the right.

As noted earlier, hydraulic head is sufficient to describe the distribution of the mechanical energy of groundwater in most groundwater projects because the fluid density is constant in space and time. Commonly, under ordinary conditions groundwater temperature and chemical variations do not significantly affect the density of the fluid so density is constant throughout the system. When wells sample groundwater that varies in density, head calculations must include adjustment to pressure heads that allow for reasonable comparisons. It is best to assess groundwater flow under variable density conditions using computer codes designed to account for the density variations. [Click here to link to Box 3](#) which presents a more detailed discussion of how hydraulic head is related to the force potential that drives fluid flow, including situations when the fluid density varies due to variation of temperature and/or dissolved substances.

Representing Hydraulic Head Distributions

Multiple measurements of hydraulic head obtained from laboratory piezometers or monitoring wells in the field are used to represent the spatial head distribution. This can

be illustrated by examining the head distribution in a column filled with sand and penetrated by a number of piezometers (Figure 21). Darcy's Law indicates that the head distribution will be linear along a homogeneous sand column because the flow is uniform and one-dimensional (uniform means each packet of water moves along its path with constant speed and the flow per unit area is constant and one-dimensional means flowing in only one direction). Consequently, the lines of equal hydraulic head (equipotential lines) within the porous medium are straight, equally spaced, parallel to each other, and perpendicular to the column walls. Head decreases from h_1 to h_7 in the direction of flow as mechanical energy is converted to heat energy due to friction as water molecules flow by grain surfaces and other water molecules.

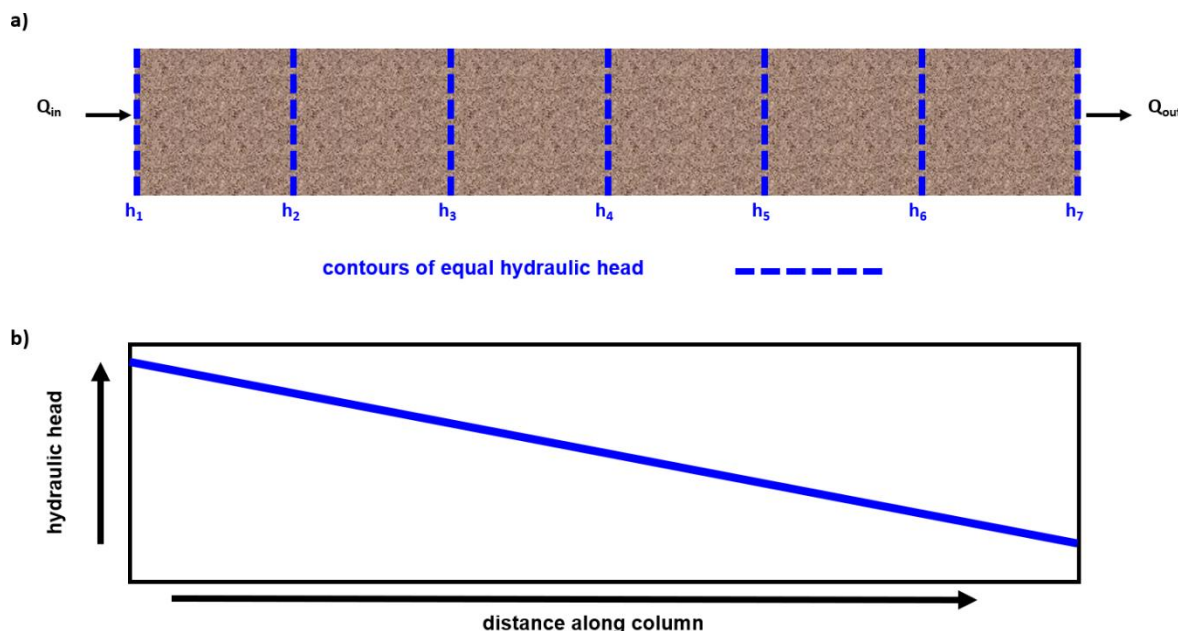


Figure 21 - Steady-state, one-dimensional flow through a homogeneous and isotropic sand column with inflow and outflow openings that are the same diameter as the column: a) the lines of equal hydraulic head (vertical dashed lines) within the saturated sand are perpendicular to the column walls, straight, parallel, and equally spaced, h_1 is the highest head and h_7 the lowest head; and, b) the head distribution is linear.

When head measurements are plotted in one-, two- or three-dimensional space, they provide a framework for understanding groundwater flow patterns. In the one-dimensional flow shown in Figure 21, the flow is in the direction of decreasing head, left to right. Hydraulic head distributions are typically represented as two-dimensional maps and cross sections of geologic settings containing a groundwater system. When head measurements are used to create a map, the head is plotted at the x,y location of the well on the land surface (Figure 22).

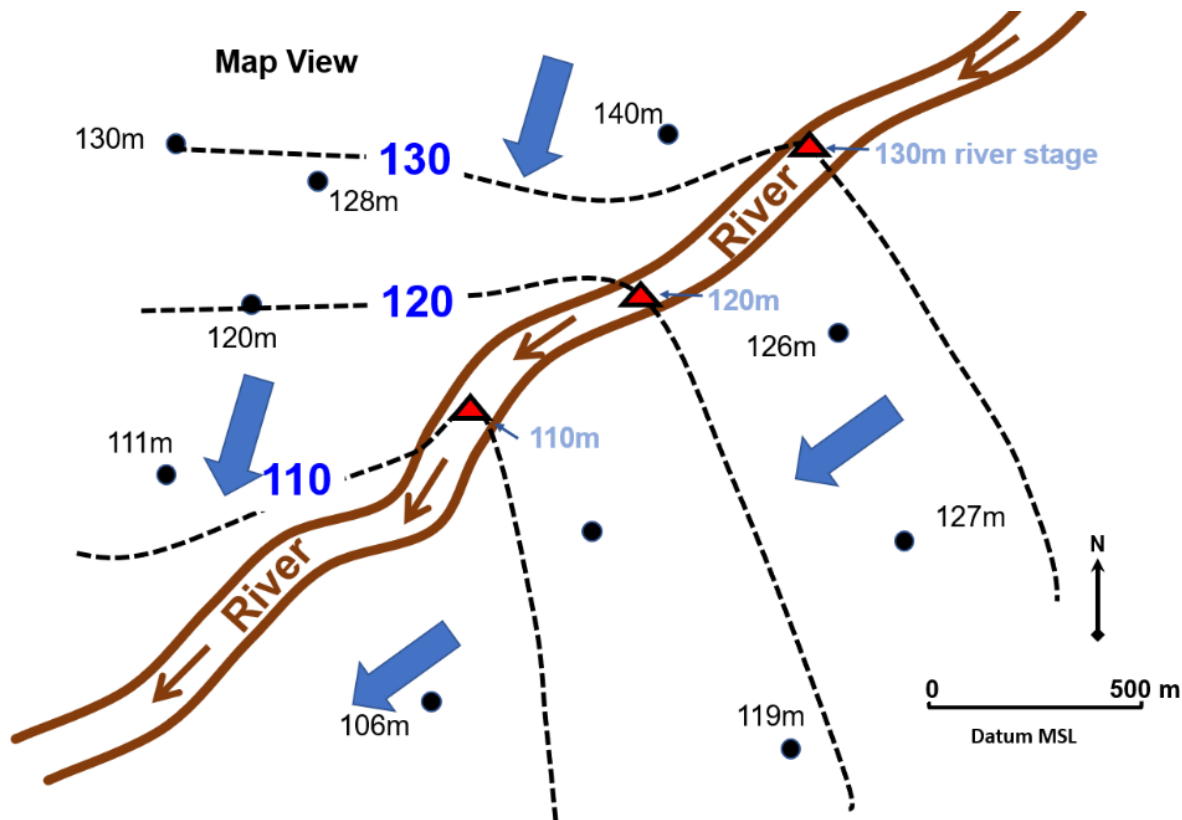


Figure 22 - Example of head data plotted at x,y well locations (black dots). Head values are plotted as the elevation above mean sea level. Dashed lines are contours of equal head (equipotential lines). The large blue arrows represent the general direction of groundwater flow, from areas of high head to areas of low head. The red triangles represent river stages that are discharge locations of groundwater.

When head measurements are plotted in cross section, the head values are plotted at the x,z location of the point of measurement (the yellow dots in Figure 23). In order to evaluate vertical components of groundwater flow, it is common for multiple piezometers to be installed at the same x,y location in the field, with each piezometer open at a different depth, z, as shown in the laboratory column of Figure 23. Head measurements are taken from three piezometers at different depths along a vertical line in the middle of the cylinder. All head measurements in Figure 23a are 10 cm because flow parallels the cylinder walls, and the column is horizontal. When the column is rotated 42° around its axis at the bottom of the mid-depth piezometer (Figure 23b), flow is still parallel to the cylinder walls, but in this position, the shallow piezometer samples upgradient of the intermediate piezometer and the deep piezometer samples down gradient.

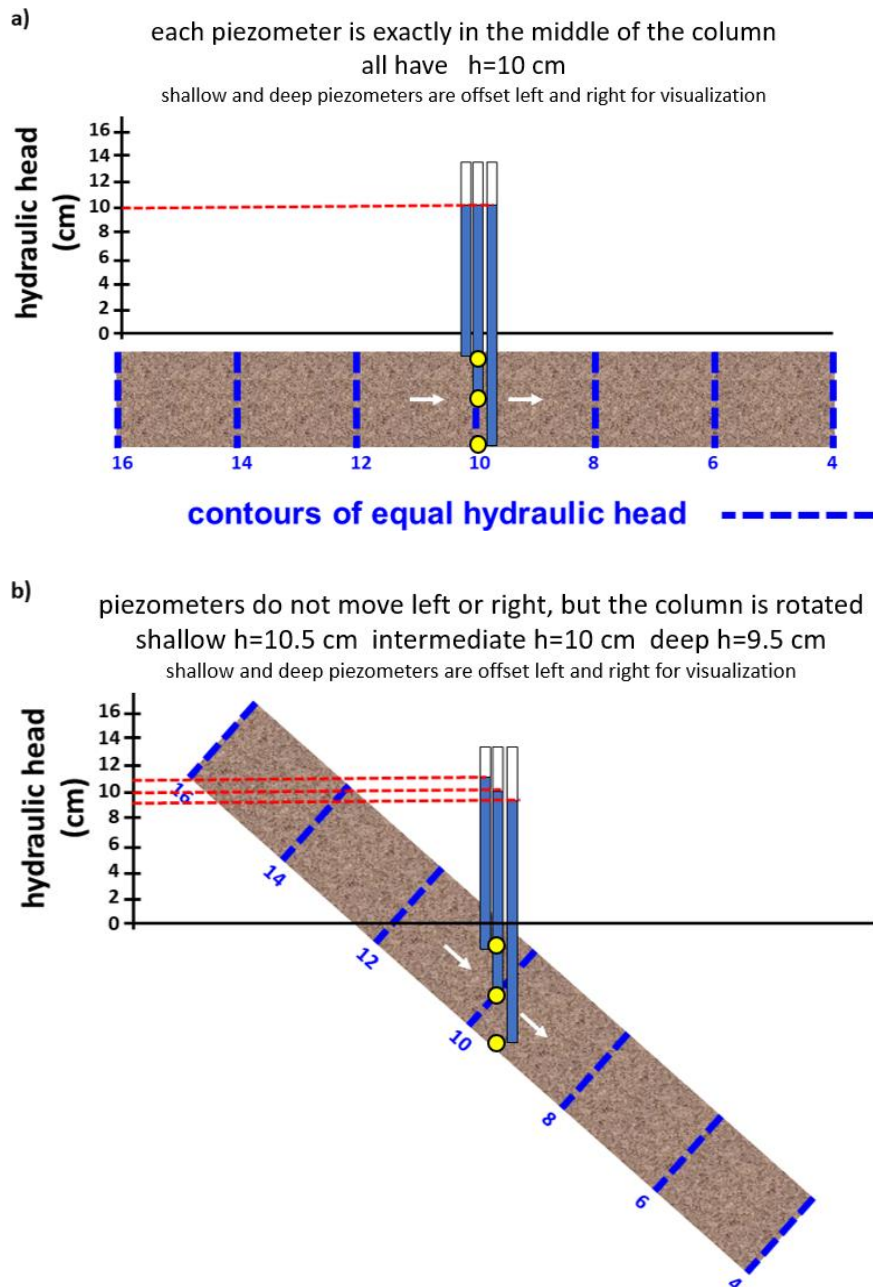


Figure 23 - Example of plotting hydraulic head values at the point of measurement where the bottom of the piezometer is open to the flow system (as indicated by the yellow dots, note the diagram of the shallow and deep piezometers are offset to the left and right of the intermediate piezometer to facilitate viewing all three water levels). The sand columns are filled with homogeneous sediment and water flows through the porous medium (white arrows) under steady-state conditions. a) Head measurements are taken from three piezometers at different depths along a vertical line in the middle of the cylinder. All head measurements are 10 cm. b) When the cylinder is rotated 42° around its axis at the bottom of the mid-depth piezometer, although flow is still parallel to the cylinder walls, the shallow piezometer now samples head conditions upgradient of the intermediate piezometer and the deep piezometer samples down gradient conditions. The heads differ between piezometers. Given that the measurement points (yellow dots) are at the same x,y location, these differing heads indicate a downward component of flow.

After head data are properly presented in space, the piezometer measurements are interpreted to infer groundwater flow directions. Interpretation of head distributions and groundwater flow directions are discussed later in Section 8 this book. Interpretation of

heads in groundwater systems containing water of different densities requires special attention as described in the Groundwater Project book "Darcy's Law in Variable Density Groundwater Systems" (Marinelli, 2024).

4.3 Hydraulic Gradient

As shown in Equation 16, the ratio of Δh and ΔL (the hydraulic head difference divided by the length of the sample or the distance separating two head locations) can be generalized into a differential called the hydraulic gradient, dh/dl as in Equation 21.

$$Q = -K \frac{dh}{dl} A \quad (21)$$

where:

$$dh = \Delta h \text{ over an infinitesimal interval (L)}$$

$$dl = \Delta L \text{ over an infinitesimal interval (L)}$$

Given that the hydraulic gradient is computed by subtracting the head, h_1 , at the origin from the head, h_2 , at a distance ΔL from the origin in the direction of flow, and then dividing by the distance ΔL , the negative sign in Equation 21 provides a positive value of volumetric flow rate from high to low hydraulic head. In the vertical column shown in Figure 19, the value of head h_2 at L_2 is subtracted from h_1 at L_1 . This results in a negative gradient, $\Delta h/\Delta L$. That is, flow proceeds in the down gradient direction. Using this convention, flow is away from h_1 and toward h_2 . With the difference in head being a lower head value minus a higher head value, the gradient is negative (Equation 22).

$$\frac{dh}{dl} = \frac{\Delta h}{\Delta L} = -\frac{Q}{KA} \quad (22)$$

Hydraulic gradient can also be represented in three dimensions when flow is not aligned with a coordinate axis, x, y, or z (Equation 23), so there is a component of flow in each axis direction as shown in Equation 23. In this case, in order to determine the direction of flow, each hydraulic gradient component is calculated with h_2 being located at a larger coordinate position than h_1 .

$$\frac{\partial h}{\partial x}, \quad \frac{\partial h}{\partial y}, \quad \frac{\partial h}{\partial z} \quad (23)$$

The partial differential (∂) representation ($\partial/\partial x$) is used because the gradient is partially dependent on the conditions in each of the coordinate directions. The resulting gradient vector (the overall magnitude and direction of the gradient) is dependent on the magnitudes of all three components of gradient in the x, y, and z directions.

The hydraulic gradient is commonly represented using the letter "i" such that Darcy's law is often written as shown in Equation 24.

$$Q = -KiA \quad (24)$$

where:

$$i = \text{hydraulic gradient } (\Delta h / \Delta L \text{ or } \frac{dh}{dl}) \text{ (dimensionless: L/L)}$$

The difference in the hydraulic head over a distance along the flow path is defined as the hydraulic gradient, $\Delta h / \Delta L$. This gradient of mechanical energy is the driving force of groundwater flow. If water is not moving, the gradient is zero, and the value of head is the same everywhere. In this situation, hydrostatic conditions exist. Under hydrostatic conditions the elevation head and pressure head at any location in the porous media combine to form the same hydraulic head value (Figure 24).

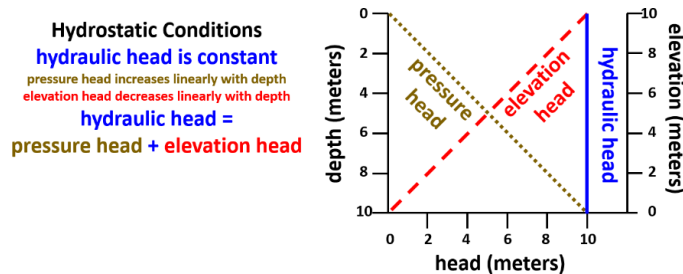


Figure 24 - Under hydrostatic conditions in this example, hydraulic head is 10 m at all depths. Hydraulic head is the sum of the pressure head and elevation head. Pressure increases linearly with depth and elevation decreases linearly with depth.

Groundwater flow occurs in the direction of the decreasing head, independent of the position of the porous medium in space (Figure 20). Local gradients are impacted by the magnitude of the hydraulic conductivity, flow rate, and cross-sectional area as stated by Darcy's Law (Equation 22) and illustrated in Figure 25.

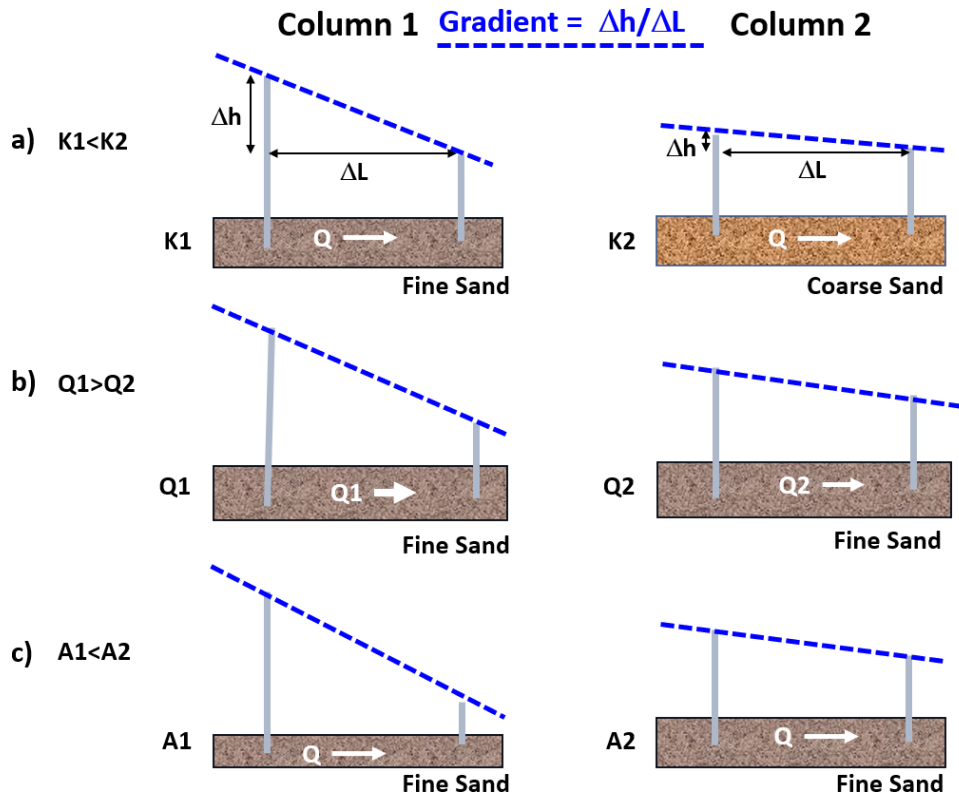


Figure 25 - The relative effects of individually varying K , Q and A on the hydraulic gradient. Darker cylinders contain fine sand and the lighter cylinder contains coarse sand. ΔL is constant. Gradients for conditions shown in Column 1 are larger than for conditions illustrated in Column 2: a) lower hydraulic conductivity results in a larger gradient; b) larger flow rate results in a larger gradient; and, c) smaller flow area results in a larger gradient (after Cohen and Cherry, 2020).

It is important to note that in addition to representations of gradients in the horizontal x,y -plane (e.g., $\Delta h / \Delta L$ as displayed in Figure 22 and Figure 25), vertical gradients, $\Delta h / \Delta z$, in the vertical x,z -plane can be assessed to examine if water is moving upward or downward at a given location (Figure 26). To evaluate vertical gradients, wells or piezometers extending to different depths are completed immediately adjacent to each other or are vertically isolated from one another in a single borehole. The magnitude of the vertical gradient is computed by comparing the absolute value of the head difference between the piezometers in the direction of flow, $\Delta h = |h_B - h_A|$, over the absolute value of the vertical distance separating their measurement locations, $\Delta L = |Z_B - Z_A|$. If piezometers or monitoring wells have screens open to the groundwater over an interval, the measuring point is designated as the midsection of the screened interval. The direction of the gradient is determined by comparing the head in the shallow piezometer, A, with that of the deeper piezometer, B. In Figure 26, the head at B is less than the head at A, so flow is downward. If the head in B was higher than A then the gradient would be upward.

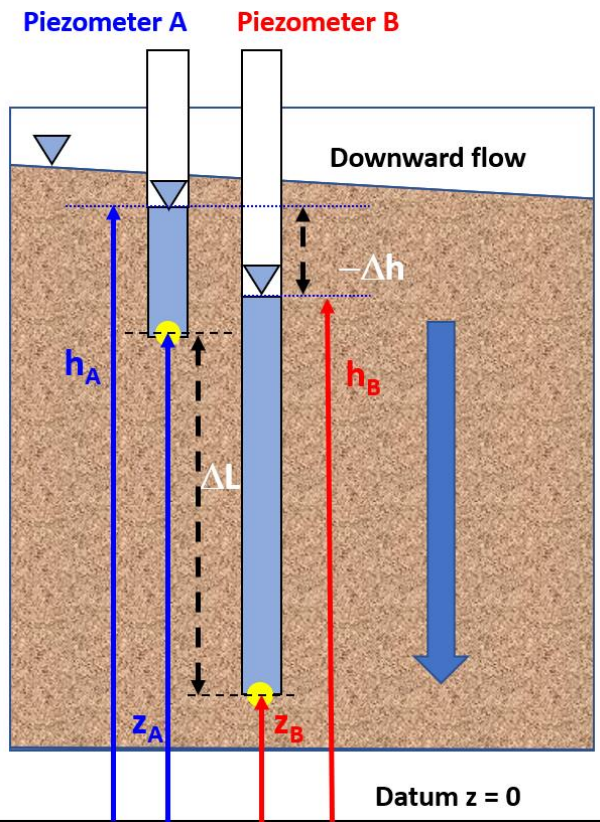


Figure 26 - Example of the factors needed to compute a vertical gradient. The stippled pattern represents saturated porous media. The absolute value of the difference in head, Δh , between shallow piezometer A and deep piezometer B is $\Delta h = |h_B - h_A|$. The gradient is computed by dividing Δh by the vertical distance between their measurement points (yellow dots), $\Delta L = |Z_B - Z_A|$. The direction of the gradient is determined by comparing the head in the shallow piezometer, A, with that of the deeper piezometer, B. In this example, the potential for ground water flow is from the higher to lower head, in this case it is downward from A to B.

Evaluation of groundwater flow in a field system requires two-dimensional maps and cross sections, and in some settings three dimensional spatial representations. The construction and interpretation groundwater flow directions are addressed in Sections 5 and 8 in this book.

Transient Changes in Gradients

The discussion of head and gradient have been presented in the context of steady-state flow conditions, in which heads and gradients do not change over time. When the heads and gradients are not constant, conditions are referred to as transient. As long as the flow rate in and out of the sediment-filled tubes presented in the previous figures remains constant, the heads in the piezometers do not change and the gradient is constant. Figure 27 illustrates how gradients change when flow rates vary with time. It illustrates the situation where, after steady-state flow is established, the inflow to the left reservoir is stopped, that is, $Q_{in} = 0$ at t_1 . At the first instant when Q_{in} stops, the rate of flow in from the reservoir is the same as during steady state, but once the inflow is cut off, water entering the sediment is derived from the slow emptying of the water-filled reservoir on the left. As the reservoir

water level declines, the rate of flow into the sand-filled tube decreases and the gradient declines in accordance with Darcy's law. The head in the sand on the left side also declines which releases some stored water from the sand (more will be said about this release of water from storage in Section 6 of this book). As water continues to flow in from the declining left reservoir the gradient becomes smaller and smaller until eventually the water level on the left side equals the water level on the right side and the system becomes static (Figure 27). In a static system there is no flow and the heads are equal everywhere.

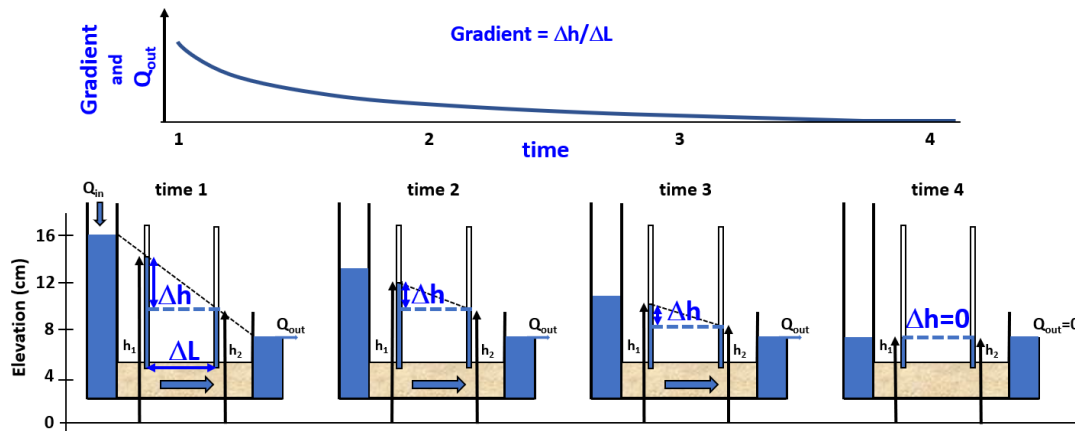


Figure 27 - Transient conditions: Initially (time= t_1) flow is steady-state, $Q_{in} = Q_{out}$, then the inflow, Q_{in} , stops. Given that the head is high in the left reservoir, the gradient ($-\Delta h/\Delta L$) continues to drive water through the tube, but the water level in the left reservoir begins to decline because there is no inflow to replenish it (time= t_2). The declining water level in the left reservoir results in a declining gradient, so the flow rate through the tube decreases with time and Q_{out} decreases with time. During transient conditions the inflow and outflow differ, $Q_{in} \neq Q_{out}$, because the change in gradient has not yet reached the other end of the tube. Head declines work their way across the tube and the outflow decreases over time (e.g., time= t_3) until eventually there is no gradient and thus no flow (time= t_4), $Q_{in} = Q_{out} = 0$ (after Cohen and Cherry, 2020).

As changes in the rates and locations of recharge and discharge to and from a groundwater system vary over time, so do heads and gradients. Groundwater systems are generally in a state of change. However, to simplify an analysis, it is often assumed that system can be treated as if conditions are in a steady-state for the time period of investigation (e.g., day, month, season, or on a long-term average). When such simplifying assumptions are applied, results must be carefully reviewed to determine if the steady-state assumption negatively impacts interpretations of actual groundwater conditions.

4.4 Hydraulic Conductivity

The hydraulic conductivity proportionality constant, K , can be conceptualized as the relative ease of fluid passage through a porous material. It has direction and magnitude and is represented as a vector; however, the first part of this discussion presents it as a scalar value. Rearranging Darcy's law to solve for hydraulic conductivity generates Equation 25.

$$K = -Q \frac{\Delta L}{\Delta h A} \quad (25)$$

In this configuration, it becomes clear that the units of K are L/T because Q units are (L^3/T) , A units (L^2), h units are (L), and L units are (L). The units are presented as Equation 26.

$$\frac{L}{T} : \frac{L^3}{T} \frac{L}{L^2} \quad (26)$$

Thus, the constant of proportionality, K , has units of velocity (e.g., meters/seconds, meters/day). However, K is not a velocity, rather it represents the transmission properties of the porous material. If water easily passes through a porous material it is described as having a high hydraulic conductivity; if water is poorly transmitted through a material it has a low hydraulic conductivity. These conditions are also referred to as permeable or of low permeability, respectively.

Intrinsic Permeability

Freeze and Cherry (1979) describe the results of hydraulic conductivity experiments used to explore the relationship between physical properties of the porous media and the fluid. A number of columns filled with different sizes of glass beads were set up as Darcy columns and changes in specific discharge were observed. Based on these observations, the relationship of the specific discharge to measurable characteristics of the porous media and were noted as shown in Equations 27, 28, and 29.

$$q \propto d^2 \quad (27)$$

where:

q = specific discharge (L/T)

d = diameter of uniform glass beads comprising the porous medium (L)

$$q \propto \rho g \quad (28)$$

where:

ρ = fluid density (M/L^3)

g = gravitational constant (acceleration of gravity) (L/T^2)

$$q \propto \frac{1}{\mu} \quad (29)$$

where:

μ = dynamic viscosity ($M/(LT)$)

When considered together with Darcy's original observation that $q \propto -dh/dl$, these three relationships lead to a definition of hydraulic conductivity that includes physical characteristics of the porous media and the influence of fluid properties (Equation 30).

$$\frac{Q}{A} = -\frac{\left(\frac{cd^2g\rho}{\mu}\right) dh}{dl} \quad (30)$$

where:

- Cd^2 = intrinsic permeability (k) of the porous medium (L^2)
 C = a constant of proportionality representing effects of particle shape,
tortuosity, and pore size distribution of the porous medium
independent of fluid properties (dimensionless)

Once the properties of the fluid are known, the hydraulic conductivity can be calculated from the intrinsic permeability as shown in Equation 31.

$$K = \frac{C d^2 g \rho}{\mu} = \frac{k g \rho}{\mu} \quad (31)$$

For sediments and rocks, intrinsic permeability (k) incorporates the influence of all the media properties that affect flow, not only the mean grain diameter as was the case for the uniform glass spheres. It has units of L^2 . The intrinsic permeability represents the magnitude of variation in the diameters of the interconnected pores as well as the amount of branching and reconnecting of the pore pathways over a linear travel path, referred as the degree of tortuosity. Tortuosity is a measure of actual distance traveled divided by the shortest distance between two locations. In general, the larger the diameter of the pores and the more efficiently they are interconnected (less tortuosity), the larger the intrinsic permeability. In contrast, a porous material with small diameter pores and many circuitous interconnected pathways (high tortuosity) would have a lower intrinsic permeability. Intrinsic permeability can also be computed if the hydraulic conductivity and fluid properties are known by rearranging Equation 31.

Fluid Properties

The specific weight and dynamic viscosity of the fluid also influence the hydraulic conductivity. The larger the specific weight of a fluid ($\gamma = g\rho$) and the lower the dynamic viscosity (μ), the higher the hydraulic conductivity. The specific weight, γ , of a fluid is its density times the gravitational constant, g , and the dynamic viscosity, μ , is the ratio of the shearing stress on a plane to the rate at which fluid velocity changes across the plane (internal resistance to flow). The influence of fluid properties on the value of hydraulic conductivity can be illustrated by visualizing how the flow rate would be affected if two Darcy sand-filled columns under the same hydraulic gradients were set up such that water flowed through one and molasses flowed through the other (Freeze and Cherry, 1979). It is assumed that the sand in each column has the same the structure and number of interconnected pores. Clearly the flow rate of the molasses would be slower than that of water. This is because the viscosity of molasses is typically more than a thousand times higher than that of water, while the specific weight of molasses is only about 1.5 times higher than water.

For groundwater systems, changes in density and viscosity caused by temperature need to be considered when computing hydraulic conductivities. Dynamic viscosity and

density of water as a function of the water temperature is shown in Figure 28. Temperature has a more significant impact on viscosity than density.

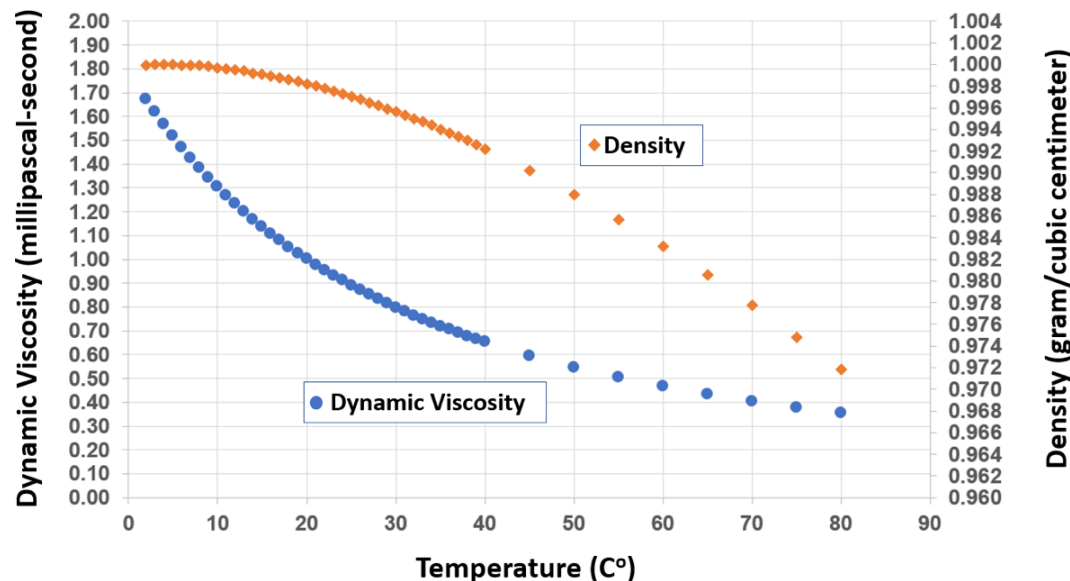


Figure 28 - Dynamic viscosity and density of water as a function of water temperature. It is useful to note that 1 millipascal-second is equivalent to 0.01 gram/centimeter-second (data from IAPWS, 2008).

For example: If a sand has an intrinsic permeability, k , of $1 \times 10^{-7} \text{ cm}^2$, and the water moving through the sand has a temperature of 10°C , then (from Figure 28):

- $\mu = 1.3 \text{ milliPascal-second}$, which is $0.013 \text{ gram/(centimeter-second)}$
- $\rho = 0.9997 \text{ g/cm}^3$, and with
- $g = 980.67 \text{ cm/s}^2$ (constant independent of temperature), then
- $K = \frac{k g \rho}{\mu} = \frac{0.0000001 \text{ cm}^2 \cdot 980.67 \frac{\text{cm}}{\text{s}^2} \cdot 0.9997 \frac{\text{g}}{\text{cm}^3}}{0.013 \frac{\text{g}}{\text{cm-s}}} = 7.54 \times 10^{-3} \text{ cm/s} \sim 8 \times 10^{-5} \text{ m/s}$

Repeating the calculation assuming the water temperature is 20°C :

- $\mu = 1.0 \text{ milliPascal-second}$, which is $0.01 \text{ gram/(centimeter-second)}$
- $\rho = 0.998 \text{ gm/cm}^3$, and with
- $g = 980.67 \text{ cm/s}^2$, then
- $K = \frac{k g \rho}{\mu} = \frac{0.0000001 \text{ cm}^2 \cdot 980.67 \frac{\text{cm}}{\text{s}^2} \cdot 0.998 \frac{\text{g}}{\text{cm}^3}}{0.01 \frac{\text{g}}{\text{cm-s}}} = 9.787 \times 10^{-3} \text{ cm/s} \sim 1 \times 10^{-4} \text{ m/s}$

These calculations illustrate that although the changes in K are rather small, K increases as water temperature increases, because the magnitude of the decrease in dynamic viscosity (in the denominator) with temperature is larger than the corresponding decrease in density (in the numerator).

As fluids of different composition pass through saturated porous medium the properties of the composition of the fluid will influence hydraulic conductivity characterization (remember the molasses example). For example, if pure benzene was

spilled during a train accident and entered the top of the 10°C groundwater system as liquid benzene, the saturated K value of the sand for benzene could be computed. In this simplified example, at a temperature of 10°C, the K of sand with an intrinsic permeability, k , of $1 \times 10^{-7} \text{ cm}^2$, for benzene would be governed by the properties of benzene, not properties of water:

- $\mu_{\text{benzene}} = 1.25 \text{ milliPascal-second}$, which is $0.0125 \text{ gram}/(\text{centimeter-second})$
- $\rho_{\text{benzene}} = 0.727 \text{ gm/cm}^3$, and with
- $g = 980.67 \text{ cm/s}^2$, then
- $$K_{\text{benzene}} = \frac{k g \rho}{\mu} = \frac{0.0000001 \text{ cm}^2 \cdot 980.67 \frac{\text{cm}}{\text{s}^2} \cdot 0.727 \frac{\text{g}}{\text{cm}^3}}{0.0125 \frac{\text{g}}{\text{cm} \cdot \text{s}}} = 5.7 \times 10^{-3} \text{ cm/s} \sim 6 \times 10^{-5} \text{ m/s}$$

This indicates the K for benzene flow ($\sim 6 \times 10^{-5} \text{ m/s}$) is lower than the K for water flow ($\sim 8 \times 10^{-5} \text{ m/s}$) at the same temperature. This is because, although benzene is less viscous than water at 10°C, the density of benzene is considerably less than that of water. If the benzene dissolved in the water such that benzene molecules were being carried as a dissolved substance (solute) within the water, the flow rate would be controlled by the properties of the water because no liquid benzene would be present.

To reiterate, hydraulic conductivity is symbolized by a capital K with units of length over time L/T. K reflects the impact of the properties of both the fluid and the medium on the ease with which fluid passes through a medium. Intrinsic permeability is usually represented by a lowercase k with units of length squared (L^2). k reflects the impact of only the properties of the medium on the ease with which fluid passes through it. Occasionally k_i is used to represent intrinsic permeability. In older literature, and a few modern writings, hydraulic conductivity is referred to as permeability or the coefficient of permeability. In some literature (e.g., Freeze and Cherry, 1979) the term “permeability” is used to represent k without the “intrinsic” modifier. Consequently, care needs to be exercised when reading a report or textbook to clearly understand and apply the information. It is useful to check the units associated with each term to decipher how the terms are being used. In the petroleum industry, the term “permeability” usually refers to k (L^2). Petroleum engineers often work with materials of low k and if the values are given in units of m^2 or cm^2 the number is very small (e.g., 1×10^{-8} to $1 \times 10^{-16} \text{ cm}^2$). As a result, they introduced a unit called a “darcy” that is equivalent to $9.87 \times 10^{-9} \text{ cm}^2$ or, approximately $1 \times 10^{-8} \text{ cm}^2$ to describe the capacity of petroleum reservoir rocks to transmit fluids. A sandstone with an intrinsic permeability of $1 \times 10^{-9} \text{ cm}^2$ would have a permeability of 0.1 darcy.

4.5 Applicability of Darcy's Law

Darcy's law is a macroscopic law applied using average values of parameters for a representative portion of the porous media, the REV as discussed in Section 3 of this book. Darcy's law is applied to the flow of fluids through porous media. It describes a linear relationship between specific discharge and the hydraulic gradient. This relationship is valid for most all groundwater conditions. However, as the flow rate approaches zero or when high rates of flow occur in high hydraulic conductivity material like fractures or karst features, flow may not be linear and thus, Darcy's law does not appropriately represent groundwater flow.

It has been suggested that a more general formulation of the law may be posed as Equation 32.

$$q = -K \left(\frac{dh}{dl} \right)^m \quad (32)$$

where:

m = coefficient (dimensionless), if $m = 1$, as in all the common situations, the flow law is linear, if m is not equal to 1 then the equation describes non-linear conditions and should not be called Darcy's law. (Freeze and Cherry, 1979)

Darcy's law is strictly applicable for laminar flow of an incompressible fluid in a solid matrix (non-deforming) porous medium in which the gradient of mechanical energy is the only driving force (Figure 29). It is applicable under steady state or transient conditions. Laminar flow occurs when a fluid flows in parallel lines with no disturbance between the lines. Laminar flow is by definition "not turbulent" (Figure 29). Under turbulent flow conditions packets of water exhibit chaotic changes in velocity (for example, flow in a white-water stream). Additional information on fluid behavior in porous media is provided in the Groundwater Project book "[Introduction to Fluid Mechanics for Groundwater Scientists](#)" (Klammler, 2023).

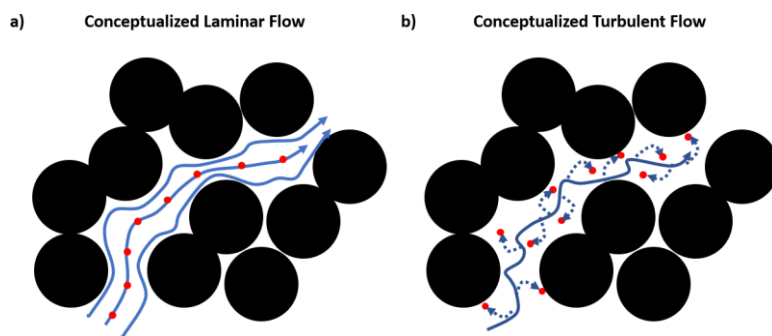


Figure 29 - Conceptualized laminar and turbulent flow at the pore scale. Small red dots represent a “packet of water” that can be tracked along a flow path: a) laminar flow occurs when packets of water follow one another in a predictable manner, not getting ahead of or behind of their original position; and, b) turbulent flow occurs when motion of the fluid becomes

chaotic (dashed arrows) and can no longer be described by equations of fluid mechanics for smooth flow. Particles do not strictly follow each other.

Turbulent conditions begin to develop as flow velocity increases. The Reynolds number that characterizes the ratio of internal forces to viscous forces acting on fluid elements is often used to test for laminar or turbulent conditions (Equation 33).

$$R_e = \frac{qd\rho}{\mu} \quad (33)$$

where:

R_e = Reynolds number characterizes the ratio of internal to viscous forces acting on fluid elements (dimensionless)

q = specific discharge (L/T)

d = characteristic length (L)

ρ = density (M/L³)

μ = dynamic viscosity (M/(LT))

The characteristic length term attempts to provide some information on the pore diameters available for flow. Authors suggest using an effective grain size (e.g., d_{10} finer than) (Todd and Mays, 2004), the mean pore dimension, mean grain diameter, or some function of the square root of the intrinsic permeability k (Freeze and Cherry, 1979). Bear (1972) states “Darcy’s law is valid as long as the Reynolds number, based on average grain diameter, does not exceed some value between 1 and 10 (page 126)”. Most authors on the topic agree that when R_e is less than one, laminar flow occurs, and Darcy’s law is valid.

Flow rates that exceed the upper limit of Darcy’s law have been noted to occur in caverns and cavities of karstic limestones and dolomites, cavernous volcanic rocks (e.g., lava tubes), and some open framework boulder dominated deposits (in short, materials with large interconnected pores and extremely high hydraulic conductivities). Under most natural conditions, groundwater flows are laminar and Darcy’s law is valid (Freeze and Cherry, 1979). However, turbulent flow may occur in a portion of a groundwater system when flow rates accelerate in the vicinity of high yield pumping wells and drains. Turbulent flow may also occur in fractures with large apertures when the system is stressed by pumping. The lower limit of Darcy’s law is of little concern to most hydrogeologists as flow rates are extremely small.

Darcy’s law as presented here is not valid for compressible fluids. Fortunately, water has a relatively low compressibility. So, although water is not completely incompressible, this requirement can be relaxed to accommodate use of Darcy’s law for the small compressibility of water. However, Darcy’s law is not applicable if the density of the fluid varies due to differing pressure, temperature, and/or high concentrations of dissolved constituents; it is not applicable if there are substantial differences in density from location to location within a flow system; and it is not applicable if thermal, chemical, or electrical gradients drive fluid flow. However, forms of flux equations based on Darcy’s Law have been developed to accommodate density variations due to compressibility, non-uniform

solute concentrations and non-uniform temperature. These equations are usually referred as representing Darcy's Law.

Again, fortunately, the density and viscosity changes of water are usually trivial at the low pressures and narrow range of temperatures occurring in most of the Earth's shallow subsurface making Darcy's law applicable.

The lengthy presentation of Darcy's Law in this section is purposeful. Darcy's Law is the key to understanding and interpreting groundwater flow in porous media. It provides the foundational relationships between head, gradients and hydraulic conductivities that hydrogeologists used every day to develop conceptual models of how natural groundwater systems work, generate groundwater budgets, identify source areas of groundwater contamination, manage groundwater supplies and quantify exchanges between surface water and groundwater systems. In the authors' experience, whenever a problem seems overwhelming or unclear, check Darcy's Law and be sure basic principles are being correctly applied. This advice has been valuable in resolving issues encountered by students attacking assigned problems as well as professional hydrogeologists and engineers managing large complex groundwater sites.

4.6 Further Investigation of Darcy's Law, Head, Gradient and Hydraulic Conductivity

Cohen and Cherry (2020) developed a [Groundwater Project module](#) ↗ that offers the reader deeper conceptual and visual understanding of hydraulic head and groundwater flow. [Exercise 3](#) ↗ provides an opportunity to think about pressure and head.

5 Hydraulic Conductivity Values

The value of hydraulic conductivity, K , is determined by measuring flow rates, lengths, water levels, and pressures (Equation 15). Resulting hydraulic conductivity values are also used in conjunction with equations to compute groundwater discharge (Equation 15), flux (Equation 17), and velocity (Equation 18) as illustrated in Section 4. Hydraulic conductivity values are also required to predict the three-dimensional head distribution in a groundwater basin, infer groundwater flow directions and anticipate groundwater impacts from municipal well fields. This section:

- describes some basic methods used to estimate hydraulic conductivities in the laboratory;
- provides an illustration showing the range of hydraulic conductivities for various earth materials;
- presents concepts used to describe the two- and three-dimensional spatial variability of hydraulic conductivity, including the spatial concepts of isotropic, anisotropic, homogeneous and heterogeneous hydraulic conductivity distributions;
- discusses methods used to assign hydraulic conductivities to field settings; and,
- explains methods to determine equivalent hydraulic conductivities for fractured systems and individual fractures.

5.1 Conditions Effecting Hydraulic Conductivity Values

Hydraulic conductivity, K , represents the relative ease of groundwater movement through an earth material as stated in Section 4. It represents the combination of the intrinsic permeability, k , and fluid properties (Equation 31). If the fluid properties are constant, then hydraulic conductivity will increase as intrinsic permeability increases, because K is directly proportional to Cd^2 . K will increase if C (which reflects pore shape and size distribution, as well as the tortuosity of pore connections) becomes larger and if the characteristic length, d , increases. In Section 4, the investigation of the relationship between K and k described by Freeze and Cherry (1979) used the diameter of glass spheres for d as a surrogate for the size of the pore spaces. Conceptually, for a group of uniform spheres, if the squared diameter of the spheres increases the squared diameters of the pores also increases (Figure 30). The doubling of the pore channel diameter increases the cross-sectional area of pores by a factor of four; thus, the capacity of the porous medium to transmit water increases.

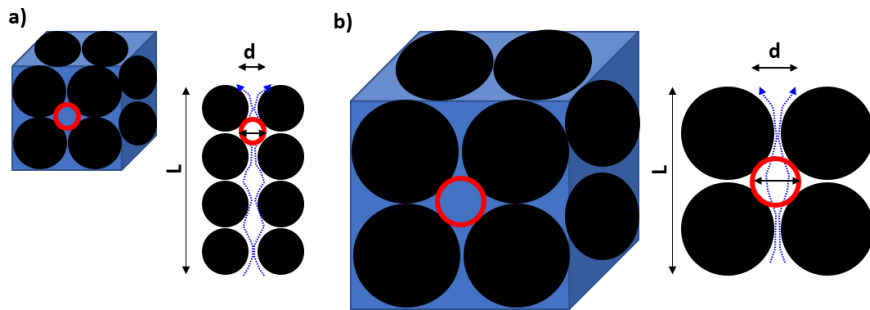


Figure 30 - K is proportional to Cd^2 . Doubling of grain-size diameter (black circles), doubles pore diameter (d , red circle), increasing K . Dotted blue arrows represent flow paths. Black solid double-headed arrows (L) represent straight line flow path distance. Increased pore size reduces tortuosity (the quotient of flow-path-length shown by dotted blue lines and straight-line-distance L) thus increasing the value of C : a) a sample of porous material with small grains and pore diameters, and more tortuous flow paths; b) a sample of porous material with grain and pore diameters twice that of the material in (a). The illustrated pore channel shape in (b) has a lower tortuosity than the sample shown in (a).

As the size of grains become more uniform, the number of pores decreases, thus reducing tortuosity (flow path length divided by the straight-line distance), and pore diameters become larger, so hydraulic conductivity increases. In contrast, if grain sizes are less uniform, finer grains fill large pores, so the number of pores increase, thus increasing tortuosity; and pore diameters become smaller, so hydraulic conductivity decreases. The effect of the magnitude of grain size and uniformity of grain size on hydraulic conductivity values is illustrated in Figure 31.

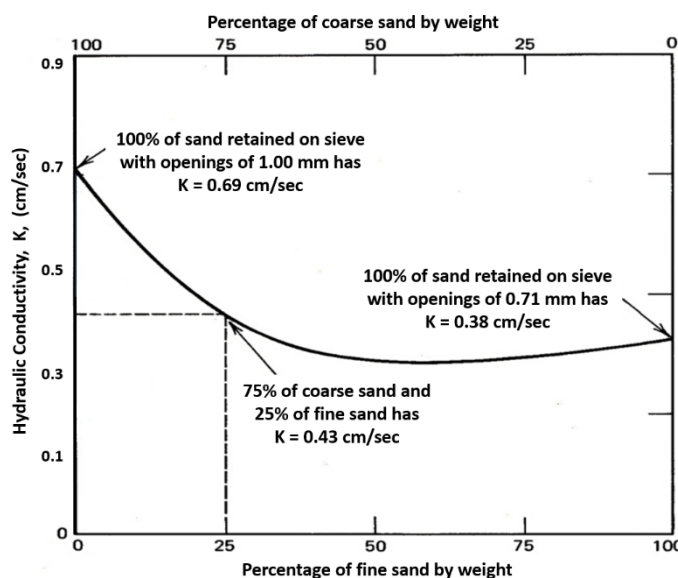


Figure 31 - Example of the influence of decreasing the uniformity of a sample of coarse sand on the hydraulic conductivity. A mix of 75% coarse and 25% fine sand alters the K to be much closer to the value of 100% fine sand (unpublished data, Courtesy of the Illinois Water Survey).

Figure 31 provides an example of how the hydraulic conductivity of a uniform coarse sand is impacted by the addition of finer particles. A mix of 75% coarse sand and

25% fine sand alters the K to be much closer to the value of the fine sand. In fact, for mixtures of more than 30% of fine sand, the hydraulic conductivity is less than that of 100% fine sand because the larger grains of the coarse sand occupy some of the pore space available for water flow in the 100% fine-sand sample.

Primary and Secondary Hydraulic Conductivity

As with porosity, earth materials have an initial hydraulic conductivity when originally formed and secondary hydraulic conductivity that develops after their original formation. Hydraulic conductivity can increase as a result of weathering, fracturing, jointing, and faulting; and can decrease as a result of mineral precipitation, and at times as a result of weathering. Like porosity, the hydraulic conductivity of a formation near the surface may be higher than the same formation buried at some depth below the surface. This is because lithostatic pressure (weight of the overlying earth) acts to reduce pore openings and interconnections. Snow (1968, 1970), observed that, in general, hydraulic conductivity of fractured rocks decreases with depth. Davis and Turk (1964) found hydraulic conductivities of crystalline rocks were significantly lower at depths greater than 100 m, whereas D'Agnese and others (1997) noted decreased hydraulic conductivity of sedimentary and volcanic rocks of Death Valley, USA, was most pronounced between 330 and 1000 m. Changes in fractured rock hydraulic conductivities with depth are described in Krasny et al. (2003) and Krasny and Sharp (2007).

5.2 Methods to Estimate Hydraulic Conductivity

There are many approaches to estimating hydraulic conductivity of earth materials. In a laboratory setting tests using the Darcy column set up can be performed to estimate values of hydraulic conductivity. If the material is unconsolidated, hydraulic conductivity can be estimated by analyzing the range of sizes of sediment grains. However, small-scale measurements often are not representative of the hydraulic conductivity at the much larger field scale as discussed in Section 3 of this book. Representative hydraulic conductivity values are needed in order to evaluate groundwater systems when designing facilities for water supply or to clean up contamination. Consequently, a large area of groundwater hydrology involves field testing to estimate hydraulic conductivities. A summary of laboratory methods for estimating hydraulic conductivity is provided in Box 4. [Click here to read Box 4 ↗](#), which includes details about the basic laboratory procedures and a brief overview of field testing referred to as aquifer testing. Determination of hydraulic conductivity and other aquifer properties using field-based methods is presented in a separate companion Groundwater Project book "*An Introduction to Hydraulic Testing in Hydrogeology: Basic Pumping, Slug, and Packer Methods ↗*" (Woessner et al., 2023). Aquifer testing is covered in detail in numerous publications by the United States Geological Survey (e.g., Lohman 1972); groundwater text books; and commercial aquifer test software manuals and packages (e.g., AQTESOLV ↗, and Aquifer Test ↗). An excellent reference is

"An Analysis and Evaluation of Pumping Test Data" by Kruseman and de Ridder (1994). A downloadable copy is available on the [Groundwater Project website](#). Regardless of the method employed, the value of hydraulic conductivity is an estimate, though it is often referred to as a measurement or determination.

5.3 Hydraulic Conductivity Values for Earth Materials

Most groundwater textbooks contain tables of hydraulic conductivity values summarized from a large number of laboratory and field tests. The tables typically include ranges of values for a given type of earth material because they are formed by a wide variety of processes that influence the size and distribution of interconnected voids and complexity of pathways. A gravel that is infilled with sand, silt and clay will have a lower hydraulic conductivity than an open framework gravel found in a river bar. Though both are classified as gravel deposits, their hydraulic conductivity may differ by orders of magnitude. As explained in Section 5.1, the larger and more interconnected the pores of a material, the higher the hydraulic conductivity.

Freeze and Cherry (1979) provide a useful table of intrinsic permeability, k , and hydraulic conductivity, K , of unconsolidated material, sedimentary rocks, and igneous and metamorphic rocks similar to that shown as Figure 32. This figure presents the range of values of hydraulic conductivity and intrinsic permeability in three systems of units. The data show that hydraulic conductivity varies over a wide range. There are few other physical parameters that take on values ranging over 13 orders of magnitude. In practical terms, this wide range of values suggests that an order-of-magnitude knowledge of hydraulic conductivity can be useful. Conversely, it implies that if a third decimal place is reported for a hydraulic conductivity value, it is likely of little significance.

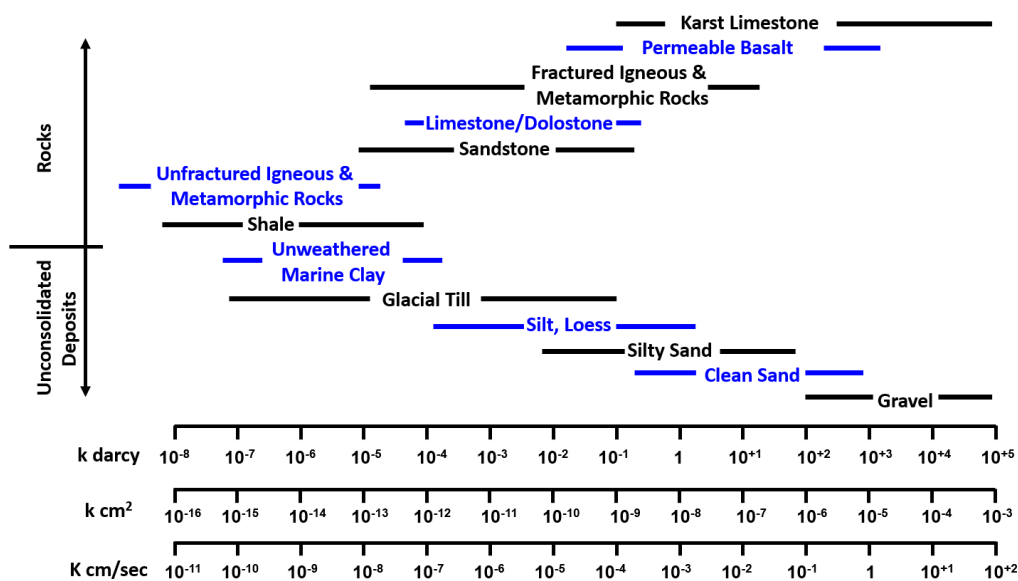


Figure 32 - Ranges of intrinsic permeability, k , and hydraulic conductivity, K , values. The alternating colors are used to make the chart easier to read. For conversion purposes, $1 \text{ cm/s} = 1.02 \times 10^{-5} \text{ cm}^2$ and $1.04 \times 10^3 \text{ darcy}$ (after Freeze and Cherry, 1979).

5.4 Spatial and Directional Variation of Hydraulic Conductivity

As discussed previously in this book, the transmission properties of earth materials are influenced by the processes that are active when the material is formed or deposited, as well as the changes in the material that occur during post-formation processes. Both sets of processes influence the direction and magnitude of hydraulic conductivity at each location throughout the material. In the general case, hydraulic conductivity varies with direction, and when aligned with the principal coordinate axes, it is represented as K_x , K_y and K_z .

If formation of the earth material results in uniform pore sizes that are well connected in all directions at a given location (e.g., $K_x = K_y = K_z$) the hydraulic conductivity at that location is isotropic. In a material with isotropic hydraulic conductivity, water passes through a material with equal ease regardless of the direction that the water is forced through the material. That is, given the same gradient in any direction, the resulting flow rate is the same. Figure 33a provides a schematic of an isotropic porous medium where K is the same in every direction at every location. In contrast, if the pore structure and connections resulted in a setting where hydraulic conductivity is lower in one direction than another, the porous medium is anisotropic, for example, where $K_x = K_y$, but K_z has a smaller value as shown in Figure 33b. The medium shown in Figure 33b could be the result of compacting the medium shown in Figure 33a, or from a depositional process that oriented non-spherical grains in a preferred direction. Anisotropy can also involve different values of K in all of the principal directions $K_x \neq K_y \neq K_z$. In most sediments and sedimentary rocks, the deposition process produces micro layering resulting in horizontal hydraulic conductivities being about the same, $K_x = K_y$, and vertical values, K_z , that are smaller. This results in isotropic conditions in the horizontal plane (map view) with anisotropic conditions in a cross-sectional representation as shown in Figure 33b.

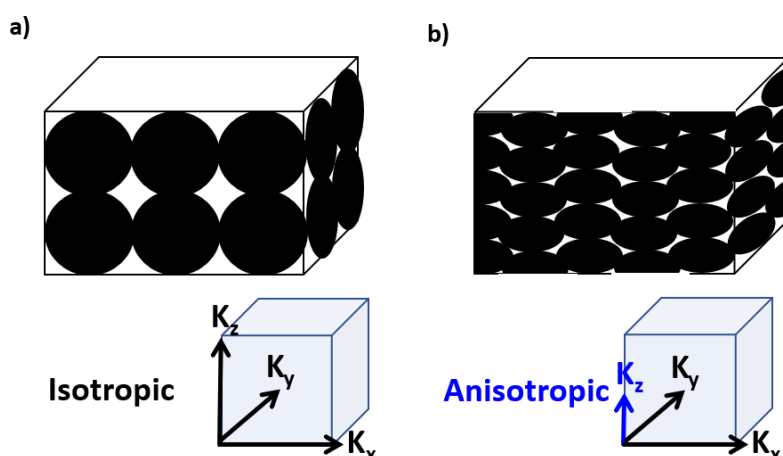


Figure 33 - Schematics of a representative volume of a porous medium with isotropic and anisotropic hydraulic conductivity: a) an isotropic porous medium where the magnitude and direction of K_x , K_y and K_z are equal; b) an anisotropic medium where the direction and magnitude of K_x equals K_y , while K_z has a smaller value. The material shown in (b) could be the result of compacting the material shown in (a).

When hydraulic conductivity distributions are observed at the broader scale of a geologic formation (not at only one location), two general conditions can be found in four combinations as illustrated in Figure 34. The formation can be either homogeneous or heterogeneous, and it can be either isotropic or anisotropic:

- If all locations have the same value of K_x , K_y , K_z , then the hydraulic conductivity distribution is isotropic and homogeneous (Figure 34a).
- If the same anisotropic conditions are present at all locations within a formation, then the hydraulic conductivity distribution is anisotropic and homogeneous (Figure 34b).
- If the hydraulic conductivity is isotropic at all locations, but the isotropic values differ from location to location, then the hydraulic conductivity distribution is isotropic and heterogeneous (Figure 34c).
- If at different locations within the formation, different sets of anisotropic conditions are present, then the hydraulic conductivity distribution is anisotropic and heterogeneous (Figure 34d).

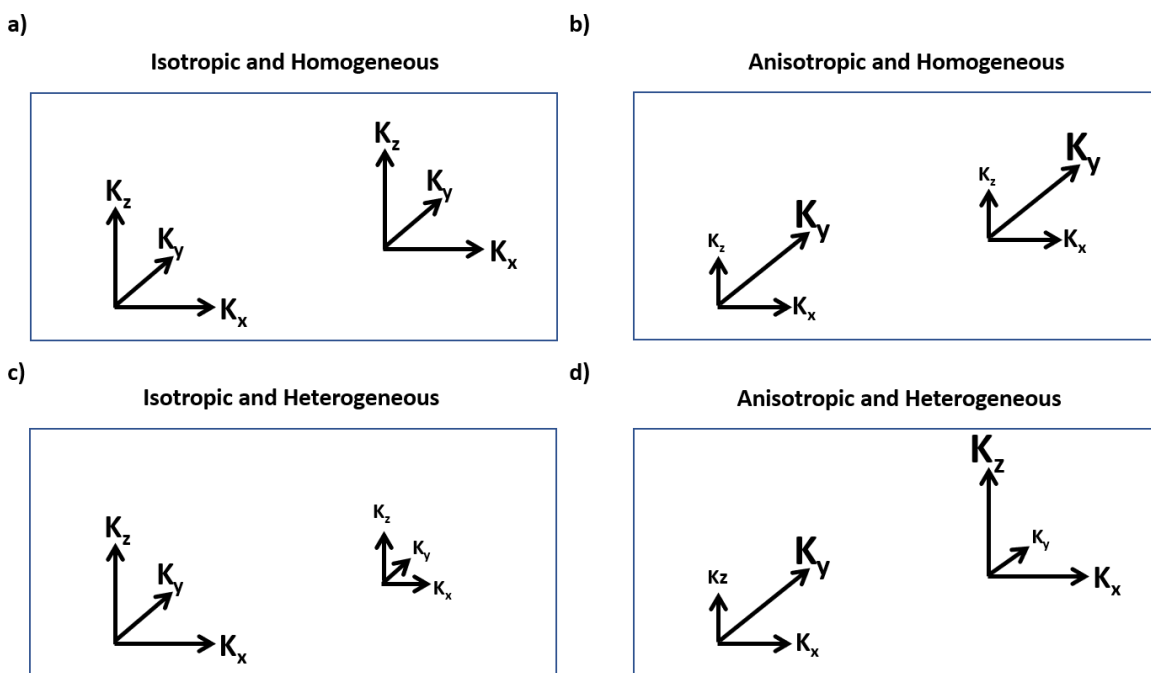


Figure 34 - Examples of hydraulic conductivity distributions for a geologic formation enclosed by the blue box. When point-values of K_x , K_y and K_z are observed at many locations in a formation, the hydraulic conductivity distribution can be described in terms of homogeneity (same throughout) or heterogeneity (variable from location to location) and having isotropy (at a location the same in all directions) or anisotropy (at a location not the same in all directions). a) Isotropic and homogeneous conditions: the values of hydraulic conductivity in each coordinate direction are equal at all locations. b) Anisotropic and homogeneous conditions: one or more of the values of hydraulic conductivity in each coordinate direction are not equal, but this relationship is the same at all locations within the region. c) Isotropic and heterogeneous conditions: hydraulic conductivity is equal in all directions at a location, but values differ at other locations. d) Anisotropic and heterogeneous conditions: one or more of the directional values of hydraulic conductivity can differ at each location and they can all be different at each location.

The three-dimensional components of hydraulic conductivity can be used to derive the hydraulic conductivity, K_s , associated with a particular groundwater flow path (q) constructed within the groundwater system. For example, if the spatial hydraulic conductivity conditions (K_x , K_y , K_z) are known, the hydraulic conductivity associated with a flow line at some angle to the coordinate system can be established using a hydraulic conductivity ellipsoid (Freeze and Cherry, 1979, Chapter 2). In two dimensions an ellipse can be constructed using the square root of K_{max} and K_{min} values as shown in Figure 35 and expressed in Equations 34 and 35.

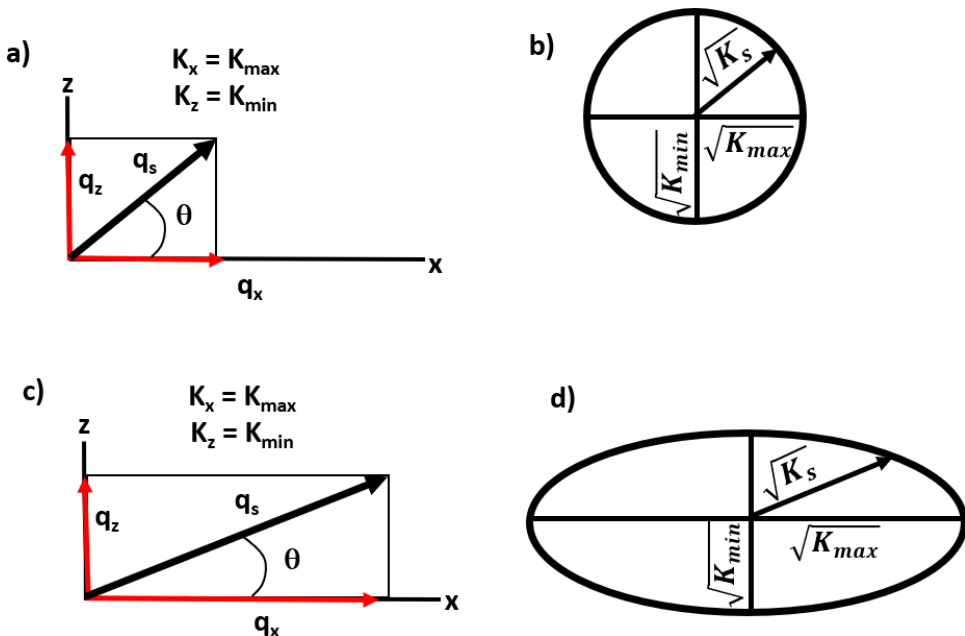


Figure 35 - The determination of the hydraulic conductivity, K_s , associated with an arbitrary flow line q_s at angle θ to the x coordinate in an isotropic and anisotropic material. a) Specific discharge q_s in an arbitrary direction of flow in an isotropic material. b) Hydraulic conductivity ellipse for isotropic conditions; K_s is the same at all angles. c) Specific discharge q_s in an arbitrary direction of flow in an anisotropic material. d) Hydraulic conductivity ellipse for anisotropic conditions showing K_s varies with angle (after Freeze and Cherry, 1979).

$$\frac{1}{K_s} = \frac{\cos^2 \theta}{K_x} + \frac{\sin^2 \theta}{K_z} \quad (34)$$

Equation 34 relates the hydraulic conductivity, K_s , in any angular direction, θ , to the components K_x and K_z . Equation 34 can be written in rectangular coordinates by setting $x = r \cos \theta$ and $z = r \sin \theta$ resulting in Equation 35.

$$\frac{r^2}{K_s} = \frac{x^2}{K_x} + \frac{z^2}{K_z} \quad (35)$$

Equation 35 is the equation of an ellipse. Major axes are the square root of K_x and K_z as shown in Figure 35d (Freeze and Cherry, 1979). As indicated in Figure 35b and d, the hydraulic conductivity in any direction, K_s , in an isotropic or anisotropic medium can be determined graphically if K_x and K_z are known. Although the x, y, and z axes are shown here in their classic orientation, the axes may be oriented in any direction within a formation as shown in Figure 36.

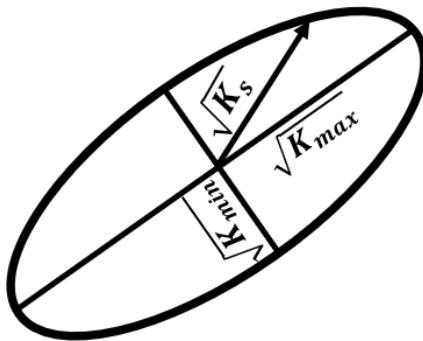


Figure 36 - The hydraulic conductivity ellipse may have any orientation in a subsurface material.

5.5 Hydraulic Conductivity of Homogeneous and Heterogeneous Materials

When hydrogeologic settings have homogeneous hydraulic conductivity distributions it is often the result of a fairly uniform set of depositional and post-depositional conditions (e.g., conditions favorable to similar pore sizes and connections; similar sediment structures; followed by similar weathering and fracturing processes). From a geologic perspective, such conditions are most common in broad areas of sedimentation with similar processes (e.g., beach deposits, sand dunes, back bay deposits). Formations that were chemically precipitated (e.g., limestones, dolostones, salt) may initially be homogeneous. Post depositional processes such as dissolution, jointing, and fracturing may result in maintaining homogeneity or the development of heterogeneous conditions. Igneous and metamorphic rocks are initially relatively impermeable and may develop homogeneous or heterogeneous properties through a secondary process (e.g., weathering, solutioning, jointing, and fracturing). Certainly, some large scale, isotropic and homogeneous hydraulic conductivity conditions occur, but most unconsolidated and consolidated formations are anisotropic and heterogeneous. The primary cause of anisotropy on a small scale is the orientation of clay minerals in sedimentary rocks, unconsolidated layering in sediments, and fracture sets in crystalline materials. Core samples of clays and shales seldom show horizontal to vertical anisotropy greater than 10:1, and it is usually less than 3:1. However, at the field scale where coarse- and fine-grained materials are interlayered or fracture sets dominate, ratios of K_x to K_z can

exceed 1000:1. In most hydrogeologic settings, heterogeneous and anisotropic distributions of hydraulic conductivity are the norm.

Equivalent Hydraulic Conductivity

Geologic formations often involve layered geologic materials in which each bed is isotropic and homogeneous. This is referred to layered heterogeneity. Sometimes the layers are thin and it is useful to obtain an equivalent representative hydraulic conductivity for a group of layers in order to make calculations such as determining flow rates or groundwater velocities through the material using Darcy's law. An equivalent horizontal and vertical hydraulic conductivity can be derived for the layered unit.

A saturated two-layered system is represented in Figure 37. The layers are isotropic and homogeneous with different values of hydraulic conductivity, K_1 and K_2 .

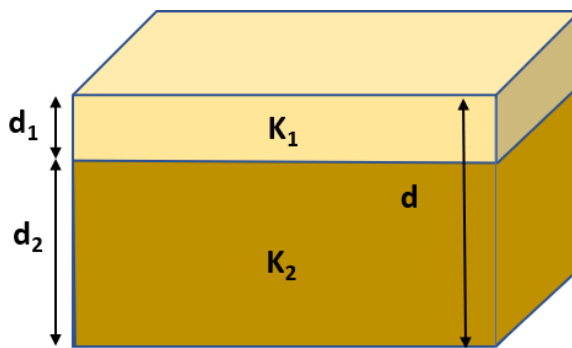


Figure 37 - Two isotropic and homogeneous layers representing a geologic material with $d = d_1 + d_2$. The thickness of layer 1 is d_1 and the homogeneous, isotropic hydraulic conductivity is K_1 . The thickness of layer 2 is d_2 and the homogeneous, isotropic hydraulic conductivity is K_2 . In this example, $K_1 > K_2$.

The equivalent horizontal hydraulic conductivity, K_h , can be computed using a thickness-weighted arithmetic average as presented in Equation 36:

$$K_h = \sum_{i=1}^n \left[\frac{K_i d_i}{d} \right] \quad (36)$$

and for conditions shown in Figure 37:

$$K_h = \frac{K_1 d_1 + K_2 d_2}{d_1 + d_2} \quad (37)$$

where:

K_h = equivalent horizontal hydraulic conductivity (L/T)

K_1 = hydraulic conductivity of layer 1 (L/T)

K_2 = hydraulic conductivity of layer 2 (L/T)

d = $d_1 + d_2$, total thickness (L)

d_1 = thickness of layer 1 (L)

d_2 = thickness of layer 2 (L)

An equivalent vertical hydraulic conductivity can be computed using a thickness-weighted harmonic average as presented in Equation 38:

$$K_v = \frac{d}{\sum_{i=1}^n \frac{d_i}{K_i}} \quad (38)$$

and for the two-layer condition shown in Figure 37:

$$K_v = \frac{d_1 + d_2}{\frac{d_1}{K_1} + \frac{d_2}{K_2}} \quad (39)$$

For example, in Figure 37, if $K_1=100$ m/d and $K_2 = 6$ m/d, and $d_1 = 10$ m and $d_2 = 30$ m, the equivalent K_h would be 29.5 m/d (Equation 37). The equivalent K_v would be 7.8 m/d (Equation 39).

The theoretical basis for these expressions and an additional example of deriving equivalent hydraulic conductivities for a four-layer system is provided in Box 5. [Click here to read Box 5](#).

There are likely as many types of heterogeneous configurations as there are geological environments, but it can be useful to draw attention to four broad classes described by Freeze and Cherry (1979): Layered heterogeneity, discontinuous heterogeneity, random heterogeneity and trending heterogeneity.

Layered heterogeneity is common in marine deposits, unconsolidated lacustrine deposits and sedimentary rocks. An example was described using Figure 37 and Equations 36 through 39. Layered heterogeneity can be comprised of materials with K values spanning nearly the full 13-order-of-magnitude range displayed in Figure 32, for example, in interlayered deposits of clay and sand.

Discontinuous heterogeneity can occur in the presence of large-scale stratigraphic features or faults that may have large contrasts in K (Figure 38). Another example of a discontinuous feature is the overburden-bedrock contact.

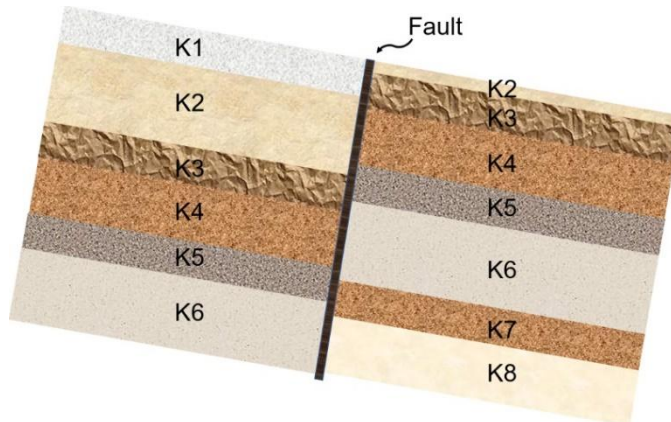


Figure 38 - Discontinuous heterogeneity caused by faulting that juxtapose formations of differing hydraulic conductivity.

Random heterogeneity can occur in the presence of a wide variety of geologic materials where mixtures of deposits that do not have any readily identifiable structure can be grouped as a unit for the purpose of calculating equivalent K values. If present, a non-random structure is often difficult to identify such as the K distribution shown in the units outlined by white in Figure 39. In this case, it has been found that calculating the geometric mean of the sample values produces an equivalent homogeneous isotropic value fairly representative of the unit as a whole (Equation 40).

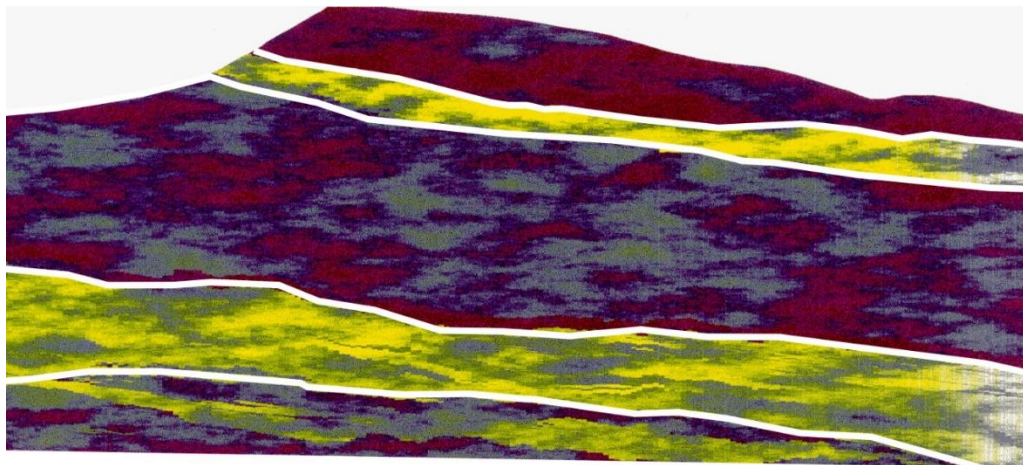


Figure 39 - A cross-sectional view of five layers of volcanic rocks comprised of a mixture of materials with varying hydraulic conductivity values (dark colors represent low values and light colors represent high values of hydraulic conductivity). The individual formation hydraulic conductivity distributions within the white outlines do not have a readily identifiable structure. Equivalent hydraulic conductivities can be computed as the geometric mean of the sample values for each formation using Equation 40.

$$K_{equivalent} = 10^{\left(\frac{1}{N} \sum_{i=1}^{i=N} \log K_i\right)} \quad (40)$$

where:

$K_{equivalent}$ = equivalent homogeneous isotropic value representative of the unit as a whole (L/T)

K_i = K for each of N samples from the unit (L/T)

N = number samples with measured K values (dimensionless)

Trending heterogeneity is illustrated on the map in Figure 40. Trends are possible in many types of geological formations, and are commonly observed in alluvial fans, deltas, and glacial outwash plains. Geologic facies representing sediments originating from different depositional environments are often mapped and can be used to identify trending heterogeneities. Variations in bedding, jointing and fracturing can also be linked to trending horizontal and vertical heterogeneity.

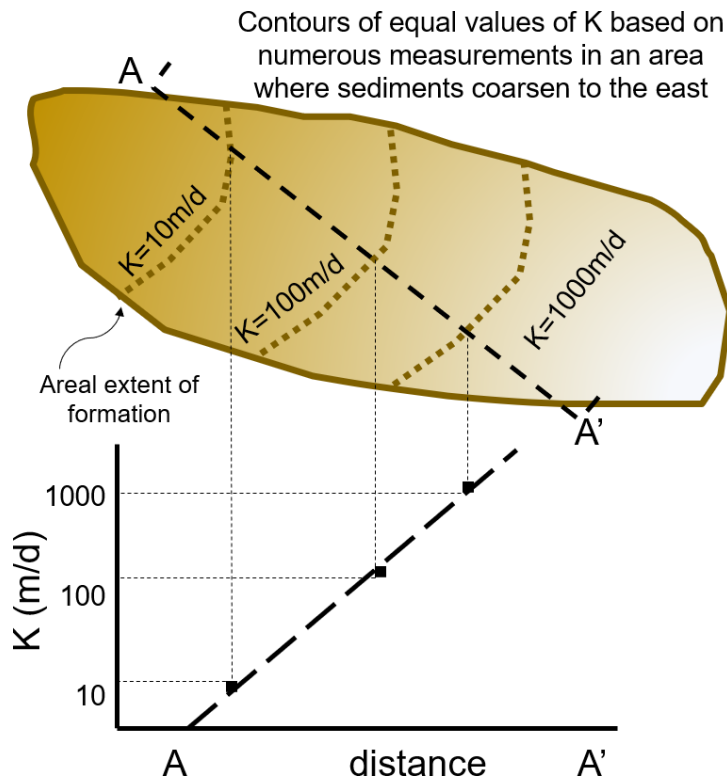


Figure 40 - Trending heterogeneity caused by a sedimentary process resulting from a geologic depositional environment with high energy in the southeast such that uniform coarse-grained materials were deposited in that area and declining energy to the northwest such that finer-grained sediments were deposited in that area.

The common heterogeneous conditions found in regional studies make assignments of equivalent hydraulic conductivity values difficult. Researchers have recognized that the hydraulic conductivity distribution in most formations follows a log normal distribution where the standard deviation of $\ln(K)$ can range from 0.5 to 4.5 (Meerschaert et al., 2013). Consequently, hydraulic conductivities derived from lab and field scale testing, are often correlated with knowledge of the geologic setting, published tables of values, as well as head and gradient information to generate representative hydraulic conductivity values. Estimates should be supported by field and laboratory measurements.

5.6 Hydraulic Conductivity in Fractured Rocks

Hydraulic conductivity of a fractured rock is dependent on its unfractured hydraulic conductivity (called matrix hydraulic conductivity) as well as the spacing between fractures, their aperture (width of the fracture opening), roughness of the fracture walls, and their interconnectedness.

When fracturing is extensive relative to the volume of material that a K value is assigned to, groundwater flow in the fracture network can be treated as a continuum and the hydraulic conductivity of the system can be used in Darcy's law to estimate flow rates (Figure 41). In that case, the transmission properties of the fractured medium are assumed

to behave as an equivalent porous medium represented by a hydraulic conductivity value in each primary direction.

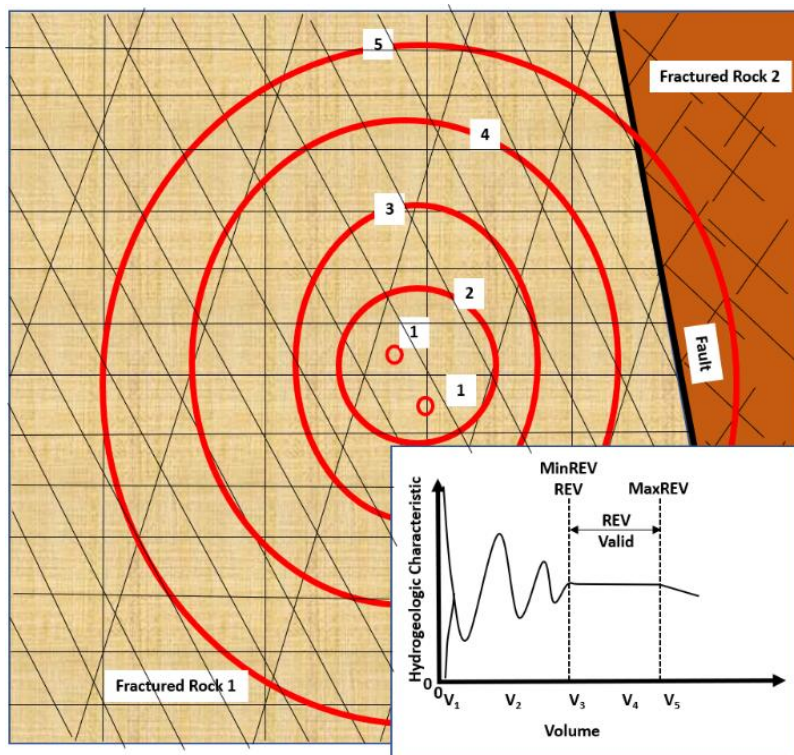


Figure 41 - Conceptualizing the REV for a fractured rock system when an equivalent hydraulic conductivity is to be used to represent the system. The red circles represent sampling of progressively larger volumes of fractured rock. V_1 represents a sample of either a fracture (black line) or the solid matrix. In this example a representative elementary volume is recognized at V_3 . Volumes larger than V_3 can be represented with the same equivalent property values until the volume is as large as V_5 . The V_5 sample volume includes an area with different fracture conditions.

The site can be conceptualized as an equivalent porous medium as long as the smallest unit of interest exceeds the volume of the REV. Figure 42 presents a conceptual model of a fractured volume of rock. Fractured rocks are typically anisotropic because of the directional variations in fractures and joints (Figure 42). In some cases, it is quite common for K_z to be greater than K_x because fractures oriented in the near vertical direction are common and tend to have larger apertures than those that are not as steep. Vertical fractures tend to have larger apertures because they do not respond to the weight of overlying material to the same degree as horizontal or fractures occurring at less than vertical orientations.

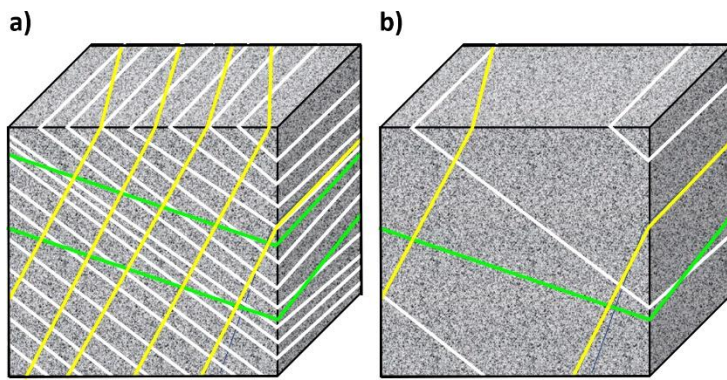


Figure 42 - Conceptual models of fractured media with white, yellow and green lines representing fractures. a) A system that is extensively fractured relative to the volume of material being investigated can be represented using an equivalent-porous-medium K and Darcy's law because groundwater flow would be similar to flow in porous media. b) A sparse fracture network cannot be well represented as an equivalent-porous-medium, so it is more appropriate to evaluate flow through individual fractures or fracture networks.

When the matrix hydraulic conductivity is minimal and groundwater is flowing through a sparse network of fractures or when groundwater transport of dissolved substances through fractures is of interest, it can be useful to determine the hydraulic conductivity of individual fractures or a fracture network (Figure 42b). For example, Snow (1968) developed an equation to estimate the equivalent hydraulic conductivity (and intrinsic permeability) of a medium with a parallel array of planar fractures (Equations 41 and 42) as shown in Figure 43. The aperture of the fractures, b , and the number of fractures per unit distance of rock face, N , are required to estimate K of the fractured system.

$$K_{\text{fracture set}} = \frac{\rho g}{\mu} N b^3 / 12 \quad (41)$$

where:

$K_{\text{fracture set}}$ = equivalent hydraulic conductivity of a fracture set (L/T)

N = the number of fractures per unit distance of rock face, $N = 1/\text{spacing}$ (s)
where spacing is the average distance between fractures (1/L)

b = fracture aperture (L)

ρ = fluid density (M/L³)

g = gravitational constant (L/T²)

μ = Dynamic viscosity M/(LT)

$$k_{\text{fracture set}} = N b^3 / 12 \quad (42)$$

where:

$k_{\text{fracture set}}$ = equivalent intrinsic permeability of a fracture set (L²)

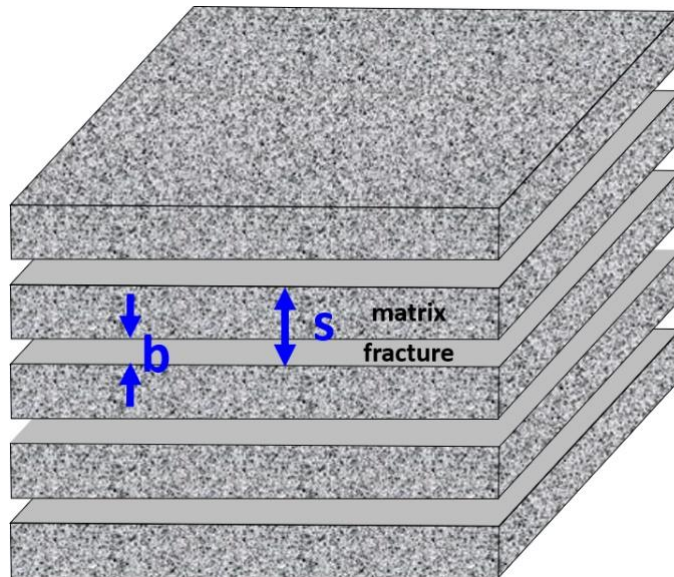


Figure 43 - Fracture aperture, b , and spacing between fractures, s . The number of fractures per unit length, $N = 1/s$.

In general, when conducting groundwater resource investigations, fractured rock systems are treated as equivalent pores media. When representations of flow in a fracture network are required, specialized groundwater modeling tools are applied. Additional information on the effect of fractures and structures on groundwater system properties and flow are provided in two Groundwater Project Books, “*Fractures and Faults in Sandstone and Sandstone-Shale/Mudstone Sequences and their Impact on Groundwater*” (Aydin, 2023) and “*Structural Geology Applied to Fracture Aquifer Characterization*” (Fernandes et al., 2023).

Even more challenging than evaluating fractured rock flow is characterizing flow in karst aquifers. This is discussed in the Groundwater Project book “*Introduction to Karst Aquifers*” (Kuniansky et al., 2022).

5.7 Exercises

[Exercise 4](#) provides an opportunity to consider the relative magnitude of hydrogeologic properties for different materials. [Exercise 5](#) explores estimating hydraulic conductivity from a laboratory apparatus. [Exercise 6](#) offers grain-size distribution data for estimating hydraulic conductivity.

6 Aquifers and Aquifer Properties

Of all the words in the hydrologic vocabulary, there are probably none with more shades of meaning than the term aquifer. It means different things to different people, and perhaps different things to the same person at different times. It is used to refer to individual geologic layers, to complete geologic formations, and even to groups of geologic formations. The term needs to be viewed in the scale and context of its usage.

An aquifer is a saturated, permeable, geologic unit that can transmit and store significant quantities of water under ordinary hydraulic gradients, and yield water to wells and springs in economically usable amounts (Freeze and Cherry, 1979). The overarching concept is that aquifers are saturated geologic materials that store and transmit water in sufficient quantities and rates such that they can be sources of water for humans. This concept is found in early definitions and the concept that an aquifer is permeable enough to yield economic quantities of water to wells has been embraced by the science and water well industry communities (Freeze and Cherry, 1979). The term is sometimes used loosely to represent all formations of earth materials that contain groundwater, but a saturated clay formation may contain groundwater yet fail to meet the requirements to yield sufficient water for use. In this case, it would not be classified as an aquifer. The definition of an aquifer does not recognize less productive groundwater systems that may support vital ecological systems, though such systems may be critical to human wellbeing. When economics are tied to the definition, a 1000 m deep groundwater system may be of value for supplying cooling water to an electrical generation plant and thus viewed as an aquifer by this industry, but may not be considered an aquifer by someone looking for agricultural water to irrigate a crop.

Geologic units that don't serve as aquifers are often referred to as aquitards, aquicludes or aquifuges. An aquifuge suggests that the material has no capacity to store or transmit water, it is impermeable. Though such settings may occur (e.g., a deep, unweathered granite), the term is not widely used. An aquiclude is a saturated geologic unit that has some storage and transmission properties, however, for practical purposes, no transmission occurs. Aquitards are units that store water and are less permeable than aquifers, so they slow the transmission of water. They may transmit water in regional layered flow systems where leakage passes through them from one aquifer to an overlying or underlying aquifer, yet their hydraulic conductivity is low enough that they cannot produce useful quantities of water. Modern usage has generally replaced the term aquitard with the term confining unit, confining bed and/or leaky confining unit. Most saturated geologic materials are classified as either aquifers or aquitards/confining units, rarely are units labeled aquiclude or aquifuges.

The most common aquifers are formations with hydraulic conductivity values in the upper half of the ranges shown in Figure 32. These include unconsolidated sands and gravels, limestones, and heavily fractured volcanic and crystalline rocks, and permeable

sedimentary rocks such as sandstones. The most common aquitards are silts, clays and shales.

It is recognized that the definitions of aquifer and aquitard are imprecise with respect to values of hydraulic conductivity. The terms are often used in a relative sense. For example, in layers of sand and silt, the sands are considered aquifers, whereas in layers of silt and clay, the silts may be considered aquifers.

Aquifers are often named for regions or associated formations. The High Plains or Ogallala Aquifer of the central United States is the largest aquifer in the world and is named after the town of Ogallala, Nebraska near the outcrop location of aquifer material. Other large aquifer systems include the Nubian Sandstone Aquifer System in Africa, the Arabian Aquifer system in the Middle-East, and the North China Aquifer. All of these aquifers provide critical water for humans, agriculture, and industries. An overview of major aquifer systems in the world is provided in the Groundwater Project book, "Large Aquifer Systems Around the World" (Van der Gun, et al., 2022).

Aquifer systems are often thought of as having uniform properties, thicknesses, and extent. However, heterogeneous and anisotropic properties with variable extent and thickness are nearly always the case. In the following discussion, simplified conditions are used to illustrate similarities and differences in aquifer types. There are three basic aquifer types: Unconfined, perched and confined.

6.1 Perched Aquifers

An unconfined aquifer can also occur as a perched aquifer. Most commonly, perched aquifers form and are maintained by recharge that accumulates on aquitards in the vadose zone. Perched groundwater forms above a layer of lower permeability material within the vadose zone where the migration of percolating recharge is slowed to the extent that it saturates the porous material above an aquitard (Figure 45). If sufficient water is available for the development of water supplies, then this is referred to as a perched aquifer. Otherwise, it is referred to as perched groundwater. The lower permeability layer also becomes partly saturated below the perched zone (Figure 45), returning to unsaturated conditions below the saturated zone. The water continues to flow slowly downward under unsaturated conditions through the rest of the aquitard and back into the underlying sediments. A line along which water pressure equals atmospheric pressure forms within, or at the base of the lens resulting in an inverted water table so the entire perched system is surrounded by a water table. Where perched groundwater systems intersect the land surface, groundwater discharges as spring flow.

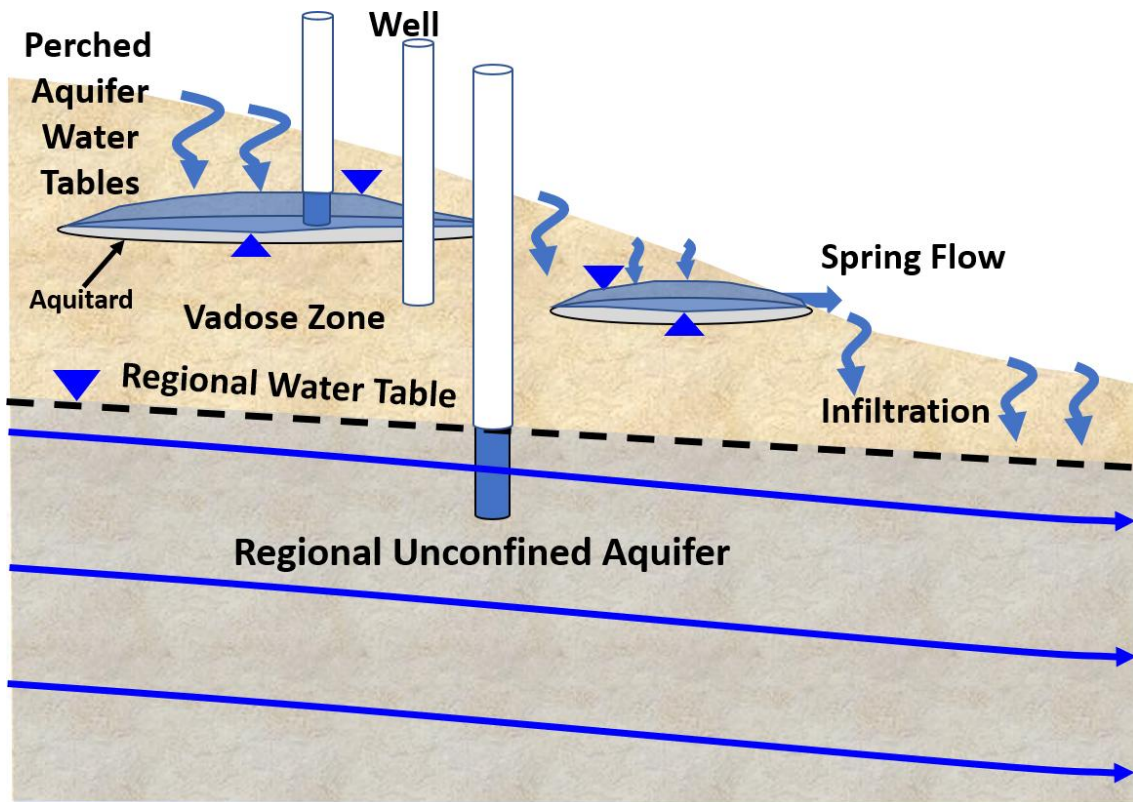


Figure 44 - Perched aquifers form on lower permeability lenses (gray) that are aquitards in the vadose zone. Precipitation infiltrates and percolates downward to the regional water table, but its progress is slowed by the presence of low permeability layers and, if sufficient infiltration occurs (solid blue arrows), the vadose zone sediments overlying the lens become saturated and a water table forms. As water leaks into the low permeable layer a portion of the aquitard becomes saturated and then flow reverts back to unsaturated conditions. A water table forms the lower boundary of the perched system (inverted triangles). The left well shows the presence of unconfined saturated perched conditions (perched groundwater flows into the well). A well that is sealed through the perched zone, but open to the vadose zone below is dry because pore spaces outside of the well bottom are filled with air and water, and the vadose water is in tension (pressures are less than atmospheric) so does not flow into the well. The well on the right is sealed through the vadose zone, but open to the regional unconfined aquifer.

6.2 Unconfined Aquifers

An unconfined aquifer, or water-table aquifer, is an aquifer with the water table as the upper boundary. The fluid pressure of water at the water table is equal to atmospheric pressure and the hydraulic head at the water table is equal to the elevation of the water table. The triangle in Figure 45 indicates the elevation of the water table.

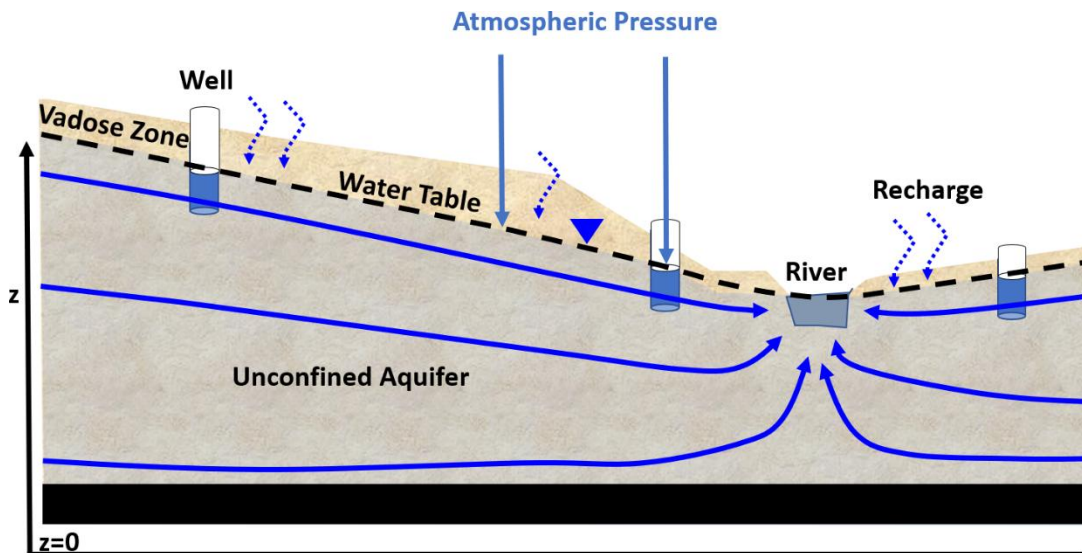


Figure 45 - Schematic of an unconfined aquifer. The upper surface is the water table (dashed black line) and the bottom boundary is typically a lower permeability unit (black bar). The water at the water table is at atmospheric pressure, $h_p = 0$, so the elevation head, z , represents the hydraulic head. Water levels in wells penetrating to depths just below the water table are shown. Recharge occurs to the water table from infiltration at the land surface (blue dashed arrows). The long solid blue arrows show general groundwater flow directions.

The term unconfined indicates there is free communication between the land surface and the water of the aquifer (Figure 44). These aquifers receive recharge from rainfall and melting snow; they are not overlain by a lower permeability unit that confines the movement of water within the aquifer. Water moves through the vadose zone and crosses the water table to become groundwater. The elevation of the water table changes in response to smaller or larger amounts of recharge, changes in rates of discharge, and the introduction or extraction of water (e.g., infiltration of surface irrigation water and pumping). When a borehole is advanced into the earth, the first groundwater encountered will be part of an unconfined aquifer. The water table may be many 10s to 100s of meters below the ground surface, especially in upland areas and arid regions. In lower areas, the water table will be near the surface where springs, rivers, wetlands and lakes occur.

6.3 Confined Aquifers

In contrast to unconfined aquifers, confined aquifers typically occur at depth (Figure 46). A confined aquifer is an aquifer that occurs beneath an aquitard which is often referred to as a confining bed. In a confined aquifer, the water level in tightly cased wells rises above the top elevation of the aquifer. Groundwater recharge entering the aquifer typically occurs at an outcrop area where hydraulic heads are higher than the elevation of the confined portion of the groundwater system as shown in Figure 46. When water flows into and through the confined aquifer, heads exceed the top elevation of the fully saturated confined aquifer zone. The overlying and underlying confining units constrain water from leaking out of the aquifer and direct flow parallel to the aquifer boundaries. The surface to which the water rises in wells and piezometers penetrating a confined aquifer is referred to as the potentiometric surface (Figure 46). Water movement is from areas where the

potentiometric surface is at a high elevation to where it is at a lower elevation. The potentiometric surface can also be used to describe head distributions in unconfined aquifers as it represents hydraulic head. When a potentiometric surface is presented it should include descriptors that state whether it is describing conditions in an unconfined or confined groundwater system.

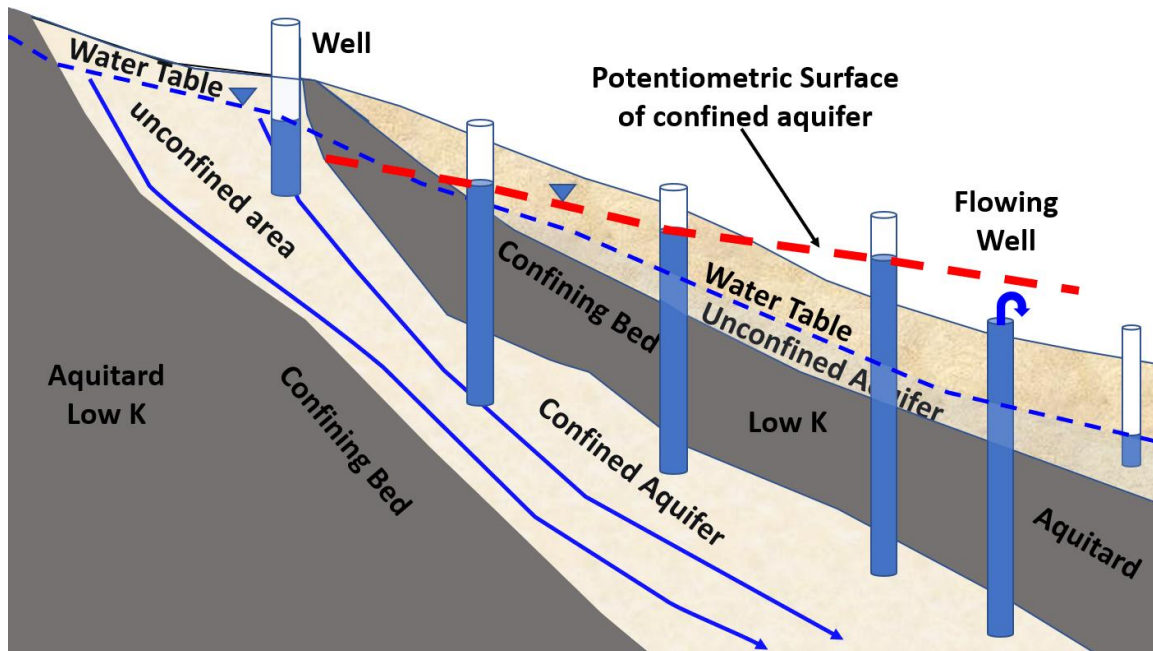


Figure 46 - Schematic of a confined aquifer. The aquifer is located between confining units (aquitards) of low hydraulic conductivity (gray). The recharge area is elevated, and groundwater flow moves into a geologic setting where the confining beds restrict the upward migration of water. Blue arrows indicate the general direction of groundwater flow. The water levels in tightly cased wells rise above the top of the confined aquifer. The surface representing total head in a confined aquifer is referred to as the potentiometric surface (dashed red line). Confined aquifer wells will flow at the land surface without pumping if the potentiometric surface is higher than the top of the well casing as shown by the rightmost confined aquifer well. Confined aquifers can be overlain by other confined aquifers, and, near the surface by an unconfined aquifer.

A confined aquifer can be simulated with a length of garden hose that is filled with water and sediment, then capped on one end. The saturated sediment represents the confined aquifer and the hose walls represent the “confining beds”. When the open end of the hose (aquifer recharge area) is raised, the potential energy of the system increases. Conditions in a confined aquifer are simulated by opening the capped end of the hose and feeding water into the upper end of the hose. If a hole is drilled in the hose (i.e., a “well” is installed) at some distance from the upper end water from the saturated sand system squirts out. By installing tall piezometers (hollow tubes) in the hose, the elevation of water in the piezometers measured from a horizontal datum represents hydraulic head data points of the potentiometric surface. The total head exceeds the height of the confining bed (hose wall) as shown in Figure 47.

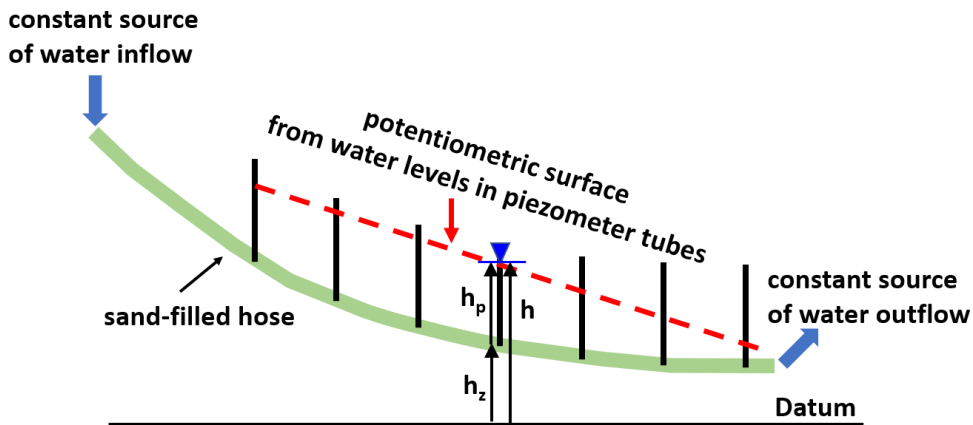


Figure 47 - Example of sediment-filled garden hose simulating a confined aquifer. The dashed red line represents the head distribution along the potentiometric surface.

Wells penetrating a confined aquifer are also called confined wells or artesian wells and the aquifer is said to exist under confined or artesian conditions. In some cases, the head in a confined aquifer may rise above the ground surface and the water level in the well casing will be higher than the elevation of the ground surface as shown for the two confined well furthest to the right in Figure 46. When this occurs, if the elevation of the top of the well casing is lower than the elevation of the potentiometric surface, water will flow freely from the well casing without pumping. This is referred to as a flowing well (Figure 46) or often as an artesian well. The term, artesian well, is associated with flowing wells constructed in the old Roman City of Artesium (currently the town of Artios in France) during the Middle Ages. The wells penetrated a confined aquifer and freely flowed at the surface. Based on a purely scientific definition, an artesian well is any well that penetrates a confined aquifer, whether it flows at the land surface or does not. However, artesian is commonly used for any flowing well whether or not it penetrates a confined aquifer. Flowing wells can also occur in discharge areas of unconfined aquifers when large upward gradients are present. Most commonly, wells penetrating a confined aquifer are described as confined wells. Additional information on flowing wells and the related hydraulics is provided in the Groundwater Project book "History and Hydraulics of Flowing Wells" (Jiang & Cherry, 2024).

6.4 Properties of Aquifers and Confining Units

The groundwater transmission and storage properties of geologic formations including aquifers and confining units can be described by three hydrogeologic terms: transmissivity, T ; specific storage, S_s ; and storativity, S .

Transmissivity

When describing the transmission capacity of a small representative volume of porous media the hydraulic conductivity is used. However, the capacity of an unconfined or confined aquifer to transmit water is described as transmissivity. Transmissivity is

defined as the product of hydraulic conductivity, K , and saturated aquifer thickness, b , as shown in Equation 43.

$$T = K b \quad (43)$$

where:

T = transmissivity, the capacity of an aquifer to transmit water (L^2/T)

b = saturated thickness of the aquifer (L)

The units of transmissivity are L^2/T . The term transmissibility is an outdated term that is occasionally used for transmissivity. Transmissivity describes the overall transmission capacity of an aquifer system, not just the properties of a small volume of the aquifer. For example, if the hydraulic conductivity of a confined aquifer is 100 m/d and the thickness is 10 m, then T is 1,000 m^2/d . If another aquifer has a hydraulic conductivity of 50 m/d and is 300 m thick, its transmissivity is $T = 15,000 m^2/d$. The higher T of the second aquifer indicates that it can transmit more water, thus if all else is equal, it would be a better target for a water supply well. Aquifers with multiple horizontal layers with different hydraulic conductivities can be represented by the sum of the T value for each layer.

The transmissivity of a confined aquifer of uniform thickness is a constant value for an isotropic and homogeneous set of conditions as shown in Figure 48a. By definition the head of a confined aquifer is higher than the top of the aquifer, so the complete thickness of the confined aquifer is saturated, thus b is a constant when T is determined. The saturated thickness of an unconfined aquifer varies with space as the water table slopes in the direction of flow, thus, T values change with distance from a given location (Figure 48b). When the water table slope is small, a single value of T is commonly used to represent the aquifer. In areas with large water table gradients, average thickness may be used to compute one representative value of T .

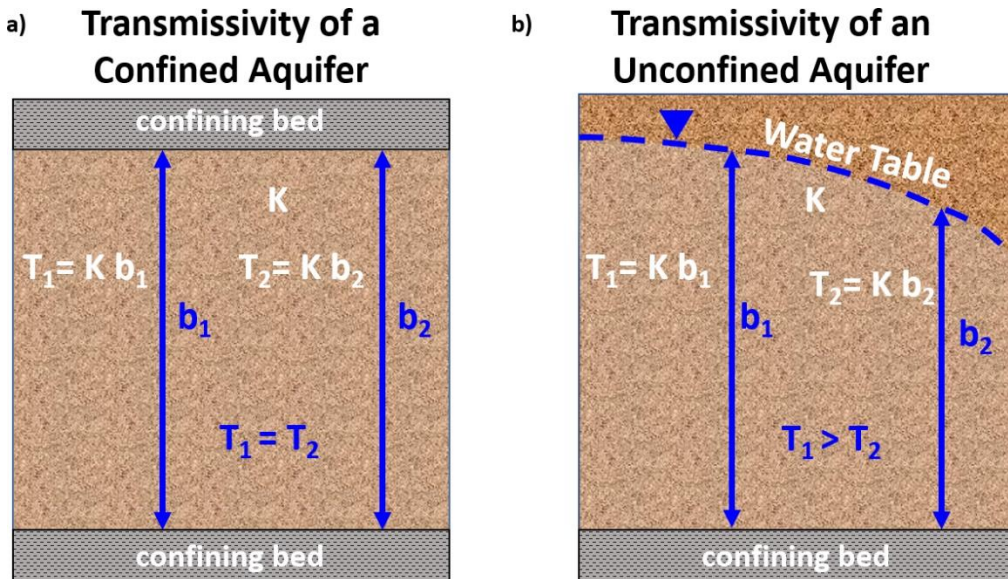


Figure 48 - Transmissivity, T , is the product of hydraulic conductivity, K , and saturated thickness, b , of the aquifer. a) In a confined aquifer of uniform geologic thickness, saturated thickness, b , is constant ($b_1 = b_2$) even when the hydraulic head is different. b) In an unconfined aquifer, transmissivity needs to be defined at a specified location because saturated thickness depends on the hydraulic head (e.g., based on the elevation of the water table). Head of an unconfined aquifer decreases in the downgradient flow direction, so saturated thickness decreases ($b_1 > b_2$) and so does transmissivity ($T_1 > T_2$).

Transmissivity values are often estimated by combining K values from laboratory tests or textbook tables with field measurements of aquifer thickness, b . Most commonly, T values are determined from carefully designed aquifer tests where wells are pumped while water levels are measured in nearby observation wells. These data are then analyzed using analytical equations and/or numerical computer simulations to estimate transmissivity values (e.g., Lohman, 1972).

Storativity

The storage capacity of an aquifer is referred to as the storativity, S . The older term, storage coefficient, is also used to describe the same aquifer storage property. Storativity describes the capacity of an aquifer to store or release water. It is defined as the volume of water removed or stored per unit change in head normal to the earth's surface over a unit area. Storativity is dimensionless and is expressed as a decimal.

Unconfined Aquifer Storativity

The storativity for an unconfined aquifer is dominated by the gravity drainage term, specific yield (S_y). Specific yield reflects the volume of water that drains by gravity when the water table is lowered, or fills with water when the water table is raised (Figure 49). The storativity (S) of an unconfined aquifer is composed of two components as shown in Equation 44.

$$S_{unconfined} = S_y + S_s b_{average} \quad (44)$$

where:

$S_{unconfined}$ = storativity of an unconfined aquifer (dimensionless)

S_y = specific yield (dimensionless)

S_s = specific storage ($1/L$)

$b_{average}$ = average thickness before and after a water level change (L)

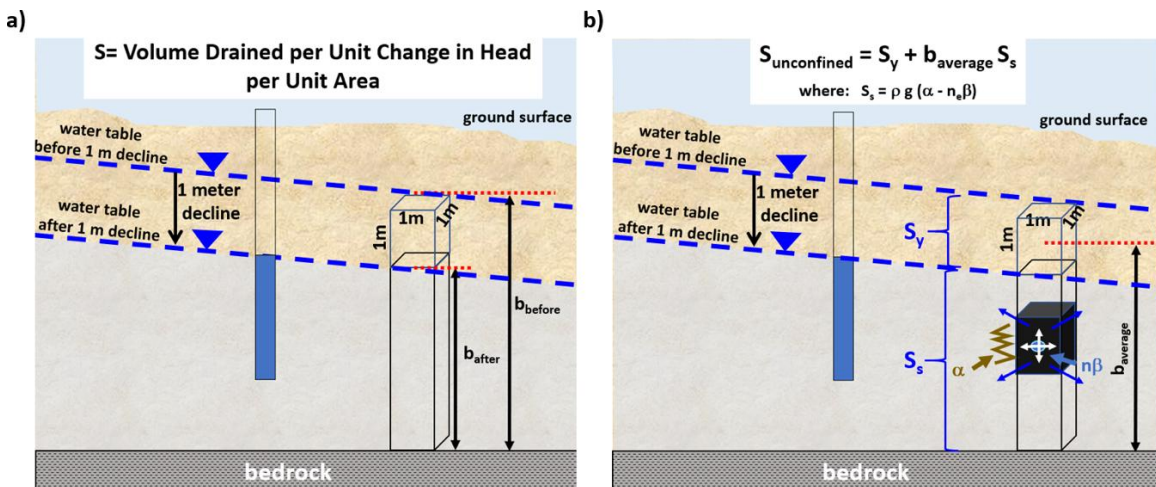


Figure 49 - Schematic of components of storativity (S) of an unconfined aquifer. a) Illustration of the definition of the storage coefficient, which is the volume of water released from, or added to, storage per unit change in head normal to the earth's surface per unit area. b) As the water table is lowered 1 meter, the volume of water released per cubic meter of unconfined aquifer is almost entirely accounted for by water that drains from pores as described by specific yield, S_y . The portion of the aquifer that underlies the drained portion also yields a small quantity of water (small blue arrows in black volume) in response to the reduced weight (because water drained from pores) of the overlying water. The structure of the solids (black volume) compresses (reducing the volume of pore space) as indicated by the compressibility of the aquifer skeleton, α , (jagged vertical line). In addition, there is a small expansion of the slightly compressible water, $n\beta$, (blue dot and white arrows). This property of the aquifer is called specific storage, S_s . The volume of water released from gravity drainage is orders of magnitude larger than the volume squeezed from the saturated portion of the aquifer, $S_s b_{average}$. As a result, S_y is used to represent unconfined aquifer storativity.

The specific yield is the volume of water that can drain by gravity from a saturated volume of material divided by the total volume of that material. The fractional volume of water that remains in the sample is called specific retention (S_r). It is assumed that, when water is added to storage and the water table rises, the pore spaces that fill already contain only the volume of water indicated by the value of specific retention.

The second term of Equation 44 is the product of the specific storage (S_s) and the average of saturated thickness before and after drainage ($b_{average}$). The specific storage is defined as the volume of water that is released from (or added to) storage per unit volume of saturated material. When multiplied by the saturated thickness it accounts for a small amount of water that is released from a unit area of aquifer in response to the relief of stress on the material below the drained pores. When the head declines the water that is released

from saturated storage through the column of aquifer underlying drained pores is produced by two mechanisms: (1) the compaction of the aquifer (reduction in pore volume) caused by an increase in the effective stress, σ_e , and (2) the expansion of the water caused by decreased pore water pressure. Effective stress is the difference between the total pressure exerted by the overlying material (soil/rock and water combined) minus the pore water pressure. An increase in pore water pressure lifts the grains of the aquifer skeleton thus relieving the stress of the overlying material on the grains. The first of the mechanisms that releases water from an aquifer for a head decline is controlled by the aquifer compressibility, α , and the second by the fluid compressibility, β . The volume of water in the porous medium is dependent on the effective porosity, n_e . The resulting equation for S_s is Equation 45.

$$S_s = \rho g (\alpha + n_e \beta) \quad (45)$$

where:

S_s = specific storage (1/L)

α = compressibility of the aquifer solid structure ($T^2 L/M$)

n_e = effective porosity (dimensionless)

β = compressibility of water ($T^2 L/M$)

To account for the thickness of saturated media that is affected by the change in pore water pressure and the consolidation of the aquifer skeleton, the specific storage is multiplied by the average saturated thickness for the given water table decline, $b_{average}$ (Figure 49), resulting in a dimensionless storativity term as shown in Equation 46.

$$S_{unconfined} = S_y + S_s b_{average} = S_y + b_{average} \rho g (\alpha + n_e \beta) \quad (46)$$

where:

$S_{unconfined}$ = Storativity of an unconfined aquifer (dimensionless)

The compressibility of water is small, $4.4 \times 10^{-10} \text{ m}^2/\text{N}$ (N is a Newton = 1 (kg m)/s²) and the compressibility of earth materials ranges from 1×10^{-11} to $1 \times 10^{-6} \text{ m}^2/\text{N}$ (Table 4). The scale of the $S_s b_{average}$ term is illustrated with this example. For an unconfined sand aquifer with a compressibility on the higher end of the range, $\alpha = 1 \times 10^{-8} \text{ m}^2/\text{N}$, an effective porosity of 0.24, a water density of 1 kg/m^3 and with $g = 9.8 \text{ m/s}^2$, then the specific storage (Equation 45) is $1 \times 10^{-7}/\text{m}$. If the aquifer is 60 m thick then the storage term related to the remaining saturated aquifer (Equation 46) is 6×10^{-6} . The computed $S_s b_{average}$ value is more than three orders of magnitude smaller than the S_y , given typical specific yields of earth materials range from 0.05 to 0.40, so the storativity term for the unconfined aquifer can be set equal to S_y and the $S_s b_{average}$ term can be ignored as presented in Equation 47.

$$\text{simplified} \quad S_{unconfined} = S_y \quad (47)$$

In fact, when S_y is obtained by a field test involving pumping a well and observing the changing water levels in nearby observation wells, the volume of water from $S_s b_{average}$

is “built in” to the interpreted S_y value (e.g., Lohman, 1972). Equation 47 is typically used to represent specific yield.

Table 4 - Range of values of compressibility of earth materials and water (after Domenico and Mifflin, 1965; Freeze and Cherry, 1979).

Compressibility of Some Common Earth Materials	
Material	Compressibility (meter⁻²/Newton)
Geologic Type	Range of Compressibility α
Clay	$1 \times 10^{-6} - 1 \times 10^{-8}$
Sand	$1 \times 10^{-7} - 1 \times 10^{-9}$
Gravel	$1 \times 10^{-8} - 1 \times 10^{-10}$
Jointed Rock	$1 \times 10^{-8} - 1 \times 10^{-10}$
Sound Rock	$1 \times 10^{-9} - 1 \times 10^{-11}$
Fluid	Compressibility β
water	4.4×10^{-10}

The volume of water removed from or added to aquifer storage over an area, A , for a change in head, Δh , is determined as shown in Equation 48. For a specific yield of 0.18, if the water table declined 1 meter over a 1 square meter area, then 0.18 cubic meters would drain from the aquifer. If the area were instead 1 km², then 180,000 cubic meters would drain from the aquifer.

$$\text{Volume of Unconfined Water for a change in head} = S_y A \Delta h \quad (48)$$

where:

$Volume$ = volume drained from an unconfined aquifer over an area, A , for a water table elevation change of Δh (L³)

S_y = specific yield (dimensionless)

A = area over which the water table changes (L²)

Δh = change in water table elevation (L)

Confined Aquifer Storativity

The storativity of a confined aquifer is defined as the volume of water released from, or added to, storage per unit change in head normal to the surface, per unit area. This is the same definition as for unconfined aquifers. The difference between the storage capacity in an unconfined aquifer and a confined aquifer is that in the confined aquifer the entire aquifer remains saturated when a unit change in head occurs (Figure 50). As a result, no gravity drainage occurs and all the water that leaves or enters storage is derived from the specific storage term, S_s , times the saturated thickness, b , as shown in Equation 49.

$$S_{\text{confined}} = S_s b = b \rho g (\alpha + n_e \beta) \quad (49)$$

where:

S_{confined} = storativity of a confined aquifer (dimensionless)

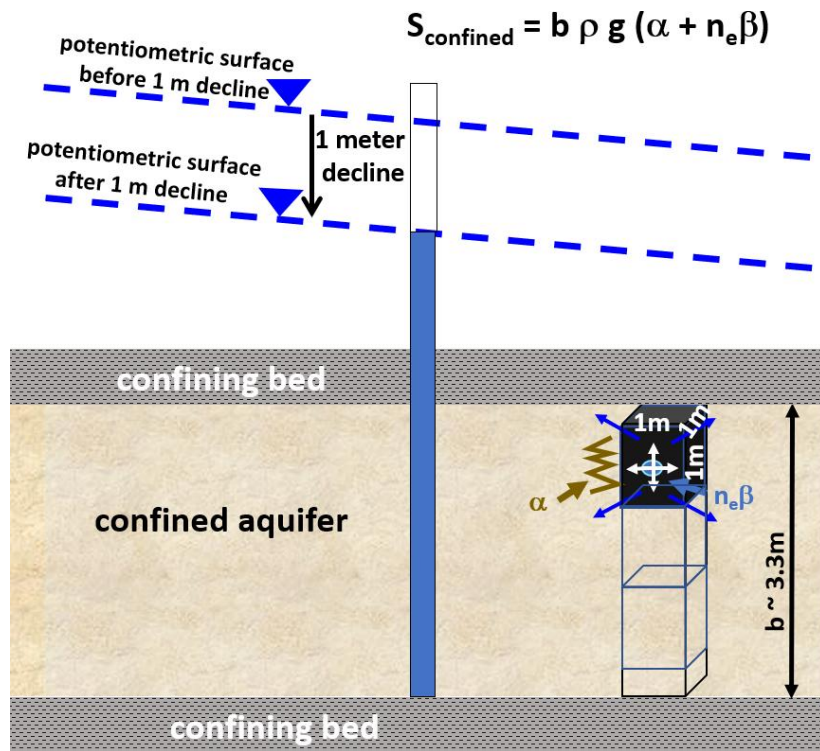


Figure 50 - Schematic of the parameters controlling storativity, S , of a confined aquifer. The aquifer remains fully saturated as a unit change in the potentiometric surface occurs. Water is released from the entire saturated thickness, b , of the aquifer by compression of the skeleton, α (jagged line), and expansion of the pore water (blue arrows), $n_e\beta$.

The specific storage of a confined aquifer can be computed as described Equation 45, with $S_y = 0$. This value is then multiplied by aquifer thickness to obtain storativity (Equation 49). Storativity of confined aquifers typically range from 0.00001 to 0.001 (1×10^{-5} to 1×10^{-3}). Lohman (1972) suggests the storativity for a confined aquifer can be approximated as $0.0000033/\text{m}$ ($0.000001/\text{ft}$) times the aquifer thickness in meters. Most commonly, site and regional scale confined aquifer storativity values are derived from carefully designed aquifer tests where the aquifer is pumped for a period of time and the response the total head distribution monitored (e.g., Lohman, 1972). Wang (2020) provides a summary of groundwater storage in confined systems in the Groundwater Project book, “[Groundwater Storage in Confined Aquifers](#)”.

The volume of water removed from or stored in a confined aquifer over an area, A , for a change in head, Δh , is determined as shown in Equation 50. For a storativity of 0.00001, if the potentiometric surface declined 1 meter over a 1 square meter area, then 0.00001 cubic meters would be released from the aquifer. If the area were instead 1 km^2 , then 10 cubic meters would be released from the aquifer. The volume of water released from a confined aquifer for a given head decline is substantially less than the volume released from an unconfined aquifer for the same head decline. This is because the water comes only from the compression of the aquifer framework and expansion of water in response to the pressure change rather than from drainage of pore spaces.

$$\text{Volume of Confined Water for a change in head} = SA\Delta h \quad (50)$$

where:

Volume = volume drained from a confined aquifer for a hydraulic head change,

Δh , over an area, A (L^3)

S = storativity (dimensionless)

A = area over which the head change occurs (L^2)

Δh = change in head (L)

6.5 Exercises

[Exercise 7](#) considers pore pressure and effective stress. [Exercise 8](#) provides an opportunity to think about the units of specific storage. [Exercise 9](#) involves estimating the volume recharge based on head changes and storage properties. [Exercise 10](#) suggests a sketch to facilitate understanding of aquifer types and gradients. [Exercise 11](#). Provides an opportunity to calculate the volume delpted from an aquifer given head change and storage properties.

7 Equations of Groundwater Flow

In almost every field of science and engineering the techniques of analysis are based on an understanding of the physical processes, and in most cases, it is possible to describe these processes mathematically. Hydrogeology is no exception. Mathematical relationships describing groundwater flow are the foundation used to develop quantitative equations and models for specific groundwater systems and sites. In the previous 6 Sections of this book, principles and definitions have been presented which will be used to develop groundwater flow equations. These include the concepts of the representative elementary volume (REV), Darcy's Law, head, gradient, hydraulic conductivity, transmissivity and storativity. These concepts are used in conjunction with the equation that describes conservation of mass (water) (e.g., mass inflow = mass outflow + change in mass storage) to develop universal mathematical equations that describe groundwater flow under various conditions. Readers may find it helpful to review material in the Groundwater Project book "[Introduction to Fluid Mechanics for Groundwater Scientists](#)" (Klammler, 2023).

The basic law governing groundwater flow in a porous medium is Darcy's Law which describes the relationships between discharge, Q , or flux, q , and the hydraulic conductivity, gradient (head per distance) and cross-sectional area. When Darcy's Law is combined with an equation of continuity that describes the conservation of fluid (water) mass, then the universal equations governing groundwater flow are formulated. Though the mathematics, which use partial differential equations, may appear daunting, it is straight forward. The equation development presented here starts with groundwater flow in one dimension and then introduces the same equations in three dimensions.

To apply these general equations to a particular groundwater problem, a problem domain, they are constrained to specific conditions by assigning site boundary conditions and, in some cases, initial conditions, that represent a particular groundwater setting. Analytical solutions and computer simulation are tools of the groundwater industry that incorporate the governing equations presented here making the equations accessible to groundwater professionals. These tools are used to quantify groundwater behavior in a wide variety of hydrogeologic settings under varied conditions. Some examples of the application of these tools to solve groundwater problems are presented in Section 7.5. It is important to understand the underlying assumptions and simplifications used to formulate methods used to solve groundwater problems. The goal of this section is to present the governing equations and explain those assumptions and simplifications.

7.1 Basis for Flow Equation Development

General groundwater flow equations are often referred to as governing equations because they describe the factors that control (i.e., govern) groundwater flow. The equations are based only on Darcy's Law and the continuity equation for the conservation of mass (of water).

Development of the governing equations is typically accomplished by conceptualizing groundwater flow through a small volume of fully saturated porous material (REV) that reflects overall hydrogeologic properties of a larger deposit. It can be visualized as a cube of porous material of sufficient size ($\Delta x, \Delta y, \Delta z$) to encompass macroscopic properties governing groundwater flow (Figure 4 and Figure 51). The mass of water within the REV (M) depends on the density of the water, the porosity of the element (assuming all pores spaces are fully connected), and the volume of the block as shown in Equation 51. Under steady-state flow conditions, the mass of water in the REV is constant, inflow equals outflow, and heads, gradients and flow rates do not vary with time (Figure 51a). When flow is transient, the mass of water in the REV varies with time, inflow does not equal outflow, and heads, gradients, and flow rates vary with time (Figure 51b).

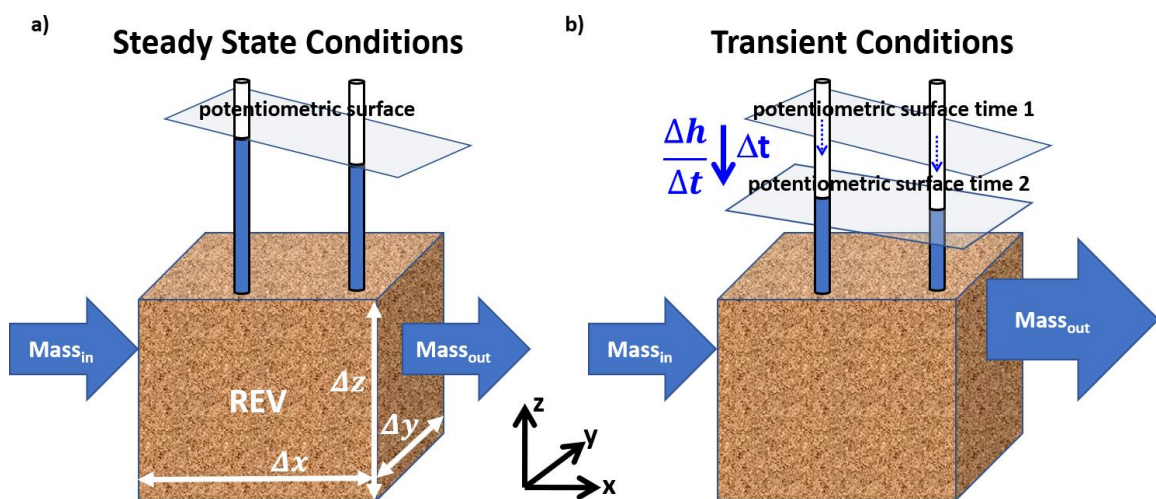


Figure 51 - A small, but representative, volume called a Representative Elementary Volume (REV) of a porous medium has dimensions $\Delta x, \Delta y, \Delta z$. The confined fully saturated cube of porous material reflects the general properties of a porous earth material. Flow is from left to right. The volume is fully saturated. a) REV for confined steady-state conditions, the gradient (potentiometric surface, illustrated as the light blue plane) does not change with time, mass flow is constant and mass inflow equals mass outflow. b) REV for confined transient conditions, the gradient represented by the potentiometric surface (blue plane) changes with time, Δt , the flow rate varies with time, mass inflow does not equal mass outflow, and the mass of water (M) in the REV changes with time.

$$M = \rho n \Delta x \Delta y \Delta z \quad (51)$$

where:

M = mass of water in the REV (M)

ρ = density of water in the REV (M/L³)

n = fully connected porosity (n_e) of the REV (dimensionless)

$\Delta x, \Delta y, \Delta z$ = length of each side of the REV (L)

7.2 Governing Equations for Confined Transient Groundwater Flow

The law of conservation of mass for flow through a saturated porous medium requires that the flux of fluid mass into the volume equals the flux of fluid mass out of the

volume plus the change in mass stored within the volume. Darcy's Law is represented by the specific discharge, q . The mass flux is ρq (Equation 52).

$$\text{Mass Flux} = \rho q \quad (52)$$

where:

Mass Flux = mass of water passing through a unit area per unit time ($M/(L^2T)$)

ρ = density of water (M/L^3)

q = specific discharge (L/T)

One-dimensional Flow

Governing equations describing groundwater flow are most often presented as representing steady state or transient conditions, and flow in two- or three-dimensional space. However, especially for readers who are not as familiar with differential equations, it is useful to consider one-dimensional flow (along the x axis) through a REV first (Figure 52). The mass flux into the REV is the product of the specific discharge and the fluid density (item 1 of Figure 52). If the head is declining, then water is coming out of storage from the porous medium and the mass flux will increase across the REV as shown in item 2 of Figure 52. Multiplying the slope of the mass-flux-vs-distance graph by the distance across the REV (Δx) determines the increase in mass flux from left to right (item 3 of Figure 52). Adding that increase of flux across the element to the influx produces the outflux (item 4 of Figure 52). It is useful to recall that a flux has units of velocity (L/T) because it is a flow rate L^3/T divided by the area of flow ($L^3/T)/(L^2)$.

The fluxes in and out of the element in Figure 52 are shown in Equations 53 and 54 respectively.

$$\text{Mass Flux In} = \rho q_x \quad (53)$$

$$\text{Mass Flux Out} = \rho q_x + \frac{\Delta(\rho q_x)}{\Delta x} \Delta x \quad (54)$$

where:

Mass Flux = mass of water passing through a unit area per unit time ($M/(L^2T)$)

ρ = density of water (M/L^3)

q_x = specific discharge (L/T)

Δx = length of the elementary volume in the x direction (L)

Change in Mass Flux across an REV with 1D Flow

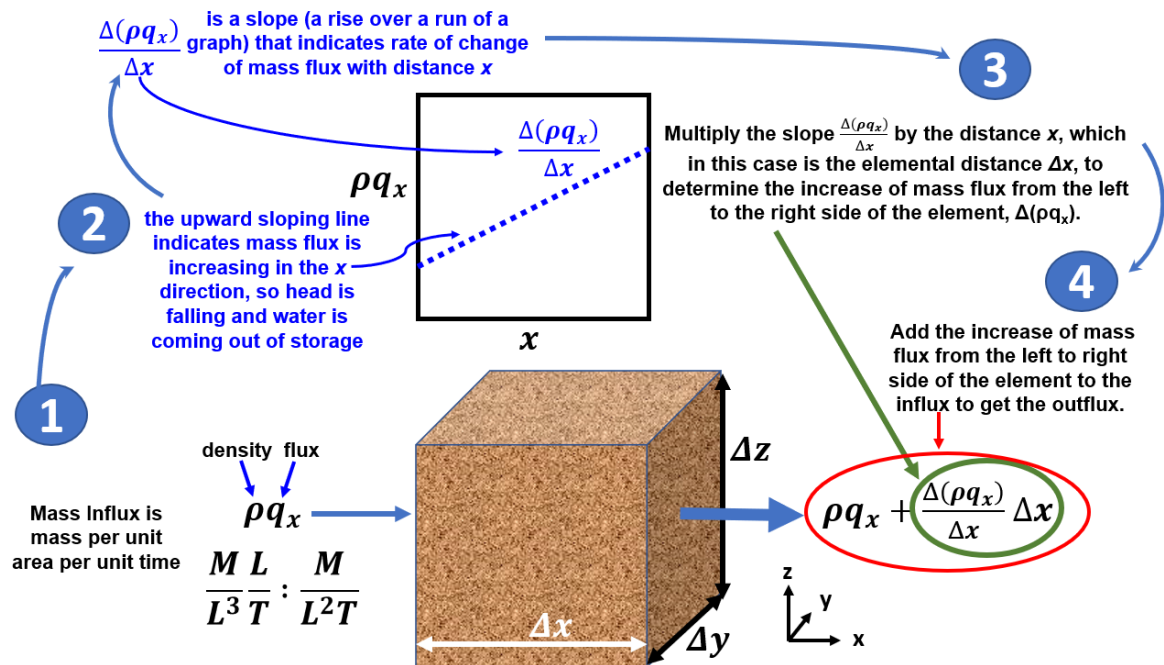


Figure 52 - Change in mass flux through a representative elementary volume of a porous material with one-dimensional flow.

Mass flow rate is obtained by multiplying the fluxes by the cross-sectional area of the elementary volume that they pass through (for one-dimensional flow in the x direction, the area is $\Delta y \Delta z$), as in Equations 55 and 56.

$$\text{Mass Flow In} = (\rho q_x) \Delta y \Delta z \quad (55)$$

$$\text{Mass Flow Out} = \left(\rho q_x + \frac{\Delta(\rho q_x)}{\Delta x} \Delta x \right) \Delta y \Delta z \quad (56)$$

where:

Mass Flow = mass of water passing into, or out of, an REV per unit time (M/T)

$\Delta y, \Delta z$ = length of the elementary volume in the y and z directions (L)

Next, the change in the inflow is examined using and analysis of the inward flow of mass. The inward flow of mass is defined as mass inflow minus outflow, a positive value of inward flow of mass indicates that the inflow exceeds the outflow and water is going into storage, while a negative value indicates outflow exceeds inflow and water is coming out of storage. The inward flow of mass is determined by subtracting the outflow (Equation 56) from the inflow (Equation 55) as shown in Equation 57.

$$\text{Inward Flow of Mass} = (\rho q_x) \Delta y \Delta z - \left(\rho q_x + \frac{\Delta(\rho q_x)}{\Delta x} \Delta x \right) \Delta y \Delta z \quad (57)$$

where:

Inward flow of Mass = mass of water flowing into the elementary volume per unit time
(M/T)

Expanding the second term of Equation 57 and subtracting yields Equation 58. The negative sign indicates that water is coming out of groundwater storage, thus inward flow of mass is negative.

$$\text{Inward Flow of Mass} = -\frac{\Delta(\rho q_x)}{\Delta x} \Delta x \Delta y \Delta z \quad (58)$$

Given that the inward flow of mass is the increase in mass in the element per unit time and mass must be conserved, then the inward mass flow per unit time must equal the change in mass storage per unit time. Recall that specific storage is the change in volume of water stored in a unit volume of aquifer for a change in head, so the change in volume with time is shown as Equation 59.

$$\frac{\Delta V}{\Delta t} = \rho g(\alpha + n\beta) \Delta x \Delta y \Delta z \frac{\Delta h}{\Delta t} \quad (59)$$

where:

ΔV = change in volume of water in the REV (L^3)

ρ = density of water in the REV (M/L^3)

g = gravitational constant (acceleration of gravity) (L/T^2)

α = compressibility of the aquifer solid structure ($L^3/L^3)/(F/L^2)$, inverse pressure

β = compressibility of water ($L^3/L^3)/(F/L^2)$, inverse pressure

n = fully connected total porosity (n_e) of the REV (dimensionless)

The change in stored mass for a unit of time is obtained by the product of Equation 59 and the water density (Equation 60).

$$\frac{\Delta M}{\Delta t} = \rho \left(\rho g(\alpha + n\beta) \Delta x \Delta y \Delta z \frac{\Delta h}{\Delta t} \right) \quad (60)$$

where:

ΔM = change in mass of water in the REV (M)

Equating the change in mass storage (Equation 60) with the inward flow of mass (Equation 58) produces Equation 61.

$$\rho \left(\rho g(\alpha + n\beta) \Delta x \Delta y \Delta z \frac{\Delta h}{\Delta t} \right) = -\frac{\Delta(\rho q_x)}{\Delta x} \Delta x \Delta y \Delta z \quad (61)$$

Although it is recognized that the water density changes slightly in response to head changes (i.e., pressure changes), the amount of compression or expansion is small enough to assume constant density for the vast majority of applications so, ρ , can be taken out of the delta-term due to its minimal change with time (Equation 62).

$$\rho \left(\rho g(\alpha + n\beta) \Delta x \Delta y \Delta z \frac{\Delta h}{\Delta t} \right) = -\rho \frac{\Delta q_x}{\Delta x} \Delta x \Delta y \Delta z \quad (62)$$

Dividing both sides by ρ and by $\Delta x \Delta y \Delta z$, then substituting the specific storage, S_s , for $\rho g(\alpha + n\beta)$ provides Equation 63.

$$S_s \frac{\Delta h}{\Delta t} = - \frac{\Delta q_x}{\Delta x} \quad (63)$$

The specific discharge can be represented by Darcy's Law, where $q_x = -K_x \Delta h / \Delta x$, assuming the principal direction of the component of hydraulic conductivity is aligned with the x-axis, as represented in Equation 64.

$$S_s \frac{\Delta h}{\Delta t} = - \frac{\Delta}{\Delta x} \left(-K_x \frac{\Delta h}{\Delta x} \right) \quad (64)$$

The Δ 's in the equation describe discrete changes across a small elementary volume. This allows translation of this relationship into a differential form when the discrete change is infinitesimal by replacing Δ with d , providing the derivative of a smooth function (Equation 65).

$$S_s \frac{dh}{dt} = - \frac{d}{dx} \left(-K_x \frac{dh}{dx} \right) \quad (65)$$

Equation 65 is the governing equation for confined, one-dimensional, transient, heterogeneous conditions of groundwater flow. Equation 65 can also be written as Equation 66.

$$S_s \frac{dh}{dt} = \frac{d}{dx} K_x \frac{dh}{dx} \quad (66)$$

Three-dimensional Flow

In most cases, the flux will not be one-dimensional along the x-axis. It will occur in an arbitrary direction with a component in each of the x, y, and z directions (see for example Section 5.4), thus the change in mass flux across the element needs to be accounted for in each of the three-dimensions as shown in Figure 53. The partial differential symbol ($\frac{\partial}{\partial x}$) is used in order to represent that only a part of the change in flux across the element occurs in the x direction, as there are also changes in the y- and z-directions ($\frac{\partial}{\partial y}, \frac{\partial}{\partial z}$); and when the system is transient, with time, $\frac{\partial}{\partial t}$. The groundwater flow equation for three-dimensional flow is the same as the equation for one-dimensional flow with additional flux terms for the y- and z-directions.

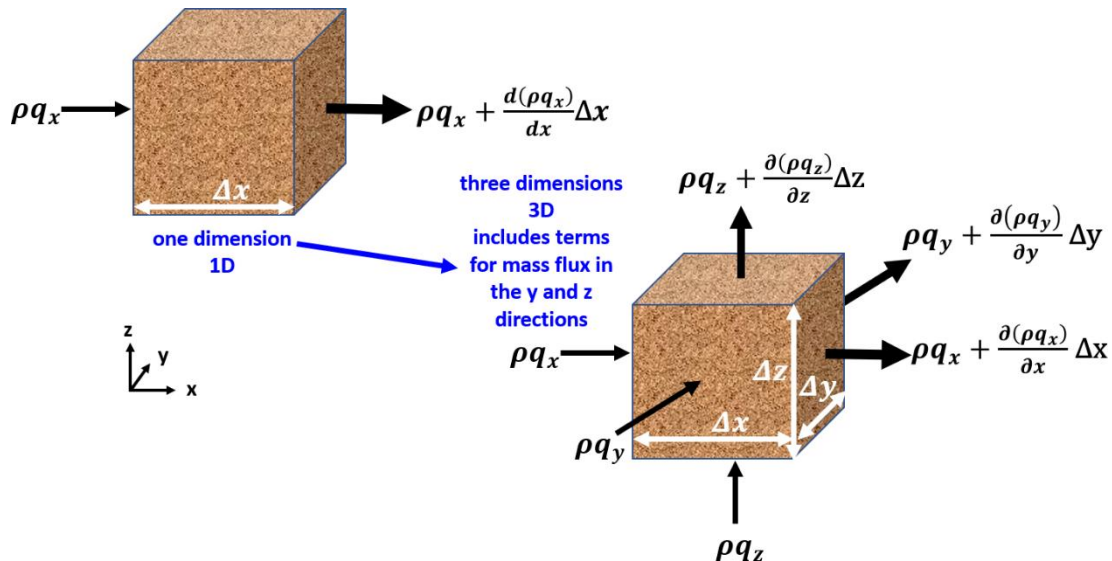


Figure 53 - Representative Elementary Volume showing three-dimensional mass influx and outflux (e.g., ρq_x) and an addition or loss of mass flux in the outflow (e.g., $(+\frac{\partial \rho q_x}{\partial x} \Delta x)$). This schematic represents confined conditions.

Confined, three-dimensional, transient, anisotropic, heterogeneous conditions of groundwater flow are represented by Equation 67.

$$S_s \frac{\partial h}{\partial t} = \frac{\partial}{\partial x} \left(K_x \frac{\partial h}{\partial x} \right) + \frac{\partial}{\partial y} \left(K_y \frac{\partial h}{\partial y} \right) + \frac{\partial}{\partial z} \left(K_z \frac{\partial h}{\partial z} \right) \quad (67)$$

When the values of K_x , K_y and K_z are constants (but not the same value) they can be taken out of the derivative resulting in Equation 68. It describes **confined, three-dimensional, transient, anisotropic, homogeneous** conditions of groundwater flow.

$$S_s \frac{\partial h}{\partial t} = K_x \frac{\partial^2 h}{\partial x^2} + K_y \frac{\partial^2 h}{\partial y^2} + K_z \frac{\partial^2 h}{\partial z^2} \quad (68)$$

For **confined, three-dimensional, transient, isotropic and homogeneous** conditions of groundwater flow, $K_x = K_y = K_z = K$, thus one value of K is sufficient to represent the hydraulic conductivity and Equation 69 is formulated.

$$S_s \frac{\partial h}{\partial t} = K \left(\frac{\partial^2 h}{\partial x^2} + \frac{\partial^2 h}{\partial y^2} + \frac{\partial^2 h}{\partial z^2} \right) \quad (69)$$

For **confined, two-dimensional (plan view), transient, isotropic, homogeneous** conditions in an aquifer of constant thickness, the z -terms for vertical flow can be omitted from Equation 69. Also, saturated thickness, b , is not dependent on head, h , (Figure 54) and assuming the aquifer thickness is constant, both sides of Equation 69 can be multiplied by the aquifer thickness leading to Equation 70 that represents horizontal flow in a map view.

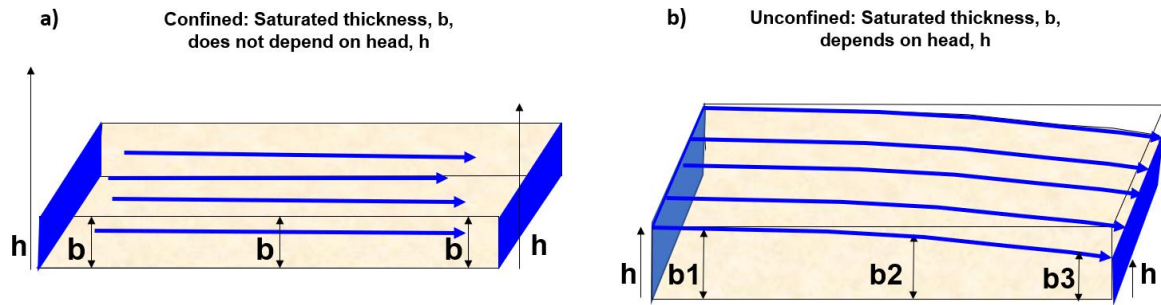


Figure 54 - Saturated thickness of confined and unconfined aquifers. a) For confined flow, the saturated thickness remains constant and is independent of hydraulic head, so the flow equations can use b for thickness. b) For unconfined flow conditions, saturated thickness depends on head as the water table surface slopes, so thickness is equal to head if the bottom of the aquifer is used as the datum for head measurements.

$$S_s b \frac{\partial h}{\partial t} = Kb \left(\frac{\partial^2 h}{\partial x^2} + \frac{\partial^2 h}{\partial y^2} \right) \quad (70)$$

Then, by using the definition of transmissivity, T , as Kb and storativity, S , as $S_s b$, Equation 70 can be written as Equation 71.

$$S \frac{\partial h}{\partial t} = T \left(\frac{\partial^2 h}{\partial x^2} + \frac{\partial^2 h}{\partial y^2} \right) \quad (71)$$

Equation 70 and Equation 71 represent groundwater flow under confined, two-dimensional (plan view), transient, homogeneous and isotropic conditions using S and T.

7.3 Governing Equations for Unconfined Groundwater Flow

Unconfined flow equations are non-linear in that the transmissivity of the aquifer depends on the saturated thickness and the saturated thickness varies in the direction of flow because the water table slopes. By definition, a confined aquifer is fully saturated, so transmissivity values are constant for a confined aquifer of constant thickness. Under water table conditions the water table slopes, flow is parallel to the water table and the saturated thickness decreases in the direction of flow (Figure 55). If the slope of the water table is small, Darcy's Law can be applied to develop governing equations by using the Dupuit simplification or Dupuit assumptions. Dupuit's simplification uses the approximate gradient (dh over the distance x , $\frac{dh}{dx}$) rather than the true gradient (dh over the flow path length, $\frac{dh}{dl}$) by assuming the flow is horizontal (no vertical components of flow) as shown by the solid arrows in Figure 55 and by Equation 72.

$$Q = -K \frac{dh}{dx} A \text{ rather than } Q = -K \frac{dh}{dl} A \quad (72)$$

Expressing the flow area as the product of the height of the water table and the unit width of the system in the y direction, the flow is shown in Equation 73.

$$Q = -K \frac{dh}{dx} h \Delta y \quad (73)$$

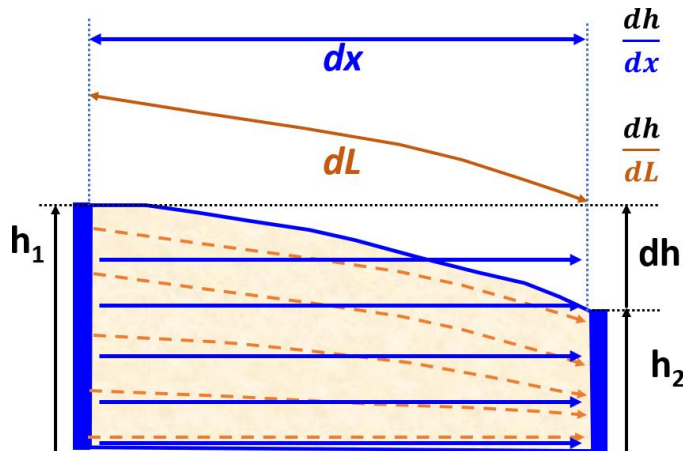


Figure 55 - Dupuit's simplification mathematically approximates unconfined flow as horizontal by using the gradient $\frac{dh}{dx}$ (blue solid arrows) instead of the gradient along the flow path $\frac{dh}{dL}$ (orange dashed lines). The calculated heads and flow rates are sufficiently accurate if the slope of the water table is small.

If the bottom of the unconfined aquifer is used as the datum, then the head defines the saturated thickness. To include this dependency in the flow equations, Equation 70 is adjusted so that aquifer thickness, b , is replaced with h , and the varying value of h has to be inside the derivative. In addition, to represent unconfined flow, specific yield, S_y , is used as the aquifer storativity. Thus, **unconfined, two-dimensional (plan view), transient, anisotropic, heterogeneous** conditions of groundwater flow are represented by Equation 74.

$$S_y \frac{\partial h}{\partial t} = \frac{\partial}{\partial x} K_x \left(h \frac{\partial h}{\partial x} \right) + \frac{\partial}{\partial y} K_y \left(h \frac{\partial h}{\partial y} \right) \quad (74)$$

For **unconfined, two-dimensional (plan view), transient, anisotropic, homogeneous** conditions of groundwater flow, hydraulic conductivities do not need to be within the derivative, resulting in Equation 75.

$$S_y \frac{\partial h}{\partial t} = K_x \frac{\partial}{\partial x} \left(h \frac{\partial h}{\partial x} \right) + K_y \frac{\partial}{\partial y} \left(h \frac{\partial h}{\partial y} \right) \quad (75)$$

Unconfined, two-dimensional, plan view, transient, isotropic, homogeneous flow is represented using only one value of K as shown in Equation 76.

$$S_y \frac{\partial h}{\partial t} = \frac{K}{2} \left(\frac{\partial^2 h^2}{\partial x^2} + \frac{\partial^2 h^2}{\partial y^2} \right) \quad (76)$$

7.4 Steady State Equations Describing Confined and Unconfined Flow

Up to this point, the development of the flow equations has represented transient conditions. For **steady-state flow**, the change in storage with time is equal to zero because the head values and gradients are constant. Consequently, the left-hand side in any of Equations 67 through 76 is set to zero. For example, the steady state equation representing

confined, three-dimensional, steady-state, anisotropic, heterogeneous conditions is represented by Equation 77.

$$0 = \frac{\partial}{\partial x} \left(K_x \frac{\partial h}{\partial x} \right) + \frac{\partial}{\partial y} \left(K_y \frac{\partial h}{\partial y} \right) + \frac{\partial}{\partial z} \left(K_z \frac{\partial h}{\partial z} \right) \quad (77)$$

Whereas the equation for **confined three dimensional isotropic and homogeneous** conditions, referred to as the Laplace equation, is represented by Equation 78.

$$0 = \frac{\partial^2 h}{\partial x^2} + \frac{\partial^2 h}{\partial y^2} + \frac{\partial^2 h}{\partial z^2} \quad (78)$$

The equation for two-dimensional flow describing *steady state unconfined anisotropic, heterogeneous* conditions is represented by Equation 79 and **unconfined steady-state two-dimensional flow under isotropic and homogeneous** conditions is presented in Equation 80. Equation 80 is the Laplace equation.

$$0 = \frac{\partial}{\partial x} K_x \left(h \frac{\partial h}{\partial x} \right) + \frac{\partial}{\partial y} K_y \left(h \frac{\partial h}{\partial y} \right) \quad (79)$$

$$0 = \frac{\partial^2 h^2}{\partial x^2} + \frac{\partial^2 h^2}{\partial y^2} \quad (80)$$

The solution to any of the Equations 67 through 80 would produce head values at any location in the groundwater flow system: for the three-dimensional equations $h(x,y,z)$; two-dimensional, $h(x,y)$ or $h(x,z)$; and $h(x)$, $h(y)$ or $h(z)$ for one-dimensional representations. Regardless of the equation form, or dimensionality, given information about the boundary conditions of the problem domain, the resulting head distributions can be used to determine hydraulic gradients, flow directions and fluxes, and with effective porosity values, groundwater velocities.

These governing equations can be modified to account for many other hydrologic conditions that would impact the mass flux of water and the resulting head terms. For example, the effect of adding a constant or variable source of water (e.g., surficial recharge or an injection well) or extracting water (pumping well) can be represented by adding additional terms to the right-hand side of the governing equation because they are an additional change in mass in the REV. Governing equations are used to represent the general conditions of a groundwater system under investigation. They are combined with values of hydraulic conductivities, aquifer geometries, boundary conditions, and source/sink terms to generate head distributions and water balances for the specific system under investigation. Section 7.5 provides a brief explanation of boundary conditions and presents an example of application of the groundwater flow equations to field settings.

7.5 Applying Governing Equations

The general mathematical governing equations that describe groundwater flow conditions in a groundwater system are the foundation of models developed to characterize groundwater flow and its transport of dissolved substances. The governing equations describe how the hydraulic heads, h , within a problem domain are distributed

under a set of specified conditions. The steps involved in formulating a groundwater model include:

1. defining the purpose of the model;
2. building a conceptual model of the groundwater system including a water balance based on field and laboratory data, and hydrogeologic theory;
3. translation of the conceptual model into a format compatible with the appropriate governing equation and solution technique;
4. application of the technique to obtain a solution;
5. calibration (adjusting hydraulic parameters and boundary conditions until the solution matches heads and fluxes measured at the field site);
6. using the calibrated model to make predictions about how the groundwater system will respond under a new stress such as pumping or a drought; and,
7. reporting model results and their uncertainty.

The Role of a Water Budget in Formulating Models

In a few places in this book, the concept of a water budget or water balance has been noted as a key component used to understand groundwater systems. When scientists develop a conceptual model of a groundwater system, they examine the characteristics of the physical geologic framework, assess hydrogeological parameters, define problem boundaries, and generate a field-based groundwater budget that accounts for the volumes of groundwater entering and leaving the problem domain. The groundwater budget is a simple accounting of the groundwater inflows, outflows and changes in groundwater storage over a specified time interval for a defined problem domain (volume). In its simplest form it is expressed as Equation 81.

$$\text{Groundwater Inflow} = \text{Groundwater Outflow} + \text{Change in Groundwater Storage} \quad (81)$$

Given the addition of the change in groundwater storage on the right-hand side of Equation 81, a sign convention is required for the change in groundwater storage. As presented here, “Change in Groundwater Storage” is negative for water coming out of groundwater storage (i.e., falling water levels) and positive for water going into groundwater storage (i.e., rising water levels). The sign convention may vary in other presentations. The convention for any presentation can be deduced by looking at the form of the expression and reasoning out which sign is required for the system to balance.

Groundwater inflow can include flow of water into the domain at boundaries including leakage from a deeper aquifer system; recharge by natural precipitation; agricultural irrigation and artificial basin recharge; and seepage from surface water features such as streams, lakes and wetlands. Outflow can include flow of water out of the domain at boundaries including leakage to a deeper aquifer system; groundwater flowing to natural discharge locations such as streams, lakes, wetlands and springs; loss of groundwater to evapotranspiration, and extraction of groundwater by water supply wells and drains. Changes in storage occur in response to natural or induced changes in the

potentiometric surface. A conceptual groundwater budget is illustrated with words in Figure 56 and as images in Figure 57.

IN	Green Mountain GW inflow + Precipitation Derived Recharge + Bright River Leakage + Irrigation Recharge		
	$GWin_{GM}$ $GWin_R$ $GWin_{BR}$ $GWin_{IR}$		
=			
OUT	Municipal Well Discharge + Discharge to Bright River + Wetland Evapotranspiration Discharge + Fish Lake Inflow		
	$GWout_{MW}$ $GWout_{BR}$ $GWout_{WL}$ $GWout_{FL}$		
+			
Change Storage	Change in Groundwater Storage $GWstor$		

Figure 56 - A word representation of a conceptual water budget for the system shown in Figure 57.

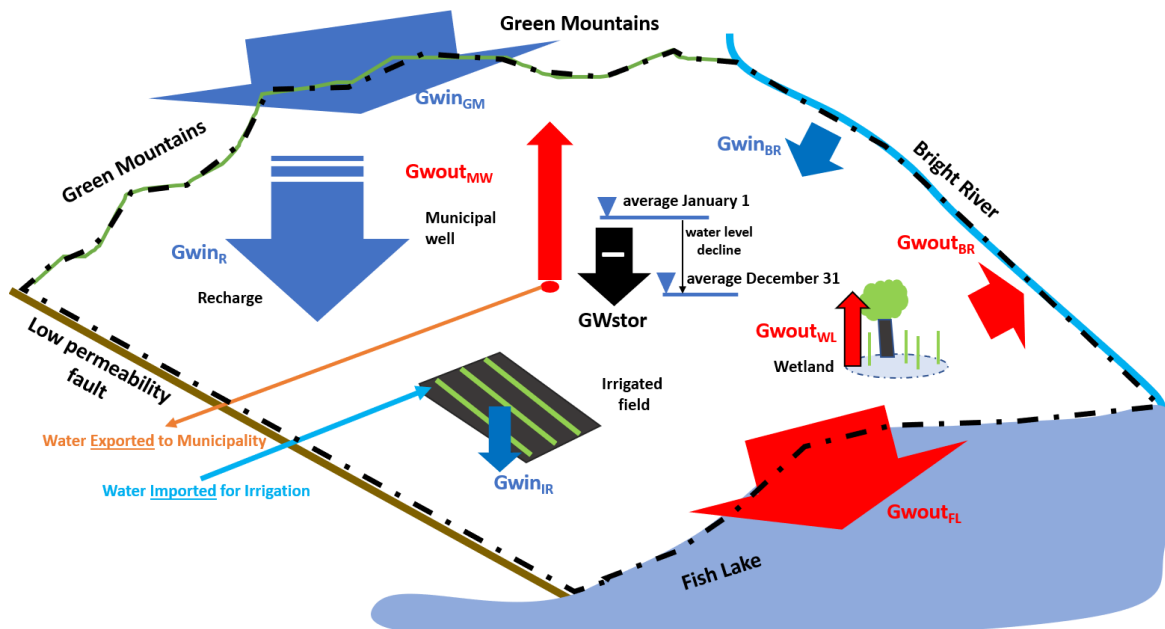


Figure 57 - A pictorial representation of a conceptual groundwater budget for one year. Terms are defined in Figure 56. The problem domain is outlined by a black dash dotted line. Blue arrows represent groundwater inflows and red arrows represent groundwater outflows. Groundwater inputs include annual inflows from the Green Mountain boundary, areal recharge, infiltration from the irrigated field and leakage from the upper reaches of the Bright River. Annual groundwater outflows include extraction and export of water from a municipal well, plant use of groundwater at a wetland (evapotranspiration), discharge to the southeastern portion of the Bright River and discharge to Fish Lake. The annual change in storage results from the decline in water levels between January 1 and December 31.

The conceptual budget is defined for a problem domain bordered by a low permeability fault (no groundwater flow into or out of the model); a permeable boundary along the Green Mountains where groundwater inflow occurs; a river boundary (Bright River) along which groundwater is recharged by river losses in the upper reaches and groundwater discharges to the gaining river in the lower reaches; and a lake where groundwater discharges to the lake as shown in Figure 57. Within the problem domain areal recharge occurs, as well as infiltration from an irrigated field. Groundwater leaves the system at a municipal well and by groundwater evapotranspiration at a wetland. The water

budget is calculated over a one-year period so the storage is the product of the specific yield and the change in water level over the year (on average for the entire domain or the sum of values if the specific yield varies over the domain).

The average rates of inflow and outflow for the year are computed and summed. The values are obtained in a variety of ways. Recharge is estimated as the spatially averaged precipitation minus evapotranspiration. Groundwater flow in from the Green Mountains and out to Fish Lake are estimated by Darcy's Law, using field measurements of gradients, hydraulic conductivity and flow areas. River seepage is estimated by noting the amount of gain and loss of stream flow between river gages. Municipal well discharge is obtained from town records. Irrigation recharge is estimated by knowing the amount of water imported for irrigation and subtracting the amount used by the type of crop in the climate of the area. Evapotranspiration from the wetland groundwater is estimated based on the local climate and character of the wetland vegetation. Change in groundwater storage is estimating by determining the average change in water levels in wells over the domain and multiplying by the area of the domain and the specific yield of the subsurface materials.

Many of the budget components are not easily determined, so they are estimates thus, the budget will not balance. If the imbalance is large, it is likely that the estimate for some component of the budget is in error, or an important component was overlooked and is not included. If the imbalance is small it may be distributed over the components of input or output, or considered to be part of the most uncertain component. When such a distribution is made, the water budget will be perfectly balanced, indicating the errors were incorporated into the component estimates. If the most uncertain component is determined by solving the budget equation, then the measurement error for all of the components is incorporated into the computed value. It is recommended that each component be measured or estimated independently and errors for each component estimated. A quantitative water budget provides the foundation for assessing whether analytical equations and numerical groundwater models make sense. A good reference for developing water budgets is available from the United States Geological Survey (Healy et al., 2007).

Boundary Value Problems

To apply the governing equation, a boundary value problem is formulated. It requires selecting a governing equation that describes the appropriate hydrogeological conditions, assigning head or flow rates at boundary conditions and assigning hydrogeologic parameters (e.g., hydraulic conductivity, recharge rates). Also, when conditions are transient, initial heads and storativity values are assigned. The boundary value problem is a model of the hydrogeological system.

Methods for Solving Groundwater Problems

Methods used to obtain solutions to groundwater problems include the following five approaches:

1. Inspection of field data

Inspection of the data for spatial and temporal trends and correlating data with the site-specific geological framework and basic hydrogeological principles allow for an initial analysis. This often includes building a conceptual model of how the groundwater system works and developing a water budget to assess interrelationships. A water budget lists the inputs and outputs (including water going into or coming out of storage) and estimates the magnitude of each budget item. The water budget must balance because mass is conserved. Inspection is also used to determine whether field data collected in simple settings contain trends that make it possible to predict future conditions.

2. Graphical techniques

Graphical methods include flow-net construction, a method discussed in Section 8.

3. Analog models

Analog models include using simple laboratory-scale systems made of materials that emulate groundwater flow under prescribed boundaries. These could be sand tanks or electric circuit boards.

4. Analytical mathematical techniques

Analytical solutions are algebraic equations that are continuous solutions to conditions described by a governing equation and assigned boundaries. A continuous solution is one that provides a value of head at every location in the system domain. Analytical solutions can be solved by hand (e.g., pencil-and-paper or hand calculator) or a spreadsheet. Analytical solutions usually require substantial simplifying assumptions and are typically only applicable to field systems with simple boundary conditions and flow patterns (for example, isotropic and homogeneous systems that can be represented by one- or two-dimensional flow).

5. Numerical mathematical techniques

Most field-scale groundwater modeling efforts require numerical methods to approximate solutions to a particular governing equation and generate values of head at discrete points in the groundwater system. The benefit of using such an approximation is that it can address complex boundary conditions and parameter distributions. Numerical modeling includes methods like finite difference and finite element modeling, which are used in many engineering fields. The United States Geological Survey has developed public domain numerical modeling software (e.g.,

<https://water.usgs.gov/software/lists/groundwater>) for simulating various aspects of groundwater systems.

Regardless of the solution technique, the governing equations are used to define the distribution of hydraulic head and fluxes within a system where the groundwater professional defines the spatial distribution of aquifer properties (e.g., K , and S) as well as boundary conditions for the volume of earth material. That volume is called the problem domain or model domain.

Boundary Conditions

Boundary conditions are generalized into three types that are defined along all boundaries of the model domain and can change with time. The three general types of boundary conditions are:

Type 1: Specified head boundary (also known as Dirichlet conditions). Steady or time-varying head values are specified along the boundary (for steady-state models the values are constant). If an unchanging value of head is defined on a boundary then the Type 1 boundary is referred to as a constant head boundary. Such a boundary could represent a large lakeshore where the lake stage elevation is assigned as a groundwater discharge boundary. When the model is solved, the model calculates flow rates at the location where the head is specified.

Type 2: Specified flux boundary (also known as Neumann conditions). Steady or time-varying flux is defined along the boundary (for steady-state models the values are constant). A special case is a no-flow or zero flux boundary. The gradient across a no-flow boundary is 0, so no flow crosses the boundary, $Q=0$. A low permeability fault zone bordering a model domain could be assigned as a no-flow boundary. When the model is solved, the model calculates head at the location where the flux is specified.

Type 3: Head-dependent flux boundary (also known as Cauchy conditions; also referred to as a mixed boundary). Steady or time-varying head values external to the model domain are specified along the boundary and a resistance layer is defined between the model domain and the external head (for steady-state models the head values are constant). Flow across the boundary is controlled by the difference between the specified head value located outside of the domain and the head calculated at the boundary of the model domain. The calculated head depends on conditions in the rest of the model domain. As the calculated head at the boundary varies, so does the flux in or out of the boundary. A Type 3 boundary could be used to represent flow into a groundwater system from alluvial sediments underlying a large river. When the model is solved, the model calculates the time-varying flow rate at each location where the head dependent flux condition is specified.

Franke et al. (1987) provide a well-written discussion of how groundwater boundaries are formulated. A few conceptual examples of the application of models to groundwater problems are provided here.

Application of Flow Equations (Unconfined Aquifer Flow Between Water Bodies)

This subsection shows how an algebraic analytical solution is developed. Groundwater professionals usually do not need to develop their own analytical solutions because many solutions have been created and published. To use a solution the professional need only understand the hydrogeological conditions being represented and how mathematical simplifications effect its application to a particular site being investigated.

Consider the steady-state, isotropic and homogeneous, one-dimensional, section of an unconfined aquifer shown in Figure 58. The constant head reservoirs on the left and right can represent any water body, for example, a reservoir, lake or river and will be represented as Type 1 specified head boundaries. To be completely accurate, the water bodies need to fully penetrate the aquifer, however if the partial penetration provides good connection, this requirement is commonly overlooked and reasonable results are obtained.

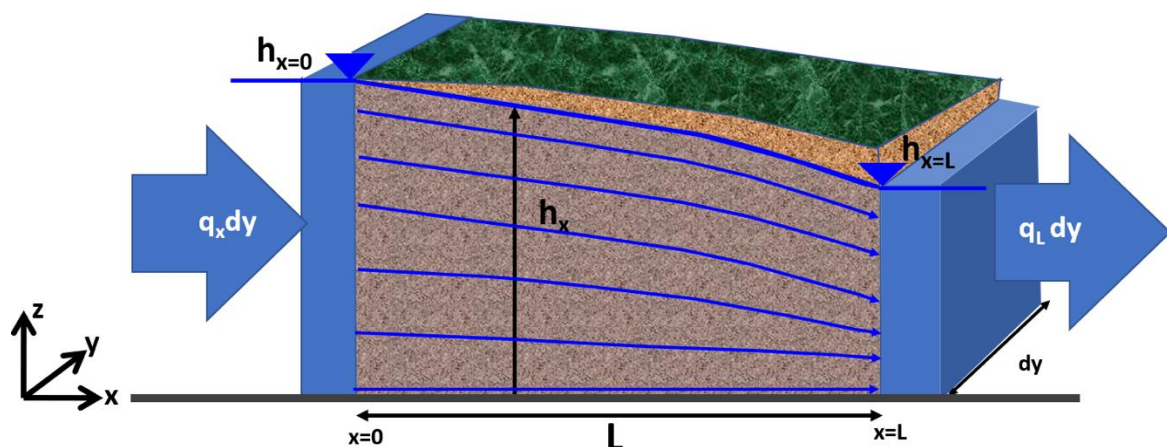


Figure 58 - Steady, unconfined groundwater flow between fully penetrating surface water bodies of constant head.

Equation 80 is applicable to this situation. When unconfined flow is formulated in one dimension, the y term is omitted, the head is measured from the aquifer base (because it also represents aquifer thickness), and the partial differential is changed to an ordinary differential becoming Equation 82. This equation represents groundwater conditions for the problem domain, the area bounded by the two water bodies, the water table and aquifer base.

$$0 = \frac{d^2 h^2}{dx^2} \quad (82)$$

Those familiar with differential equations will see that the general solution to Equation 82 by integration is shown as Equation 83. Those who are unfamiliar with differential equations can, for now, accept that this is the case because this step is not vital to understanding and use of the final solution.

$$h_x^2 = C_1 x + C_2 \quad (83)$$

where:

h_x = head at location x (L)

C_1, C_2 = constants of integration (L, L², respectively)

x = position on the x axis (L)

By applying the boundary condition $h = h_1$ at $x = 0$ on the left face (a Type 1 boundary) and the condition $h = h_2$ at $x = L$ on the right face (also a Type 1 boundary), the values of the constants of integration can be determined. By substituting at $x = 0$, the first term, C_1 , of Equation 83 is zero and so, $C_2 = h_1^2$. As shown in Equation 84.

$$h_1^2 = C_2 \quad (84)$$

Knowing the value of C_2 and substituting $h = h_2$ at $x = L$ into Equation 83 produces Equation 85.

$$h_2^2 = C_1 L + h_1^2 \quad (85)$$

$$\frac{h_2^2 - h_1^2}{L} = C_1$$

Returning to Equation 83 and substituting Equation 84 and Equation 85 for C_1 and C_2 , respectively, results in Equation 86, which is then rearranged with respect to the order of h_1 and h_2 , and solved for h_x (the head at any distance x from $x = 0$) in any of the three forms shown in Equation 86.

$$h_x^2 = \left(\frac{h_2^2 - h_1^2}{L} \right) x + h_1^2 \quad (86)$$

$$h_x^2 = h_1^2 - \left(\frac{h_1^2 - h_2^2}{L} \right) x$$

$$h_x = \sqrt{h_1^2 - \left(\frac{h_1^2 - h_2^2}{L} \right) x}$$

The heads at any x location in the system can be derived using Equation 86. For example, referring to Figure 58, if h_1 is 15 m, h_2 is 10 m, and L is 1000 m, what would be the value of head (h_x) at $x = 343$ m? Using the third representation of Equation 86, the head at $x=343$ m is calculated as follows.

$$h_x = \sqrt{(15 \text{ m})^2 - \left(\frac{(15 \text{ m})^2 - (10 \text{ m})^2}{1000 \text{ m}} \right) 343 \text{ m}} = 13.5 \text{ m}$$

For a similar situation, the groundwater professional need not develop an analytical solution from scratch, because an existing solution is available. Once an appropriate existing analytical solution is identified, problem-specific parameters are inserted, and a head is calculated.

The next task is evaluating the flow rate per unit width, q' . Expressing the flow area as the product of the height of the water table and the unit width of the system in the y direction, the flow is shown in Equation 87.

$$Q = -K \frac{dh}{dx} h \Delta y \quad (87)$$

With $\Delta y=1$ it can be removed from the expression, so that q' is the flow per unit width ($\Delta y=1$) with units of L^2/T (Equation 88). The symbol q' is used here to differentiate it from specific discharge, q (L/T).

$$q' = -K \frac{dh}{dx} h \quad (88)$$

where:

$$q' = \text{flow per unit width } (\Delta y=1) (L^2/T)$$

Rearranging and integrating from $x = 0$ to $x = L$ and from h at $0 = h_1$ to h at $L = h_2$, as shown in Equation 89, results in Equation 90.

$$q' dx = -K h dh \quad \text{and integrating:} \quad \int_0^L q' dx = -K \int_{h_1}^{h_2} h dh \quad (89)$$

$$q' = -\frac{K}{2L} (h_2^2 - h_1^2) \quad \text{or} \quad q' = -\frac{1}{2} K \left(\frac{h_2^2 - h_1^2}{L} \right) \quad (90)$$

Again, using Figure 58, if h_1 is 15 m, h_2 is 10 m, L is 1000 m, and $K = 25 \text{ m/d}$ then the flow per unit width, q' , can be computed using Equation 90 as follows.

$$q' = -\frac{1}{2} 25 \left(\frac{10^2 - 15^2}{1000} \right) = 1.56 \frac{\text{m}^2}{\text{day}}$$

If the cross-sectional area perpendicular to the boundaries is 100 m wide, the discharge of groundwater through the 100 m wide aquifer would be q' (100 m) = 156 m^3/d .

Box 6 extends the boundary value problem by adding constant recharge to the one-dimensional model. Box 6 also includes a simple spreadsheet that allows the reader to input values for this problem, including recharge rates and quickly see the head distribution and flow rates for the groundwater system. [Click here to read Box 6](#) ↴ and experiment with the interactive spreadsheet.

It is important to remember that in this unconfined system the heads not only determine the gradient, but also the saturated thickness so the aquifer base must be used as the datum if a reasonable flow rate is to be obtained. At times, a hydrologist forgets this issue and calculates outrageous values for flow rate because sea level is used as a datum for a system that is at a high elevation with an aquifer base only 10 meters below the surface (e.g., perhaps at 2000 m on a continental divide instead of 10 m). Also, because the head, as measured from the aquifer base, determines the saturated thickness and the gradient, error will be introduced if the Dupuit assumptions are applied to an aquifer with a sloping base.

It should be noted that when the water table slope is small approximations of q and v are often derived by directly using Darcy's law and assuming confined conditions as a reasonable approximation. In this case the confined conditions state the change in the water table is linear and it is assumed the thickness does not change significantly (T is constant).

Example Numerical Application of Flow Equations to a Dewatering Problem

This subsection shows how a numerical groundwater model, that incorporates a governing equation to describe groundwater conditions, can be applied to a field problem. Groundwater professionals often use software developed by mathematicians and computer programmers to solve problems. There are a number of standard, open-source, groundwater modeling software packages available to groundwater professionals (e.g., <https://water.usgs.gov/software/lists/groundwater/>). The basics of using a numerical code, MODFLOW, developed by the United States Geological Survey, are presented in a Groundwater Project book “*Getting Started with MODFLOW*” (Winston, 2023). Guidance to conceptualizing geological settings useful in structuring a modeling effort are available in the Groundwater Project book “*Geologic Frameworks for Groundwater Flow Models*” (Brandenburg, 2020).

The professional does not need have all the skills needed to develop new software, but does need to understand how to apply models to solve problems.

The model presented here is intended to provide the reader with a general idea of a numerical model application in order to illustrate how groundwater systems are simplified for modeling and appreciate what they can achieve after mastering knowledge of groundwater science.

Often, large construction projects or mining endeavors need to dewater a groundwater system to accomplish their work. This example illustrates a situation in which a mining company wants to construct an exploratory mine shaft and needs to keep the shaft dewatered by maintaining a water level in the shaft at an elevation of 900 m. The shaft will be sealed through overlying formations including a thick shale layer overlying the confined aquifer in which the shaft terminates.

The model formulation is illustrated in Figure 59. To allow flexibility in assigning parameter values to the problem domain, the governing equation for confined three-dimensional, anisotropic, heterogeneous hydraulic conductivity distributions (K_x , K_y , K_z) is selected (Equation 67). A long-term pumping rate is sought, so a steady-state formulation of the problem is selected (left-hand side is set to 0). In addition to the flow equation, assignment of internal hydrogeologic parameters at multiple locations (e.g., K_x , K_y , K_z), and the domain boundaries are specified based on information from field-based hydrogeologic investigations. In this hypothetical example, water levels from boreholes in the field are used to estimate values of head that are specified on the left and right boundaries (Type 1). Recharge is estimated from local precipitation and soil conditions and is applied as a constant flux at the top of the model. The unconfined aquifer is also represented using Equation 67 however the computer code continually changes the unconfined hydraulic properties ($T = Kb$) as the saturated thickness of the unconfined layer changes. The boundaries on the front and back faces and the base are assigned as Type 2, zero flux, no-

flow, boundaries, where water cannot pass into or out of the model domain. By defining the head on the bottom of the shaft as a constant 900 m, the model will calculate the outflow required to maintain that water level (large red arrow in Figure 59).

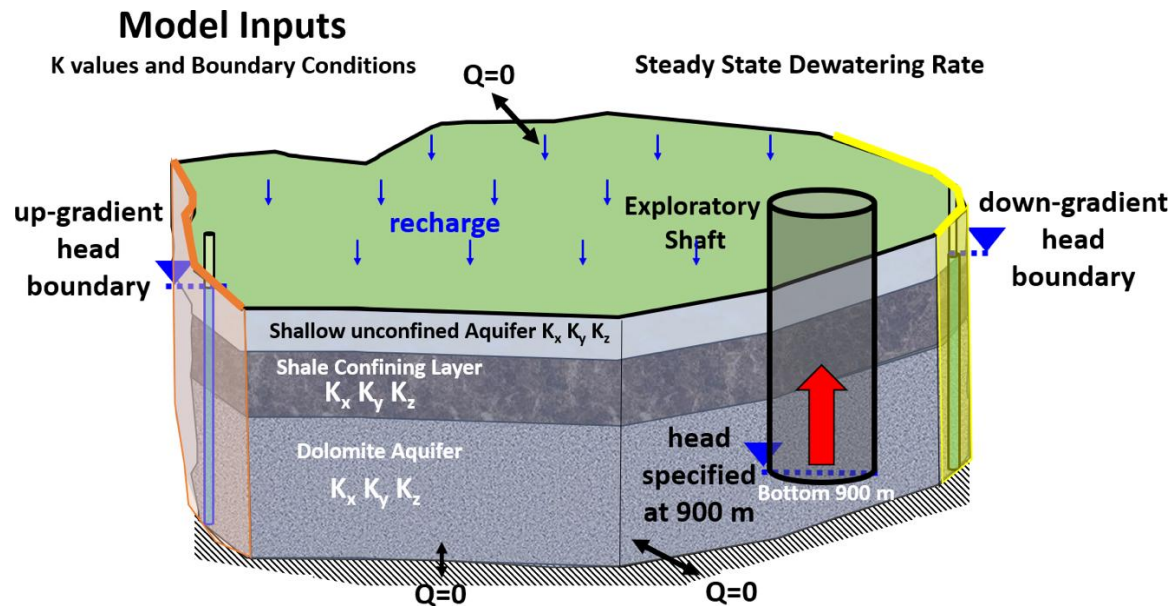


Figure 59 - Schematic of a three-dimensional, three-layer aquifer model. The governing equation describing conditions represents confined three-dimensional anisotropic and heterogeneous groundwater conditions. Hydraulic conductivity assignments (K_x , K_y , K_z) can be different at each location within all layers. The external boundary conditions include Type 1 specified heads over the entire left (orange) and right sides (yellow) of the model with a lower value on the right side. A flux boundary equal to the estimated recharge rate is applied at the top of the model. The boundaries on the front and back faces and the base are assigned as no flow, $Q=0$, water cannot cross the boundary. The location of the exploratory shaft is also shown and a constant head of 900 m is defined at the base of the shaft. The red arrow represents the outflow from the shaft.

Finally, to solve the governing equation, a public-domain computer code that uses a numerical mathematical technique to generate heads and a water budget is applied. Figure 60 schematically illustrates the model results including: head distribution within each of the three geologic layers; flow rates into the left and right boundaries; leakage rates between model layers; and the answer to the question that prompted the model formulation (i.e., the steady-state pumping rate required to maintain the water level in the shaft at 900 m). The software also provides a water budget that accounts for the volume of water flowing in and out of every model boundary and from applied sources (recharge) and sinks (water extracted at the shaft). The water budget must balance (for steady-state conditions, inflow must equal outflow). A water budget that does not balance indicates a problem with the model formulation and the modeler must not use the results, but rather determine the causes and modify conditions to obtain a reasonable water balance.

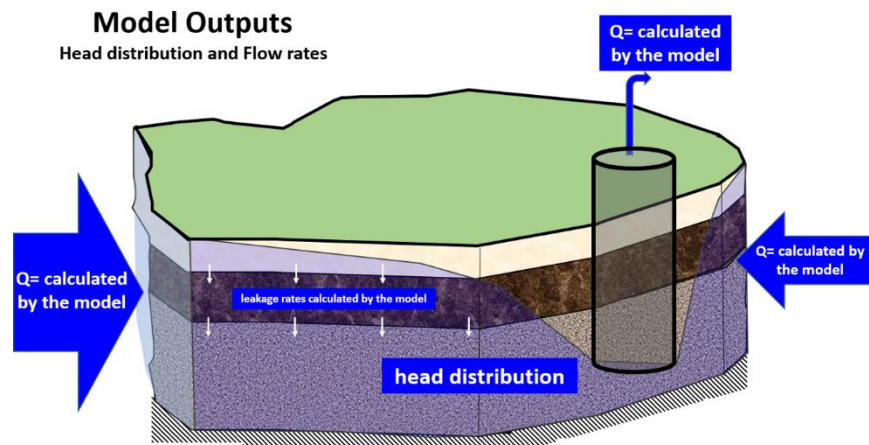


Figure 60 - Schematic of the outputs computed by the numerical model shown in Figure 59. The outputs include: the head distributions within each of the three geologic layers; flow rates into the left and right boundaries and within and between each model layer; and the answer to the question that prompted the model formulation (i.e., the steady-state pumping rate required to maintain the water level in the shaft at 900 m). The software also provides a water budget that accounts for the volume of water flowing in and out of the entire model domain.

If the mining company wanted to know how long they would need to pump in order to lower the water level to the bottom of the shaft, they could construct a model using the transient formulation as presented in Equation 67 and begin pumping the shaft at a fixed rate to explore how pumping at various rates would impact water levels in the vicinity of the shaft.

7.6 Exercises

[Exercise 12](#) offers practice in writing groundwater flow equations. [Exercise 13](#) provides an opportunity to identify flow equations.

8 Interpreting Groundwater Flow

The water in groundwater systems is always in motion. Groundwater flows from recharge areas (areas of high hydraulic heads) to discharge areas (areas of low hydraulic heads). Water enters the groundwater system in recharge areas and leaves the system in discharge areas. When striving to understand groundwater flow at one location, it is useful ask the question: Where is the water coming from and where is it going?

Toth (1963) provided some foundation for conceptualizing groundwater flow systems. His work showed that multiple unconfined flow systems can occur in landscapes with sufficient recharge. He paired recharge and discharge areas to define the flow systems. He described three levels of flow systems: local, intermediate and regional, as shown in Figure 61. Local flow systems form between adjacent recharge and discharge areas, and local system flow paths are relatively short. Intermediate flow systems originate in recharge areas and discharge downgradient, but not to the nearest discharge location. Intermediate flow systems encompass at least one local flow system. Regional flow systems originate at regional recharge areas and flow to distant discharge locations, with relatively long flow paths. The regional system often surrounds one or more local and/or intermediate flow systems.

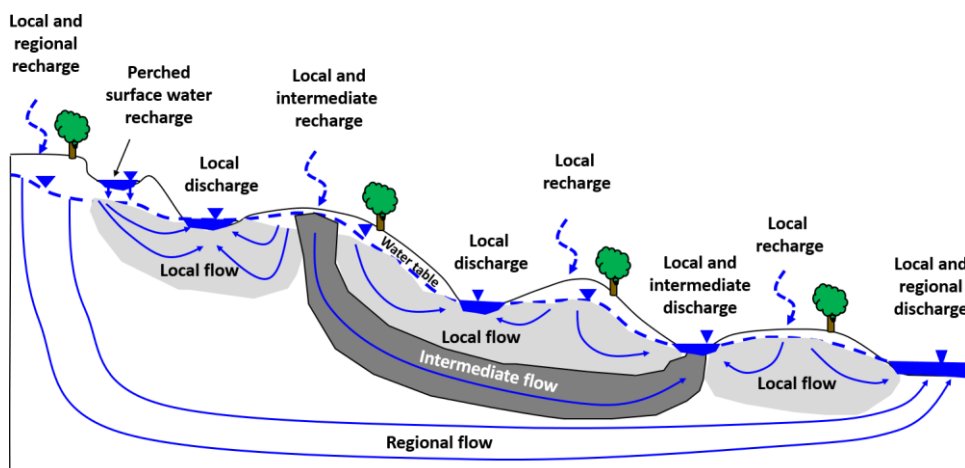


Figure 61 - Schematic of groundwater flow in an unconfined aquifer with multiple recharge and discharge areas showing local, intermediate and regional flow systems.

Toth's conceptual model provides a framework for investigation of unconfined groundwater systems. Groundwater flow systems do not only occur in aquifers, groundwater moves through all the saturated materials between a recharge and discharge area. This can include multiple aquifers (unconfined, and confined) as well as aquitards as illustrated in Figure 62. Confined aquifers are recharged at outcrop sites or by downward leakage of water from overlying aquifers. In down gradient areas they may discharge in the form of upward leakage of water into overlying aquifers.

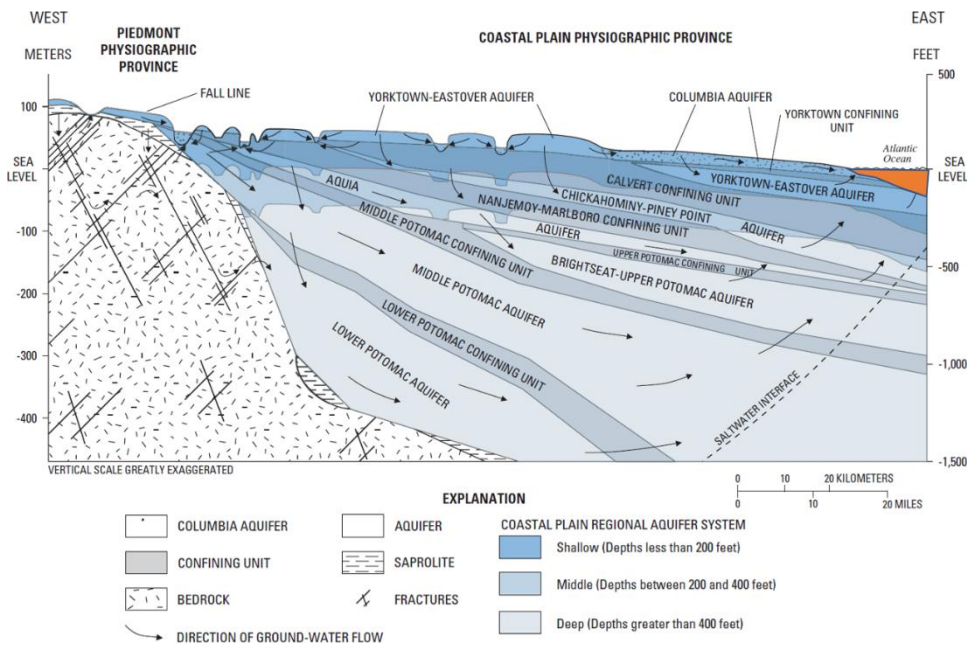


Figure 62 - Groundwater flow (black arrows) in multiple, stacked, aquifer systems of the Coastal Plain of Virginia, USA. Aquifers are composed of terrestrial and marine sediments and separated by finer-grained marine sediments (confining units). Groundwater originates as recharge at both regional and local recharge areas associated with the shallow aquifer and at the western outcrop areas of the deeper confined aquifers. Groundwater flow is generally downward in the western portion of the region, horizontal in confined aquifers and then upward at the eastern regional discharge area located at the ocean (orange shading) (modified from Nelms et al., 2003).

This section addresses how to assess hydraulic gradients and flow directions using field data. It includes discussions of plotting and interpreting hydraulic heads; accounting for the influence of contrasts in and anisotropy of hydraulic conductivity on flow direction; as well as the effect of physical and hydraulic boundaries on groundwater flow directions and rates.

8.1 Mapping the Head Distribution

A plot of the spatial distribution of hydraulic head at a given time is used to interpret groundwater gradients, flow directions, fluxes and velocities. The elevation (relative to a horizontal datum, i.e., mean sea level) of the water level in a well bore represents hydraulic head. Head data are gathered in the field by surveying the location and elevation of the top of the casing (TOC) of wells or piezometers, then measuring from the top of the casing to the depth of the water level as shown in Figure 63. The depth to water is then subtracted from the TOC elevation to generate a head value (the elevation of the water level). Typically, a steel tape or an electric water-level-depth probe (dipmeter) is used to determine the depth to water. Wells can also be instrumented with electrical transducers that record the change in the depth of water overlying the transducer over a selected time interval.

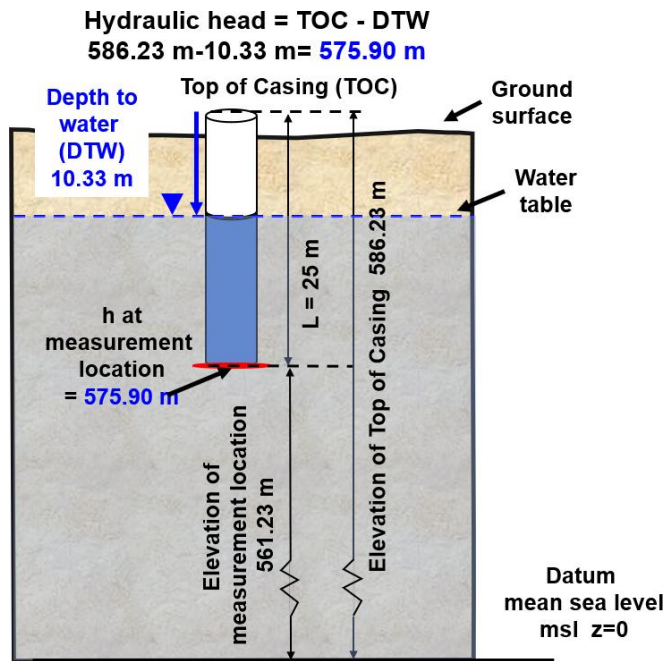


Figure 63 - Determining total head using a well that is open at the bottom. L is the total length of well casing. TOC is the top of casing, the surveyed measuring point location. The water level depth below the TOC measuring point is determined. The total head is derived by subtracting the depth to water from the TOC elevation. The head is then assigned to the location that corresponds with the bottom of the well when plotted on a cross section and at the x,y location of the well when potted on a map.

It is recognized that measuring tools have errors associated with them. Neilson (1991) prepared a table comparing measuring methods and associated accuracy that showed instrument errors varied from 2 to 10 mm. Error also occurs during the survey of TOC elevations (survey error) and as a result of the approach the instrument operator uses to measure the water level (operator error). Thus, measured heads may have a combined error +/- that is larger than the instrument error. In most regional settings, values can be rounded to tenths of a meter to account for errors. When a small area is being evaluated or gradients are small, however, head differences of a few centimeters are usually needed to distinguish gradients and great care is required to minimize error during surveying and water level depth measurement. An error study that quantifies the measurement error associated with head values should be performed and results reported with raw head data and when discussing heads plotted on maps and cross sections.

The next step is to assign the head value to the correct position in a cross sectional or map view of the field site (Figure 64). The open portion of the well is the location of the head measurement. In Figure 63 it is at the bottom of the well. Some wells are perforated or screened over a portion of their length, this is called an open- or screened-interval. Such intervals may range from less than a meter to the entire well depth. In this case, the head value is typically plotted at the midpoint of the open interval. Once a number of head values are plotted on a cross section, the distribution of head (x,z) can be contoured creating equipotential lines. Equipotential lines connect locations of equal head (dashed red lines of

Figure 64a). In map view, heads are plotted at the well casing locations (x,y) as shown in Figure 64b. The head values are independent of the surface elevation. Once a number of head values are plotted on a map, heads are then contoured creating equipotential lines and lateral flow directions are inferred.

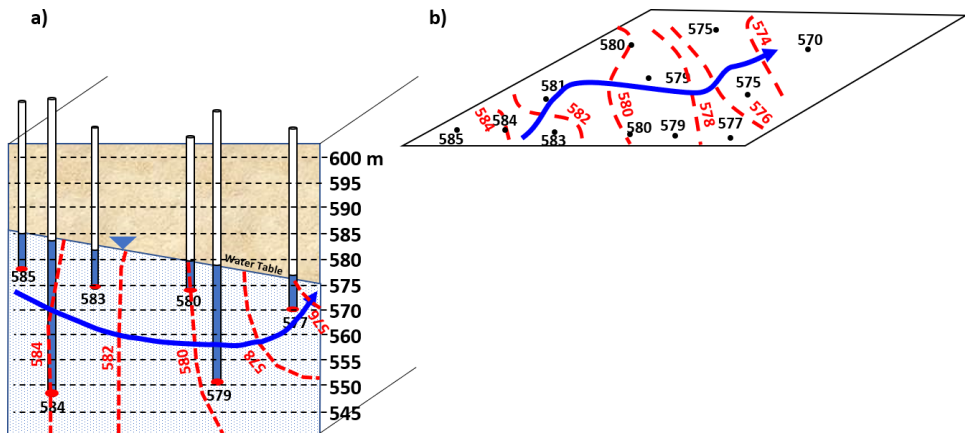


Figure 64 - Heads measured in the field (black numbers) are plotted and then contoured to estimate equipotential lines with a contour interval of 2 m (red dashed lines). The general groundwater flow directions are inferred from areas of high heads to areas with low heads (blue arrows). a) A cross-section view based on wells open only at the bottom. Flow is generally from the left to the right, but with a downward component on the left and an upward component to the discharge area on the right. b) A map view of the same area with wells indicated by black dots. The cross section is along the south boundary of the map view, while other head data were collected at additional wells that are not shown on the cross section.

The construction of cross sections and map views of head data is a standard practice. The map view for a confined or unconfined aquifer is referred to as a representation of the potentiometric surface. An example is shown for the confined Memphis Sand aquifer, Memphis, USA in Figure 65. A map of the total head for an unconfined aquifer can also be referred to as a water table map. However, because the water table is a representation of head (energy per unit weight) it is also referred to as representing a potentiometric surface. So, when using the term potentiometric surface, it should be placed in context as either representing a confined or unconfined groundwater system.

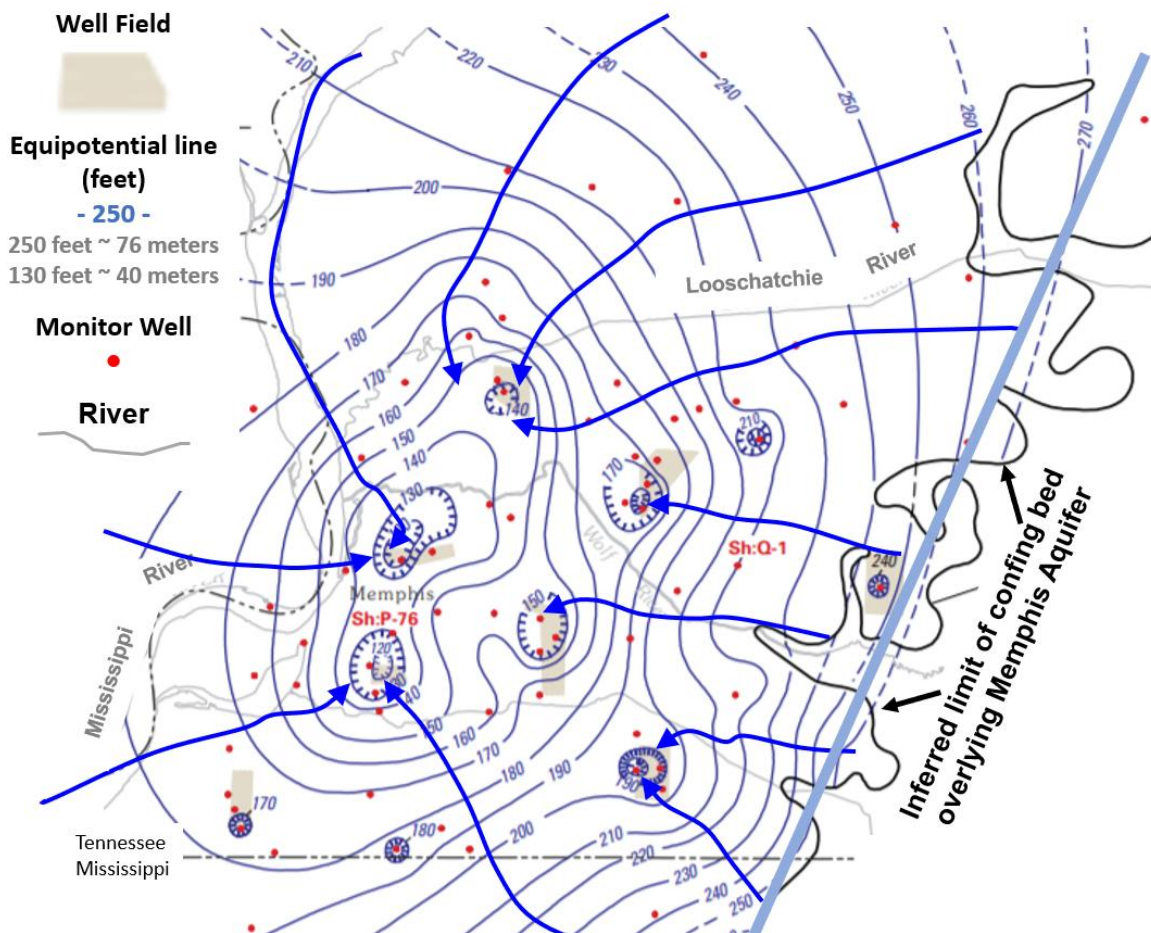


Figure 65 - Potentiometric map (from 1995) of the confined Memphis Sand aquifer in the vicinity of Memphis, TN, USA. Light blue lines are equipotential lines (in feet), divide by 3.28 to convert to meters) interpolated from head data collected at wells (red dots). Dashed lines are inferred. The head distribution shows depressions (areas of lower head) that are indicated by hatched equipotential lines. These areas are associated with long-term pumping of municipal and industrial wells (modified from Taylor and Alley, 2001).

8.2 Determining Groundwater Flow Directions

When evaluating the direction of groundwater flow, the first step is to plot the head data on a map or cross section, then create contours of equal head, i.e., equipotential lines, as shown in Figure 64 and Figure 65. Representations in cross-sectional views are created using axes that are equally scaled, x and z . In geologic investigations cross-sectional representations are often shown with the vertical scale exaggerated (e.g., horizontal to vertical ratios of 1 to 10, 1 to 100, etc.); this allows small changes in features to be visible. However, cross sections without vertical exaggeration are required when attempting to interpret groundwater flow directions. Maps are already scaled equally in the x and y direction and are most commonly used to represent two-dimensional groundwater flow patterns. An example of the process used to construct equipotential lines is illustrated in Figure 66.

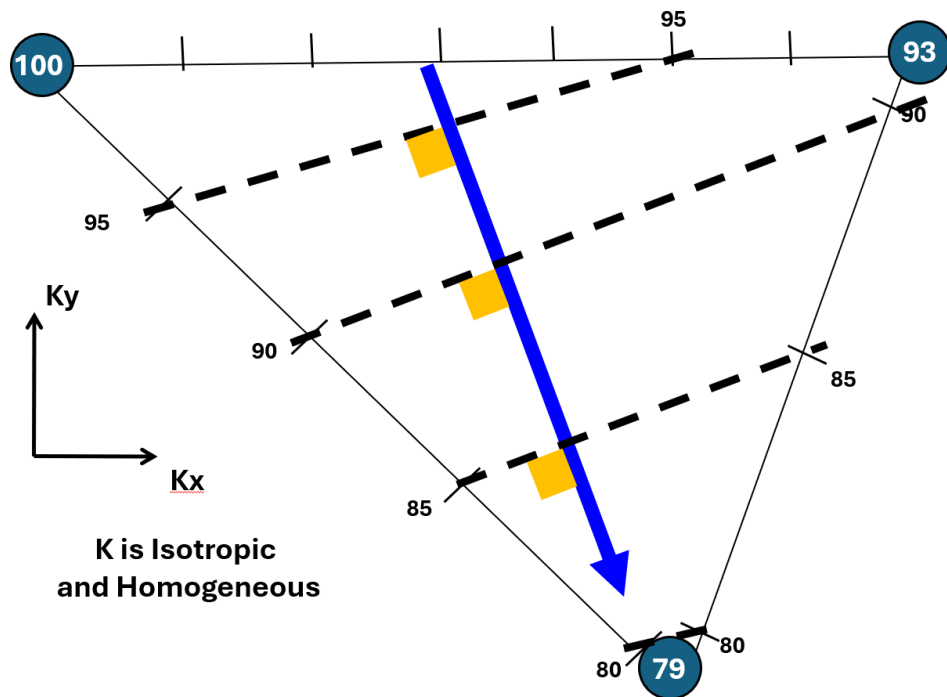


Figure 66 - Example of constructing equipotential lines using measurements from three wells (blue circles). The three values of head are shown as 100, 93, and 79. The space between wells is divided into segments to linearly interpolate the values of head between the wells. Then dashed black equipotential lines are drawn connecting equal values of interpolated heads. If the material has isotropic and homogeneous hydraulic conductivity, then groundwater flow (large blue arrow) will occur in the direction of the maximum gradient (from high values to low values), which is at right angles (yellow boxes) to the equipotential lines.

Alternatively, equipotential lines can be drawn using computer software to interpolate sparse data points to a regular grid (e.g., the public domain, open-source, geographical information system [QGIS](#); the commonly-used, commercial gridding and contouring program [SURFER](#); or code in [Python](#) or [Matlab](#)). These interpolated values are then contoured. There are many interpolation methods that are not discussed here, but often their name makes it easy to envision their procedure (e.g., closest point; nearest neighbor; triangulation, inverse-distance weighting of surrounding data; kriging which includes functions describing continuity of trends in the coordinate directions; trend surface polynomials).

One challenge with automated interpolation is that the conditions at the boundaries of the data are usually poorly represented because the programs infer data trends beyond the measured data field (extrapolation). Many practitioners prefer to use digitized versions of their own hand drawn contour maps over computer generated versions because this allows geologic insight to be incorporated into the interpretation and often allows boundary conditions to be represented in a more realistic manner. This is particularly so when the number of data points (monitoring wells) are relatively few and when they are not uniformly distributed within the study area. With any method of interpolation and contouring, results must be scrutinized to see if they make hydrogeologic sense. This process is referred to as a sensibility analysis. Ask the question, “What would this look like

if it was hand contoured?" Some interpolation methods yield poor representations of a system. When the output doesn't make sense, data quality and interpolation methods need to be reviewed, and in some cases additional field data collection proposed.

Gradient and Flow Directions in Isotropic Material

The head distribution and interpolated equipotential lines can be used to calculate a hydraulic gradient at any location within the flow field. A gradient is a vector, that is it has both magnitude and direction. The maximum gradient is used to determine the direction of groundwater flow and is referred to as $-\text{grad } h$, with the negative sign indicating that groundwater flow is from high head to low head (Figure 67a). In Figure 67b the gradient $(h_2 - h_1)/L_1$ is greater than the gradient $(h_2 - h_1)/L_2$, and there is no direction with a larger gradient than $(h_2 - h_1)/L_1$. In this case, $-\text{grad } h$ is defined over the distance L_1 . For isotropic and homogeneous material, the path of groundwater flow is parallel to $-\text{grad } h$ and flow lines are constructed at right angles to equipotential lines as illustrated in Figure 68.

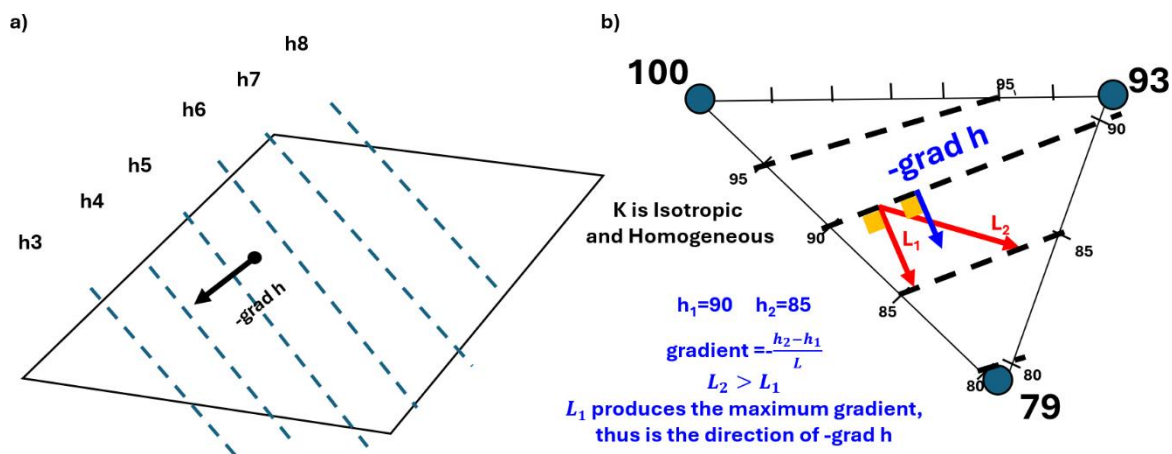


Figure 67 - The relationship of the hydraulic gradient vector $-\text{grad } h$ to mapped head (dashed blue equipotential contours): a) $-\text{grad } h$ for a map view of a head field where $h_8 > h_3$; and, b) $-\text{grad } h$ for a flow field interpreted from head measurements at three wells (blue dots). Head values are the large values adjacent to the well locations. $-\text{grad } h$ is defined by the maximum hydraulic gradient.

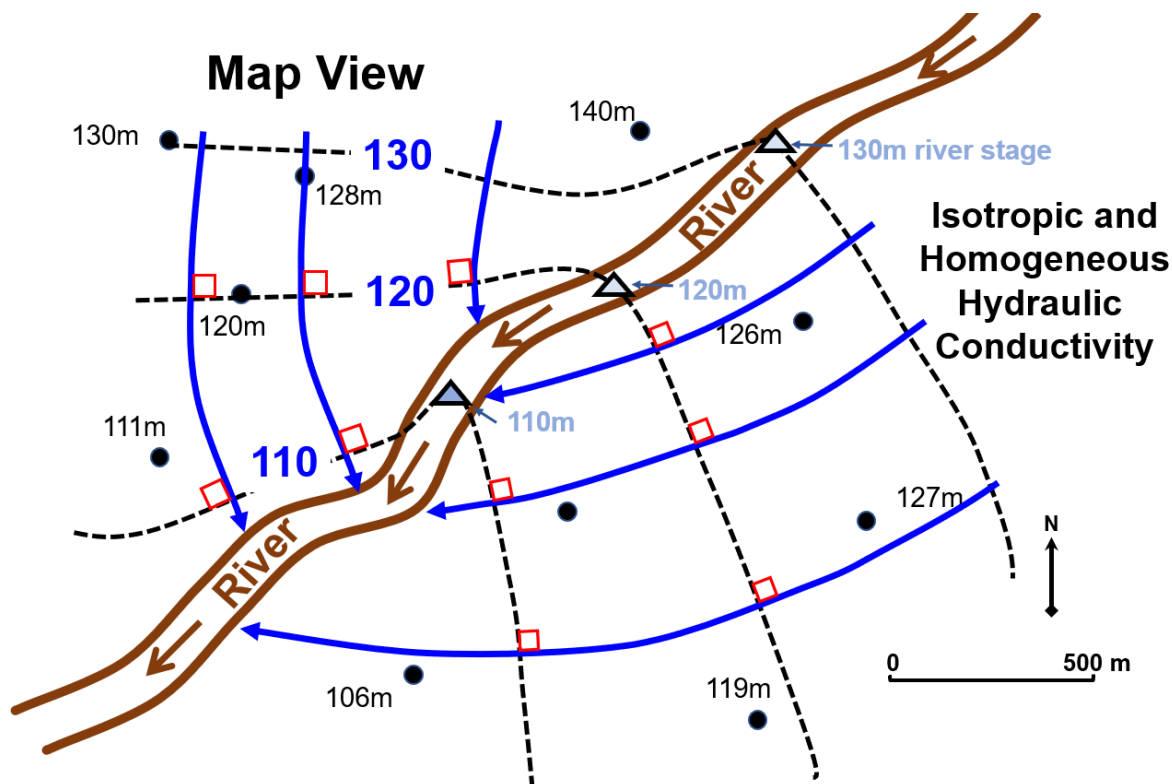


Figure 68 - Water table map of an isotropic and homogeneous unconfined aquifer. Head measurements are plotted at well locations (black dots). The surveyed river stages (blue triangles) also represent head values as groundwater is discharging to the river and the water table is connected to the river stage. Heads are contoured using a 10 m interval creating the equipotential lines shown as dashed black lines. Blue arrows represent flow lines constructed at right angles (indicated by red squares) to the equipotential lines.

Flow Directions in Anisotropic Materials

As stated previously in Sections 4 and 5, most sediments and sedimentary rocks are deposited such that their hydraulic conductivity is similar in all directions of the horizontal plane (K_x and K_y). However, those same depositional process create anisotropy in the vertical direction due to layering of the sediments, thus vertical hydraulic conductivity, K_z , is commonly orders of magnitude less than horizontal hydraulic conductivity (K_x and K_y).

When the two-dimensional hydraulic conductivity distribution is anisotropic and homogeneous ($K_x \neq K_y$, or $K_x \neq K_z$) groundwater flow is influenced by the maximum component of hydraulic conductivity. If the component of maximum hydraulic conductivity does not parallel $-\text{grad } h$, then flow lines cross equipotential lines at an angle other than a right angle.

The flow directions in anisotropic settings are dependent on the magnitude of the component hydraulic conductivities illustrated by using an inverse hydraulic-conductivity tensor ellipse (Figure 69). Once $-\text{grad } h$ is identified for a set of equipotential lines and the inverse hydraulic-conductivity tensor ellipse is constructed with axes of $1/K_{\max}^{0.5}$ and $1/K_{\min}^{0.5}$, the anisotropic flow direction at a given location can be determined by graphical construction (Liakopoulos, 1965). The hydraulic-conductivity tensor ellipse described in

Section 5.4 (Figures 34 and 35) is used to illustrate the directional nature of K whereas the inverse hydraulic-conductivity tensor ellipse is used to determine groundwater flow directions.

Figure 69 presents the steps used to construct flowlines in an anisotropic setting where K_x is greater than K_z .

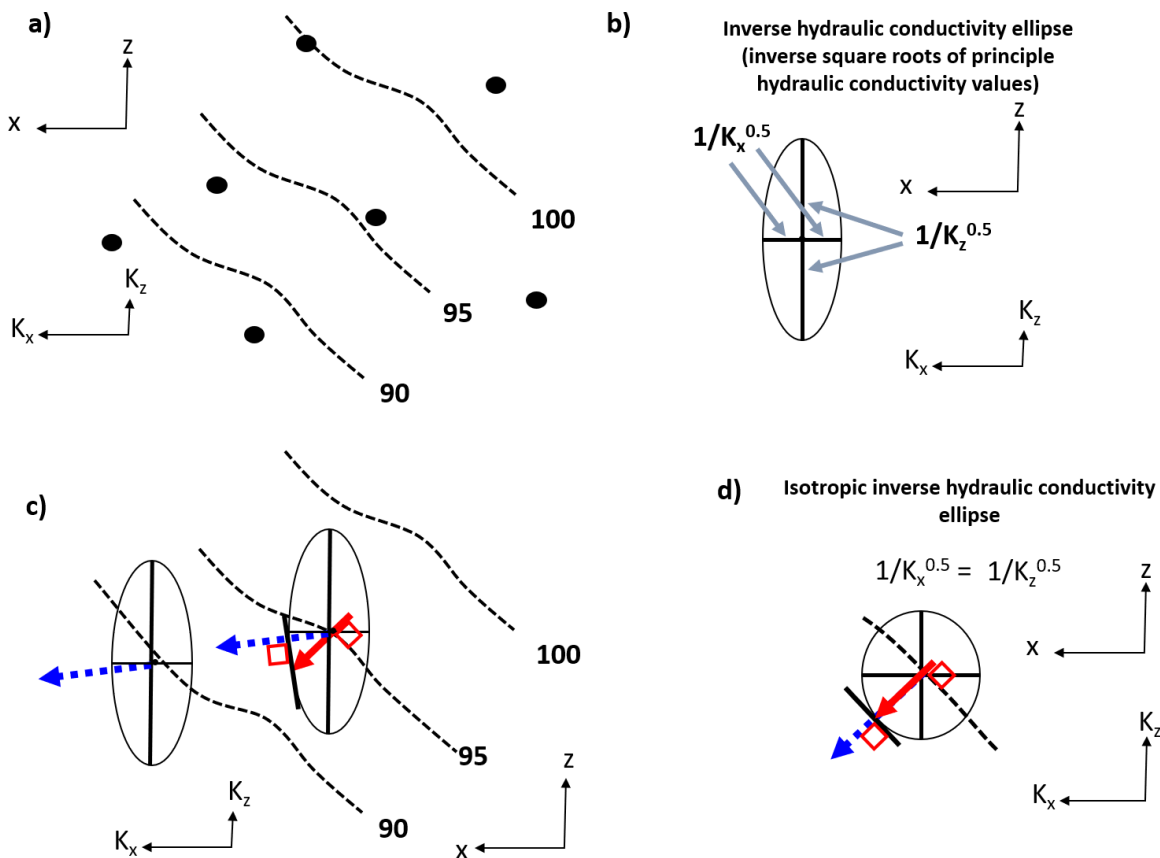


Figure 69 - Determining flow direction in a cross section of anisotropic homogeneous material is illustrated for a case where $K_x > K_z$: a) head values are obtained (black dots are heads from wells) and equipotential lines (dashed lines) are constructed; b) then an inverse hydraulic-conductivity tensor ellipse is generated for site conditions; and, c) the ellipse is placed with its center on an equipotential line at the location where the flow direction is to be determined. The ellipse axes are aligned with the direction of maximum and minimum K on the map and cross section. A line representing $-grad h$ (red solid arrow) is drawn from the ellipse center (at a right angle [red square] to the equipotential line) to the ellipse perimeter. A tangent to the ellipse at the point where $-grad h$ intercepts its perimeter is constructed (black solid line). Then the anisotropic flowline (blue dashed arrow) is constructed from the center of the ellipse to the tangent line crossing it at a right angle (red square). The flow path is traced through the system by plotting additional inverse hydraulic-conductivity tensor ellipses where the dashed blue flow line crosses the next equipotential line. d) The inverse hydraulic-conductivity tensor ellipse is a circle under isotropic and homogeneous conditions. This results in flow lines being parallel to $-grad h$ at all locations.

Figure 70 illustrates how flow direction is impacted by the orientation of the equipotential lines in an anisotropic media.

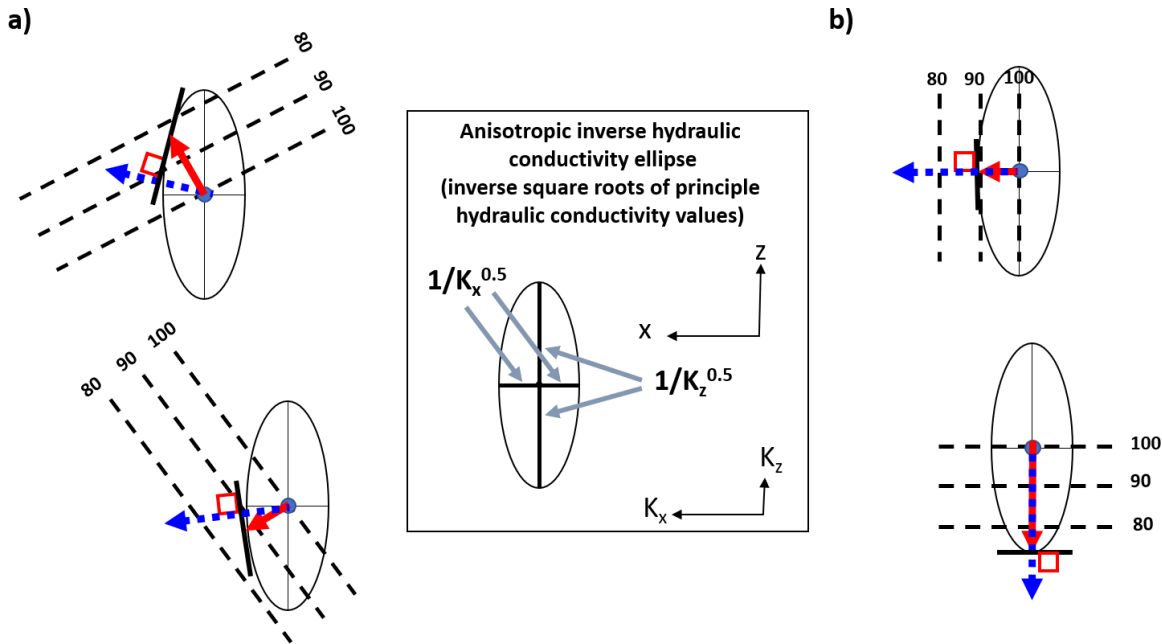


Figure 70 - Examples of using the inverse-hydraulic-conductivity tensor ellipse graphical method to determine flow directions in four examples of equipotential line orientations in the x-z field. Values of K_x are greater than K_z . The method and symbols shown here are defined in Figure 69. a) Two non-parallel or non-vertical orientations of equipotential lines with the anisotropic flow path indicated by the dashed blue arrow. b) Equipotential lines oriented parallel to the K_x axis (upper diagram) and K_z axis (lower diagram). For the cases shown in (b), the $-\text{grad } h$ (red arrow) and anisotropic flow line (dashed blue arrow) are identical.

A second graphical approach for representing flow in an anisotropic system is presented in Box 7. [Click here to read Box 7](#) about a graphical method of axis transformation to draw two-dimensional flow in an anisotropic, homogeneous medium.

Flow Directions at Interfaces of Differing Hydraulic Conductivity

Groundwater flow is also impacted by contrasts in hydraulic conductivity as flow passes from one isotropic homogeneous region to another (Figure 71). If a flow line intersects the hydraulic conductivity boundary at an angle other than 90° , it is refracted into the adjacent formation. The magnitude of refraction relates to the ratio of the hydraulic conductivity values as shown in Equation 91. The refraction occurs because discharge through in the area between two flow lines, the flow tube or stream tube, must be the same on both sides of the interface ($Q_1 = Q_2$) under steady state conditions and Darcy's Law must be honored on both sides of the interface. Given that, the equipotential lines must be closer together (larger hydraulic gradient) and the stream tubes must be wider (flow through a larger cross-sectional area) in the lower hydraulic conductivity side of the interface than on the higher hydraulic conductivity side. In addition to the flow line refraction, the equipotential lines also refract as they cross the hydraulic conductivity boundary.

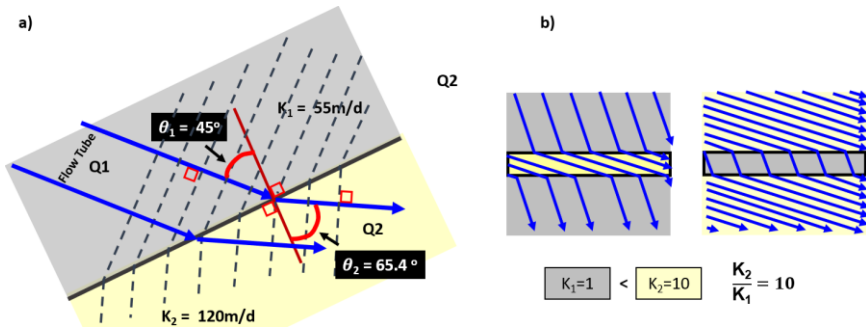


Figure 71 - Examples of flow lines and equipotential lines refracting at the interface between layers of different hydraulic conductivities. Gray and yellow areas are saturated, isotropic, homogeneous materials of different hydraulic conductivity. a) Dashed lines are equipotential lines decreasing from upper left to the lower right. In the gray area $K_1=55$ m/d and in the yellow area $K_2=120$ m/d. The flow lines (blue arrows) intersect the boundary at 45° . They are refracted into the yellow area at an angle of 65.4° . The equipotential field is also refracted. b) Flow line refraction in a sequence of isotropic, homogeneous aquifers with K_2 (yellow) 10 times K_1 (gray).

$$\frac{K_1}{K_2} = \frac{\tan \theta_1}{\tan \theta_2} \quad (91)$$

where:

K_1 = hydraulic conductivity of layer 1 (L/T)

K_2 = hydraulic conductivity of layer 2 (L/T)

θ_1 = angle the flow line makes with a perpendicular to the boundary in stratum 1 (degrees)

θ_2 = angle the flow line makes with a perpendicular to the boundary in stratum 2 (degrees)

The derivation of the tangent law is presented in Box 8. [Click here to read Box 8](#) ↴ which presents the derivation of the tangent law.

8.3 The Influence of Boundary Conditions

Generally, groundwater system boundaries can be referred to as physical boundaries or hydraulic boundaries. Physical boundaries do not move as the flow directions and rates within a groundwater system change. They represent a measurable change in hydrogeologic properties such as those that occur at formation contacts, faults, and large water bodies. Hydraulic boundaries can move when the flow field changes because they are formed by hydraulic conditions such as locations and rates of recharge and the divergence or convergence of multiple flow systems.

Physical Boundaries

Non-flow or Zero Flux Boundaries

Physical boundaries such as a hydraulic conductivity contrast, control flow paths in a groundwater system. For example, if a permeable sand and gravel aquifer abuts a low

hydraulic conductivity granite, the groundwater flow within the aquifer parallels the boundary (Figure 72a) and the equipotential lines meet the boundary at right angles (Figure 72a). This is a Type 2 specified flux boundary referred to as a no-flow or zero flux boundary.

Constant Head Boundaries

In contrast, if a large lake forms a boundary of the aquifer, groundwater flow lines are perpendicular to the lake shore because the water level of the lake is an equipotential line, so equipotential lines in the aquifer near the lake are parallel to the boundary (Figure 72b). This boundary is a specified head Type 1 boundary, referred to as a constant head boundary.

Water Table Boundary

The water table is the upper boundary of an unconfined aquifer. A water table is a unique boundary in that pressure head is, by definition, zero so head is equal to elevation. If recharge enters the unconfined aquifer, water flows across the boundary at an angle and equipotential lines meet the water table at an angle (Figure 72c). If there is no recharge, the water table is a flow line the equipotential lines meet the water table at right angles (Figure 72d). Regardless of whether flow occurs across the water table, or not, the value of an equipotential line where it intersects the water table is equal to the elevation of the water table.

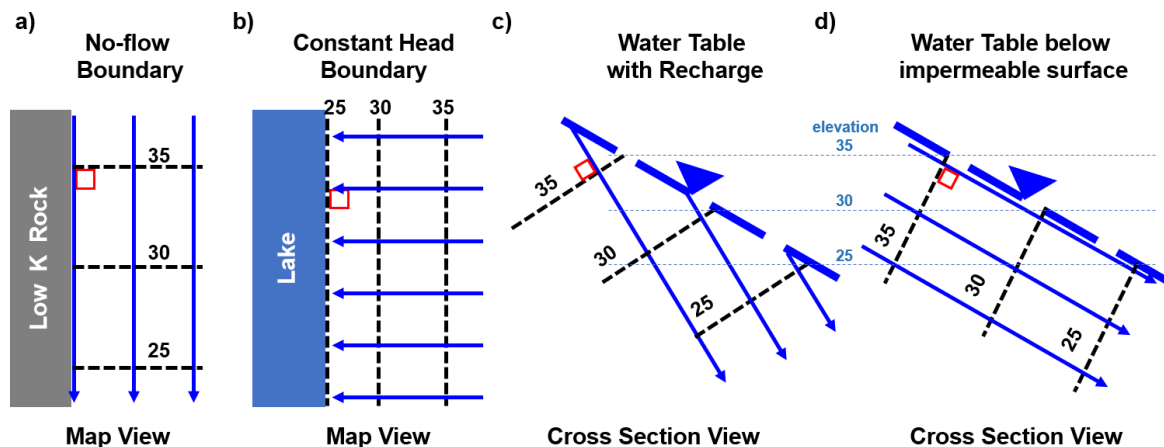


Figure 72 - Relative positions of the flow lines (blue arrows) and equipotential lines (dashed black lines) at domain boundaries. a) At an impermeable or low K boundary flow lines parallel the boundary and equipotential lines intersect it at right angles. b) Groundwater flow into a lake with a constant water level equal to the water table elevation. Flow lines intersect the boundary at right angles and equipotential lines parallel it. c) When recharge crosses a water table, flow lines meet the water table at an angle and equipotential lines intersect the water table at the elevation equal to their value, but at angle other than 90° . d) When there is no recharge at the water table, flow lines parallel the water table and equipotential lines intersect the water table at the elevation equal to their value and are perpendicular to the water table.

Boundaries at Subsurface Features

Faults

Faults or shear zones can also form physical flow boundaries (Figure 73). The behavior of groundwater in the vicinity of these features depends on whether the faulting created conditions that significantly reduced the hydraulic conductivity (e.g., by creating fault gouge, or juxtaposing formations of substantially different hydraulic conductivity) or enhanced the hydraulic conductivity (e.g., by creating numerous, well-connected, open, large aperture fractures within and adjacent to the feature). When fault or shear zones restrict groundwater flow, they may be considered Type 2 no-flow boundaries. If a conductive fault zone is located near the perimeter of the model domain and is connected to a source of water, it may be treated as a Type 2 constant flux or Type 3 variable flux boundary. In some settings, conditions within a single zone vary spatially such that some sections may enhance flow while others limit flow. It is advisable to inspect outcrops and place wells near and within faults and shear zones to determine if they limit or enhance flow.

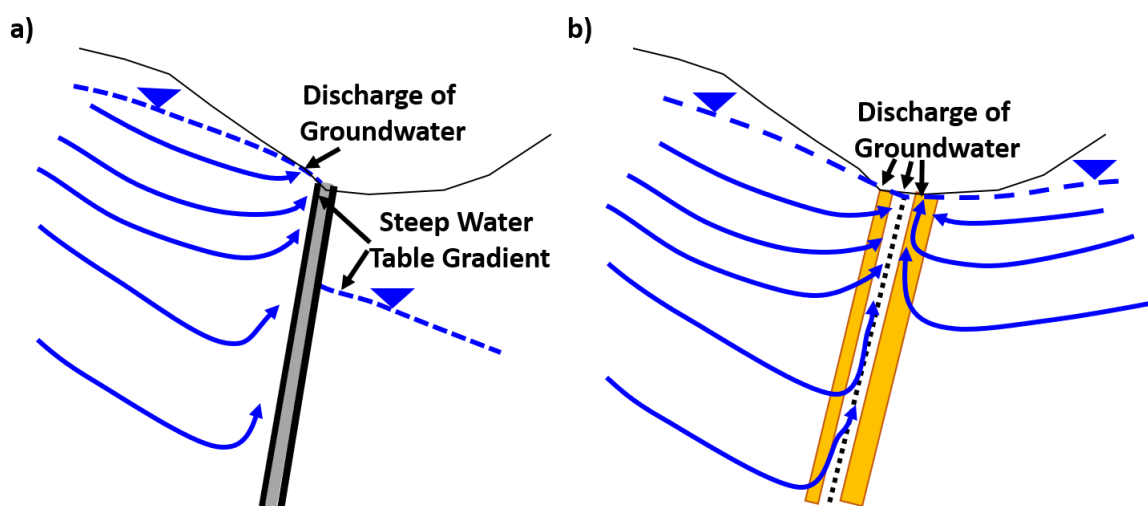


Figure 73 - The role of faults, fracture zones and shear zones as boundaries in cross sections: a) A fault system filled with low hydraulic conductivity fault gouge (gray). The generalized groundwater flow (blue) arrows show the fault acts as a barrier to flow, forcing the upper portion of the flow system to discharge at the surface on the upgradient side of the fault. The restriction of flow causes the water table on the down gradient side of the zone to be lower. b) A conductive fault or shear zone in which fracturing enhanced the hydraulic conductivity of the region adjacent to the fault (orange zones) and along the fault itself (dashed line). Generalized flow lines (blue arrows) show the system concentrates groundwater discharge in the swale. In other settings the conductive zone may carry recharge deep into the system.

Seawater-Freshwater Interface Boundaries

Near coastlines the subsurface seawater-groundwater interface creates a boundary to fresh groundwater flow (Figure 62 and Figure 74). The boundary acts as a physical boundary that limits flow, forcing fresh unconfined groundwater to discharge along the coastline. The interface behaves as a Type 2 no-flow boundary. The boundary is not a sharp

interface because its position shifts with the tidal cycles and as freshwater discharge rates vary. A mixing zone between freshwater and seawater occurs and is referred to as the transition zone. Groundwater flow projects near coastlines often require modeling tools that account for variable density flow. In its simplest form it can be assumed the boundary acts as an impermeable physical boundary.

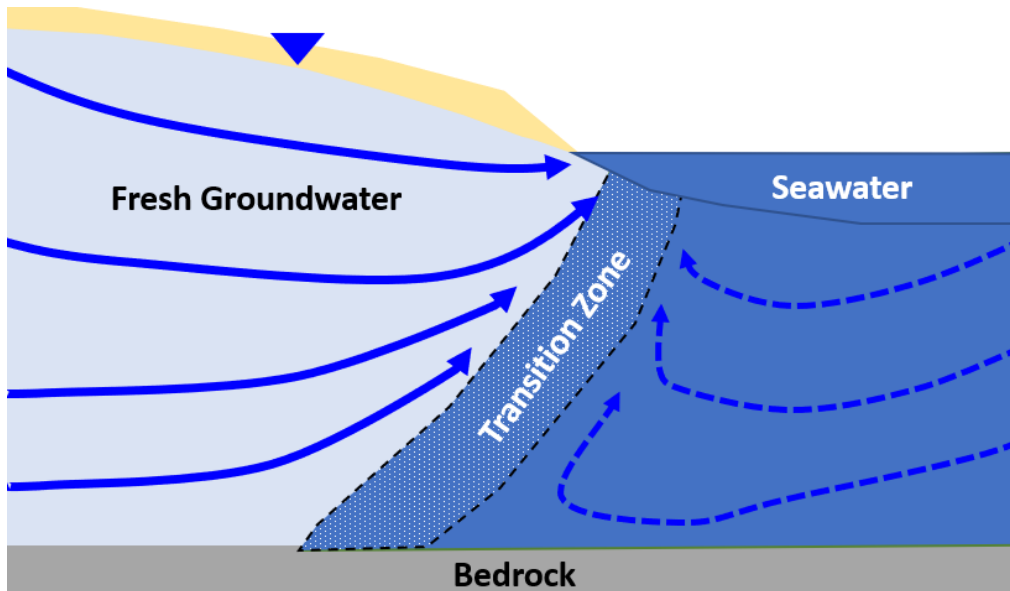


Figure 74 - Schematic cross section of groundwater flow at the coastline. The seawater-fresh groundwater interface is a boundary to the freshwater groundwater system. The interface is not sharp because cyclic tides and varying freshwater discharge rates shift the position of the interface. At the interface the fresh and salt water mix such that a transitional zone develops. The boundary forces freshwater groundwater to discharge along the coastline.

Hydraulic Boundaries

Hydraulic boundaries form when two or more flow systems converge. They are defined where parallel groundwater flowlines separate groundwater flows originating from common or differing recharge sources. They are typically drawn on cross sections, but sometimes hydraulic divides at recharge and discharge areas are indicated on maps. Hydraulic boundaries occur in both unconfined and confined systems.

In an unconfined system, groundwater flow lines originate in a recharge area and continue to discharge areas. A vertical hydraulic divide is formed below both the recharge area and the discharge area (Figure 75, red dashed lines). As groundwater flow paths cannot cross, the divide boundaries act as no flow boundaries (Type 2). When a drop of water recharges the system on the divide, half of the drop moves along one side of the divide and the other half along the other side. Divides can be vertical, horizontal or some combination of conditions depending on the nature of the flow systems (Figure 75). Hydraulic boundaries are defined by the flow system conditions. They can change with time, including, in some cases, disappear as the head distribution changes in response to variations in the magnitude and timing of recharge and discharge.

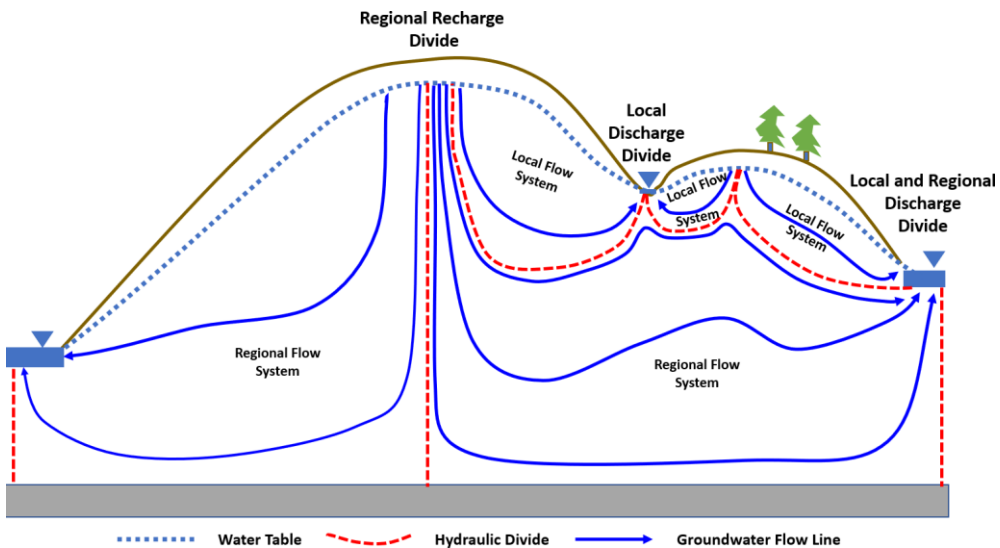


Figure 75 - Cross section of groundwater flow showing the water table (dashed blue line), hydraulic divides (red dashed lines) and groundwater flow lines (blue arrows). Recharge from the regional recharge area flows to both local and regional discharge areas. Local recharge also discharges at local and regional locations.

Flow Systems with Distant Boundaries

It is not unusual to assess groundwater flow conditions in a portion of the system that is a long distance from physical boundaries. This problem domain would be considered to have distant boundaries. In some cases when analytical solutions are developed it is assumed that the boundaries impacting groundwater flow are sufficiently distant that the aquifer can be thought of as infinite in extent, a factor that simplifies the mathematics.

When groundwater modeling techniques are used and physical boundaries of the domain area are far away from a site of investigation, setting up local boundaries for the investigation may be appropriate. As an example, examine the setting shown in Figure 76a. Assume the area of interest is shown by the concentration of wells near the lake. The sand and gravel aquifer is unconfined, assumed to behave as an isotropic and homogeneous system, and is surrounded by a number of physical boundaries. These physical boundaries include a fault and low permeable granites to the south, water flowing out of the Green Mountains on the west, a major river to the north, and the lakeshore to the east. The purpose of the investigation is to determine the effect of pumping a new well (the location shown by the orange dot) on the water levels in existing wells in the area. In this setting, it may be appropriate to set local boundaries in the vicinity of the site of interest (Figure 76b). The lake elevation (a physical boundary of constant head (Type 1)) is set to the east. The western boundary is designated as a constant head (Type 1) using the value of the equipotential line established from contouring head measurements. The northern and southern boundaries are designated as no-flow (Type 2) because they are parallel to defined groundwater flow lines. This smaller model area is appropriate under transient flow conditions when the area

of influence of the well (red dotted line in Figure 76b) is small and not affected by the local boundary conditions on the north, west, and south (impacting the eastern boundary would not be a problem because it is a physical boundary). However, if the area of influence is large like that shown in Figure 76c then the selection of the smaller area would not be appropriate because the artificial boundaries will influence the results. It should be noted that, if steady-state pumping was being investigated the local boundaries would influence the predictions. Steady-state analyses should be performed using the entire problem domain.

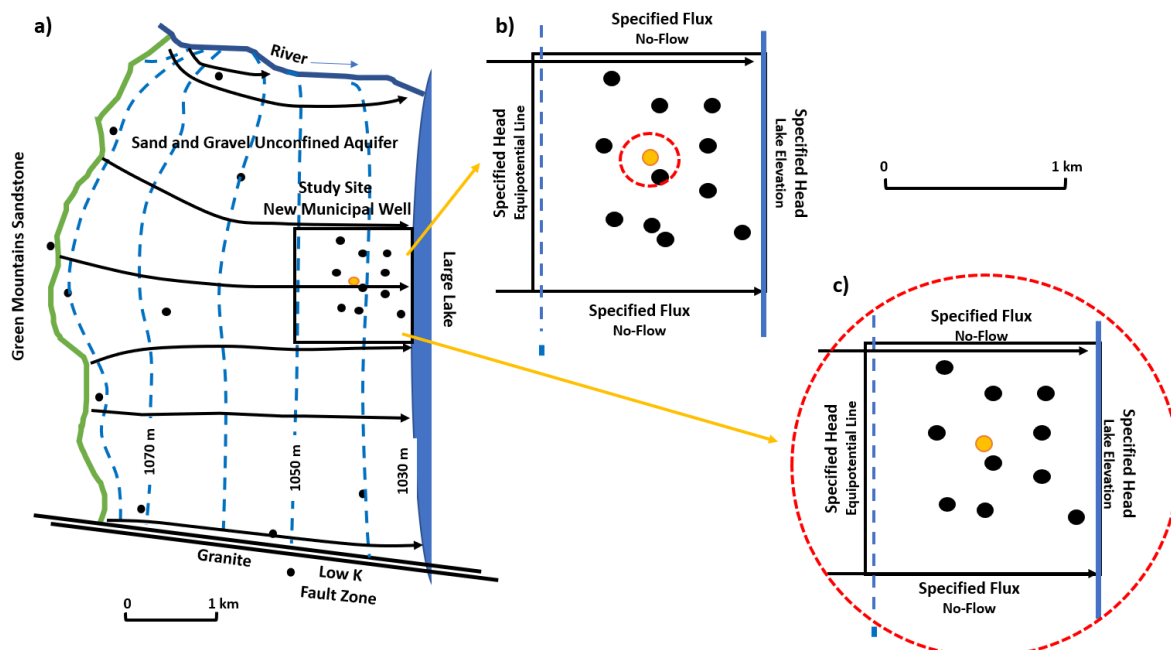


Figure 76 - Setting boundary conditions for a smaller site model located in a larger problem domain. a) The modeling effort is designed to examine the effect of pumping a new well (orange dot) on water levels in existing wells (black dots). Physical boundaries, equipotential lines (dashed blue lines) and groundwater flow lines (black arrows, assuming isotropic and homogeneous conditions) are shown. The site investigation area is surrounded by a black box. b) Setting local boundaries for the site investigation. This approach may be appropriate if the water level changes caused by pumping (dashed red line) do not extend to the local boundaries. c) Setting where the area of influence extends beyond the proposed local model boundaries. In this case the entire domain should be used instead of the local model site.

8.4 Analysis of Groundwater Flow Systems

Hydrogeologic investigations have specific goals defined to answer questions related to applied groundwater projects or to meet research objectives. Meeting these goals requires an understanding of the geologic framework forming the aquifer system, physical and hydraulic boundary conditions, as well as the locations, rates and timing of groundwater sources (e.g., recharge, stream leakage) and sinks (e.g., pumping, evapotranspiration). In most cases, it is necessary to determine the groundwater flow system behavior under both steady-state and transient conditions, and to prepare a water budget.

Developing Potentiometric Maps and Cross Sections

A key component of evaluating groundwater flow conditions is the construction of potentiometric maps of unconfined and confined aquifers and, in complex groundwater systems, representations of multiple aquifers and aquitards. Head measurements obtained from field investigations are used to interpret horizontal and vertical groundwater flow directions and rates, and the potential for exchange between aquifers and aquitards. Interpretation of the mapped gradients and behavior of groundwater flow can shed light on the aquifer conditions including changes in hydraulic conductivity, aquifer thickness, and can be used to identify the location of recharge and discharge areas. Challenges to presenting, developing and interpreting potentiometric information are included in this section.

Potentiometric Maps, Cross Sections and Flow Nets

Strictly speaking, a potentiometric map or cross section is a representation of the distribution of head (head values and equipotential lines). When flow lines are added to sets of equipotential lines the potentiometric map becomes a flow net (Figure 77). However, it may be referred to as a potentiometric map, water table map or a flow net. As presented in the previous sub sections, a set of parallel flow lines encompasses a flow tube. Conceptually, the discharge through flow tubes is constant under steady state conditions. Potentiometric maps can have an infinite number of flow tubes as there are as many tubes as there are pairs of flow lines. Most maps or cross sections show a number of flow tubes to represent general groundwater flow conditions (Figure 77a).

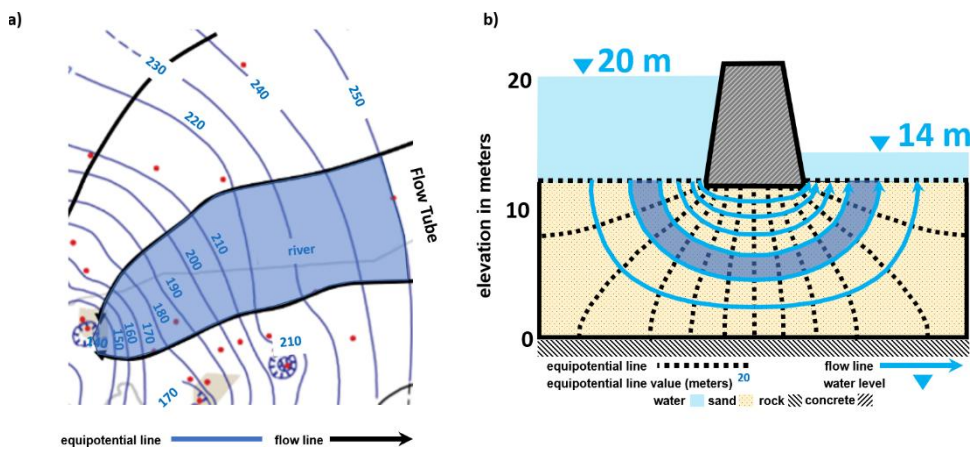


Figure 77 - Schematics of flow nets. Flow tubes are bordered by flowlines. a) A qualitative flow net for which head data at the red dots are hand-contoured and flow lines are drawn at right angles to equipotential lines assuming isotropic and homogeneous conditions. One flow tube is shaded in blue (after Brahana and Borshears, 2001). b) A scaled, hand-drawn flow net of groundwater flow under a dam can be used to quantify flow per unit width of aquifer (Poeter and Hsieh, 2020). A flow tube is shaded in blue.

Although the term flow net can refer to any map or cross section with equipotential lines and flow lines, flow nets constructed under a series of rigorous rules (scaled flow nets) can be used to quantitatively examine groundwater flux (Figure 77b). Scaled flow nets can

be hand drawn or produced using groundwater models. They are used in both map view and cross section view to compute the volume of water that would discharge into excavations or under berms or dams, and to design drainage systems.

Considerations When Developing Potentiometric Maps and Cross Sections

Potentiometric maps represent flow in the horizontal plain and they are often used to represent conditions in a single hydrogeologic unit or aquifer. Flow within an aquifer or between aquifers can be represented by the construction of vertical cross sections and/or multiple potentiometric maps.

To generate a potentiometric map of a groundwater system, care must be taken to assure that piezometers and wells used to collect data represent horizontal flow conditions (or near-horizontal conditions). In most groundwater systems, water flows horizontally in large portions of the aquifers. Figure 78 shows the equipotential lines and a flow line in an unconfined aquifer. Horizontal flow is represented by the shallow wells screened near the water table and by any of the wells where equipotential lines are near vertical (vertical equipotential lines indicate horizontal flow). Wells screened at variable depths in the recharge area and discharge area reflect vertical flow with lower heads in deeper wells in the recharge area and higher heads in deeper wells in the discharge area. Potentiometric maps need to exclude the data from these deeper wells in order to portray a reasonable representation of near-horizontal flow in the system. Cross-sectional representations would use all of the data to show vertical components of flow (Figure 78).

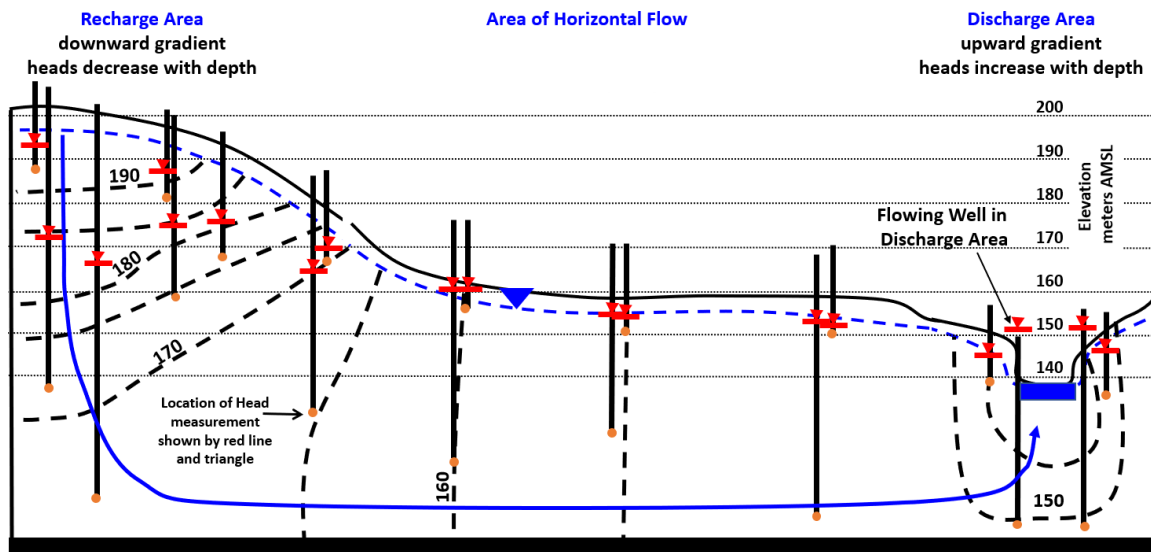


Figure 78 - Schematic of the head distribution in an isotropic and homogeneous unconfined aquifer. Wells are open only at the bottom as indicated by the orange circle. The head associated with that location is shown as a red line and triangle. Equipotential lines are dashed black lines. In the recharge area, heads are lower in deeper wells (heads decrease with depth and flow is downward). A zone of horizontal flow occurs where equipotential lines are vertical and heads in deep and shallow wells at approximately the same location are about equal. In the discharge area deeper wells have higher heads (heads increase with depth and flow is upward). When the head in a well is above the top of the well casing, water flows from the well without a pump.

Maps of potentiometric surfaces are also used to represent flow in confined aquifers. In confined systems, the aquifer is constrained by confining beds and has substantially higher hydraulic conductivity than confining beds, so near-horizontal flow occurs in much of the system (vertical equipotential lines) when the confined aquifer is a horizontal layer. When confined aquifers dip, flow is near-parallel to the aquifer boundaries. The exception to flow being parallel to the aquifer boundaries in confined aquifers occurs in recharge and discharge areas where vertical gradients are present as is the case in unconfined systems (Figure 79). When producing a potentiometric map for confined aquifers, it is generally appropriate to exclude head data from deeper wells located in the recharge and discharge areas so the flow lines will represent flow parallel to the aquifer boundaries. It is sometimes useful to represent areas containing vertical gradients by shading areas of a potentiometric map and labelling them as areas where gradients are upward or downward.

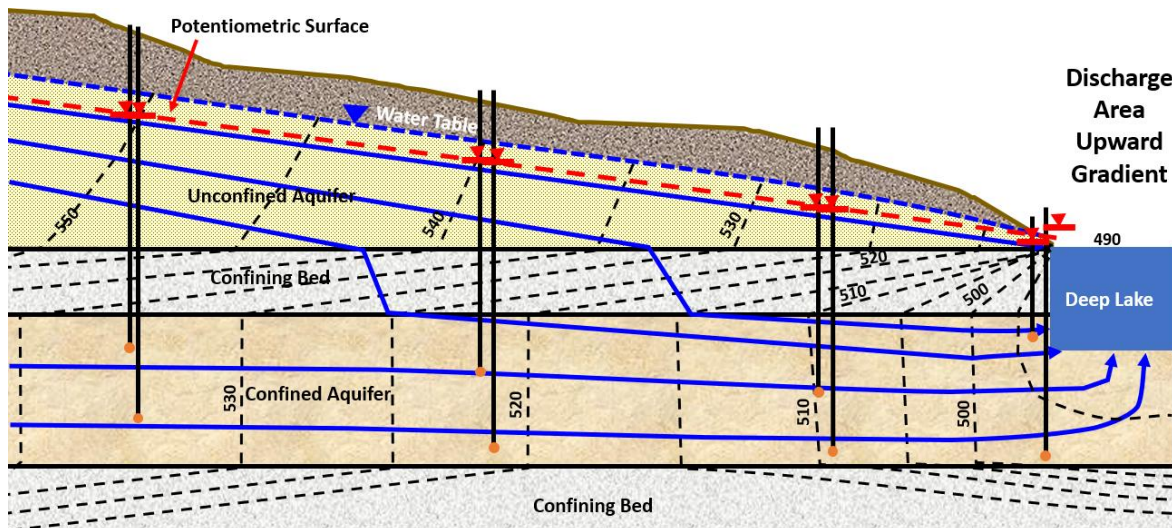


Figure 79 - A schematic cross section of flow in a confined aquifer that discharges to a deep lake. Formation conditions are assumed to be isotropic and homogeneous. Flow lines are blue arrows and equipotential lines are dashed black lines. Water levels in pairs of wells penetrating to different depths in the confined aquifer are the same where flow is essentially horizontal. Upward gradients occur in the discharge area.

Construction of flow nets representing cross-sectional views rely on monitoring well data from wells screened at multiple depths (Figure 78 and Figure 79). Cross section flow nets are constructed as scaled sections without vertical exaggeration in the direction of flow (Figure 80). They must be constructed in the direction of groundwater flow in map view (section W-E of Figure 80a and b) so that flow is parallel to the plane of the drawing. This ensures meaningful flow lines because there is no flow in or out of the plane of the drawing. If cross sections are constructed at some angle other than parallel to groundwater flow, they will not represent vertical flow conditions along the flow path even though a vertical distribution of head can be plotted on the section (e.g., the W-NE section of Figure 80c and d).

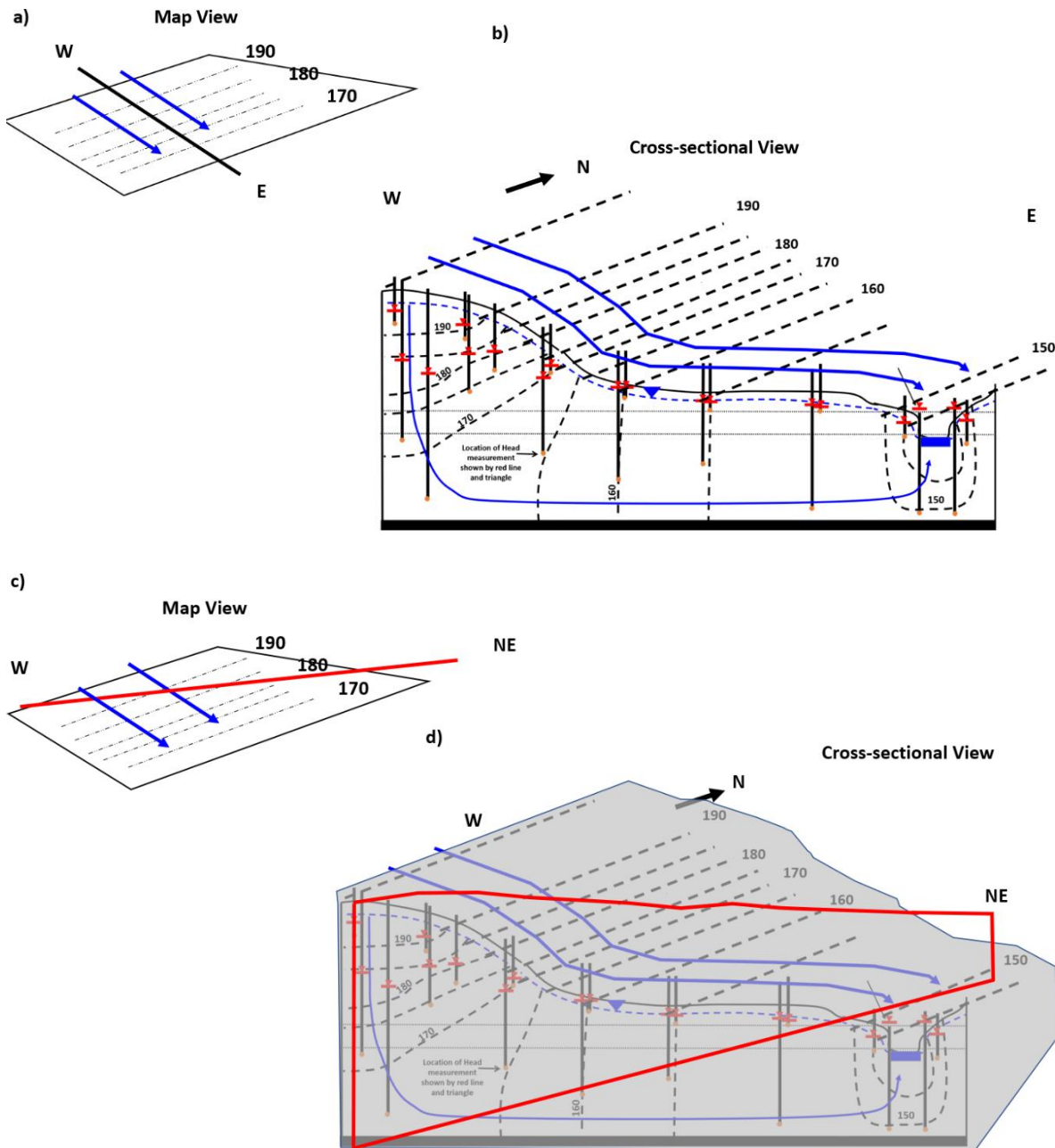


Figure 80 - Schematic representation of plotting hydrogeologic cross sections that parallel the groundwater flow in a region. Equipotential lines are shown as dashed black lines, monitoring wells as vertical solid black lines with horizontal red lines representing water levels recorded in wells. The black and gray bars represent earth materials with a lower hydraulic conductivity. a) Map insert of the general groundwater flow direction (blue arrows) and the location of the W-E cross section. b) The cross section parallels the groundwater flow as represented in the map view. Equipotential lines and flow lines represent conditions in the vertical dimension. c) Map insert of the general groundwater flow direction (blue arrows) and the location of a cross section, W-NE, plotted so it is not parallel to groundwater flow. d) The red frame represents the location of the cross section relative to the groundwater flow direction. If vertical heads were plotted on this cross section and flow directions interpreted, flows would have no relationship to vertical flow in the direction of groundwater flow.

Head data used for construction of potentiometric maps and cross sections need to be accompanied by the following information to assure the data are representative of the appropriate aquifer or cross section of earth materials:

- well completions, including depths and the extent of the casing open to the aquifer;
- types and configuration of aquifers and aquitards penetrated; and,
- location of recharge/discharge areas as well as areas of groundwater pumping, which can cause vertical gradients.

Representing Steady State and Transient Conditions

Steady state is represented by data collected over a period of time when heads and gradients are not changing. At smaller sites, a single hydrogeologist (or a team of people) makes all head measurements on the same day. When study areas are much larger, the data may be collected within the same week, or some other short period of time. The data sets are then represented as a snapshot in time when conditions are constant (e.g., March 15, 2020; or March 2019 to May 2019, average water levels). If data are collected over a period when the water table or potentiometric surface is changing in a consistent way (e.g., declining 2 cm per day) then either the data sets need to be corrected for this change (by generating comparable values for a short time period that are adjusted to a single day or week), or an error analysis should be generated. Often, well hydrographs that reflect groundwater level changes over time are recorded during the data collection period and can be referred to for data adjustments or error analyses. In large regional studies, where head changes in the down gradient direction are large, transient head errors may not impact interpretations of flow directions and fluxes because changes are small (a few centimeters) compared to the spatial variation in heads (meters).

If the system is changing in an irregular way (e.g., localized groundwater mounds or depressions are growing or shrinking) only the most general conclusions can be made using steady-state assumptions. In such cases a transient analysis should be undertaken.

Transient representations of changes in head distributions and flow paths are most often represented as a time series or “snapshots” of head distributions on maps and cross sections (e.g., a potentiometric map for each month; or a period of lowest water levels and highest water levels). These data sets and representations illustrate the system dynamics by documenting the timing and magnitude of changes. When head changes over time are small, it may be appropriate to generalize the system as steady state. However, when values change significantly over time, transient conditions should be presented.

Influence of Variation in Hydraulic Conductivity and Cross-Sectional Area on Head Distribution and Flow Pattern

As discussed in Section 4, construction of potentiometric maps and cross sections allow for the interpretation of groundwater flow directions. Gradients observed on maps and cross sections can be analyzed to shed light on: variations in aquifer thicknesses and hydraulic conductivity distributions; the locations of recharge and discharge areas; and the

addition or loss of water along a flow path. The impact of these conditions on hydraulic gradient along a one-dimensional flow path are illustrated in Figure 81.

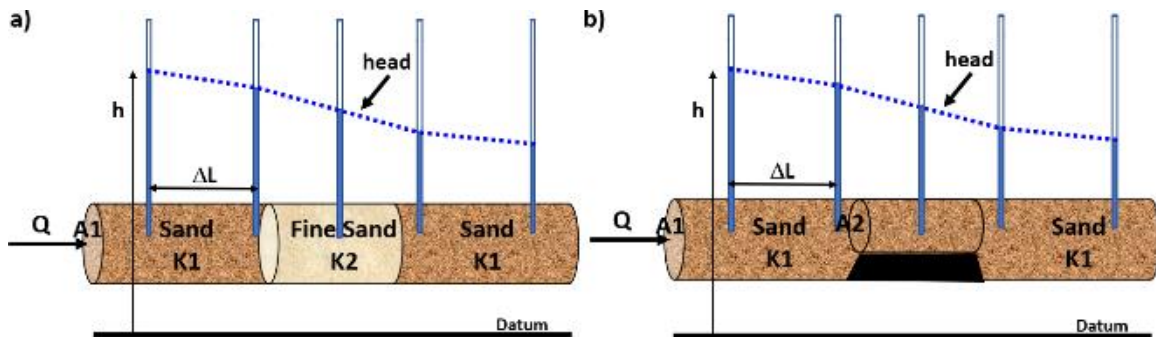


Figure 81 - Effect of changes in K and A on the head distribution/gradient along the flow path. Q is a constant value in space and time because the flow is steady state. Gradients are calculated between piezometers as $\Delta h/\Delta L$. a) The effect of groundwater entering and leaving a lower hydraulic conductivity zone. To maintain the same discharge Q , the gradient needs to be higher through the lower K zone (after Cohen and Cherry, 2020). b) The effect of groundwater encountering a smaller cross-sectional area, A_2 . The black zone is impermeable ($K = 0$). The gradient increases to maintain a constant discharge.

Similar concepts can be illustrated in two dimensions. To initiate the thought process, envision the steady state head distribution in an isotropic and homogeneous aquifer of constant thickness. The gradient would be constant in space and equipotential lines would be evenly spaced (Figure 82a). When equipotential lines are not evenly spaced, (e.g., the gradients are changing in space) there is an underlying reason (as indicated by Darcy's law). The changing gradient could be due to a change in hydraulic conductivity (Figure 82b(1)) and/or cross sectional area (Figure 82b(2)), or due to water entering the aquifer as recharge or as leakage from an underlying/overlying zone (Figure 82b(3)).

When parallel flow lines converge and diverge, again the relationships defined by Darcy's law can be used to hypothesize possible subsurface conditions. The change in width between the flow lines might reflect a change in hydraulic conductivity, cross-sectional area, and/or an increase or decrease of the discharge within the flow tube resulting from recharge or leakage to/from an adjacent formation (Figure 83).

Changes in gradients can also be caused by increasing the flow of water into the groundwater system in some areas (e.g., recharge), and decreasing the flow via discharge, pumping of wells, or direct groundwater evapotranspiration (Figure 82b(3) and Figure 83c).

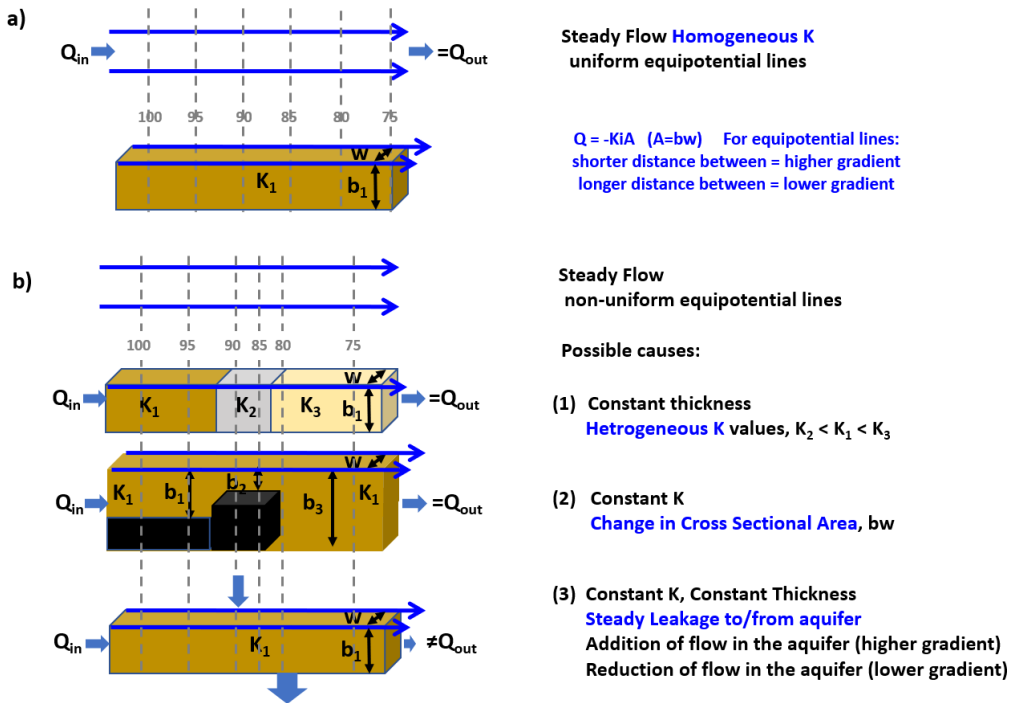


Figure 82 - Factors effecting spacing of equipotential lines when head measurements are contoured for a steady-state system. Equipotential lines are dashed gray lines and flow lines are blue arrows. a) Equipotential lines are evenly spaced and flow line spacing is constant. If the volumetric flow rate and flow area are constant then the hydraulic conductivity, K_1 , is constant. b) Equipotential lines are not evenly spaced indicating the gradient is changing along the flow tube. The observed changes could be attributed to (1) a variation in hydraulic conductivity, (2) a change in the cross-sectional area, (3) a steady inflow or outflow of water, or some combination of 1, 2, and 3.

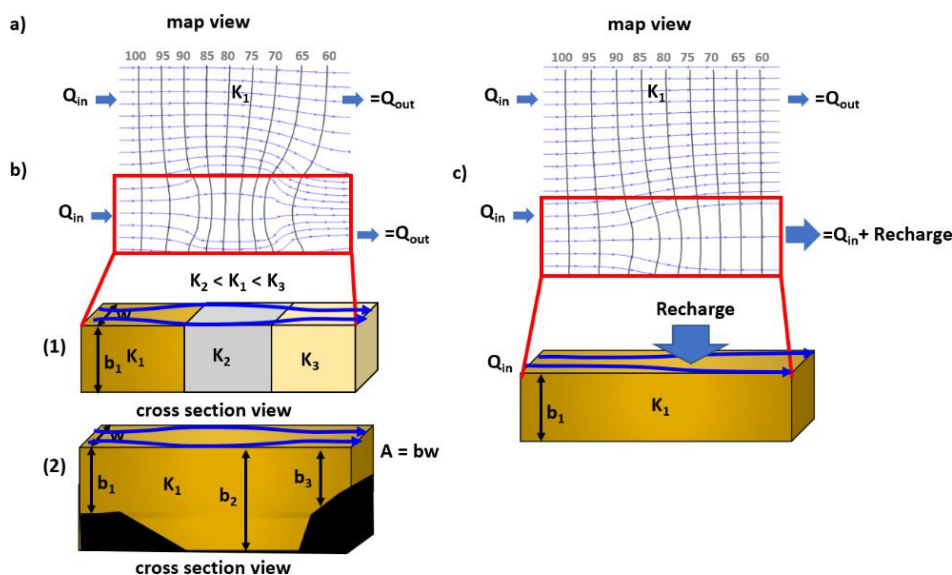


Figure 83 - Factors effecting spacing of flow lines and equipotential lines when head measurements are contoured. Equipotential lines are dashed gray lines and flow lines are blue arrows. a) Uniform equipotential line spacing and constant distance between flow lines homogeneous conditions. b) Irregular distance between flow lines might be caused by (1) changes in the hydraulic conductivity [larger distance for lower K_2 , smaller distance for higher K_3] and/or (2) changes in flow area, $A = bw$, [larger distance for larger b_2 , smaller distance for smaller b_3]; and/or, c) a steady-state addition or reduction of water flowing in the aquifer.

Addition of steady recharge along the flow path results in a steepening of the gradient and/or a widening of the flow tube. Steady-state leakage of water out of an aquifer to, for example, an underlying aquifer results in a decreased gradient and/or a narrowing of the flow tube. When water is withdrawn from a well at a steady rate of pumping for an extended period of time, the head in the aquifer is lowered in a curved conical shape and recharge is captured in the area around the pumping well (Figure 84). This causes water to flow towards the well to sustain the rate of water discharging from the pump. The change in head in the potentiometric or water table surface is referred to as a cone of depression of the head field (or a drawdown cone). The cone of depression grows with time as water is released from storage in the aquifer and eventually the withdrawal rate is balanced by inflow in the form of leakage from overlying/underlying aquifers, capture of surficial recharge water, and/or inflow from (or decrease of outflow to) a surface water body such as a lake or river.

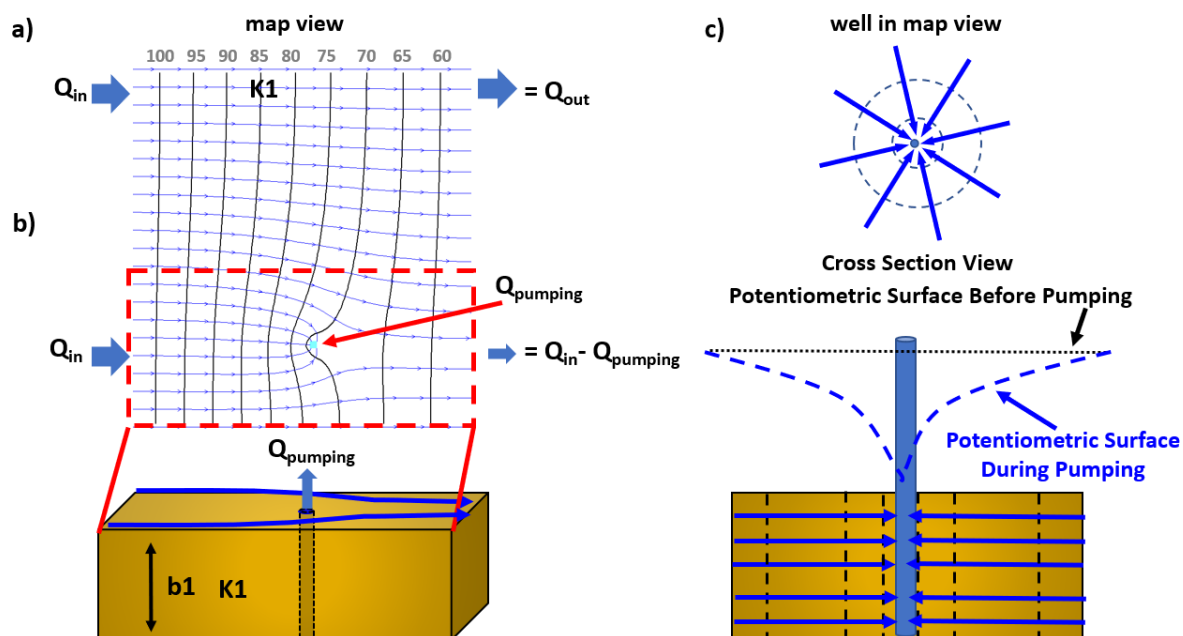


Figure 84 - Pumping of wells effects spacing of equipotential lines and the corresponding distance between flow lines when head measurements are contoured. a) Initial condition under isotropic and homogeneous conditions. b) Changes in the equipotential lines and flow lines as a result of long-term, steady-state pumping. The flow lines get closer together as water flowing to the well is captured and so, less water flows through the aquifer downgradient of the well. This representation assumes the capture of the upgradient groundwater flow is sufficient to equal the steady-state pumping rate. c) Conceptual models of how pumping reduces the head in the vicinity of the well when water flows toward a well. Heads decrease towards the well.

Putting the Concepts Together

Flow nets are created from head data collected in the field. The head data need to be representative of nearly horizontal flow in map view, or of a flow path in cross section. In addition to head data, the type, thickness and composition of aquifers including estimates of hydraulic conductivities are also collected as part of a hydrogeological

investigation. These data are paired with flow nets to interpret causes of changes in observed gradients and flow paths yielding valuable insight to the nature of the groundwater flow system.

8.5 Examples of Flow Systems

Three groundwater potentiometric maps are presented in this section to illustrate basic principles of constructing groundwater flow lines based on contours of head and interpreting the factors influencing the head configurations.

High Plains Aquifer in Wyoming, USA

A potentiometric map of a portion of the High Plains Aquifer in Wyoming, USA is shown as Figure 85. Groundwater is obtained from the unconsolidated and consolidated sediments of the Ogallala Formation, Arikaree Formation and the White River Group that are underlain by lower permeability Cretaceous sedimentary rocks (Bartos and Hallberg, 2011). These formations outcrop east of the Laramie Mountains in the western portion of the region shown. Formations slope to the east forming the major regional High Plains Aquifer found in portions of Colorado, Kansas, Nebraska, New Mexico, Oklahoma, South Dakota, Texas, and Wyoming.

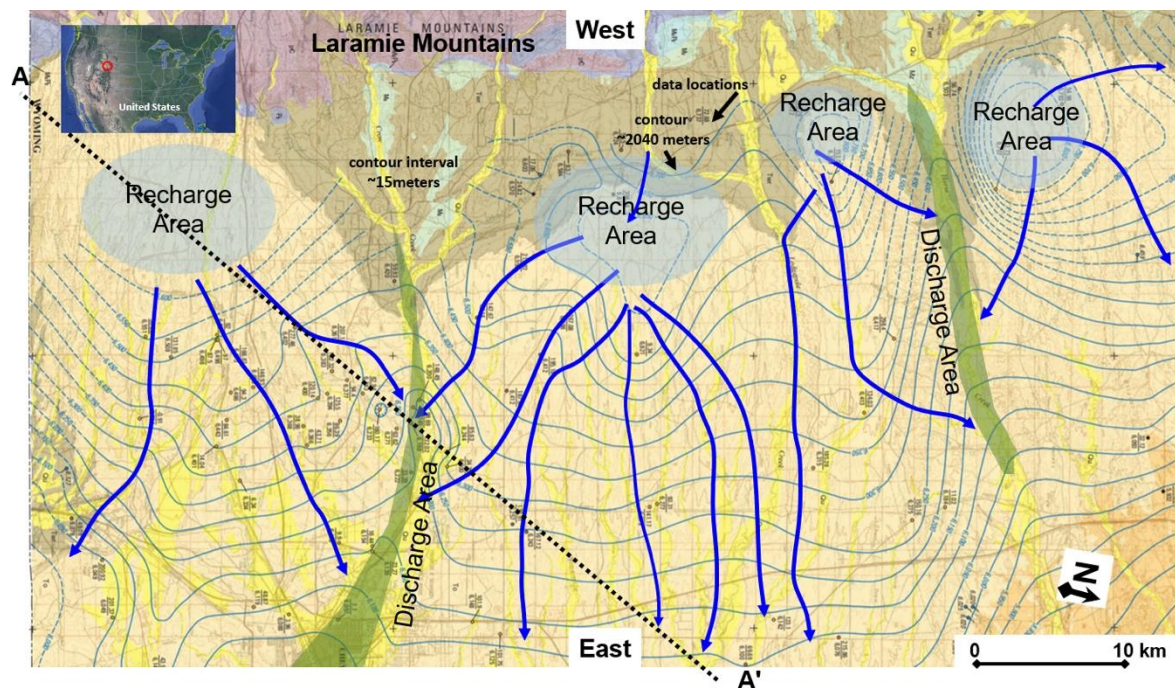


Figure 85 - Potentiometric map of a portion of the High Plains Aquifer located in Laramie County, Wyoming, USA. Equipotential lines (thin blue-green lines) represent conditions from March to June 2009. Recharge areas are shaded in light blue. Local discharge areas associated with streams are shaded in light green. Flow lines (thick blue arrows) were constructed assuming isotropic and homogeneous conditions. The approximate location of cross section A – A' shown in Figure 86 is indicated by the dashed line. This map covers only a small portion of the cross section shown in Figure 86 which extends far to the northeast (modified from Bartos and Hallberg, 2011).

The formations are considered hydraulically connected and water levels from wells penetrating these formations between March and June 2009 were used to create the generalized equipotential map. Flow lines were constructed assuming that flow behaves as if hydraulic conductivity is isotropic and homogeneous. Areas of recharge are inferred from the equipotential surface and are labeled and shaded light blue. These are areas of the highest heads and flow lines diverge with water flowing in multiple directions away from these elevated outcrop areas. Local flow systems discharge to local streams (labeled and shaded light green) where flow lines converge. The general regional groundwater flow is to the east (bottom of the map). It is useful to peruse the spacing of equipotential lines and the shape of flow lines and consider them in light of the information expressed in Figure 82, Figure 83, and Figure 84. A schematic geologic section along the dashed line A – A' of Figure 85 is shown as Figure 86.

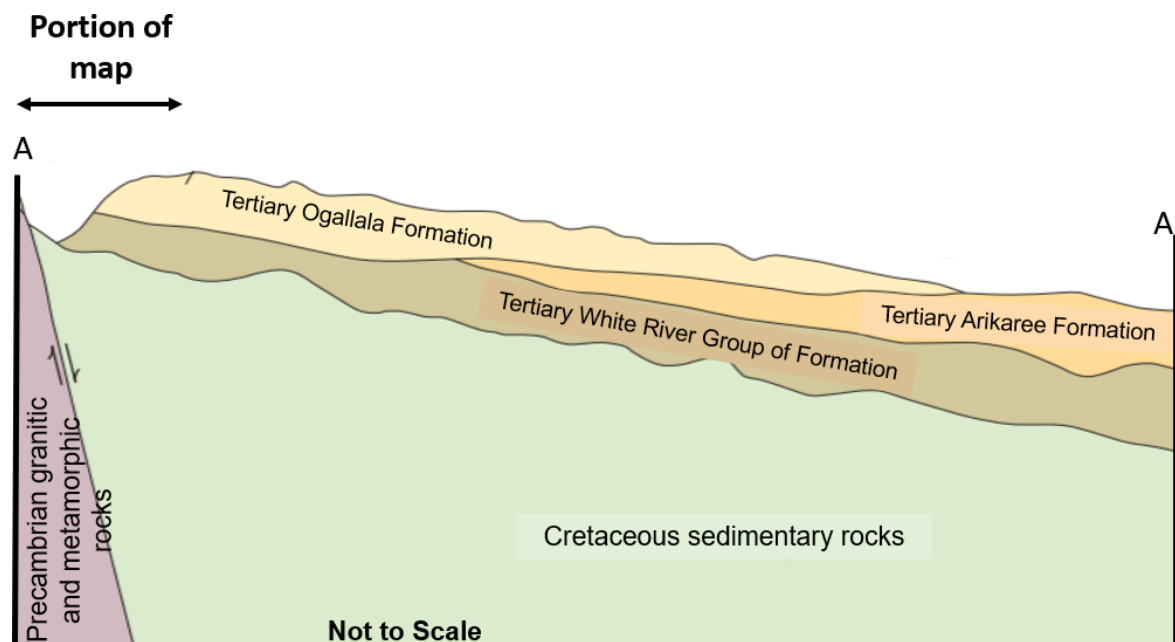


Figure 86 - Schematic southwest to northeast cross section of the High Plains Aquifer along A – A' of Figure 85 extending over 200 km. The portion of the section represented on the map shown in Figure 85 is indicated (modified by Bartos and Hallberg, 2011; from Denson and Bergebdahl, 1961).

Memphis Sand Aquifer, Memphis Tennessee, USA

A contoured map of head data from the Memphis Sand aquifer representing generalized conditions in September-November 2010 is provided as Figure 87 (Kingsbury, 2018). The aquifer is confined and separated from the water table alluvial system by clays and fine-grained sediments. The aquifer supplies 100 % of the water to the city of Memphis, TN, USA. In the area shown, aquifer thickness varies from about 200 m in the east to over 250 m in the west. Prior to pumping, groundwater flow was from the east towards the Mississippi River on the western border of the map. The potentiometric surface and flow lines show the effect of long-term pumping on the confined aquifer flow system. Pumping

has lowered the heads overall and formed closed lows in local areas around the well fields (shaded areas and hatched contours). The pumping captures groundwater flow coming from the east and draws water from the Mississippi River and western portions of the aquifer. Groundwater flow lines were drawn by assuming isotropic and homogeneous conditions. The flow lines converge and the gradient increases as they approach the pumping centers. Since 2010, water levels have risen in some areas in response to a slight decrease in water demand (Kingsbury, 2018). This can be observed by comparing the 1995 potentiometric map presented in Figure 65 with Figure 87. A cross section of the basin along the line shown in the southwest quadrant of Figure 87 is shown in Figure 88.

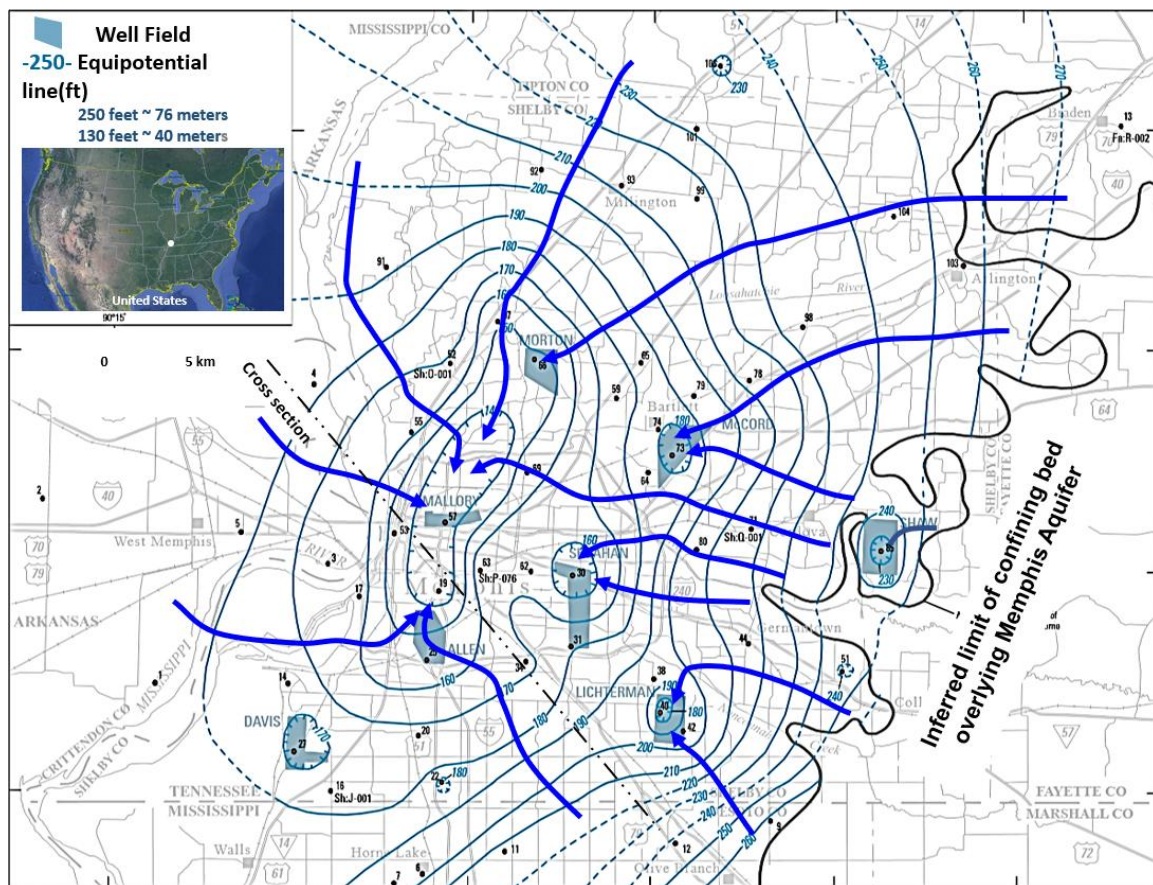


Figure 87 - Potentiometric surface based on September to November 2010 water level data for the Memphis Sand Aquifer located beneath Memphis, Tennessee, USA. Equipotential lines are solid green and dashed where inferred. Hatched contours indicate depressed areas of the potentiometric surface associated with pumping centers that have operated for an extended period-of-time. The curved black solid line in the eastern portion of the area represents the location of the transition from unconfined conditions in the east to confined conditions in the west. Flow lines are blue arrows. Pumping has captured groundwater flowing through the area as flow lines converge at well locations (modified from Kingsbury, 2018).

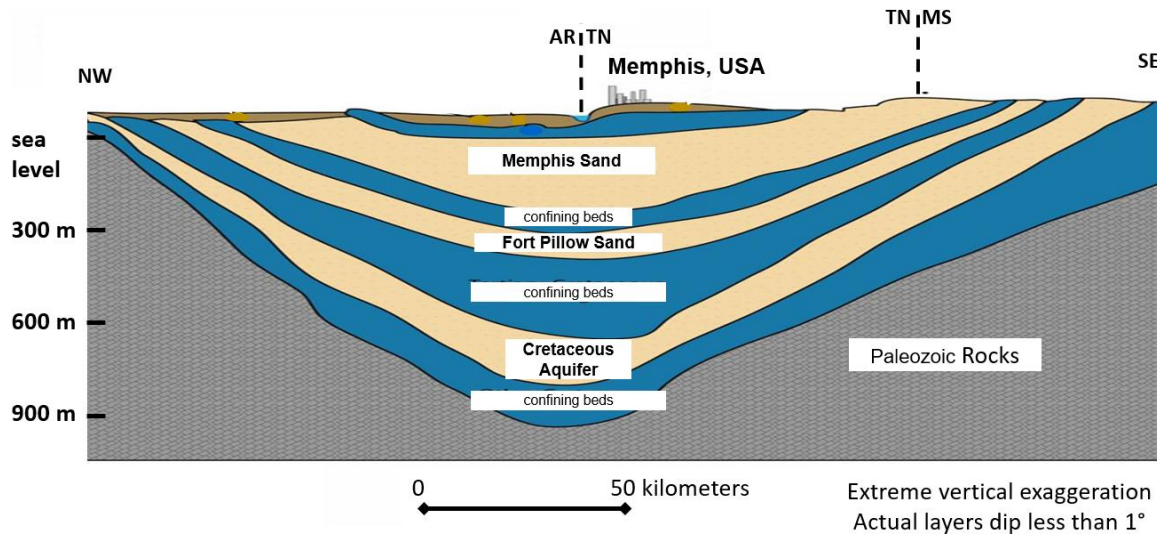


Figure 88 - A schematic cross section of the aquifer and confining beds in the Memphis area. The vertical dashed lines on the surface of the cross section represent where it crosses state boarders (AR Arkansas, TN Tennessee, and MS Mississippi). The approximate position of the schematic NW-SE cross section location is shown in Figure 87 as a dot-dashed line (modified from Taylor and Alley, 2001; Kingsbury, 1996 and 2018).

Unconfined Aquifer in East Helena, Montana, USA

Groundwater conditions in the unconfined aquifer system of East Helena, Montana, USA are shown in Figure 89. The southern portion of the area is overlain by a lead smelter that operated between 1888 and 2001. The aquifer is composed of sand and blends of sand and gravel that slope from higher ground in the south toward the Helena Valley in the north. The location of the cross section is shown as a dotted yellow line in Figure 89. The near-surface aquifer is contaminated with arsenic and selenium that originate from the smelter site. The groundwater flow system has transported plumes of contaminants northwest of the smelter site. The dissolved selenium plume originates at the smelter site and extends about 5 km to the northwest in the direction of groundwater flow. A stream (light blue line) flowing to the north passes through the site. It is losing stream water to the shallow groundwater system. This infiltrating stream water effects the groundwater flow paths forcing them to the northwest. The flow tubes originating from the smelter site narrow to the north as the aquifer thickens and stream water recharges the system.

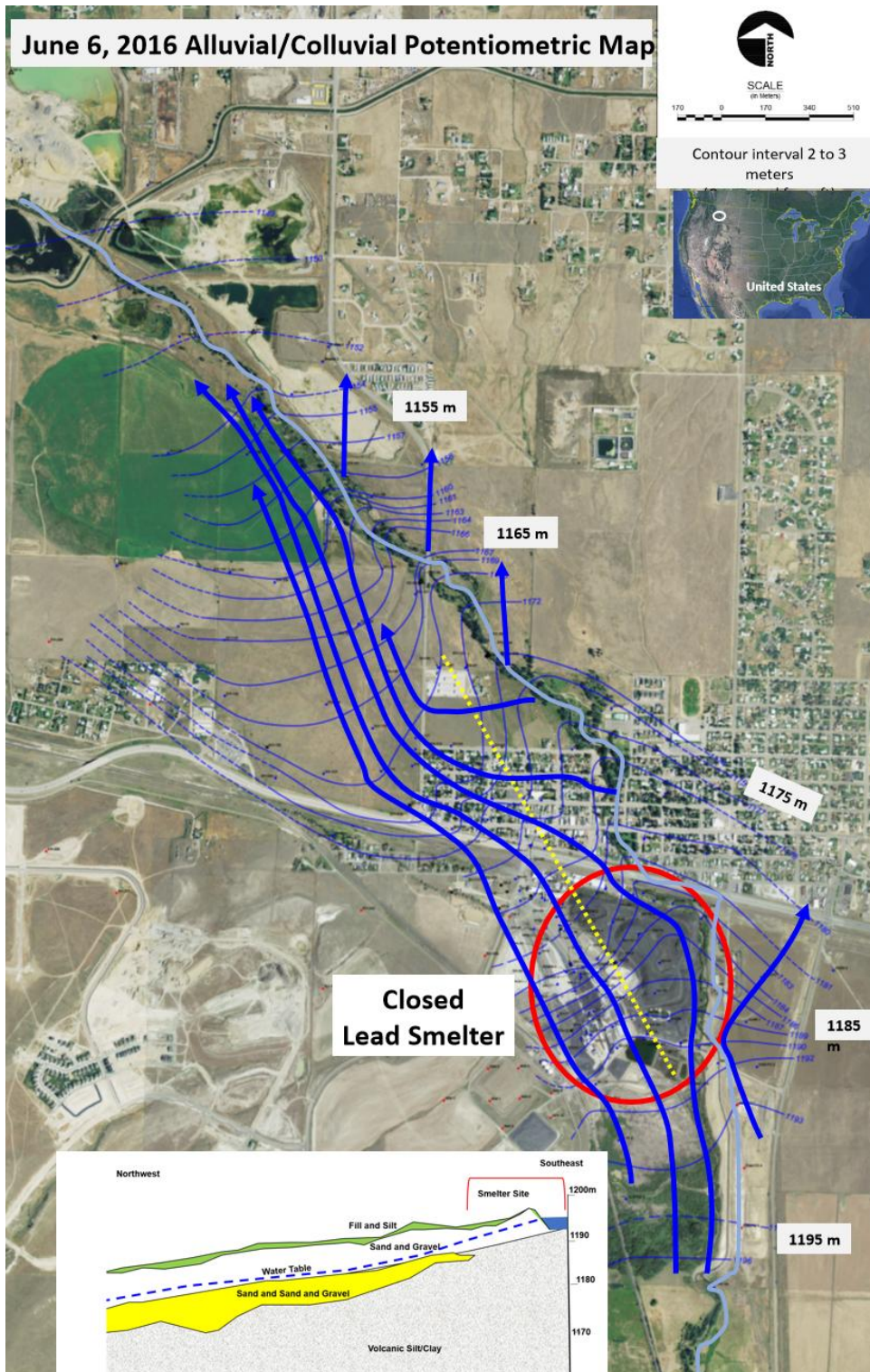


Figure 89 - Unconfined groundwater conditions in the vicinity a closed lead smelter (red circle) East Helena, Montana, USA. The region is underlain by a shallow sand and sand and gravel aquifer as shown in the cross section that is located on the map with a dashed yellow line. Groundwater flow is from the southeast to northwest though the industrial site. Equipotential lines (thin blue lines) originally labeled in feet, were converted to meters and represent water levels in June 2016. Flow lines (blue arrows) were constructed assuming isotropic and homogeneous conditions. A stream (light blue line) flowing to the north is losing water to the aquifer and this recharge is forcing groundwater flow from the smelter site to the northwest (with permission, modified from Hydrometrics, Inc., 2017).

Summary of Flow System Examples

In each of these examples head data were collected and contoured to create a potentiometric or water table map that represents horizontal flow conditions. Flow lines were constructed assuming conditions were locally isotropic and homogeneous. Evaluation of flow lines provides an opportunity to develop an understanding of site conditions. When field data indicating aquifer thickness and the distribution of hydraulic conductivity are available, then coupling observations of changing hydraulic gradients and flow line spacing with the principles stated in Darcy's law can reveal additional information about the groundwater flow system. Building and analyzing flow nets allows groundwater scientists to investigate how boundary conditions influence groundwater flow, providing the foundation for developing a conceptual model of the groundwater system. Groundwater flow analysis encompasses all aspects of the physical and hydraulic conditions as described in this book. This section is intended as an overview to introduce the basic concepts applied during interpretation of groundwater flow.

8.6 Exercises

[Exercise 14](#) provides data for use in constructing and evaluating a potentiometric map. [Exercise 15](#) offers an opportunity to determine flow paths from a potentiometric map for aquifers with isotropic and anisotropic hydraulic conductivity. [Exercise 16](#). Explores equipotentials in flow tubes with different aquifer geometries.

9 Conclusion

This book presented the principles and concepts that form the physical foundation of groundwater science and underpins the information in other [Groundwater Project books](#). Basic terms and tools used to describe the hydrogeologic properties of earth materials, compute groundwater flow directions, rates, fluxes and velocities were presented. Generalized mathematical descriptions that govern groundwater flow under standard flow conditions and their use in describing groundwater systems were outlined. This information serves as the foundation for further study of groundwater.

One critical concept to take away from this book is the relationship described by Darcy's law: that groundwater discharge is directly proportional to hydraulic conductivity, hydraulic gradient and the cross-sectional area perpendicular to the flow direction. An increase in any of those parameter values increases the groundwater discharge. When confronted with an obstacle while attempting to complete a hydrogeologic analysis, it is useful to go back to the basics of Darcy's law, $Q = -KiA$. Usually, it reminds the investigator of how basic hydrogeologic concepts can be applied and leads to a solution.

Another important concept is that flow systems are controlled by aquifer properties and boundary conditions, as well as the locations and magnitudes of sources and sinks. When confronting challenges in conceptualizing the system, it is useful to sketch cartoons representing where water enters the system and where it exits; and to build a water budget to evaluate if the system components are sufficiently known. Answer the question: Where is the water coming from and when is it going? Envision how you could represent the field system on your desk as a miniaturized version in a sand box with recharge sprinkled on the surface and tanks representing water bodies where water enters and exits. Such a simplification can help you focus on the most important aspects of the system so as to develop a better conceptual model of how the system works.

Physical principles and concepts cover a wide range of subjects. The [Groundwater Project books](#) that follow this one rely on principles and concepts presented here, and present further, more advanced, principles and concepts.

10 Exercises

Exercise 1

A 100 cubic centimeter (cm^3) sample of soil has an initial weight of 227.1 grams. It is oven dried at 105°C to a constant weight of 222.0 grams. The sample is then saturated with water and has a weight of 236.6 grams. Next, the sample is then allowed to drain by gravity in an environment of 100% humidity and is reweighted at 224.4 grams. Assuming that $1 \text{ cm}^3 \text{ of water} = 1 \text{ gram}$ at 15.5°C :

- a) Calculate the porosity;
- b) Calculate the specific yield;
- c) Calculate the specific retention;
- d) Evaluate whether the resulting particle density is reasonable;
- e) Calculate the void ratio;
- f) Calculate the initial moisture content;
- g) Calculate the initial degree of saturation.

[Solution to Exercise 1](#) ↴

[Return to where text linked to Exercise 1](#) ↑

Exercise 2

Show that $n = \frac{e}{1+e}$ where n is porosity and e is the void ratio.

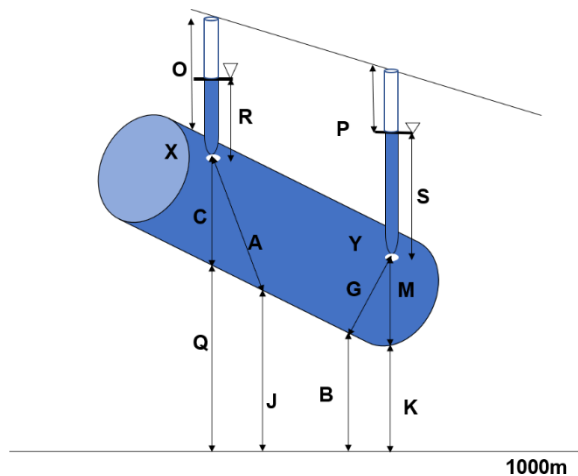
[Solution to Exercise 2](#) ↴

[Return to where text linked to Exercise 2](#) ↑

Exercise 3

Hydraulic head controls the flow of groundwater. A sand filled column is set up as shown in the accompanying figure using a datum of 1000 m. If O=9 cm, K=5 cm, P=5 cm, S=12 cm, A=12 cm, G=5 cm, R=4 cm, M=4 cm, B=7 cm, J=9 cm, Q=15 cm, C=6 cm, answer the lettered items below. To answer b through d write the answer first as the letters for the relevant line segments, and then as the total value, e.g., for G+M write, 5 cm + 4 cm = 9 cm.

- Which way is the water flowing?
- What is the total head at the white mark labeled X relative to the 1000 m datum?
- What is the elevation head at the white mark labeled Y relative to the 1000 m datum?
- What is the pressure head at the white mark labeled X?



[Solution to Exercise 3](#) ↴

[Return to where text linked to Exercise 3](#) ↑

Exercise 4

Rank the materials from the sediment with the largest value (1) to the material with the smallest value (3) for hydraulic conductivity, K , specific yield, S_y , and porosity n .

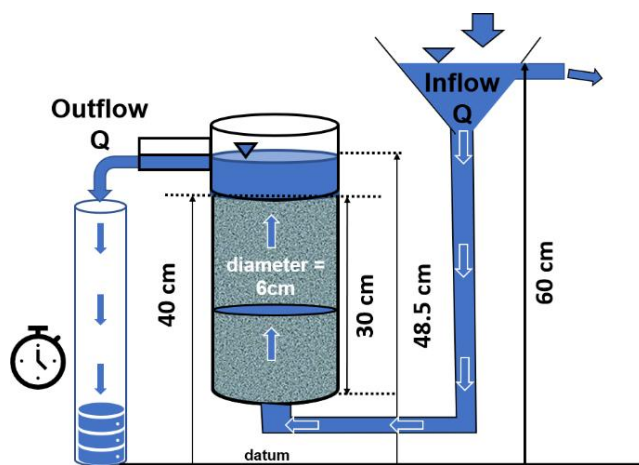
	K	S_y	n
Silty Sand	_____	_____	_____
Clay	_____	_____	_____
Equally mixed sand and gravel	_____	_____	_____

[Solution to Exercise 4](#) ↴

[Return to where text linked to Exercise 4](#) ↑

Exercise 5

A factory is disposing of hot waste water by injecting it into a 1000 m deep well that penetrates a confined aquifer. The sandstone aquifer contains water at 35°C, a similar temperature as the waste water. A regulator wanted the company to model how far the contaminated water would travel in the aquifer over a 10-year period. Hydraulic conductivity values were sparse. They required the company to core part of the 50 m thick confined aquifer and determine a representative value of hydraulic conductivity. A portion of the core was placed in a constant head permeameter as illustrated in the accompanying figure.



- If an average of 34.0 ml/min was collected at the outlet, what is K in cm/s?
- If the laboratory experiment was completed using 15°C water, what is the intrinsic permeability of the sandstone in cm^2 ?
- What is the hydraulic conductivity of the sandstone if the water temperature is 35°C (in cm/s)?

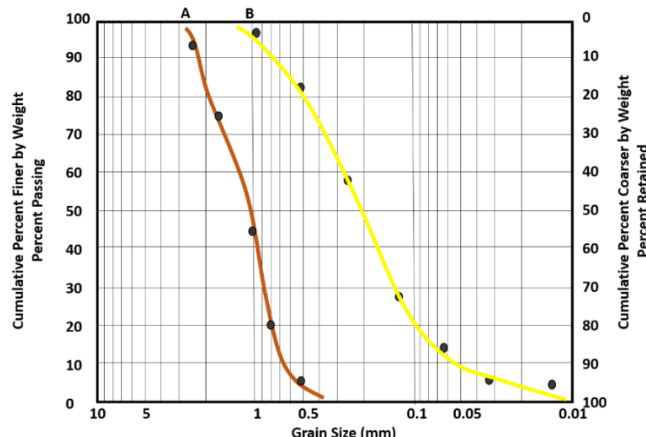
[Solution to Exercise 5](#) ↗

[Return to where text linked to Exercise 5](#) ↑

Exercise 6

K can be estimated for unconsolidated samples using empirical equations. Grain size distribution data for Sample A, a coarse sand with a porosity of 0.26 (red line), and Sample B, a fine sand with a porosity of 0.3 (yellow line), are shown on the accompanying graph.

- By inspection of the graphs, which sample is likely to have the highest hydraulic conductivity? Why?
- Compute the uniformity coefficient for each sample. Compare and contrast the results. Do the coefficients appear to support your observations in part a?
- Using the Hazen approximation and Slichter method, estimate K in cm/s.
- Are the K values computed in part c characteristic of sands? Do both methods produce similar values? Why or why not?



[Solution to Exercise 6](#) ↴

[Return to where text linked to Exercise 6](#) ↑

Exercise 7

Storage in confined aquifers relies on squeezing water in and out of the saturated skeleton. Explain the effects on the effective stress and pore water pressure when water is pumped into a confined aquifer and the water level in tightly cased wells penetrating the aquifer rises 1 m.

[Solution to Exercise 7](#) ↴

[Return to where text linked to Exercise 7](#) ↑

Exercise 8

Show that the units of S_s are 1/L.

[Solution to Exercise 8](#) ↴

[Return to where text linked to Exercise 8](#) ↑

Exercise 9

A confined aquifer underlies a 10 km^2 area. The average water level in a number of wells penetrating the confined system rose 2.5 m from April through June. An overlying unconfined aquifer showed an average water table rise of 2.5 m over the same period of time.

Assume the storativity for the confined system is 3.6×10^{-5} , and specific yield is 0.12 for the unconfined system. How much water (in m^3) recharged each aquifer based on the responses of each potentiometric surface?

[Solution to Exercise 9](#) ↴

[Return to where text linked to Exercise 9](#) ↑

Exercise 10

Draw and clearly label a cross section of a water table aquifer overlying a confined aquifer. Label the confining units as aquitards. Place two observation wells in each aquifer and show the water level in each of the wells so that groundwater flow is from the left to the right for the water table aquifer and from the right to the left for the confined aquifer. The illustration should suggest that leakage from the confined aquifer is upward into the unconfined aquifer. Show the corresponding water table and potentiometric surface positions.

[Solution to Exercise 10](#) ↴

[Return to where text linked to Exercise 10](#) ↑

Exercise 11

A regional unconfined sand aquifer was developed during 1990. As a result of the extraction of water the water table dropped about 40 m over a 1 square km area. If the porosity is 34% and the specific retention is 12%, how much water (m^3) was withdrawn from the impacted area? How might this volume differ if the aquifer were a 100 m thick confined sand with water at a temperature of 8°C? Calculate an estimate of the volume of water withdrawn if the potentiometric surface dropped about 40 m. Use an appropriate storativity based on an estimate of aquifer compressibility and water density.

[Solution to Exercise 11](#) ↴

[Return to where text linked to Exercise 11](#) ↑

Exercise 12

- 11) Write the governing equation that describes two-dimensional (x and y), steady-state flow in a confined anisotropic and homogenous aquifer.

[Solution to Exercise 12](#) ↴

[Return to where text linked to Exercise 12](#) ↑

Exercise 13

What conditions does the following governing equation represent? Explain the features of the terms of the equation that indicate each condition.

$$S_s \frac{\partial h}{\partial t} = \frac{\partial}{\partial x} \left(K_x \frac{\partial h}{\partial x} \right) + \frac{\partial}{\partial y} \left(K_y \frac{\partial h}{\partial y} \right) + \frac{\partial}{\partial z} \left(K_z \frac{\partial h}{\partial z} \right)$$

[Solution to Exercise 13](#) ↴

[Return to where text linked to Exercise 13](#) ↑

Exercise 14

Ten wells are located in a valley setting. Glacial material underlies the land surface and a confined sandstone aquifer underlies the region. All wells shown in the accompanying diagram tap the confined aquifer. DATA: All water levels (WL) are measured depths below the top of casing (TOC) elevation. TD is the total well depth below land surface. The head measurement is at the bottom of each well.

Well A TD 150 m, TOC 1105 m, WL 57 m **Well B** TD 160 m, TOC 1100 m, WL 39 m

Well C TD 170 m, TOC 1108 m, WL 76 m **Well D** TD 150 m, TOC 1100 m, WL 59 m

Well E TD 180 m, TOC 1098 m, WL 67 m **Well F** TD 160 m, TOC 1090 m, WL 57 m

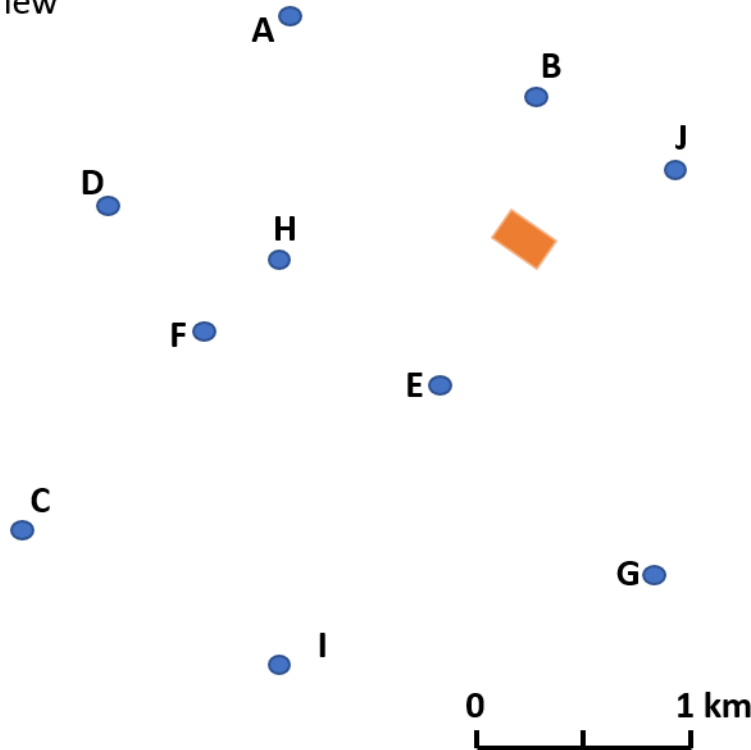
Well G TD 180 m, TOC 1080 m, WL 53 m **Well H** TD 170 m, TOC 1079 m, WL 41 m

Well I TD 180 m, TOC 1070 m, WL 50 m **Well J** TD 170 m, TOC 1100 m, WL 41 m

a) Create a potentiometric surface map view.

b) If the confined aquifer water at the orange rectangle became contaminated with dissolved nitrate from downward leakage of water in the overlying unconfined aquifer, would any other monitoring wells become contaminated under steady state flow conditions? Construct equipotential lines and flow lines to support your answer.

Map View



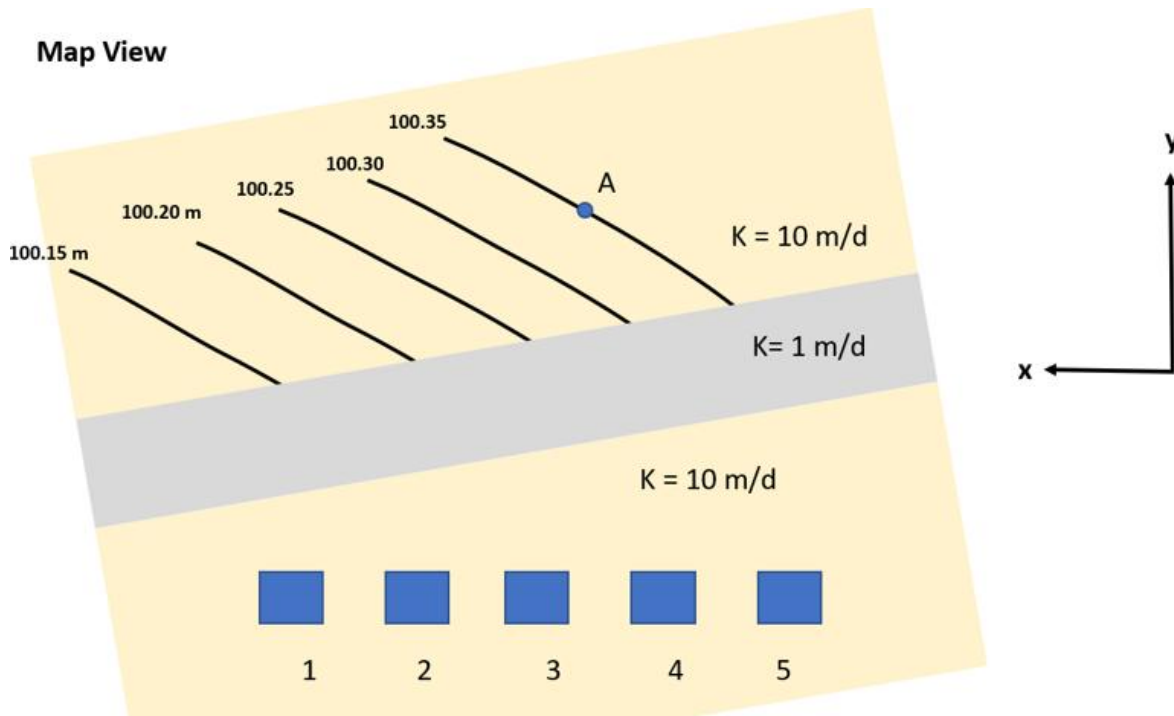
[Solution to Exercise 14 ↴](#)

[Return to where text linked to Exercise 14 ↑](#)

Exercise 15

A map view of a heterogeneous and isotropic field site containing a complex confined aquifer system is presented in the accompanying figure. If a contaminant is released at A and each zone of hydraulic conductivity is isotropic and homogeneous:

- Map the flowline from A to the row of houses. Would wells at any of the houses be impacted?
- Now assume that only the northern portion of the aquifer is anisotropic $K_x = 10 \text{ m/d}$ and $K_y = 1 \text{ m/d}$. Starting at A construct the anisotropic flow path and show which, if any, of the houses (blue rectangles) will be affected by this new flow path. Present your construction and show how you determined the flow path in the northern portion of the aquifer.



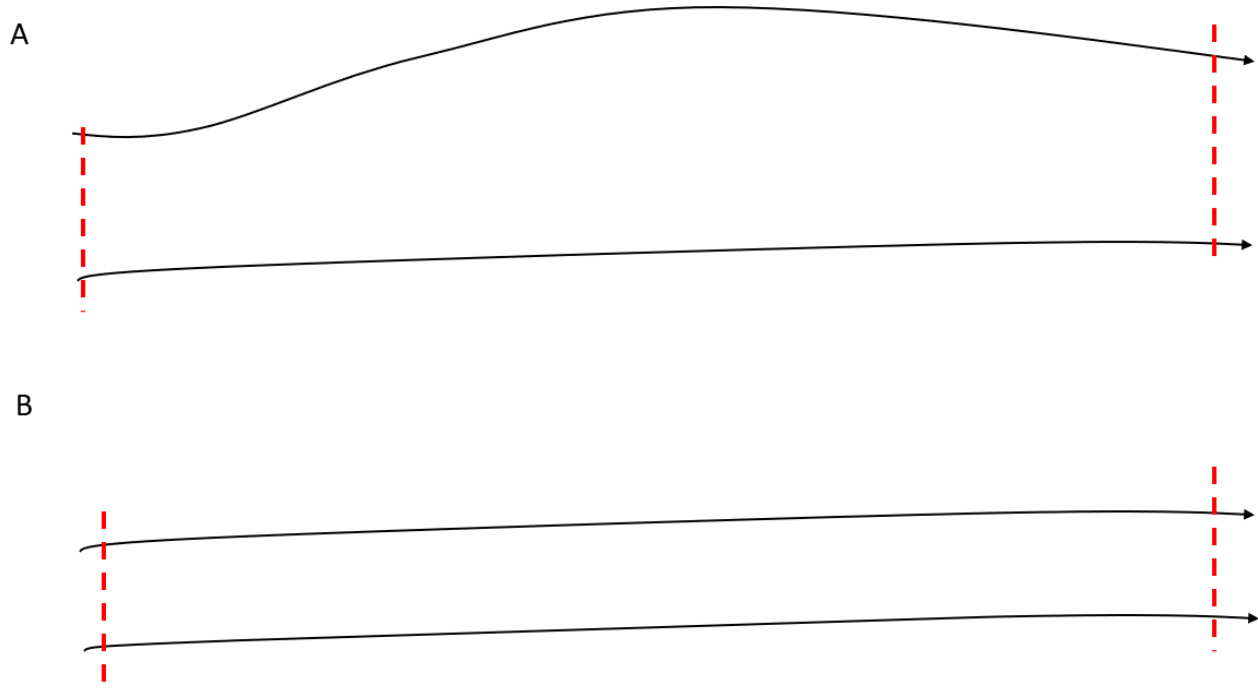
[Solution to Exercise 15 ↴](#)

[Return to where text linked to Exercise 15 ↑](#)

Exercise 16

In the accompanying figure flow lines (black lines) form two flow tubes, A and B. If conditions are isotropic and homogeneous and flow is at steady state, create equipotential lines under the following conditions.

- For A, assume the aquifer thickness and hydraulic conductivities are constant.
- For B, assume the thickness of the aquifer increases from left to right while all other conditions remain constant.



[Solution to Exercise 16](#) ↴

[Return to where text linked to Exercise 16](#) ↑

11 References

- ASTM (American Society for Testing and Materials), 1991, Annual Book of ASTM Standards. Designation D2434-68: Standard Test Methods for Permeability of Granular Solids (Constant Head), American Society of Testing and Materials, West Conshohocken, Pennsylvania, USA.
- ASTM (American Society for Testing and Materials), 2019, Standard Test Methods for Sieve Analysis for Fine and Coarse Aggregates. American Society of Testing and Materials, ASTM International.
- Aydin, A., Ahmadov, R., Antonellini, M., Cherry, J., Cilona, A., Deng, S., Flodin, E., de Joussineau, G., Parker, B., & Zhong, J. (2023). *Fractures and Faults in Sandstone and Sandstone-Shale/Mudstone Sequences and Their Impact on Groundwater*. The Groundwater Project. <https://doi.org/10.21083/978-1-77470-012-9>.
- Bartos, T.T., and L.L. Hallberg, 2011, Generalized Potentiometric Surface, Estimated Depth to Water, and Estimated Saturated Thickness of the High Plains Aquifer System, March-June 2009, Laramie County, Wyoming. United States Geological Survey Wyoming Water Science Center, Cheyenne, Wyoming, USA.
- Bear, J., 1972, Dynamics of Fluids in Porous Media, American Elsevier, New York, 764 pages.
- Brahana, J.V., and R.E. Broshears, 2001, Hydrogeology and Ground-water Flow in the Memphis and Fort Pillow Aquifers in the Memphis Area, Tennessee. United States Geological Survey Water Resources Investigation Report 89-4131, 56 pages.
- Brandenburg, J.P., 2020, Geologic Frameworks for Groundwater Flow Models. The Groundwater Project, <https://doi.org/10.21083/978-1-7770541-9-9>.
- Cedergren, H.R., 1989, Seepage, Drainage and Flow Nets. John Wiley and Sons, New York, USA, 465 pages.
- Cohen, A.J.B., and J.A. Cherry, 2020, Conceptual and Visual Understanding of Hydraulic Head and Groundwater Flow. The Groundwater Project, Guelph, Ontario, Canada, <https://gw-project.org/books/conceptual-and-visual-understanding-of-hydraulic-head-and-groundwater-flow/>.
- Cormican, A., J.F. Devlin, and C. Divine, 2020, Grain size analysis and permeametry for estimating hydraulic conductivity in engineered porous media. *Groundwater Monitoring and Remediation*, volume 40, Number 2, pages 65-72, <https://doi.org/10.1111/gwmr.12379>.
- D'Agnese, F.A., C.C. Faunt, K.A. Turner, and M.C. Hill, 1997, Hydrogeologic evaluation and numerical simulation of the Death Valley regional ground-water flow system, Nevada and California. United States Geological Survey Water-Resources Investigations Report 96- 4300, 124 pages.

- Darcy, H., 1856, Les fountains publiques de la Ville de Dijon, *in* Exposition et Application des Principes à Suivre et des Formules à Employer dans les Questions de Distribution d'Eau, Paris, editor, Victor Dalmont, English translation by P. Bobeck, 2004. Kendall/Hunt Publishing Company, Dubuque, Iowa, 584 pages.
- Davis, S.N., and L.J. Turk, 1964, Optimum depth of wells in crystalline rocks. *Ground Water*, volume 2, number 2, pages 6-11, <https://doi.org/10.1111/j.1745-6584.1964.tb01750.x>.
- Demcheck, Dennis, 2010, United States Geological Survey Louisiana Water Science Center, www.usgs.gov/media/images/usgs-collects-sediment-samples-grand-isle-beach, accessed June 12, 2020.
- Denson, N.M., and M.H. Bergendaho, 1961, Middle and upper Tertiary rocks of southeastern Wyoming and adjoining area, *in* Short papers in the Geologic and Hydrologic Sciences. United States Geological Survey Professional Paper 424-C, pages C168-C172.
- Devlin, J.F., 2015, HydroGeoSieve XL: An Excel-based tool to estimate hydraulic conductivity for grain size analysis. *Hydrogeology Journal*, volume 23, number 4, pages 837-844, <https://doi.org/10.1007/s10040-115-1255-0>.
- Devlin, J.F. (2020). Groundwater Velocity. The Groundwater Project.
<https://doi.org/10.21083/978-1-77470-000-6>.
- Domenico, P.A., and M.D. Mifflin, 1965, Water from low permeability sediments and land subsidence. *Water Resources Research*, volume 4, pages 563-576.
- Domenico, P.A., and F.W. Schwartz, 1998, Physical and Chemical Hydrogeology, second edition, John Wiley and Sons, New York, USA, 506 pages.
- Eckis, R., 1934, South Coast Basin investigations, geology and groundwater storage capacity of valley fill. California Division of Water Resources Bulletin 45, Sacramento, California, USA, 279 pages.
- Enviro Wiki contributors, 2019, Advection and Groundwater Flow, Enviro Wiki, Page Version ID: 12554,
www.enviro.wiki/index.php?title=Advection_and_Groundwater_Flow&oldid=12554, accessed May 31, 2020.
- EPA, 2020, Field photo, accessed July 10, 2020,
clu-in.org/contaminantfocus/default.focus/sec/Fractured_Rock/cat/Overview/, from
- Short, N.M., 2010, Remote Sensing Tutorial, NASA (USA National Aeronautics and Space Administration) website, Federation of American Scientists.
- EVO, 2020, EVO pumps, accessed August 1, 2020,
<http://www.evopumps.com/img/inline/gruntsudens%20pazeminasana/gruntsudens-pazeminasana-9.jpg>.

- Fair, G.W., and L.P. Hatch, 1933, Fundamental factors governing the streamline flow of water through sand. Journal of the American Water Works Association, volume 25, pages 1551-1556.
- Fernandes, A.J., Rouleau, A. & Vargas Jr., E.A. (2023). Structural Geology Applied to Fractured Aquifer Characterization. The Groundwater Project.
<https://doi.org/10.21083/978-1-77470-009-9h>.
- Folk, R.L., and W.C. Ward, 1957, A study in the significance of grain-size parameters. Journal of Sedimentary Petrology, volume 27, pages 3-26.
- Franke, O. Lehn, Thomas E. Reilly, and Gordon D. Bennett, 1987, Definition of boundary and initial conditions in the analysis of saturated ground-water flow systems - An introduction. United States Geological Survey Techniques of Water-Resources Investigation, Book 3, Chapter B5. <https://doi.org/10.3133/twri03B5>.
- Fraser, H.J., 1935, Experimental study of the porosity and permeability of clastic sediments. Journal of Geology, volume 43, number 7, pages 910-1010.
- Freeze, R.A., and J.A. Cherry, 1979, Groundwater. Prentice-Hall, Inc, Englewood Cliffs, New Jersey, USA, 604 pages.
- Gale, J.E., 1982, Assessing the Permeability Characteristics of Fractured Rock, *in* Recent Trends in Hydrogeology, editor, T. N. Narasimhan. Geological Society of America, <https://doi.org/10.1130/SPE189-181p163>.
- Goode, Daniel, 2006, Field photo, United States Geological Survey Research Hydrologist Pennsylvania Water Science Center, www.usgs.gov/media/images/bed-oriented-fracturing-lockatong-formation-newark-basin, accessed July 10, 2020.
- Hazen, A., 1911, Discussion: Dams on sand foundations. Transactions of the American Society of Civil Engineers, volume 73, 199 pages.
- Healy, Richard W., T.C. Winter, J.W. LaBaugh, and O.L. Franke, 2007, Water Budgets: Foundations for Effective Water-Resources and Environmental Management. United States Geological Survey Circular 1308, 90 pages.
- Heath, R.C., 1983, Basic Ground-Water Hydrology. United States Geological Survey Water Supply Paper 2220.
- Hubbert, M. K., 1940, The theory of groundwater motion. Journal of Geology, volume 48, pages 785-944.
- Hydrometrics, Inc., 2017, Potentiometric map 2016, 2015/2016 Water Resources Monitoring Report, East Helena Facility. Prepared for Montana Environmental Trust Group, Limited Liability Company, December 2017.
- IAPWS (International Association of the Properties of Water and Steam), 2008, Release the IAPWS Foundation 2008 for the Viscosity of Ordinary Water Substance: R12-08. International Association of the Properties of Water and Steam,
<http://www.iapws.org/index.html>, accessed July 10, 2020.

- Jiang, X.-W., & Cherry, J. (2024). *History and hydraulics of flowing wells*. The Groundwater Project. <https://doi.org/10.21083/CPET1503>.
- Johnson, A.I, 1967, Specific Yield - Comparison of Specific Yields for Various Materials. United States Geological Survey Water-Supply Paper 1662-D, 42 pages.
- Kingsbury, J.A., 1996, Altitude of the Potentiometric Surfaces, September 1995, and Historical Water-level Changes in the Memphis and Fort Pillow Aquifers in the Memphis area, Tennessee. United States Geological Survey Water-Resources Investigations Report 96-4278, 1 sheet.
- Kingsbury, J.A., 2018, Altitude of the potentiometric surface, 2000–15, and historical water-level changes in the Memphis aquifer in the Memphis area, Tennessee. United States Geological Survey Scientific Investigations Map 3415, 1 sheet, <https://doi.org/10.3133/sim3415>.
- Klammler, H. (2023). *Introduction to fluid mechanics for groundwater scientists*. The Groundwater Project. <https://doi.org/10.21083/GXAT7083>.
- Klute, A., 1965, Laboratory measurement of hydraulic conductivity of saturated soil, in Methods of Soil Analysis, Part 1, Physical and Mineralogical Properties, including Statistics of Measurement and Sampling. Agronomy Monographs, Section 9.1.
- Krasny, J., Z. Hrkal, and J. Bruthans, editors, 2003, Groundwater in Fractured Rocks. International Association of Hydrogeologists, IHP-VI, Series on Groundwater, number 7, 426 pages.
- Krasny, J., and J.M. Sharp, editors, 2007, Groundwater in Fractured Rocks, in International Association of Hydrogeologists Selected Papers in Hydrogeology, volume 9. Taylor and Francis of Balkema, Leiden, the Netherlands, 646 pages.
- Kruseman, G.P., and N.A. de Ridder, 1994, Analysis and Evaluation of Pumping Test Data, second edition with assistance from J.M. Verweij. International Institute for Land Reclamation and Improvement, The Netherlands, Publication 47, 377 pages, available for download at gw-project.org/books/analysis-and-evaluation-of-pumping-test-data/.
- Kuniansky, E. L., Taylor C. J., Williams J.H., & Paillet F. (2022). *Introduction to karst aquifers*. The Groundwater Project. doi.org/10.21083/978-1-77470-040-2.
- Liakopoulos, A.C., 1965, Variation of the permeability tensor ellipsoid in homogeneous anisotropic soils. Water Resources Research, volume 1, pages 135-141.
- Lohman, S.W., 1972, Ground-Water Hydraulics. United States Geological Survey Professional Paper 708, 70 pages.
- Marinelli, F. (2024). *Darcy's law in variable density groundwater systems*. The Groundwater Project. <https://doi.org/10.62592/VJGQ3476>.

- Masch, F.D., and K.J. Denny, 1966, Grain size distribution and its effect on the permeability of unconsolidated sands. Water Resources Research, volume 2, pages 665-677.
- Meerschaert, M.M., M. Dogan, R.L. Van Dam, D.W. Hyndman, and D. Benson, 2013, Hydraulic Conductivity Fields: Gaussian or Not?. Water Resources Research, volume 49, <https://doi.org/10.1002/wrcr.20376>.
- Morris, D.A., and A.I. Johnson, 1967, Summary of Hydrologic and Physical Properties of Rock and Soil Materials as Analyzed by the Hydrologic Laboratory of the United States Geological Survey, 1948-60. United States Geological Survey Water-Supply Paper 1839-D, 42 pages.
- Nelms, D.L., G.E. Harlow, L.N. Plummer, and E. Busenberg, 2003, Aquifer Susceptibility in Virginia, 1998-2000. United States Geological Survey Water-Resources Investigations Report 03-4278, 58 pages.
- Neilson, D.M., 1991, Ground-Water Monitoring. Lewis Publishers, Chemical Rubber Company Press (CRC Press), 91 pages.
- Poeter, Eileen, and Paul Hsieh, 2020, Graphical Construction of Groundwater Flow Nets. The Groundwater Project Guelph, Ontario, Canada, <https://gw-project.org/books/graphical-construction-of-groundwater-flow-nets/>.
- Rivera, A., 2014, Chapter 2 of Groundwater Basics in Canada's Groundwater Resources, editor, A. Rivera. Fitzhenry and Whiteside, Markham, Ontario, Canada, pages 24 -61.
- Sharp, Jr., J. M. (2023). *A glossary of hydrogeology*. The Groundwater Project. <https://doi.org/10.21083/978-1-77470-079-2>.
- Shepherd, Russell G., 1989, Correlations of Permeability and Grain Size. Groundwater, volume 27, issue 5, pages 633-638. <https://doi.org/10.1111/j.1745-6584.1989.tb00476.x>.
- Shepherd, R.B., 1989, Correlations of permeability and grain size. Ground Water, volume 27, number 6, pages 633-638.
- Slichter, C.S., 1899, Theoretical Investigation of the Motion of Groundwater. United States Geological Survey 19th Annual report, 1897-98, Part 2, pages 295-384.
- Snow, D. T. 1968, Rock fracture spacings, openings, and porosities. Journal of Soil Mechanics and Foundations Division, Proceedings of the American Society of Civil Engineers, volume 94, pages 73-91.
- Snow, A.T., 1970, The frequency and apertures of fractures in rock. International Journal of Rock Mechanics and Mining Sciences and Geomechanics Abstracts, volume 7, number 1, pages 23-30.
- Taylor, C.J., and W.M. Alley, 2001, Ground-Water-Level Monitoring and the Importance of Long-Term Water-Level Data. United States Geological Survey Circular 1217, 68 pages.

- Terzaghi, C., 1925, Principles of Soil Mechanics. Engineering News Record, volume 95, 832 pages.
- ThoughtCo, 2020, Densities of Common Rocks and Minerals, <https://www.thoughtco.com/densities-of-common-rocks-and-minerals-1439119>, accessed July 11, 2020.
- Todd, David Keith, and Larry W. Mays, 2004, Groundwater Hydrology, third edition. John Wiley and Sons, Incorporated, 656 pages.
- Toth, J. 1963, A theoretical analysis of groundwater flow in small drainage basins. Journal of Geophysical Research, volume 68, pages 475-481.
- United States Bureau of Reclamation, 1993, Drainage Manual: A Water Resources Technical Publication, Third Printing. United States Bureau of Reclamation, 319 pages, www.usbr.gov/tsc/techreferences/mands/mands-pdfs/DrainMan.pdf.
- United States Bureau of Reclamation, 1995, Ground Water Manual: A Water Resources Technical Publication. United States Bureau of Reclamation, 661 pages.
- USGS (United States Geological Survey), 2016, Field photo, Geochemical and Microbiological Processes that Affect Migration and Natural Attenuation of Chlorinated Solvents in Fractured Sedimentary Rock, Naval Air Warfare Center (NAWC), West Trenton, New Jersey, USA, https://toxics.usgs.gov/photo_gallery/nawc_page2.html, accessed July 10, 2020.
- USGS (United States Geological Survey), 2004, Field photo, Western Region Geology and Geophysics Science Center, <https://pubs.usgs.gov/of/2004/1007/granite.html>, accessed July 10, 2020.
- Van der Gun, J. (2022). *Large aquifer systems around the world*. The Groundwater Project. doi.org/10.21083/978-1-77470-020-4.
- Vukovic, M., and A. Soro, 1992, Determination of hydraulic conductivity of porous media from grain-size composition. Water Resources Publications, Littleton, Colorado, USA, 83 pages.
- Wang, H.F. (2020). *Groundwater Storage in Confined Aquifers*, The Groundwater Project, <https://doi.org/10.21083/978-1-7770541-7-5>.
- Weight, W.D., 2019, Practical Hydrogeology: Principles and Field Applications, third edition. McGraw Hill Education, New York, USA, 777 pages.
- Winston, R.B. (2023). *Getting Started with MODFLOW*. The Groundwater Project. <https://doi.org/10.21083/978-1-77470-030-3>.
- Woessner, W. W., Stringer, A. C. & Poeter, E.P. (2023). *An introduction to hydraulic testing in hydrogeology: Basic pumping, slug, and packer methods*. The Groundwater Project. <https://doi.org/10.21083/978-1-77470-090-7>.

12 Boxes

Box 1 Density of Common Minerals, Rock Types and Soils

The most common minerals on Earth are feldspar and quartz, with particle densities of 2.56 and 2.65 g/cm³, respectively (Figure Box 1-1a). However, the particle density of many common rock-forming minerals ranges from 2.16 g/cm³ for salt to 2.8 g/cm³ for talc, with the exception of minerals containing iron such as tourmaline, hornblende, olivine, sphalerite, pyrite, magnetite and hematite with densities ranging from 3 to 5.25 g/cm³. Clays, like kaolinite, are typically slightly less dense than quartz, with densities on the order of 2.6 g/cm³. Metals have a broad range of density with lithium at 0.53 g/cm³, aluminum at 2.7 g/cm³, and iridium, which is used in phones, at 22.6 g/cm³. The wet bulk density of rocks depends on the total porosity of the specific sample, so rocks of similar type have a broad range of bulk density due to differences in porosity (Figure Box 1-1b).

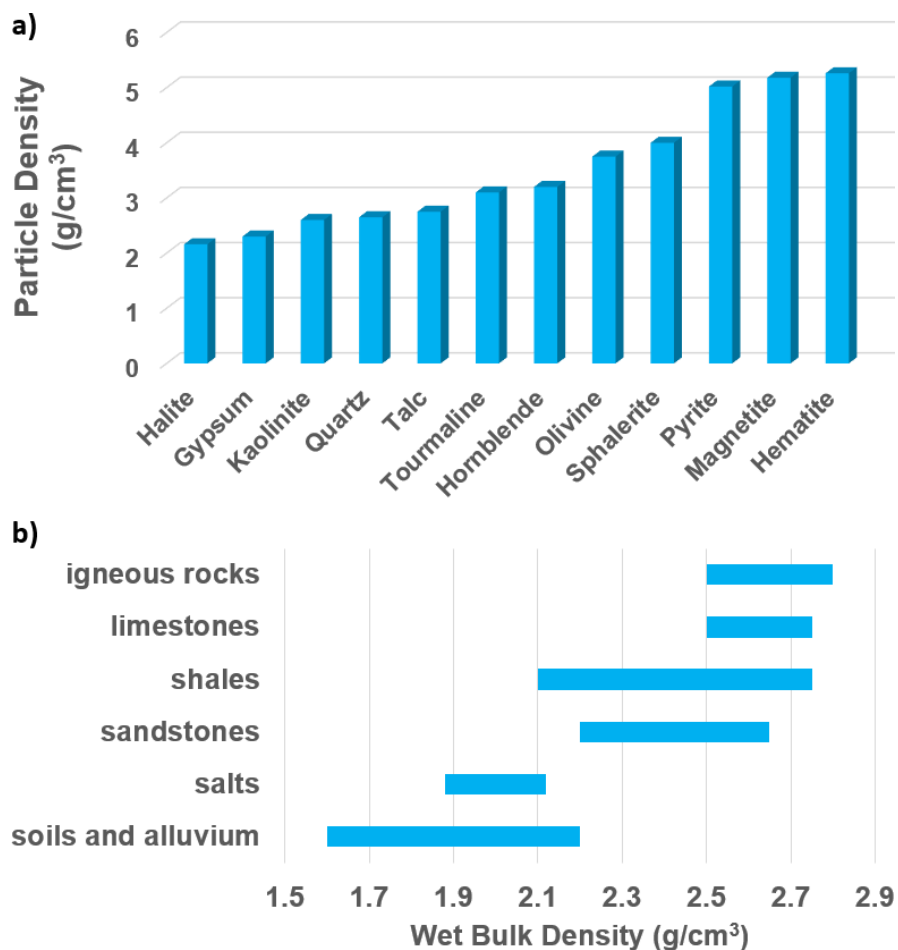


Figure Box 1-1 Particle densities of some common minerals (g/cm³) and range of wet bulk density of soils and common rock types (g/cm³) (data from ThoughtCo (2020)).

[Return to where text links to Box 1 ↑](#)

Box 2 Analyzing Grain-size Distribution

The standard approach to describing the grain-size distribution of a granular, unconsolidated sample is to start with a dry volume of granular material, weigh it, and place it on top of a nest of sieves that have progressively smaller mesh openings (Figure Box 2-1). The sieves are shaken for a period of time so each sieve holds only grains with diameters larger than its mesh size and smaller than the mesh size of the sieve immediately above it. Then the material on each sieve is collected and weighed. Sieve analyses methods are outlined in the American Society of Testing and Materials ASTM C136/C136M-19 Standard Test Method for Sieve Analysis of Fine and Coarse Aggregates (ASTM, 2019).

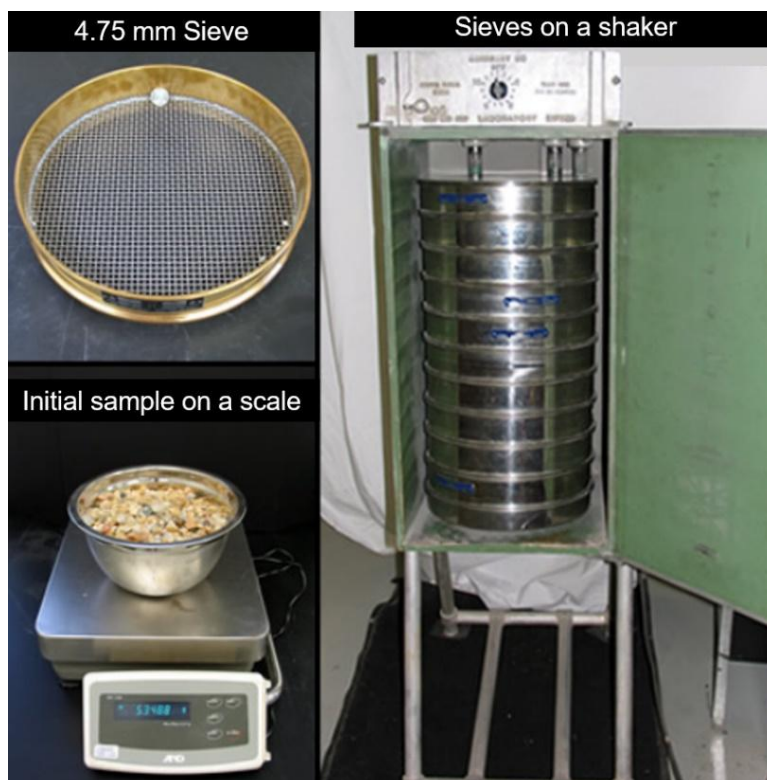


Figure Box 2-1 - To determine grain size distribution, the sample is dried, weighed and placed in a nest of sieves with the largest openings on top and the smallest on the bottom. A pan with a solid bottom is placed to catch any portion of the sample not retained on the sieves. The sample is shaken and the weight of the sample on each sieve is recorded (images from <https://pavementinteractive.org/reference-desk/testing/aggregate-tests/gradation-test/>, accessed July 10, 2020).

A table is created (Figure Box 2-2) that shows the cumulative percent retained (weight of the sample on the coarsest sieve plus the weight on consecutive sieves of decreasing size). A synonymous term is cumulative percent coarser than. Values can also be reported as cumulative percent finer than (100% minus cumulative percent coarser than) or cumulative percent passing (100% minus cumulative percent retained). These data provide the grain-size distribution as shown in (Figure Box 2-3).

Weight of total sample 100 grams		Weight on Sieve (grams)	Cumulative % Retained	Cumulative % Finer Than
Sieve Opening (mm)				
4.0 fine gravel		5	5	95
2.0 coarse sand		15	20	80
1.0		24	44	56
0.5		30	74	26
0.25 medium sand		13	87	13
0.13		6	93	7
0.06		5	98	2
0.004 silt				
Solid pan		0		

Figure Box2-2 - Example of grain-size distribution data from a sieve analysis. The cumulative percent retained and/or finer-than is computed from the weights on each sieve relative to the total sample weight. Note that in this example 98 grams of sample were recovered from the sieves suggesting either 2 grams entered the pan or part of the sample stuck to the sieves.

Once the grain size distribution table is generated, the cumulative percent data are plotted on a standard grain size distribution curve (Figure Box 2-3).

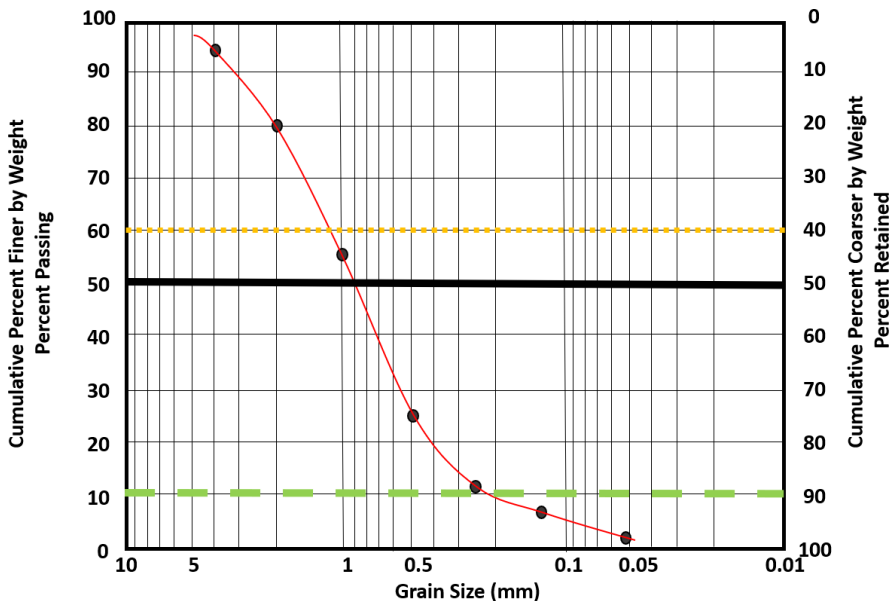


Figure Box2-3 A cumulative percent grain size distribution curve for the data presented in Figure Box 2-2. The grain size (mm) is on a log scale. The green line represents the effective grain size: d_{90} retained ($d = \text{diameter}$) or d_{10} finer-than. The value for this distribution is taken from where the green, dashed line crosses the red line. The black line at 50% provides the median grain size where it crosses the red line, d_{50} . The sample uniformity is computed using the value where the distribution crosses the yellow dotted line, d_{40} retained and/or d_{60} finer-than, and the effective grain size (e.g., cumulative percent retained, uniformity coefficient = d_{40}/d_{90}).

Grain-size distributions (Figure Box 2-3) are most commonly described by their effective grain size (size of particle for which 90% of the sample is coarser than that value, which is d_{90} cumulative percent retained or d_{10} cumulative percent finer-than) as defined in Equations Box 2-1 and Box 2-2, and the median grain size (d_{50} for both cumulative percent

retained and cumulative percent finer-than) as defined in Equation Box 2-3. A third parameter, the uniformity coefficient, provides information about how uniform (with uniform meaning similar size) the grain sizes are within the sample: uniformity coefficient = d_{40}/d_{90} for cumulative percent retained data and d_{60}/d_{10} for cumulative percent finer-than data (Equations Box 2-4 and Box 2-5). If the ratio is less than two, the sample is considered fairly uniform. A perfectly uniform sample size distribution curve is a vertical line on a grain-size distribution graph (all the grains are the same size) and has a uniformity coefficient of one.

$$\text{Effective grain size} = d_{90} \text{ cumulative percent retained} \quad (\text{Box 2-1})$$

$$\text{Effective grain size} = d_{10} \text{ cumulative percent finer than} \quad (\text{Box 2-2})$$

$$\text{Median grain size} = d_{50} \quad (\text{Box 2-3})$$

$$\text{Uniformity Coefficient} = \frac{d_{40}}{d_{90}} \text{ cumulative percent retained} \quad (\text{Box 2-4})$$

$$\text{Uniformity Coefficient} = \frac{d_{60}}{d_{10}} \text{ cumulative percent finer than} \quad (\text{Box 2-5})$$

In some empirical equations the mean particle grain size and/or the inclusive standard deviation are used to estimate sample hydrogeological properties. These values cannot be derived directly from the standard grain-size distribution curve. Folk and Ward (1957) developed a method to compute these values. Their method requires converting cumulative percent grain size distribution data to what they call phi units, ϕ . Phi units can be calculated from grain size as shown in Equation Box 2-6. Consequently, values of phi can be positive and negative.

$$\phi = -\log_2 \left(\frac{\text{size mm}}{1 \text{ mm}} \right) \quad (\text{Box 2-6})$$

where:

$$\log_2(x) = \frac{\ln(x)}{\ln(2)}$$

x = diameter in millimeters divided by 1 millimeter in order to render the value dimensionless

The mean phi size is computed as shown in Equation Box 2-7.

$$\text{Mean phi size} = \left(\frac{\phi_{16} + \phi_{50} + \phi_{84}}{3} \right) \quad (\text{Box 2-7})$$

The mean equation can use either cumulative percent retained or finer-than data. The inclusive standard deviation of a size distribution, σ_I , is defined for cumulative percent retained as shown in Equation Box 2-8.

$$\text{Inclusive standard deviation} = \sigma_I = \left(\frac{\phi_{84} - \phi_{16}}{4} \right) + \left(\frac{\phi_{95} - \phi_5}{6.6} \right) \quad (\text{Box 2-8})$$

With a grain size distribution in hand, a number of empirical equations can be applied to estimate the value of hydrogeologic properties.

[Return to where text links to Box 2 ↑](#)

Box 3 Foundation for Understanding Hydraulic Head and Force Potentials

David B. McWhorter, Eileen P. Poeter, William W. Woessner

As illustrated in the main body of this book, Darcy's Law indicates the rate of groundwater flow is proportional to the gradient of a scalar quantity called hydraulic head as shown again here in Equation Box 3-1. A scalar quantity is one that can be represented by a single number describing magnitude (as opposed to a vector that requires two numbers, magnitude and direction (an angle)). Scalar quantities include entities such as pressure, concentration and temperature; while velocity is an example of a vector quantity.

$$q = \frac{Q}{A} = -K \frac{dh}{dL} \quad (\text{Box 3-1})$$

where:

q = specific discharge (L/T)

Q = volumetric flow rate (L^3/T)

A = cross-section area of flow perpendicular to the direction of flow (L^2)

K = hydraulic conductivity (L/T)

$\frac{dh}{dL}$ = derivative of hydraulic head in direction L (dimensionless)

Science is rife with instances in which the rate of flow of some quantity of interest is expressed in this form. Heat conductance in response to a temperature gradient, flow of electricity in response to differences in voltage, and diffusion of a solute due to a concentration gradient are familiar examples. The simple proportionality of such flux laws often mask the deeper connection between the scalar quantity and the factors responsible for the flux under consideration. Hubbert (1940), in his classic treatise on groundwater flow, makes this point in reference to hydraulic head by stating that "*to adopt it without further investigation would be like reading the length of a mercury column of a thermometer without knowing that temperature is the physical quantity being indicated*". Hubbert went on to show that hydraulic head is a contribution to the total mechanical energy of the water, a quantity he referred to as "*fluid potential*". Water flow from high to low hydraulic head is tantamount to flow from high to low mechanical energy. Hubbert points out that mechanical energy is converted to thermal energy by the friction generated as the viscous fluid flows through the interstitial pore space. But is hydraulic head a physically meaningful concept under all circumstances? If not, is there an alternative way to calculate groundwater flow when hydraulic head is not a meaningful quantity? These questions can be answered by an analysis that begins with a consideration of the mechanical forces acting on groundwater.

Consider flow along a curved path as would occur when groundwater passes under an obstruction as depicted in Figure 77 in the main body of this book. Forces acting on flowing groundwater fall into one of two categories: 1) those that resist the fluid motion and 2) those that drive the fluid motion. The dominant resistive force is the drag on the

fluid that results from viscous shear as the fluid makes its way through the tiny openings among the solid grains. A second resistive force, almost always negligible, is an inertial force that occurs because the water is following a curved path (convective acceleration in fluid mechanics). Inertial forces act on the groundwater when the flow is non-uniform (as in Figure 77) or unsteady, or both. Viscous and inertial forces only exist when the groundwater is in motion. Groundwater motion is caused by the driving forces. The driving forces are related to hydraulic head.

Force on Groundwater Due to Pressure Difference

Variable water pressure and gravity are the fundamental forces that drive flow through the porous medium in all common circumstances of groundwater occurrence. These forces are the same as the forces that drive flow in a pressurized pipe and in a stream channel. Although fluid motion results from the combined effect of these forces, it is useful to consider the individual effects of each force before combining them. We consider the force due to variable pressure first.

Water contained within the volume element of porous medium depicted in Figure Box 3-1 experiences a force due to the difference in pressure acting on either end at points 1 and 2. The pressure at point 2 exerts a force on the water in the element equal to the product of pressure, p_2 , and the area of exposed water, nA , where n is porosity and A is the area of the base of the cylinder of the volume element at point 2. Similarly, the pressure at point 1 exerts the force nAp_1 . These forces are indicated by the bold red arrows in Figure Box 3-1.

The difference between these two forces is the driving force on the water in the coordinate direction L due to variable water pressure (Equation Box 3-2). By convention, forces exerted in positive coordinate directions are considered positive, so the negative sign in Equation Box 3-2 assures compliance with that convention.

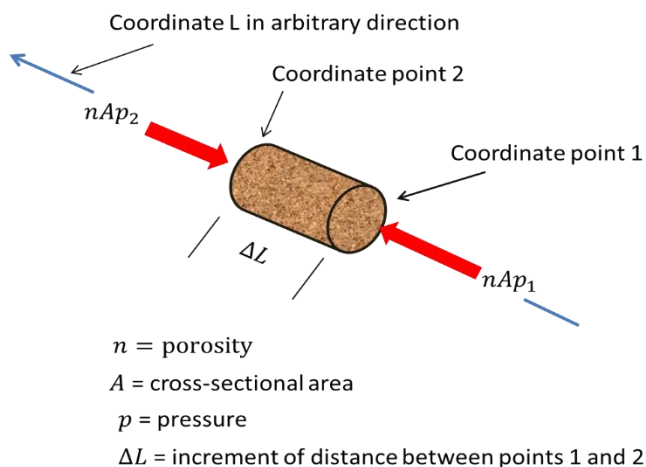


Figure Box 3-1 - Depiction of pressure forces acting on water within a volume element of porous medium.

$$\text{Driving force due to pressure difference} = -(p_2 - p_1)nA = -\left(\frac{\Delta\rho}{\Delta L}\right)nA\Delta L \quad (\text{Box 3-2})$$

where:

p_i = water pressure at location i (F/L²)

n = porosity (dimensionless)

A = cross-sectional area of volume element (L²)

Δp = difference in water pressure between points 1 and 2 (F/L²)

ΔL = distance between points 1 and 2 (L)

Divide the force in Equation Box 3-2 by the volume of water ($A \Delta L n$) to obtain the force per unit volume of fluid, f_p , due to the pressure difference Equation Box 3-3 expresses the result in derivative form.

$$f_p = -\frac{dp}{dL} \quad (\text{Box 3-3})$$

The derivative in Equation Box 3-3 evaluates the rate of change of pressure in the direction of L (from point 1 to point 2) and is called a directional derivative.

Forces on Groundwater Due to Gravity

It was natural and convenient to adopt a unit volume of water as our reference when considering the force resulting from spatial variation of pressure. This force is a surface force and can be computed without any need to know the mass of the reference element. In contrast, gravitational force on groundwater is a body force that is proportional to mass, and it is natural to adopt a unit mass for our reference entity in this case. However, forces referenced to different entities cannot be added or compared, so a common reference entity must be selected. We elect to express the force on groundwater due to gravity as a force per unit volume of water so it can be added directly to the force expressed in Equation Box 3-3. As demonstrated in a later paragraph, it is a simple matter to convert force per unit volume to force per unit weight or mass of fluid.

Throughout this book, z is the vertical coordinate measured as a positive value upward from some convenient datum as in Figure Box 3-2. Gravitational force acts vertically downward, so is considered negative in accordance with convention. Thus, the gravitational force per unit volume of fluid is $-\rho g$, where ρ is the fluid mass density (mass per unit volume) and g is the gravitational constant. Note that this is simply the familiar weight per unit volume (also called unit or specific weight) with dimensions of force per unit volume. The component of this vertical force acting in the coordinate direction L is shown in Figure Box 3-2 and is calculated by Equation Box 3-4.

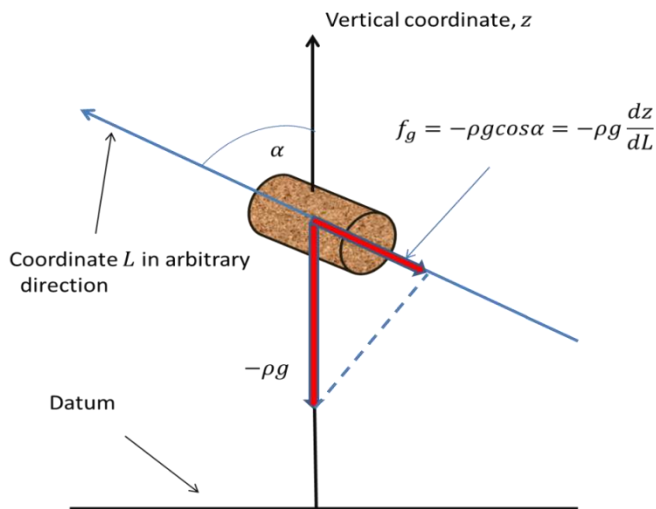


Figure Box3-2 - Throughout this book, z is the vertical coordinate measured positive upward from some convenient datum. Gravitational force acts vertically downward, so is considered negative in accordance with convention.

$$f_g = -\rho g \frac{dz}{dL} \quad (\text{Box 3-4})$$

where:

- f_g = component of force per unit volume of fluid due to gravity acting along L coordinate (F/L^3)
- ρ = fluid density (M/L^3)
- g = gravitational constant (acceleration of gravity) (L/T^2)
- z = elevation above a horizontal datum (L)

Net Driving Force

The forces in Equations Box 3-3 and Box 3-4 are added to arrive at the net driving force, F_v , exerted in the arbitrary direction, L , on a unit volume of groundwater as shown in Equation Box 3-5.

$$F_v = - \left(\frac{dp}{dL} + \rho g \frac{dz}{dL} \right) \quad (\text{Box 3-5})$$

where:

- F_v = driving force per unit volume of fluid (F/L^3)

The subscript, v , denotes volume as the reference entity. The individual forces appearing in Equation Box 3-5 may point in the same or opposite directions along L . The net driving force is zero when the individual forces are equal in magnitude but point in opposite directions. In that case, there is no flow and Equation Box 3-5 becomes Equation Box 3-6.

$$\frac{dp}{dz} = -\rho g \quad (\text{Box 3-6})$$

This is the familiar equation of hydrostatics and is the same equation one would use to compute the pressure in any column of standing water (e.g., a reservoir or standpipe).

It is a simple matter to express the net driving force in reference to either unit mass or unit weight. To obtain the net driving force per unit mass of fluid, divide Equation Box 3-5 by the mass density to obtain Equation Box 3-7:

$$F_m = - \left(\frac{dp}{\rho dL} + g \frac{dz}{dL} \right) \quad (\text{Box 3-7})$$

where:

$$F_m = \text{driving force per unit mass of fluid (F/M)}$$

Equation Box 3-8 calculates the force per unit weight of fluid and is obtained by dividing Equation Box 3-5 by the unit weight, ρg .

$$F_w = - \left(\frac{dp}{\rho g dL} + \frac{dz}{dL} \right) \quad (\text{Box 3-8})$$

where:

$$F_w = \text{driving force per unit weight of fluid (dimensionless)}$$

Few restrictions were invoked to enable the development of these expressions for the forces that drive the motion of groundwater. In particular, these expressions can vary and still remain applicable. The force equations remain valid for groundwater of variable density due to fluid compressibility, non-uniform solute concentration or non-uniform temperature. Furthermore, these results apply to a wide variety of other liquids (e.g., petroleum products, solvents) and even to gases.

Force Potentials and Hydraulic Head

A force potential associated with a particular force field is a scalar function, the negative gradient of which is the force in question. The word potential in the present context is related to the familiar concept of potential energy. The common example is the potential energy of a fluid particle (e.g., a unit mass) that is dependent upon the position of the particle in the gravitational force field. But a fluid particle may also possess potential energy owing to its position in force fields other than the gravitational field. There is potential energy associated with the convective force field that exists in non-uniform flow and the force field due to variable pressure, for example.

The potential energy possessed by a fluid particle at a particular point is the work done on the particle by the force field when the particle is repositioned from a reference point to the point in question. This is a meaningful definition only if the work done on the particle by the force field is the same for every path that can be taken in route from the reference point to the point in question. Otherwise, the value of potential energy would not be unique.

The work done on a fluid particle when it is moved a differential distance, dL , in the direction of a force F , is the differential work, $F dL$. Integration of the differential work

between the reference point and any point of interest is the potential energy at the point of interest, provided the integration is independent of the path taken between the points. This condition is satisfied if the differential work is an exact differential (see any elementary calculus book or on the web at [Wolfram MathWorld](#) for more information on exact differentials). If the fluid density is constant, the differential work is an exact differential for each of the three net driving forces in Equations Box 3-5, Box 3-7, and Box 3-8.

For example, consider the net driving force per unit weight of fluid as expressed in Equation Box 3-8. Because both ρ and g are constant, their product can be placed inside the differential operator, d , to obtain Equation Box 3-9.

$$F_w dL = - \left(d \left(\frac{p}{\rho g} \right) + dz \right) = -d \left(\frac{p}{\rho g} + z \right) \quad (\text{Box 3-9})$$

where:

$$F_w dL = \text{Differential work on a unit weight (FL)}$$

Equation Box 3-9 can be integrated up to an arbitrary constant of integration that is set to zero for convenience to provide an expression for the potential energy per unit weight of fluid, also known as hydraulic head shown in Equation Box 3-10.

$$- \int F_w dL = \frac{p}{\rho g} + z = h \quad (\text{Box 3-10})$$

where:

$$h = \text{hydraulic head, (L)}$$

Thus, we see that hydraulic head at a point can be viewed as the potential energy per unit weight of fluid. It is, also, a force potential in the sense that the negative gradient of hydraulic head is the driving force on the fluid per unit weight. Force potentials, particularly hydraulic head, are of more than academic interest. Hydraulic head is determined by a single measurement of water level relative to an arbitrary datum, a valuable attribute in groundwater field work (Figure 19 in the main body of book). Further, the negative derivative of hydraulic head in any direction evaluates the net driving force in that direction such that when h is constant throughout the system, flow is zero (i.e., there is no flow). None of this requires explicit consideration of the individual forces. In addition, the validity of using hydraulic head to determine groundwater flow does not require negligible inertial forces. For these reasons, hydraulic head enjoys an exalted status among the potentials relevant to groundwater flow. However, use of hydraulic head to evaluate flow systems requires that the fluid has constant density, even though the basic force equations that led up to the calculation of hydraulic head remain valid for fluids of variable density.

What If the Density Is Variable?

Hydraulic head is not a meaningful concept when the fluid density varies due to variable solute concentration or temperature. However, Equations Box 3-5, Box 3-7, and Box 3-8 remain valid and provide a means of calculating specific discharge in such cases.

In particular Equation Box 3-1, valid for water of constant density, can be replaced by Equation Box 3-11 for cases of variable density.

$$q = -K \left(\frac{dp}{\rho g dL} + \frac{dz}{dL} \right) \quad (\text{Box 3-11})$$

Equation Box 3-11 is obtained by using Equation Box 3-8 for the driving force and provides a valid starting point for the analysis of the complex problems of variable density.

[Return to where text links to Box 3 ↑](#)

Box 4 Methods for Estimating Hydraulic Conductivity

Hydraulic conductivity, K , is used to describe the capacity of a porous material to transmit water. Estimating representative values of hydraulic conductivity for a wide variety of porous media is required to quantitatively describe groundwater flow rates (Q), fluxes (q) and velocities (v), and determine the spatial and temporal distribution of hydraulic heads. Without hydraulic conductivity data neither simple analytical solutions nor complex computer simulations of groundwater flow are possible. As a result, a number of methods have been developed to characterize the hydraulic conductivity of earth materials. Laboratory and empirical methods are applied to small sample volumes and, although the values provide insight into the general magnitude of hydraulic conductivity at a field site, they may not provide values that are appropriate to fully predict how a groundwater system will behave at the field scale. Generally, field tests involve pumping one well while observing groundwater levels in nearby wells (aquifer testing), but some field tests use individual small diameter wells, and/or boreholes, to observe groundwater responses to sudden changes in water levels (slug testing). Field tests provide values of K that incorporate the broad complexities of the natural system such as the interconnectedness of subsurface zones of high and low hydraulic conductivity (Figure Box 4-1).

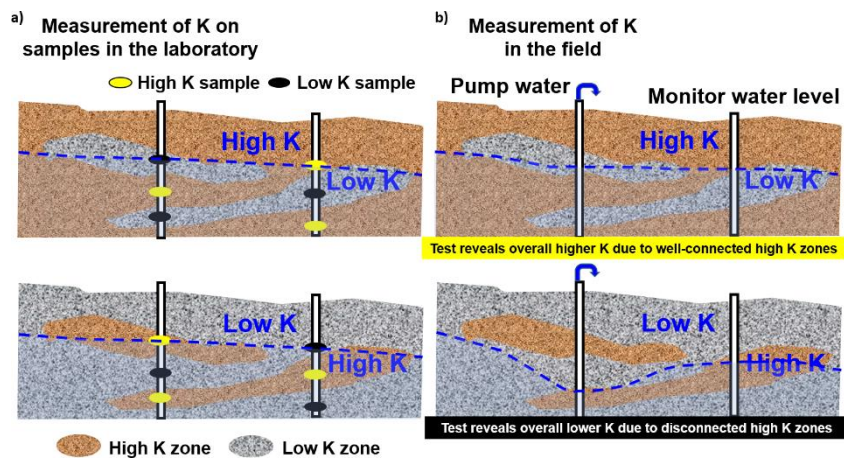


Figure Box 4-1 - Measurements of K : from: a) small laboratory samples provide insight to the range and distribution of high and low K zones at a field site, but do not reveal the interconnectedness of high hydraulic conductivity units important to developing groundwater resources and designing remedial actions for cleaning up groundwater contamination; and, b) field tests, commonly referred to as aquifer tests, sample a larger volume of material and reveal the overall magnitude of K . Field testing is essential to developing groundwater resources because the overall response of the system to pumping needs to be understood. A combination of laboratory and field testing is important to evaluation of contaminated sites because the detailed distribution of hydraulic conductivity is important to the remedial design.

Field methods for measuring hydraulic conductivity are not presented here. These methods are covered in publications by the United States Geological Survey, hydrogeology textbooks, and commercial aquifer testing software documentation. A comprehensive discussion of the use of field aquifer testing to determine aquifer properties is presented by

Kruseman and de Ridder (1994). Their book is available on the [Groundwater Project website](#). The material in this box focuses on laboratory testing methods and linking these methods with empirically generated relationships between sediment characteristics and hydraulic conductivity.

Permeameters

One approach to determining K for a sample of earth material in the laboratory is to saturate the sample and drive water through it while observing the flow rate and hydraulic heads. The sample is placed in a cylindrical chamber and water flow is set either at a constant rate (steady state flow) or allowed to decline over time.

The most useful samples are collected using a coring tool or a split-spoon sampler while drilling a borehole because they provide relatively undisturbed samples of the subsurface. Sample collection techniques that drive sample tubes into sediment may compact the sample and change its hydraulic conductivity. Sometimes disturbed granular material is collected and repacked to the approximate consolidation measured in the field. Field consolidation conditions are determined using a resistance-to-penetration test which can be achieved with a variety of tools and procedures, but, in brief, reflects either the pressure required to push a tool into the earth, or a record of the number of blows needed to drive a split spoon coring device a specified distance into the sediments exposed at the bottom of a borehole. Loose repacked samples have lost the layering and complex microstructures that may exist at the field site and influence K . Consequently, hydraulic conductivity measurements conducted on such samples provide only a rough estimate of the field value. In some cases, repacked samples are tested a number of times using varying degrees of consolidation and the measured values are averaged.

Standard permeameter operating procedures have been outlined in guidelines provided by the American Society of Testing and Materials (ASTM, 1991). Procedures such as these should be consulted when designing and operating permeameters.

Constant Head Permeameter

For a constant head permeameter test, an undisturbed core, or repacked sample, is place in the chamber (Figure Box 4-2). Determining K from a constant head permeameter test requires application of Darcy's Law. The apparatus maintains a constant flow of water and hydraulic gradient ($\Delta h/\Delta L$) as water flows through a fixed length of sample of a given cross-sectional area. Measurements are made under steady-state conditions. K is computed by solving Darcy's law for the hydraulic conductivity as shown in the main text of this book and repeated here for convenience (Figure Box 4-2 and Equation Box 4-1).

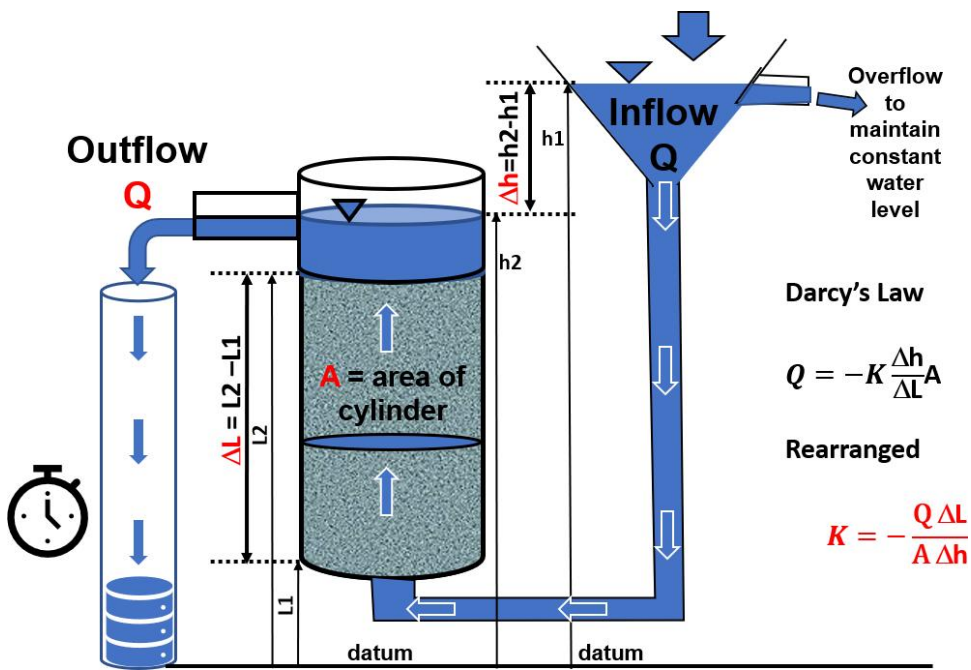


Figure Box 4-2 - Constant head permeameter. The sample is saturated from the bottom to the top by adding water to the funnel until it overflows and the water level stabilizes. Once stabilized, the volumetric flow rate, Q , is constant. The outflow is collected in a graduated cylinder, or on a weighing scale, to measure the volume that flows out as a function of time, Q . The difference between the constant water level in the funnel and the elevation of the outflow is Δh . K is calculated using the measured values of parameters shown in red.

$$K = - \frac{Q \Delta L}{A \Delta h} \quad (\text{Box 4-1})$$

A classroom-scale Darcy apparatus is shown in Figure Box 4-3. Water is pumped from the sump in the lower left to an upper constant-head reservoir in the upper left. That head is maintained by allowing the water to overflow the top of the reservoir where it is collected and returned to the sump. Water flows from the reservoir into the sand-filled column which has an inner diameter of 2 inches (5.08 cm), and an area of 20.27 cm². There is essentially no resistance to flow in the tube that carries water to the sand and so the head in the reservoir is the head at the face of the sand. Piezometers monitor head at a few locations along the column within the sand. Outflow from the column is controlled by the constant head at the lower reservoir. Once steady flow is established, the outflow is collected in a graduated cylinder. For example, a volume of 148 milliliters (148 cm³) is collected in 90 seconds so the flow rate, Q , is 1.64 cm³/s. The gradients between the piezometers vary, being -0.36, -0.34, and -0.44 from left to right, respectively. Rearranging Equation Box 4-1 to solve for $K = -Q/(Ai)$ results in K values corresponding to the measured gradients of 0.23, 0.24, 0.18 cm/s respectively. These are a reasonable value for sand. The column can be rotated at the midpoint because the piezometers are flexible tubes. The angle of the column does not affect the head or flow rate because they are controlled only by the reservoir heads, the geometry of the tube (area and length), and the K of the sand.

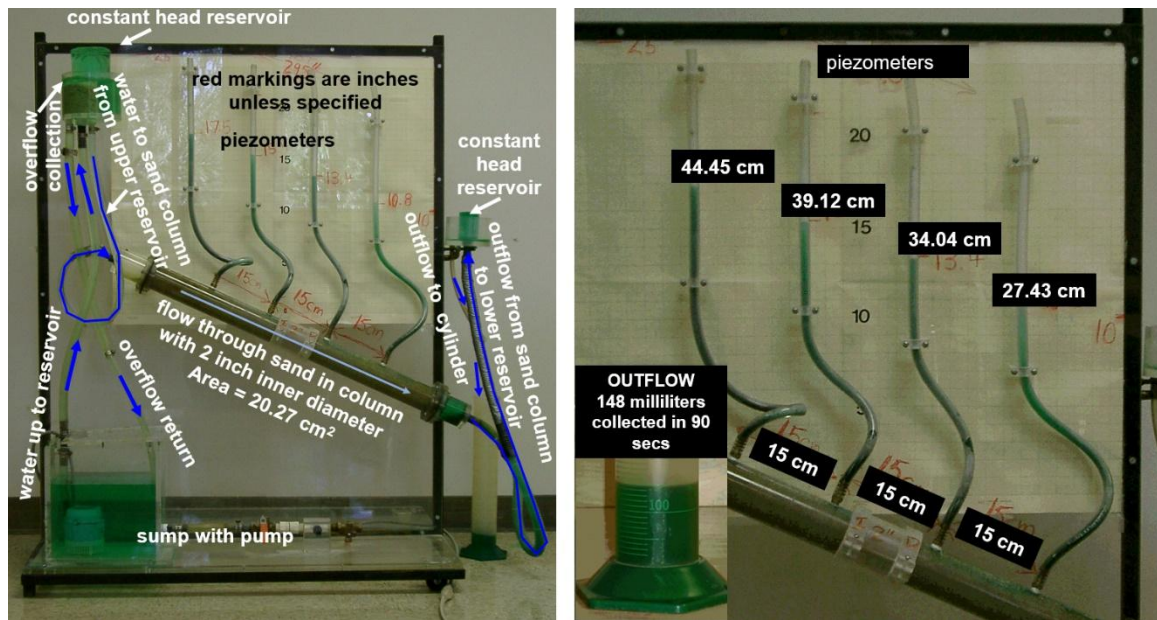


Figure Box 4-3 - Classroom-scale constant head permeameter. Heads are measured in centimeters from the horizontal line on the graph paper behind the plexiglass. The individual gradients between piezometers range from 0.34 to 0.44 such that when Darcy's Law is used to estimate K values, they range from 0.18 to 0.24 cm/s (in round numbers, all values are 0.2 cm/s, which is typical for sand). For practical groundwater work, this sand would be assigned a K of 0.2 cm/s.

The observed variation in gradients along the flow column could be due to slightly different packing of the sand, or errors in the piezometer readings which might result from something like an air bubble in one of the tubes. For practical groundwater work, this sand would be assigned a K of 0.2 cm/s. Often knowing K within an order of magnitude is beneficial in groundwater analysis. There is much uncertainty in quantifying groundwater flow, and the range of the K values from this experiment is small compared with the many other sources of error in groundwater analysis.

When water is flowing through a constant head permeameter the flow needs to be low enough that unconsolidated sediment grains are not being separated and frictional losses in the apparatus are too large. Cormican et al. (2020) suggest that a reasonable gradient can be determined by making K measurements with progressively lower gradients until two consecutive runs yield the same value. Klute (1965) noted that for most constant head permeameters the lower limit of measurement was about 0.00016 cm/s (0.14 m/d).

Falling Head Permeameter

The constant head permeameter is useful for measuring K of samples with higher values of hydraulic conductivity. When K is low, it is difficult to establish a constant flow rate over a relatively short time interval (minutes-hours), so instead, a falling head permeameter is used. In this method the water levels and flow rates change over time. Data

requirements include the dimensions of the sample and connected tube, and the change in water level over time (Figure Box 4-4).

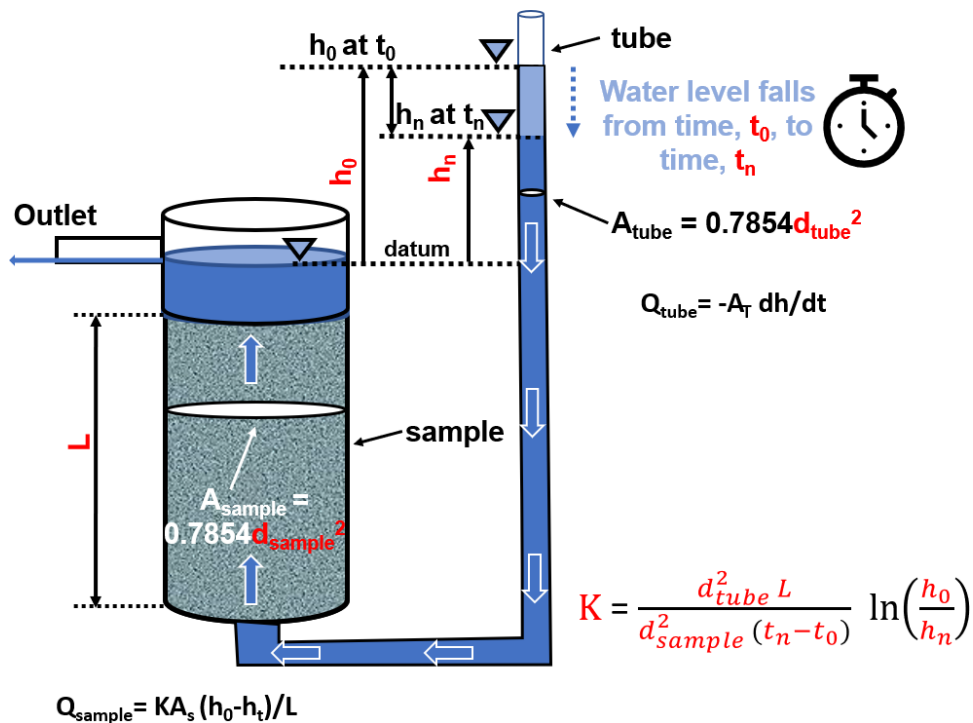


Figure Box 4-4 - Schematic of a falling head permeameter. The sample of length L is placed in a chamber of area A_{sample} , and saturated by adding water to the attached tube of area A_{tube} . Once the sample is saturated and water seeps from the outlet, the permeameter is ready to be used. At time t_0 the water level measurement above the sample outlet, h_0 is recorded. After an interval of time, $t_n - t_0$, a second measurement of the water level in the tube is made, h_n . These parameters are then used to compute the hydraulic conductivity of the sample as shown, where d_{tube} and d_{sample} are the diameters of the tube and sample, respectively.

Over a specified period of time, $t_n - t_0$, the flow rate from the tube, Q_{tube} , and the flow of water through the sample, Q_{sample} , are equal.

$$Q_{tube} = \frac{\text{Volume Change}}{\text{Time}} = \frac{A_{tube}(h_n - h_0)}{(t_n - t_0)} = A_{tube} \frac{dh}{dt} \quad (\text{Box 4-2})$$

where:

Q_{tube} = average volumetric discharge from tube during test (L^3/T)

A_{tube} = area of the tube is $0.7854 d_{tube}^2 (\text{L}^2)$

h_0 = height of water in the tube relative to the outlet at start time (L)

h_n = height of water in the tube relative to the outlet at end time (L)

t_n = end time (T)

t_0 = start time (T)

$\frac{dh}{dt}$ = change in head over the duration of the test (L/T)

$$Q_{sample} = -KiA = -K \frac{(h_n - h_0)}{L} A_{sample} \quad (\text{Box 4-3})$$

where:

Q_{sample} = average volumetric discharge through sample during test (L^3/T , volume over time)

A_{sample} = area of the sample is $0.7854d_{sample}^2$ (L^2)

L = length of sample (L)

$\frac{(h_n - h_0)}{L}$ = average gradient across the sample during the test because outlet elevation is the datum (L/L, unitless)

Equating Equation Box 4-3 to Equation Box 4-2 results in Equation Box 4-4.

$$-K \frac{(h_n - h_0)}{L} A_{sample} = A_{tube} \frac{dh}{dt} \quad (\text{Box 4-4})$$

where:

K = hydraulic conductivity of the sample (L/T)

Rearranging Equation Box 4-4 leads to Equation Box 4-5.

$$\frac{K \left(\frac{h}{L} \right) A_{sample}}{A_{tube}} dt = -dh \quad (\text{Box 4-5})$$

where:

h = hydraulic head measured from the outlet datum (L)

Integrating with the conditions that $h = h_0$ at t_0 and $h = h_n$ at t_n , provides a solution for K as Equation Box 4-6.

$$K = \frac{A_{tube} L}{A_{sample} t} \ln \left(\frac{h_0}{h_n} \right) \quad (\text{Box 4-6})$$

Substituting the areas of the sample and tube with $A_{sample} = 0.7584 d_{sample}^2$ and $A_{tube} = 0.7584 d_{tube}^2$ because the area is πr^2 , or $\pi \left(\frac{d}{2}\right)^2$, which is $\frac{\pi}{4}d^2$ as indicated in (Figure Box 4-4), the hydraulic conductivity is computed as shown in Equation Box 4-7.

$$K = \frac{d_{tube}^2 L}{d_{sample}^2 t} \ln \left(\frac{h_0}{h_n} \right) \quad (\text{Box 4-7})$$

Empirical Relationships Used to Estimate Hydraulic Conductivity

Over time researchers have attempted to generate relationships between physical parameters of unconsolidated samples (especially grain size) and hydraulic conductivity. Researchers often perform grain size distribution analysis of granular samples to determine

engineering and hydrogeologic properties. The procedure for determining grain-size distribution is described in Box 2 of this book.

The most commonly developed empirical relationships relate K to grain-size distribution data (median grain size, effective grain size, uniformity of grain size and mean grain size). A correlation supported by observing functional relationships between measurements of different related parameters on many individual samples are referred to as empirical relationships or empirical equations. Such relationships were developed by conducting both grain size analysis and a permeameter tests on the same sample for 10's to 100's of samples. Most all of the equations were developed for sand-rich samples. Four of these relationships are included here: Slichter (1899), Hazen (1911), Terzaghi (1925), and the USBR (United States Bureau of Reclamation) method as described in Vukovic and Soro (1992). Devlin (2015) developed an Excel based tool to estimate hydraulic conductivity from grain size analysis data sets that applies up to 15 empirical equations. The tool for estimating hydraulic conductivity from grain size can be accessed by [clicking here ↗](#). To properly apply this public domain software tool, the documentation should be carefully reviewed in order to understand the equations and their associated assumptions and limitations.

It is important to know that empirical expressions do not usually rely on use of consistent units. Consequently, it is imperative that the user of the expression take note of the input units for each variable and the associated output units for K .

K estimated from grain-size data using the Slichter method

Slichter (1899) developed an empirical equation for K that related the square of the mean grain diameter, d , to a constant related to porosity. Fraser (1935) provides additional details on the development of the equation as shown in Equation Box 4-8.

$$K = 10.22 \frac{\text{gram}}{\text{cm}^2 \text{s}^2} \frac{d^2}{\mu C_s} \quad (\text{Box 4-8})$$

where:

K = estimated hydraulic conductivity in centimeters per second

d = mean grain diameter in centimeters

μ = dynamic viscosity at a given temperature in gram/cm s

C_s = a constant for a given porosity (n) based on the following non-linear relationship: ($n=26\% C_s=84.3$; $n=36\% C_s=28.8$; $n=47\% C_s=11.8$)

The relationship of C_s to porosity is shown in Figure Box 4-5.

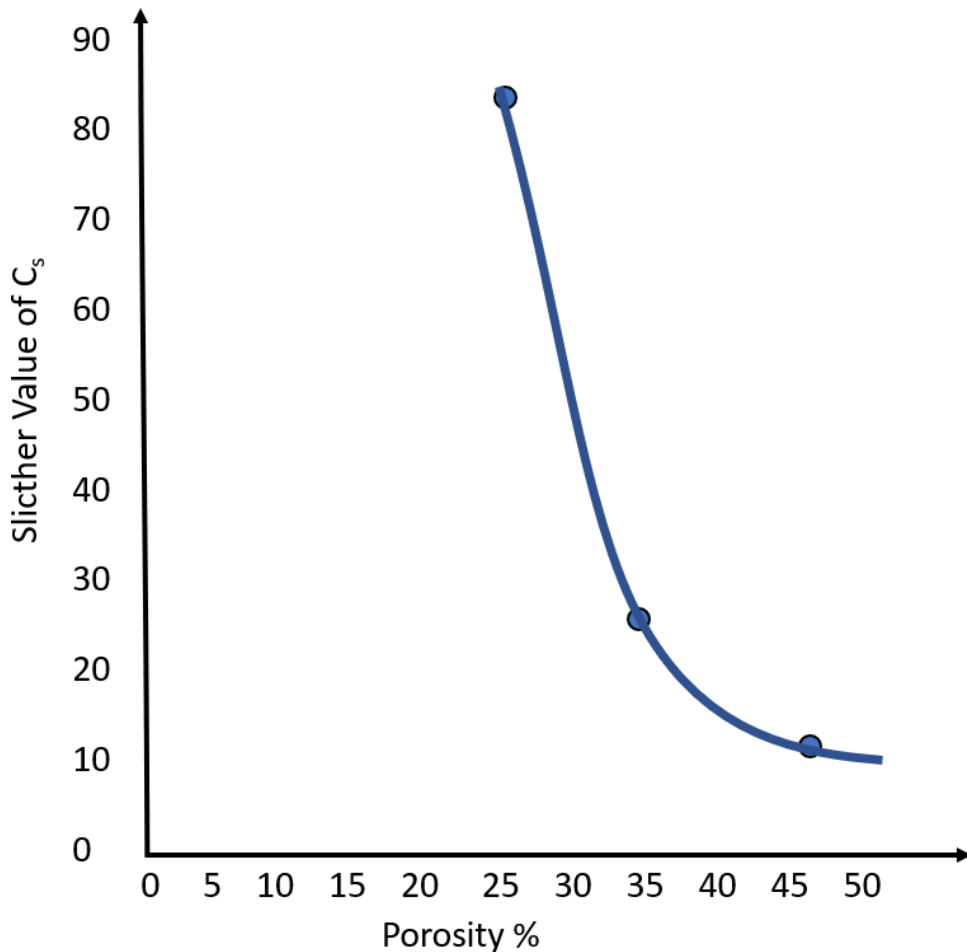


Figure Box 4-5 - Slichter relationship for C_s and porosity.

Slichter's relationship was formulated assuming grains are uniform spheres regularly distributed so the value d represents the mean diameter of the grains. He stated that the value of d for a sample of grains of various sizes should be equal to the diameter of a sample with grains of a single size that would yield an appropriate coefficient of permeability (hydraulic conductivity). The mean grain diameter is computed from the grain size distribution curve and is presented in Box 2 of this book.

Vukovic and Soro (1992) formulated C_s as $1/n^{3.287}$ (error +/- 5%) and interpreted d as the effective grain size (d_{10} percent finer than grain size distribution, see Box 2 of this book) when they presented a formulation of the Slichter equation. The use of the effective grain size, which is directly derived from the grain size distribution curve, is smaller than the mean grain diameter and its use reduces the computed hydraulic conductivity value. They suggest that the use of the Slichter method is appropriate when a sample uniformity coefficient is less than 5.

K estimated from grain size data using the Hazen method

Hazen (1911) developed a relatively simple equation for K based on the effective grain size (d_{90} cumulative percent retained or d_{10} finer-than) and a constant that varied with the dominate material type and sorting as shown in Equation Box 4-9.

$$K = \frac{C d_{10}^2}{\text{cm s}} \quad (\text{Box 4-9})$$

where:

K = estimated hydraulic conductivity in centimeters per second

d_{10} = effective grain size in centimeters (d_{10} finer-than, d_{90} retained)

C = dimensionless coefficient defined as follows:

Material	C
Very fine sand, poorly sorted	40-80
Fine sand with appreciable fines	40-80
Medium sand, well sorted	80-120
Coarse sand, poorly sorted	80-120
Coarse sand, well sorted, clean	120-150

Often, as a first estimate, the Hazen approximation constant, C , is set to 100. Professional judgement is used in applying this approach. Sorting used here is assumed to refer to the general uniformity of grain sizes. A uniformity coefficient analysis of the size distribution data is useful when selecting a value of C . Uniformity coefficient is discussed in Box 2 of this book. Vukovic and Soro (1992) suggest the Hazen method is applicable for samples with a uniformity coefficient of less than 5.

K estimated from grain size data using the Terzaghi method

Terzaghi (1925) worked in soil mechanics and developed an equation for K of sand samples that accounted for sample porosity and the effective grain diameter, while adjusting for the difference in fluid viscosity between the testing temperature and typical field temperature, as shown in Equation Box 4-10.

$$K = \left(\frac{C}{\text{cm s}} \right) \left(\frac{V_0}{V_T} \right) \left(\left(\frac{n - 0.13}{(1 - n)^{0.33}} \right) \right)^2 d_{10}^2 \quad (\text{Box 4-10})$$

where:

K = estimated hydraulic conductivity in centimeters per second (L/T)

C = Terzaghi coefficients ranging from 600 to 800 to reflect variation from irregular to smooth particles respectively (dimensionless)

V_0 = viscosity at 10°C in the same units used for V_T

V_T = viscosity at the test temperature in the same units used for V_0

n = porosity (dimensionless)

d_{10} = effective grain diameter (d_{10} finer-than, d_{90} retained) in centimeters (L)

The constants (Terzaghi coefficients) represent a range of particle conditions, generally, 800 is used for samples with rounded and smooth grains and 600 for coarse grains with irregular shapes. Vukovic and Soro (1992) summarized the literature and found

the following values for Terzaghi coefficients: sea sand, 750-663; dune sand 800; pure river sand, 696-460; muddy river sand 203.

K estimated from grain size data using the USBR method

The United States Bureau of Reclamation (1978, as reported in Vukovic and Soro, 1992) developed a relationship shown in Equation Box 4-11 for medium sands with a uniformity coefficient of less than 5.

$$K = 0.36 (d_{20})^{2.3} \quad (\text{Box 4-11})$$

where:

K = estimated hydraulic conductivity in centimeters per second (L/T)

d_{20} = grain size in centimeters (d_{20} finer-than) (L)

Other empirical equations for estimating K

Other authors have formulated empirical equations, though most are complex or require professional judgement in their use. Shepherd (1989) used median grain size raised to an exponent between 1.5 and 2, and a shape factor to estimate K . Masch and Denny (1966, pp. 665-677) developed a graphical empirical relationship based on the median grain diameter, d_{50} in phi units, and the inclusive standard deviation, σ_I . Using their graph, the median grain diameter is projected from the x axis to the appropriate plotted line of measured intrinsic standard deviation, then the corresponding K is read from the y-axis. Slichter (1899), Terzaghi (1925), the Kozeny-Carmen equation (Bear, 1972), Fair and Hatch (1933) and others have attempted to use porosity as a factor in grain size relationships for computing hydraulic conductivity. However, porosity is poorly correlated to K and relationships that are proposed are non-linear. Also, most empirical equations based on grain size require a coefficient to bring grain size data into line with permeameter results. Most empirical relationships have been developed for unconsolidated sand rich materials. Cedergren (1989, page 42) describes the use of laboratory consolidation tests to estimate the hydraulic conductivity of clays and silts. The hydraulic conductivity is directly proportional to a time factor for a given percent of consolidation.

Clearly, estimates of K can be made based on grain size analysis, however, if multiple methods are used, they may not agree. Cormican et al. (2020) evaluated the use permeameter and grain size analyses to determine the hydraulic conductivity of engineered porous media used in groundwater remediation. They compared the results of 16 empirical methods with permeameter results. For the material they tested, the methods of Slichter (1898) and Shepard (1989) were most representative. If empirical equations are used to characterize K for a groundwater project, it is recommended that some site samples be analyzed with both a laboratory-based permeameter test and a grain size distribution analysis so that the most representative of the empirical equations can be used and their coefficient can be adjusted to better represent site-specific conditions.

As stated previously, a challenge in using both permeameter and grain size analyses to estimate K arises from the fact that they represent only a small portion of the field setting, essentially a point sample. Also, disturbed samples don't include the micro structures and packing of the field sediments. Thus, the values may not appropriately represent conditions at the field site. However, they are commonly used to establish the range K values for field sites and to estimate groundwater flow rates.

Field Tests to Establish Hydraulic Conductivities

Characterizing the hydraulic conductivity of unconsolidated and consolidated earth materials in a field setting is often accomplished by using boreholes and wells to observe the response of a groundwater system to the withdrawal of water. The general principle of deriving a representative field-scale value of hydraulic conductivity is to use boreholes or wells installed in such a way that the earth material properties are not altered. Then the groundwater system is manipulated, usually by pumping one of the wells, and monitoring water level declines in nearby wells. The water level declines are called drawdowns and the approximate cone-like shape of the head distribution around the pumping well is called a drawdown cone. When the pumping is stopped, water levels rise (recover). If the K value of the aquifer is high, water levels will not change as much in response to pumping and recovery as when the same process is performed in material with a low K . Thus, observing groundwater responses to changes in the groundwater system yields information on hydraulic conductivities. Analytical equations, numerical methods, and computer simulations of groundwater flow, are used in conjunction with the measurements of drawdown versus time to characterize hydraulic conductivities at both local and regional scales. A schematic of a field test in a simple setting is shown in Figure Box 4-6.

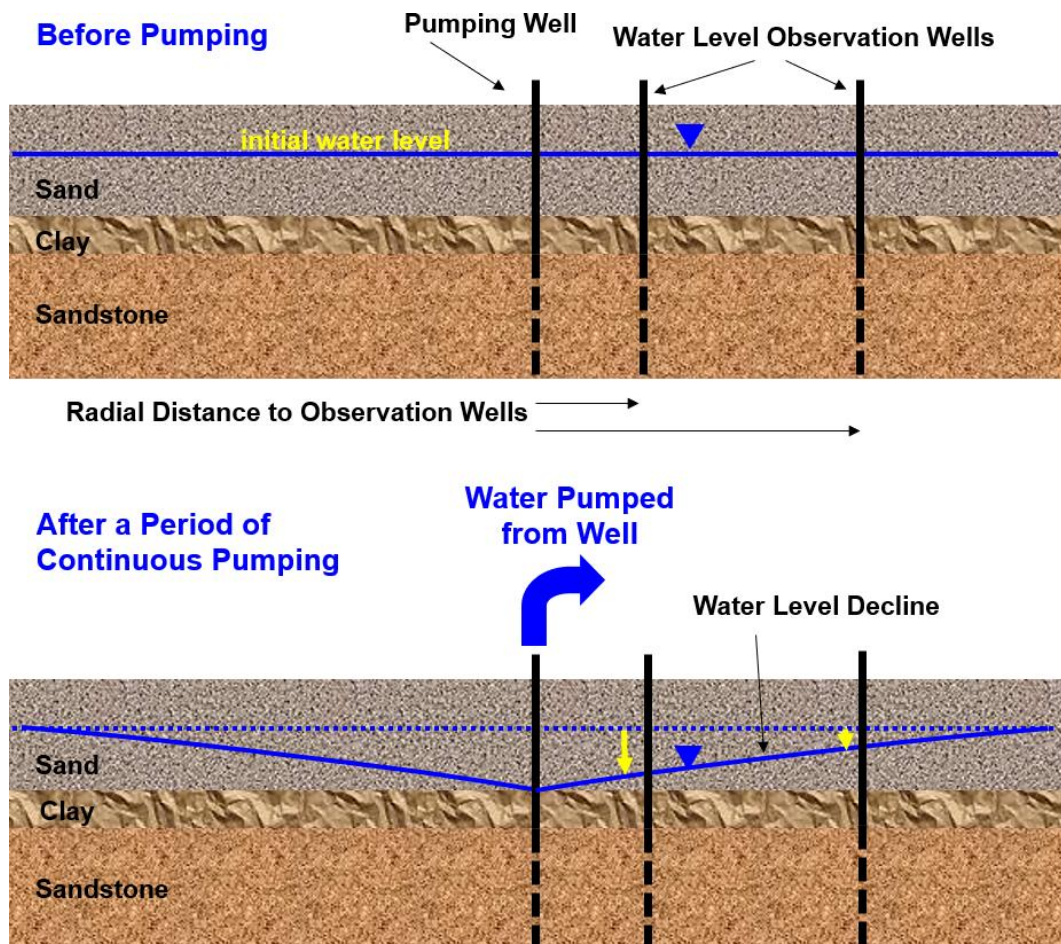


Figure Box 4-6 - When one well is pumped from the screened section of sandstone (shown as dashed line portions of the pumping well), the declining water levels are monitored in the screened portions of nearby observation wells at varying radial distances from the pumping well. The changes in water levels with time at the observation wells during and after pumping are used along with knowledge of the aquifer thickness to estimate hydraulic properties such as hydraulic conductivity and specific storage.

Field methods used to determine hydraulic conductivity are explained in a number of modern and older references. A companion Groundwater Project book "[An Introduction to Hydraulic Testing in Hydrogeology: Basic Pumping, Slug, and Packer Methods ↗](#)" (Woessner et al., 2023) provides practical information on planning, conducting, and interpreting hydraulic test to estimate field scale hydrogeologic properties. Foundational material on groundwater hydraulics including the presentation of a wide range of aquifer test methods can be found in the United States Geological Survey Professional Paper 708 by Lohman (1972). The comprehensive book, "An Analysis and Evaluation of Pumping Test Data", by Kruseman and de Ridder (1994) is available on the [Groundwater Project website ↗](#). It describes theory, field test setups, testing methods and data analyses. Another good description of how field-scale K values are derived is also found in the publicly available Ground Water Manual: A Water Resources Technical Publication, (United States Bureau of Reclamation, 1995).

[Return to where text links to Box 4 ↑](#)

Box 5 Equation Derivation for Equivalent K and a 4-layer Application

To calculate the equivalent hydraulic conductivity parallel to layers, K_x , consider flow through the system shown in Figure Box 5-1. Define Δh as the hydraulic head difference over a horizontal distance ΔL_x (so that $\Delta h/\Delta L_x$ is the hydraulic gradient). The volumetric discharge Q (L^3/T) through a unit width (into the image) of the system is the sum of the volumetric discharges through each layer. The specific discharge is $q = Q/A$. Here the area is equal to the product of the thickness d and one unit of distance into the image, so $A = d(1)$, thus $q = Q/d(1)$, or $q = Q/d$. Knowing that $q = -Ki$, this logic can be applied to the stack of layers as follows in Equations Box 5-1 through Equation Box 5-3. Equation Box 5-1 indicates the horizontal flow through each layer.

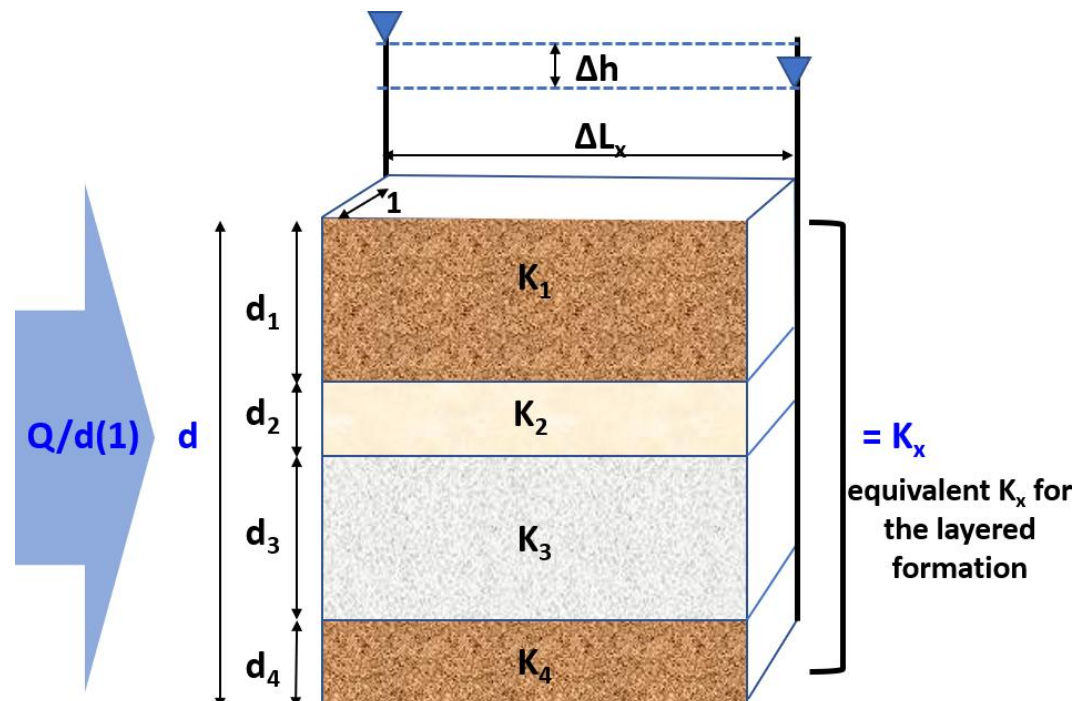


Figure Box 5-1 - Calculating the equivalent K_x of a layered heterogeneous system composed of isotropic and homogeneous layers. The original system is made up of four layers that have different thicknesses (d_1 , d_2 , d_3 , and d_4) and hydraulic conductivities (K_1 , K_2 , K_3 , and K_4). The total horizontal flux per unit thickness into the image is represented by $Q/d(1)$ where Q is the flow through a cross sectional area that is d long and the unit thickness is 1 unit wide. Conceptually, flow in the x direction passes through all of the layers under the same gradient, $\Delta h/\Delta L_x$. The equivalent K_x for the entire thickness, d , is computed using Equation Box 5-3.

$$Q_i = -K_i d_i \frac{\Delta h}{\Delta L_x} \quad (\text{Box 5-1})$$

where:

Q_i = volumetric discharge through an individual layer of a unit width denoted by i (L^3/T)

d_i = thickness of individual layer i (L)

ΔL_x = length of the layers in the x -direction (L)

Δh = hydraulic head difference over horizontal distance ΔL_x (L)

Equation Box 5-2 provides the specific discharge for the entire section by summing the flow through every layer and dividing by the total flow area of the section, and shows that the specific discharge for the entire stack of layers is equal to the product of the equivalent K_x and the gradient.

$$q = - \sum_{i=1}^n \left[\frac{K_i d_i}{d} \right] \frac{\Delta h}{\Delta L_x} = -K_x \frac{\Delta h}{\Delta L_x} \quad (\text{Box 5-2})$$

where:

q = specific discharge through the entire section per unit width in the horizontal direction (L)

K_x = equivalent K_x of the entire section (L/T)

Then, simplifying Equation Box 5-2 by cancelling the gradients, the equivalent K in the x direction is as shown in Equation Box 5-3.

$$K_x = \sum_{i=1}^n \left[\frac{K_i d_i}{d} \right] \quad (\text{Box 5-3})$$

This calculation of the equivalent K_x for the layered formation is a thickness-weighted arithmetic mean. This is the same as K_h , equivalent horizontal hydraulic conductivity, referred to in the main text. Some readers may find it useful to note that the equation for calculating equivalent K parallel to layers is identical to the equation used to calculate the equivalent conductance through electrical resistors that are wired in parallel.

To calculate the equivalent the hydraulic conductivity perpendicular to the layers, K_z , consider vertical flow through the system shown in Figure Box 5-2. Let Δh be the hydraulic head difference over a vertical distance ΔL_z (so that, $\Delta h/\Delta L_z$ is the overall hydraulic gradient). Mass must be conserved, so the volumetric inflow Q (L³/T) through a unit width (into the image) of the system at the bottom must be equal to the outflow at the top. In fact, water cannot be created nor destroyed along the flow path, so the specific discharge must be the same through each layer of the system. Given that the hydraulic conductivities differ between layers, then by Darcy's law, with a constant flow rate through each layer, the gradient will be different in each layer, as indicated by Equation Box 5-4.

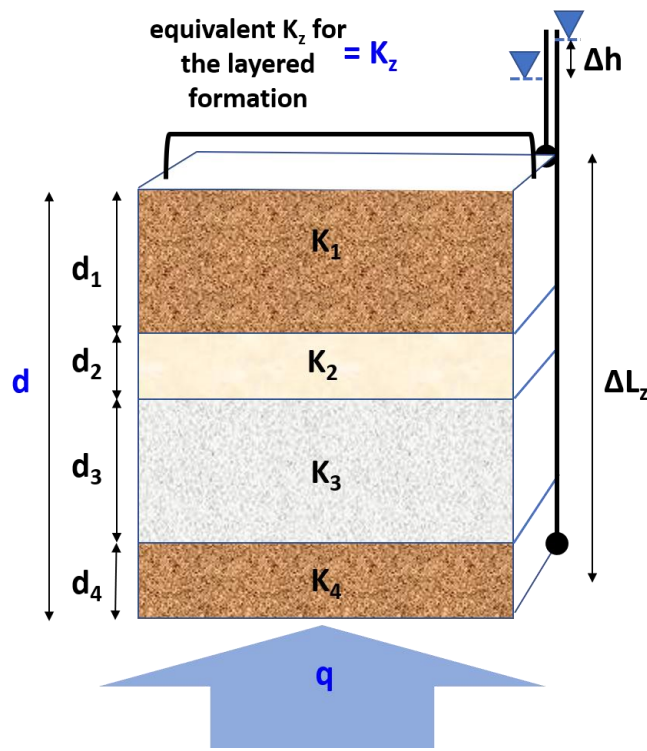


Figure Box 5-2 - Calculating the equivalent K_z of a layered heterogeneous system composed of isotropic and homogeneous layers. The vertical flux rate, q , is constant. The original system is made up of four layers that have different thickness (d_1 , d_2 , d_3 , and d_4) and hydraulic conductivity (K_1 , K_2 , K_3 , and K_4). Conceptually flow in the z direction passes through all of the layers under the overall gradient, $\Delta h/\Delta L_z$. Because mass must be conserved the flow rate through each layer will be the same, and given their differing K values, the gradients will differ. The equivalent K_z for the entire thickness, d , is computed using Equation Box 5-6.

$$q = -\frac{K_1 \Delta h_1}{d_1} = -\frac{K_2 \Delta h_2}{d_2} = -\frac{K_3 \Delta h_3}{d_3} = -\frac{K_4 \Delta h_4}{d_4} = -\frac{K_z \Delta h}{d} \quad (\text{Box 5-4})$$

where:

q = specific discharge in the vertical direction (L/T)

Δh_i = hydraulic head difference across each layer in the vertical direction, the values of Δh_i sum to Δh (L)

K_z = equivalent K_z of the entire section (L/T)

Rearranging Equation Box 5-4 produces Equation Box 5-5, where Δh is expanded into the sum of the layer Δh_i values, and, by Darcy's law, each Δh_i can be expressed as $\frac{qd_i}{K_i}$.

$$K_z = \frac{qd}{\Delta h} = \frac{qd}{\Delta h_1 + \Delta h_2 + \Delta h_3 + \Delta h_4} = \frac{qd}{\frac{qd_1}{K_1} + \frac{qd_2}{K_2} + \frac{qd_3}{K_3} + \frac{qd_4}{K_4}} \quad (\text{Box 5-5})$$

By cancelling the q 's and summing the $\frac{d_i}{K_i}$, Equation Box 5-6 provides the procedure for calculating the equivalent K_z .

$$K_z = \frac{d}{\sum_{i=1}^n \frac{d_i}{K_i}} \quad (\text{Box 5-6})$$

This calculation of the equivalent K_z for the layered formation is a thickness-weighted harmonic mean. It is the same value as the K_v , equivalent vertical hydraulic conductivity in the main text. Some readers may find it useful to note that the equation for calculating equivalent K perpendicular to layers is identical to the equation used to calculate conductance through electrical resistors that are wired in series.

Equations Box 5-3 and Box 5-6 provide the K_x and K_z values for a homogeneous but anisotropic formation that is hydraulically equivalent to the layered heterogeneous system of homogeneous, isotropic geologic formations (Figure Box 5-3). Given that K_x is a thickness-weighted arithmetic mean, the high hydraulic conductivity values dominate its value, whereas the low hydraulic conductivity layers dominate the thickness-weighted harmonic mean K_z value. For example, suppose the materials from top to bottom are coarse sand, medium gravel, silty sand and fine gravel. The layers from top to bottom have K values of $K_1 = 100 \text{ m/d}$, $K_2 = 1000 \text{ m/d}$, $K_3 = 0.1 \text{ m/d}$ and $K_4 = 400 \text{ m/d}$ and corresponding thicknesses of $d_1 = 125 \text{ m}$, $d_2 = 58 \text{ m}$, $d_3 = 125 \text{ m}$ and $d_4 = 67 \text{ m}$. The computed horizontal and vertical hydraulic conductivities are $K_x = 260 \text{ m/d}$ and $K_z = 0.3 \text{ m/d}$ (using Equations Box 5-3 and Box 5-6). The anisotropy ratio, K_x/K_z , is on the order of 900. In the field, it is common for layered heterogeneity to lead to regional anisotropy values on the order of 10:1 and in many settings much greater values.

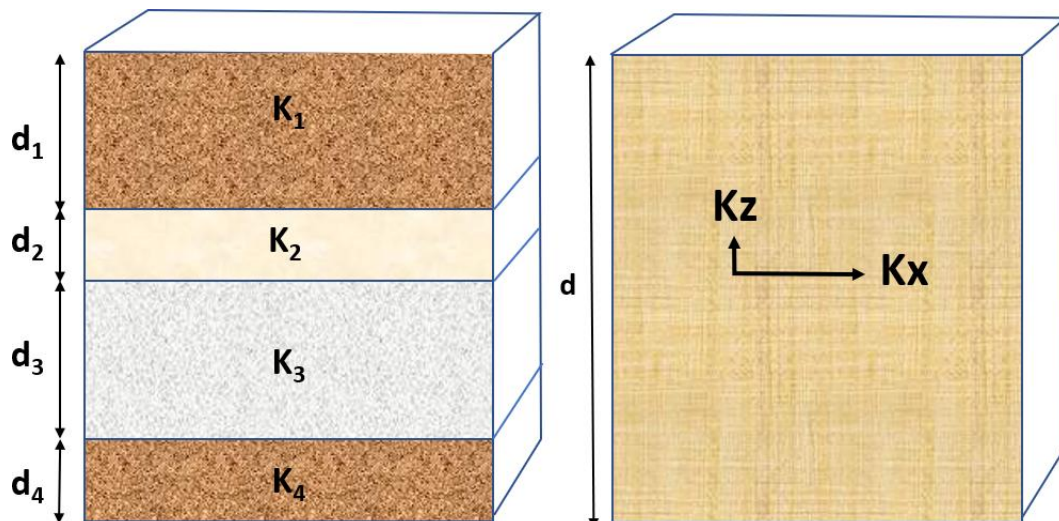


Figure Box 5-3 - Equivalent hydraulic conductivities can be calculated for layered materials using Equations Box 5-3 and Box 5-6.

[Return to where text links to Box 5 ↑](#)

Box 6 Adding Recharge to the Unconfined Aquifer System

Consider the addition of a flux boundary condition on the top of the model. This could represent uniform recharge to the upper surface between the constant-head boundaries (Figure Box 6-1). Now the flow rate will vary from one x -location to another. Depending on the relative values of h_1 , h_2 , recharge, W , hydraulic conductivity, K , and boundary heads, the flow may be entirely to the right, to the left, or a groundwater divide may form within the land mass at which the flow, q' , is zero with increasing flow volume in opposite directions from the divide to the boundaries.

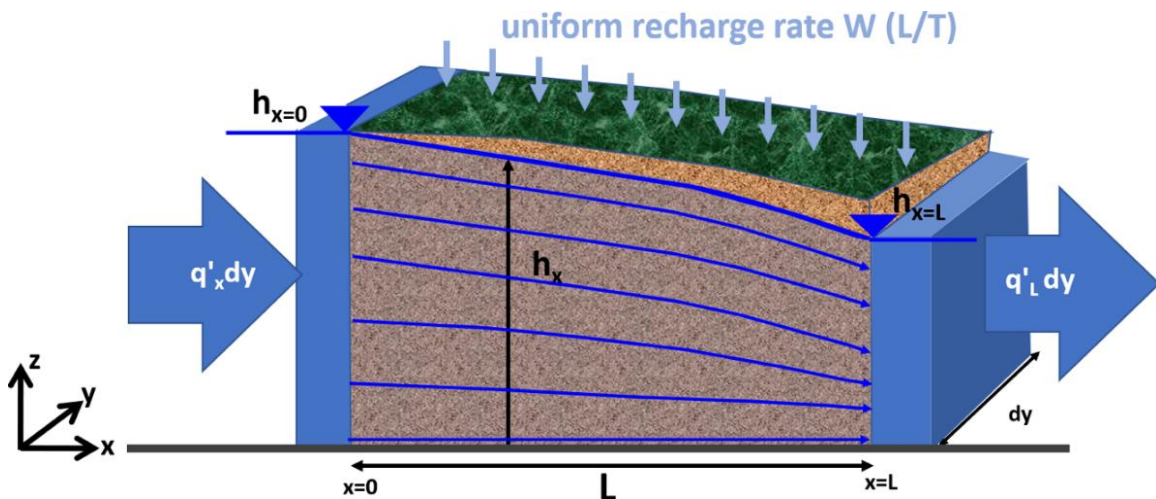


Figure Box 6-1 - Including uniform recharge on a steady-state, unconfined groundwater flow system between fully penetrating surface water bodies of constant head.

A few schematics of possible configurations are shown in Figure Box 6-2 to illustrate the substantial variations that can occur in this simple one-dimensional system. Flow directions and velocities, as well as the shape of the water table can be drastically different.

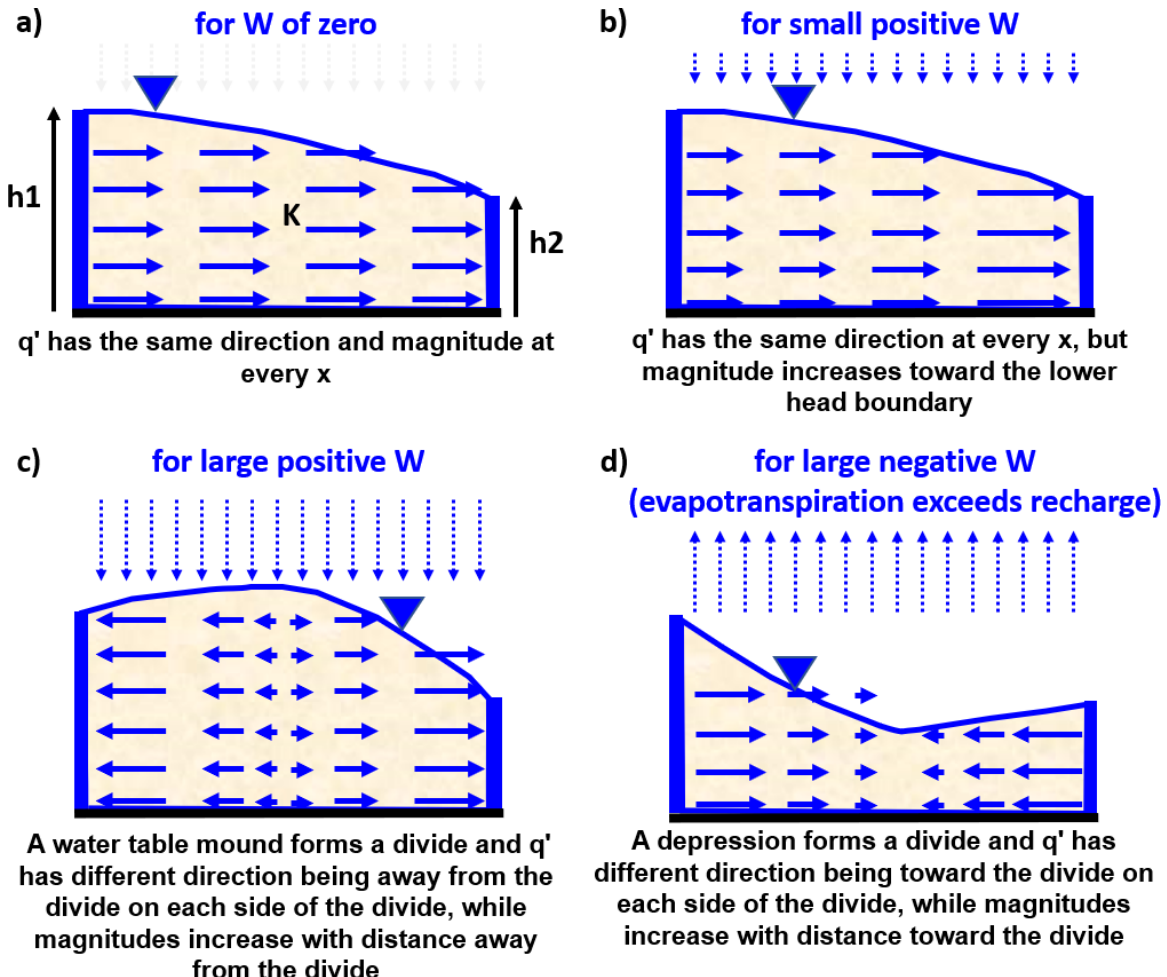


Figure Box 6-2 - Depending on the relative values of boundary heads, h_1 , h_2 , W , and K , the flow, q' (solid blue arrows) may be entirely to the right, to the left, or a groundwater divide may form within the groundwater system. The response of the water table: a) for recharge, W , of zero; b) for a small recharge rate relative to the through flow in the aquifer; c) for a large recharge rate relative to the through flow in the aquifer; d) for a large negative recharge rate (loss of water from the water table, e.g., evapotranspiration) relative to the through flow in the aquifer.

To incorporate surficial recharge into the analytical solution, first consider a small prism of the aquifer, as shown in Figure Box 6-3.

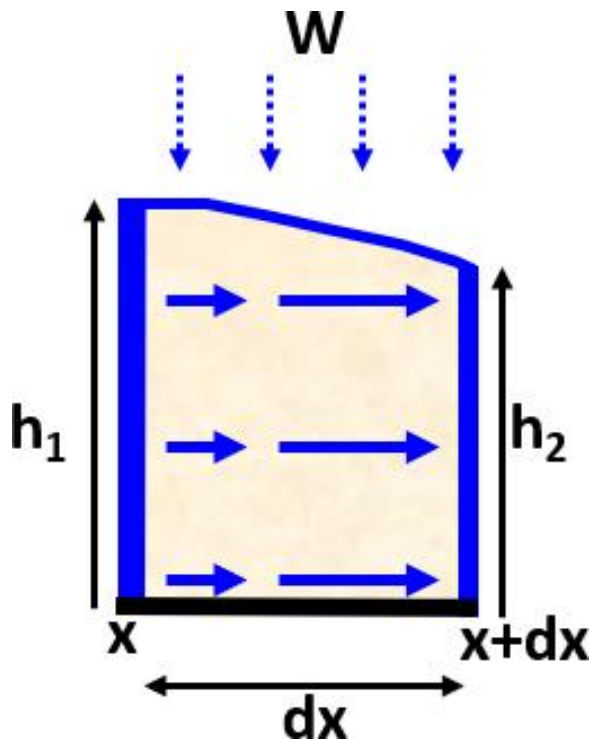


Figure Box 6-3 - A small prism of the aquifer.

Flow through the left face of Figure Box 6-3 is shown in Equation Box 6-1.

$$q'_x dy = -K \left(h \frac{dh}{dx} \right)_x dy \quad (\text{Box 6-1})$$

where:

q'_x = flow per unit width (L^2/T)

dy = width of the face into the page (L)

Flow through the right face of Figure Box 6-3 is shown in Equation Box 6-2.

$$q'_{x+dx} dy = -K \left(h \frac{dh}{dx} \right)_{x+dx} dy \quad (\text{Box 6-2})$$

The value of $h \left(\frac{dh}{dx} \right)$ is different on each side of the element, so the value of $Q(q'dy)$ is different on each side. The difference between flow on each side of the element must equal the amount of flow entering as recharge from the top of the system. The difference in flow can be expressed in terms of the one-dimensional, unconfined, steady-state groundwater flow equation, and equated to the amount of flow that enters the element from the top between the two sides ($W dx dy$) as in Equation Box 6-3.

$$(q'_{x+dx} - q'_x) dy = -K \frac{d}{dx} \left(h \frac{dh}{dx} \right) dx dy = W dx dy \quad (\text{Box 6-3})$$

where:

W = recharge rate from the surface (L/T)

Gathering the derivative terms and dividing both sides by $-K$ provides Equation Box 6-4.

$$\frac{1}{2} \frac{d^2 h^2}{dx^2} = -\frac{W}{K} \quad (\text{Box 6-4})$$

Integrating Equation Box 6-4 yields Equation Box 6-5.

$$h^2 = -\frac{Wx^2}{K} + C_1 x + C_2 \quad (\text{Box 6-5})$$

where:

C_1, C_2 = constants of integration (L and L², respectively)

By applying boundary conditions as done for the case without recharge ($h = h_1$ at $x = 0$ and $h = h_2$ at $x = L$), the constants can be determined. Solving for the constants provides Equation Box 6-6. Solving Equation Box 6-6 for h at x results in Equation Box 6-7. See Figures Box 6-1 and Box 6-3 for terms.

$$h_x^2 = h_1^2 - \frac{(h_1^2 - h_2^2)x}{L} + \frac{W}{K}(L-x)x \quad (\text{Box 6-6})$$

$$h_x = \sqrt{h_1^2 - \frac{(h_1^2 - h_2^2)x}{L} + \frac{W}{K}(L-x)x} \quad (\text{Box 6-7})$$

where:

h_x = head at x some distance from the origin, $x = 0$ (L)

x = distance from the origin (L)

h_1 = head at the origin (L)

h_2 = head at L (L)

L = distance from the origin to h_2

K = hydraulic conductivity (L/T)

W = recharge rate (L/T)

To determine q' as a function of x , Equation Box 6-6 can be differentiated with respect to x resulting in Equation Box 6-8.

$$h \frac{dh}{dx} = -\frac{(h_1^2 - h_2^2)}{2L} + \frac{W}{K} \left(\frac{L}{2} - x \right) \quad (\text{Box 6-8})$$

Multiplying Equation Box 6-8 by $-K$ provides Equation Box 6-9.

$$-Kh \frac{dh}{dx} = \frac{K(h_1^2 - h_2^2)}{2L} - W \left(\frac{L}{2} - x \right) \quad (\text{Box 6-9})$$

Substituting q'_x for the left-hand side of Equation Box 6-9 provides Equation Box 6-10.

$$q'_x = \frac{K(h_1^2 - h_2^2)}{2L} - W \left(\frac{L}{2} - x \right) \quad (\text{Box 6-10})$$

The next task is to determine the location of the groundwater divide. An expression for the location of the divide, d , can be determined by setting q'_x equal to zero in Equation Box 6-10 and solving for the x position of the divide (d) as shown in Equation Box 6-11.

$$d = \frac{L}{2} - \frac{K}{W} \frac{(h_1^2 - h_2^2)}{2L} \quad (\text{Box 6-11})$$

where:

d = x location of the groundwater divide (L)

The maximum head (or minimum in the case of a negative value of W) can be determined by substituting d for x in Equation Box 6-7 resulting in Equation Box 6-12.

$$h_{max/min} = \sqrt{h_1^2 - \frac{(h_1^2 - h_2^2) d}{L} + \frac{W}{K} (L - d) d} \quad (\text{Box 6-12})$$

where:

$h_{max/min}$ = maximum head for positive W and minimum for negative W (L)

Earlier revisions of this book provided a spreadsheet for exploring the nature of this flow system for various input parameter values. It has been replaced by a more robust interactive educational tool called [WTR \(Water Table Recharge\)](#)↗.

[Return to where text links to Box 6↑](#)

Box 7 Axis Transformation for 2-D Flow in an Anisotropic Medium

A second graphical method for determining flow directions in anisotropic materials involves transforming one axis of the map or cross section to account for the anisotropy, plotting the head values then drawing equipotential lines and flow lines as if the system were isotropic. Subsequently, the entire drawing is transformed back to the original scale. The transformation involves either stretching the drawing in the direction of the minimum hydraulic conductivity or compressing the drawing in the direction of the maximum hydraulic conductivity. The most convenient way to explain the process is to orient the x and z axes parallel to K_{max} and K_{min} of the field system, respectively.

Consider the system shown in Figure Box 7-1, where a water body with an elevation of 8 meters overlies the ground surface at an elevation of 6 meters. A 1-meter diameter drain with a head of 0 (at atmospheric pressure) is centered 2 meters above the bedrock such that the bottom of the drain is 1.5 meters above bedrock. All boundaries other than the ponded water and the drain are no-flow. The horizontal hydraulic conductivity, K_x , is 0.16 m/day and the vertical hydraulic conductivity, K_z , is 0.01m/day.

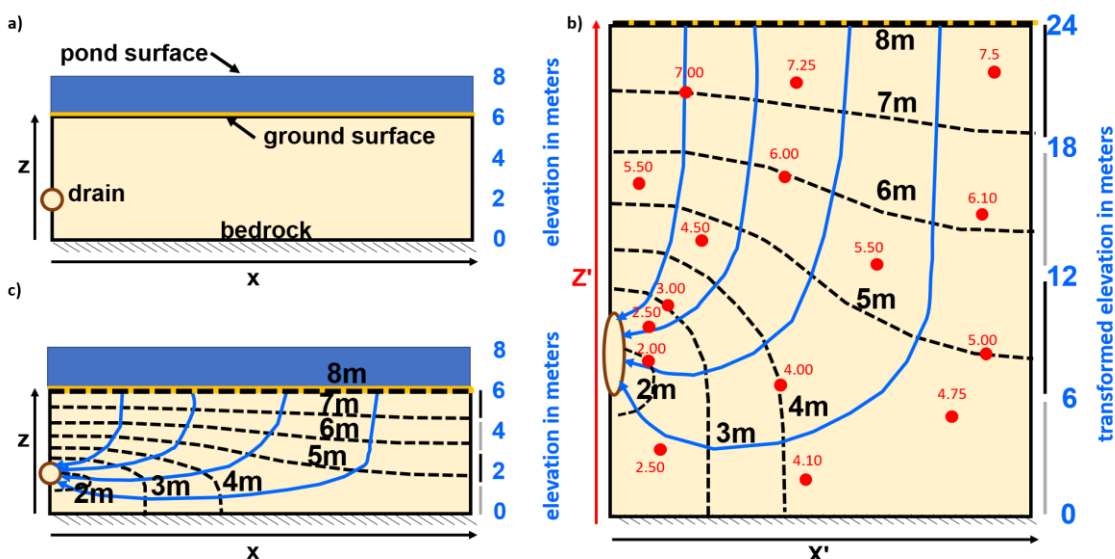


Figure Box 7-1 Example of using the axis transformation to determine flow lines in an anisotropic homogeneous system. a) The problem domain is a sand represented in cross section with no vertical exaggeration where saturated flow occurs through anisotropic material from a pond bottom (the pond surface is 8 m above the underlying low permeability bed and the bottom of the pond is 6 m above the bed). There is a 1 m diameter drain pipe at atmospheric pressure on the left boundary. All boundaries other than the pond and the drain are no-flow boundaries. The hydraulic conductivity ellipse has a ratio of the square root of K_x to the square root of K_z , which is 4. b) Transformation of the z axis and drawing of flow lines at right angles to the equipotential lines. c) The final flow lines at the original scale (z axis is returned to the original scale). (all after Freeze and Cherry, 1979).

To generate the anisotropic flow field the plot scale is transformed into X' and Z' based on the hydraulic conductivity ellipse. The scale of the x axis remains the same, $X' = x$, and the z -axis is transformed as $Z' = z \left(\frac{K_x}{K_z} \right)^{0.5}$. Substituting the values for K_x and K_z results in:

$$Z' = z \left(\frac{0.16^{0.5}}{0.01^{0.5}} \right) = z \left(\frac{0.4}{0.1} \right) = 4z$$

So, the z-axis is expanded by a factor of 4 as shown in Figure Box 7-1b. If the head values were not plotted on the pre-transformed scaled section, then the head data are plotted at the x, Z' location with their Z' four times their z value (red dots and values on Figure Box 7-1b). Next, the head data are contoured (dashed black lines) and flow lines are drawn perpendicular to the equipotential lines (solid blue arrows). Finally, the Z' location of every point in the image is transformed back to the original scale as shown in Figure Box 7-1c to obtain flowlines for the anisotropic system. After the reverse transformation, the flow lines are no longer perpendicular to the equipotential lines. The transformation is only valid when the original cross-sectional representation is plotted without vertical exaggeration.

[Return to where text links to Box 7↑](#)

Box 8 Deriving the Tangent Law of Refraction

Eileen Poeter, William Woessner, and Paul Hsieh

Figure Box 8-1 shows flow lines and equipotential lines at an interface between materials of different hydraulic conductivity. One side of the interface, Region 1 has hydraulic conductivity K_1 ; the other side of the interface, Region 2 has hydraulic conductivity K_2 . Under steady state conditions the discharge in a flow tube formed by two parallel flowlines must be the same on both sides of an interface ($Q_1 = Q_2$), and given that Darcy's Law must be followed, the gradient and flow area (A) must differ on each side of the interface to accommodate the differing hydraulic conductivities. This causes the flow lines to refract at the interface as shown in Figure Box 8-1 because the gradient ($h\text{diff}_1/l_1$ in Region 1 and $h\text{diff}_2/l_2$ in Region 2) and the flow area (indicated by the width of the flow tubes, d_1 and d_2 , times a unit width into the image) must adjust to carry the same volumetric flow in materials of different hydraulic conductivity.

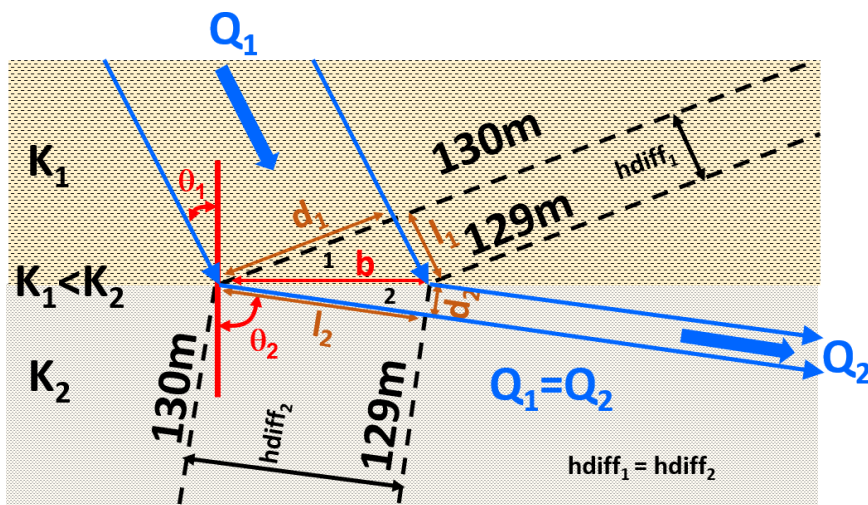


Figure Box 8-1 - Geometry of flow lines at an interface between materials of differing hydraulic conductivity showing the angle of refraction, the width of the flow tube d_1 and d_2 , and the distance between equipotential lines l_1 and l_2 on different sides of the interface.

Darcy's Law can be written for either Region 1, or 2, with the subscript $n = 1$ to represent region 1 or $n = 2$ to represent region 2, using Equation Box 8-1.

$$Q_n = -K_n i_n A_n \quad (\text{Box 8-1})$$

where:

Q_n = volumetric flow through a unit width into the image for region n (L^3/T)

K_n = hydraulic conductivity of region n (L/T)

i_n = hydraulic gradient in region n (dimensionless) = $-\frac{\text{head difference}}{\text{distance}} = -\frac{h\text{diff}_n}{l_n}$

A_n = area perpendicular to flow in tube of region n (L^2), $A_n = d_n w$ where w is a unit width into the image

Setting $Q_1 = Q_2$ leads to Equation Box 8-2.

$$-K_1 \frac{hdif\mathit{f}_1}{l_1} d_1 w = -K_2 \frac{hdif\mathit{f}_2}{l_2} d_2 w \quad (\text{Box 8-2})$$

where:

$hdif\mathit{f}_1$ = head difference between equipotential lines region 1 (L)

$hdif\mathit{f}_2$ = head difference between equipotential lines region 2 (L)

d_1, d_2, l_1, l_2 , = distances defined in Figure Box 8-1 (L)

w = a unit width into the image (L)

note: in this case $hdif\mathit{f}_1$ equals $hdif\mathit{f}_2$, $hdif\mathit{f} = hdif\mathit{f}_1 = hdif\mathit{f}_2 = (129\text{m} - 130\text{m} = -1\text{m})$.

Cancelling the equal head differences, $hdif\mathit{f}$, and canceling the equal distances perpendicular to the flow direction, w , Equation Box 8-2 simplifies to Equation Box 8-3.

$$K_1 \frac{d_1}{l_1} = K_2 \frac{d_2}{l_2} \quad (\text{Box 8-3})$$

Given the distance b and angles of θ 's as defined in Figure Box 8-1, trigonometric relationships result in Equations Box 8-4 and Box 8-5.

$$d_1 = b \cos \theta_1 \quad (\text{Box 8-4})$$

$$d_2 = b \cos \theta_2 \quad (\text{Box 8-5})$$

where:

θ_n = angles shown in Figure Box 8-1 (degrees)

Substituting Equations Box 8-4 and Box 8-5 for d_1 and d_2 in Equation Box 8-3 yields Equation Box 8-6.

$$K_1 \frac{b \cos \theta_1}{l_1} = K_2 \frac{b \cos \theta_2}{l_2} \quad (\text{Box 8-6})$$

Using rules of trigonometry, the Equation Box 8-7 and Equation Box 8-8 are true.

$$\frac{b}{l_1} = \frac{1}{\sin \theta_1} \quad (\text{Box 8-7})$$

$$\frac{b}{l_2} = \frac{1}{\sin \theta_2} \quad (\text{Box 8-8})$$

Substituting Equation Box 8-7 and Equation Box 8-8 into Equation Box 8-6 and canceling b , results in Equation Box 8-9.

$$K_1 \frac{\cos \theta_1}{\sin \theta_1} = K_2 \frac{\cos \theta_2}{\sin \theta_2} \quad (\text{Box 8-9})$$

Rearranging by multiplying both sides first by $\sin \theta_1$ and then by $\sin \theta_2$, and dividing both sides first by $\cos \theta_1$ and then by $\cos \theta_2$ results in Equation Box 8-10.

$$K_1 \frac{\sin \theta_2}{\cos \theta_2} = K_2 \frac{\sin \theta_1}{\cos \theta_1} \quad (\text{Box 8-10})$$

Using the Trigonometric identity of Equation Box 8-11.

$$\tan \theta = \frac{\sin \theta}{\cos \theta} \quad (\text{Box 8-11})$$

Equation Box 8-10 can be expressed as Equation Box 8-12.

$$K_1 \tan \theta_2 = K_2 \tan \theta_1 \quad (\text{Box 8-12})$$

Then dividing both sides of Equation Box 8-12, first by K_2 and then by $\tan \theta_2$, the tangent law of Equation Box 8-13 is obtained.

$$\frac{K_1}{K_2} = \frac{\tan \theta_1}{\tan \theta_2} \quad (\text{Box 8-13})$$

where:

K_1 = hydraulic conductivity of layer 1 (L/T)

K_2 = hydraulic conductivity of layer 2 (L/T)

θ_1 = angle the flow line makes with a perpendicular to the boundary in stratum 1 as shown in Figure Box 8-1 (degrees)

θ_2 = angle the flow line makes with a perpendicular to the boundary in stratum 2 as shown in Figure Box 8-1 (degrees)

[Return to where text links to Box 8 ↑](#)

13 Exercise Solutions

Solution to Exercise 1

1) A 100 cubic centimeter (cm^3) sample of soil has an initial weight of 227.1 grams. It is oven dried at 105°C to a constant weight of 222.0 grams. The sample is then saturated with water and has a weight of 236.6 grams. Next, the sample is then allowed to drain by gravity in an environment of 100% humidity and is reweighted at 224.4 grams. Assuming that 1 cm^3 of water = 1 gram at 15.5°C:

1a) Calculate the porosity using Equation 6 of this book.

$$n_e = \frac{V_I}{V_T}$$

where:

n_e = effective porosity (dimensionless)

V_I = volume of interconnected pore space (L^3)

V_T = volume of sample (L^3)

Recognizing that water weight in grams is equivalent to volume in cm^3 because 1g of water is 1 cm^3 use water weight where water volume is needed, so the volume of water in the sample is the saturated weight in grams minus the oven dried weight in grams:

$$n_e = \frac{(\text{saturated weight} - \text{dry weight}) \text{ as volume}}{100 \text{ cm}^3} = \frac{236.6 \text{ cm}^3 - 222.0 \text{ cm}^3}{100 \text{ cm}^3}$$

$$n_e = \frac{14.6 \text{ cm}^3}{100 \text{ cm}^3} = 0.146 \text{ or } 14.6\%$$

1b) Calculate the specific yield using Equation 11 of this book.

$$S_y = \frac{V_D}{V_T}$$

where:

S_y = specific yield (dimensionless)

V_D = volume of water that drains by gravity (L^3)

V_T = volume of sample (L^3)

Recognizing that water weight in grams is equivalent to volume in cm^3 because 1g of water is 1 cm^3 use water weight where water volume is needed, so the volume of water drained from the sample is the weight of drained water in grams:

$$S_y = \frac{12.2 \text{ g}}{100 \text{ cm}^3} = 0.122 \text{ or } 12.2\%$$

1c) Calculate the specific retention using Equation 12 of this book.

$$S_r = \frac{V_r}{V_T}$$

where:

S_r = specific retention (dimensionless)

V_r = volume of water retained against gravity after drainage ceases (L^3)

V_T = volume of sample (L^3)

Recognizing that water weight in grams is equivalent to volume in cm^3 because 1g of water is 1 cm^3 use water weight where water volume is needed, so the volume of water retained in the sample is the total water in the sample (i.e., saturated weight in grams minus the dry weight in grams) minus the weight of water drained:

$$S_r = \frac{(saturated\ weight - dry\ weight - water\ drained) \text{ as volume}}{V_T}$$

$$S_r = \frac{236.6\ g - 222.0\ g - 12.2\ g}{100\ cm^3} = \frac{2.4\ g}{100\ cm^3} = 0.024 \text{ or } 2.4\%$$

$$S_r = 0.024 \text{ or } 2.4\%$$

Check that, as in Equation 13 of this book:

$$n_e = S_y + S_r$$

$$0.146 = 0.122 + 0.024 = yes\ 0.146$$

1d) Evaluate whether the resulting particle density is reasonable using Equation 3 of this book.

$$\rho_b = (1 - n) \rho_p + n \rho_f$$

where:

ρ_b = bulk density (M/L^3)

n = total porosity (dimensionless)

ρ_p = particle density (M/L^3)

ρ_f = fluid density (M/L^3)

Rearrange to solve for particle density:

$$\rho_p = \frac{\rho_b - n \rho_f}{(1 - n)}$$

From the laboratory data:

ρ_b = saturated weight over total volume ($236.6\ g / 100\ cm^3$) = $2.37\ g/cm^3$

n = assume effective porosity is total porosity = 0.146

$$\rho_f = 1 \text{ g/cm}^3$$

Substitute and solve for particle density:

$$\rho_p = \frac{\frac{2.37\text{g}}{\text{cm}^3} - 0.146 \frac{\text{1g}}{\text{cm}^3}}{(1 - 0.146)} = 2.6 \frac{\text{g}}{\text{cm}^3}$$

Yes, this is a reasonable particle density for soil. Soil is generally a mix of quartz, feldspars and clays and this particle density fall within the range of those materials, being less than quartz (2.67 g/cm^3), greater than feldspar (2.56 g/cm^3), and typical of clay densities (2.6 g/cm^3).

1e) Calculate the void ratio using Equation 8 of this book, where e is the void ratio.

$$n = \frac{e}{1 + e}$$

Rearranging to solve for e:

$$\begin{aligned} n(1 + e) &= e \\ n + ne &= e \\ n = e - ne &= (1 - n)e \\ e &= \frac{n}{1 - n} \\ e &= \frac{n}{1 - n} = \frac{0.146}{1 - 0.146} = 0.17 \end{aligned}$$

1f) Calculate the initial moisture content of the sample before it was dried using Equation 9 of this book.

$$\theta = \frac{V_W}{V_T}$$

where:

θ = moisture content (dimensionless)

V_W = volume of water in the pore space (L^3)

Recognizing that water weight in grams is equivalent to volume in cm^3 because 1g of water is 1 cm^3 use water weight where water volume is needed, so the initial volume of water in the sample is saturated sample weight minus the dry weight:

$$\begin{aligned} \theta &= \frac{V_W}{V_T} = \frac{(\text{initial sample weight} - \text{dry sample weight}) \text{ as volume}}{10 \text{ cm}^3} \\ \theta &= \frac{V_W}{V_T} = \frac{(227.1 \text{ cm}^3 - 222.0 \text{ cm}^3)}{100 \text{ cm}^3} = \frac{0.51 \text{ cm}^3}{100 \text{ cm}^3} \\ \theta &= 0.051 \text{ or } 5.1\% \end{aligned}$$

g) Calculate the initial degree of saturation using Equation 10 of this book.

$$\text{Degree of Saturation} = \frac{\theta}{n_e}$$

$$\text{Degree of Saturation} = \frac{0.051}{0.146} = 0.35 \text{ or } 35\%$$

[Return to Exercise 1↑](#)

[Return to where text links to Exercise 1↑](#)

Solution to Exercise 2

2) Show that $n = e/(1 + e)$, where n is porosity and e is the void ratio.

Porosity is defined by Equation 6 of this book. And, when the effective porosity equals the interconnected porosity then $V_I = V_v$.

$$n_e = \frac{V_I}{V_T} = \frac{V_V}{V_T} = n$$

Void Ratio is defined by Equation 7 of this book.

$$e = \frac{V_V}{V_S}$$

The total volume is the sum of the solid and the void volume.

$$V_T = V_V + V_S$$

Using the three relationships we can show:

$$\begin{aligned} n &= \frac{V_V}{V_V + V_S} \\ \frac{1}{n} &= \frac{V_V + V_S}{V_V} = 1 + \frac{V_S}{V_V} = 1 + \frac{1}{e} \\ \frac{1}{n} &= \frac{e + 1}{e} \\ n &= \frac{e}{e + 1} \end{aligned}$$

This matches Equation 8 of this book.

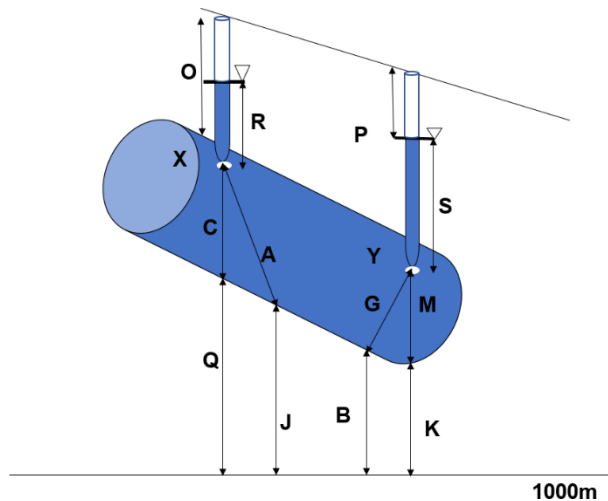
$$n = \frac{e}{1 + e}$$

[Return to Exercise 2↑](#)

[Return to where text links to Exercise 2↑](#)

Solution to Exercise 3

- 10) Hydraulic head controls the flow of groundwater. A sand filled column is set up as shown in the accompanying figure using a datum of 1000 m. If O=9 cm, K=5 cm, P=5 cm, S=12 cm, A=12 cm, G=5 cm, R=4 cm, M=4 cm, B=7 cm, J=9 cm, Q=15 cm, C=6 cm, answer the lettered items below. To answer b through d write the answer first as the letters for the relevant line segments, and then as the total value, e.g., for G+M write, $5 \text{ cm} + 4 \text{ cm} = 9 \text{ cm}$.



There are many more arrows and letters than needed to answer these questions.

- 10a) Which way is the water flowing?

Using the horizontal datum and the total elevation of the two water levels in the piezometers, the water is flowing from left to right as the head (as measured from the datum) is higher in the left piezometer than the right piezometer.

- 10b) What is the total head at the white mark labeled X relative to the 1000 m datum?

The total head at X is the elevation head ($Q+C$) plus the pressure head, R , $Q+C+R = 9 \text{ cm} + 6 \text{ cm} + 4 \text{ cm} = 19 \text{ cm}$ above the datum of 1000 m.

- 10c) What is the elevation head at the white mark labeled Y relative to the 1000 m datum?

The elevation head at Y is $(K+M) = 5 \text{ cm} + 4 \text{ cm} = 9 \text{ cm}$ above the 1000 m datum.

- 10d) What is the pressure head at the white mark labeled X?

The pressure head at X is R , $R = 4 \text{ cm}$

[Return to Exercise 3↑](#)

[Return to where text links to Exercise 3↑](#)

Solution to Exercise 4

- 3) Rank the materials from the sediment with the largest value (1) to the material with the smallest value (3) for hydraulic conductivity, K , specific yield, S_y , and porosity n .

	K	S_y	n
Silty Sand	2	2	2
Clay	3	3	1
Equally mixed sand and gravel	1	1	3

Estimation of these orders requires a number of assumptions and depending on one's thinking slight differences in ordering are acceptable.

For hydraulic conductivity see Figure 32 of this book, the order is fairly clear.

For specific yield see Table 3 of this book. Sand infilling the pores of the gravel will decrease its hydraulic conductivity compared to either sand or gravel, decrease its porosity and decrease its specific yield. Also, the materials have a wide range of values. Consequently, the proper ordering is not entirely clear.

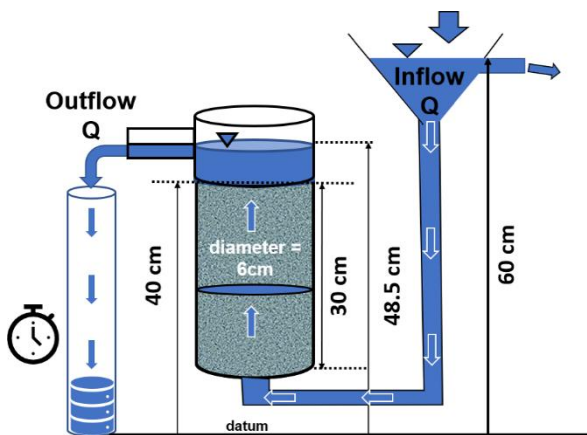
For porosity see Tables 1 and 2 in this book.

[Return to Exercise 4](#) ↑

[Return to where text links to Exercise 4](#) ↑

Solution to Exercise 5

5) A factory is disposing of hot waste water by injecting it into a 1000 m deep well that penetrates a confined aquifer. The sandstone aquifer contains water at 35°C, a similar temperature as the waste water. A regulator wanted the company to model how far the contaminated water would travel in the aquifer over a 10-year period. Hydraulic conductivity values were sparse. They required the company to core part of the 50 m thick confined aquifer and determine a representative value of hydraulic conductivity. A portion of the core was placed in a constant head permeameter as illustrated in the accompanying figure.



5a) If an average of 34.0 ml/min was collected at the outlet, what is K in cm/s?

Hydraulic conductivity can be determined by rearranging Equation 15 of this book

$$Q = -K \frac{\Delta h}{\Delta L} A$$

where:

Q = volumetric flow rate (L^3/T)

K = hydraulic conductivity, is the proportionality constant reflecting the ease with which water flows through a material (L/T)

Δh = difference in hydraulic head between two measuring points (L)

ΔL = length between locations where hydraulic heads are measured (L)

$\frac{\Delta h}{\Delta L}$ = gradient of hydraulic head (dimensionless)

A = cross-sectional area of flow perpendicular to the direction of flow (L^2)

Rearranging:

$$K = -\frac{Q \Delta L}{A \Delta h}$$

$$K = -\frac{\frac{34 \text{ cm}^3}{\text{min}} 30 \text{ cm} \frac{1 \text{ min}}{60 \text{ s}}}{\frac{17 \text{ cm}^4}{\text{s}}} = \frac{17 \text{ cm}^4}{325 \text{ cm}^3} = 0.052 \frac{\text{cm}}{\text{s}}$$

5b) If the laboratory experiment was completed using 15°C water, what is the intrinsic permeability of the sandstone in cm²?

If the test was conducted at 15°C, the intrinsic permeability, k , of the sandstone in cm² can be calculated using Equation 31 of this book, using the relationships for the physical properties of water and temperature shown as Figure 28 of this book.

$$K = \frac{C d^2 g \rho}{\mu} = \frac{k g \rho}{\mu}$$

where:

k = intrinsic permeability (L²)

ρ = fluid density (M/L³)

g = gravitational constant (acceleration of gravity) (L/T²)

μ = dynamic viscosity (M/(LT))

rearranging:

$$k = \frac{K\mu}{g\rho} = \frac{0.052 \frac{\text{cm}}{\text{s}} 0.011 \frac{\text{g-cm}}{\text{s}}}{980 \frac{\text{cm}}{\text{s}^2} 0.998 \frac{\text{g}}{\text{cm}^3}} = 5.8 \times 10^{-7} \text{ cm}^2$$

5c) What is the hydraulic conductivity in cm/s of the sandstone if the water temperature is 35°C?

If the water temperature in the sandstone is 35°C, Equation 31 of this book can be used to calculate K of the sandstone at that temperature in cm/s, using the relationships for the physical properties of water and temperature shown as Figure 28 of this book.

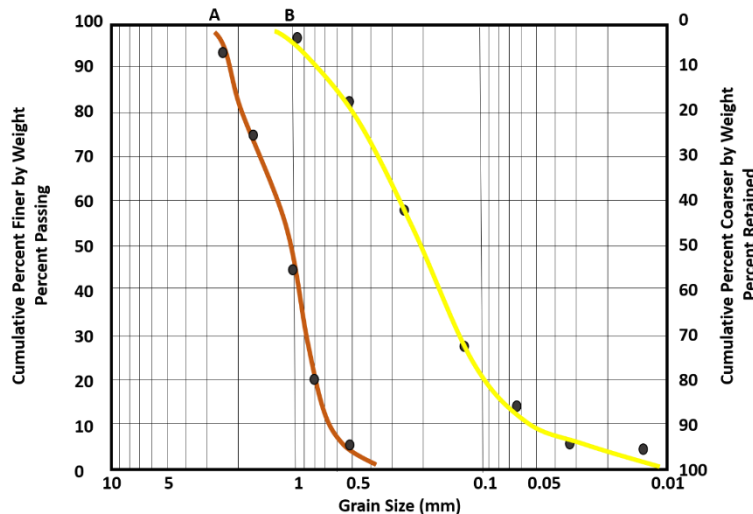
$$K = \frac{5.8 \times 10^{-7} \text{ cm}^2 980 \frac{\text{cm}}{\text{s}^2} 0.994 \frac{\text{g}}{\text{cm}^3}}{0.007 \frac{\text{g-cm}}{\text{s}}} = \frac{0.08 \text{ cm}}{\text{s}}$$

[Return to Exercise 5↑](#)

[Return to where text links to Exercise 5↑](#)

Solution to Exercise 6

K can be estimated for unconsolidated samples using empirical equations. Grain size distribution data for Sample A, a coarse sand with a porosity of 0.26 (red line), and Sample B, a fine sand with a porosity of 0.3 (yellow line), are shown on the accompanying graph.

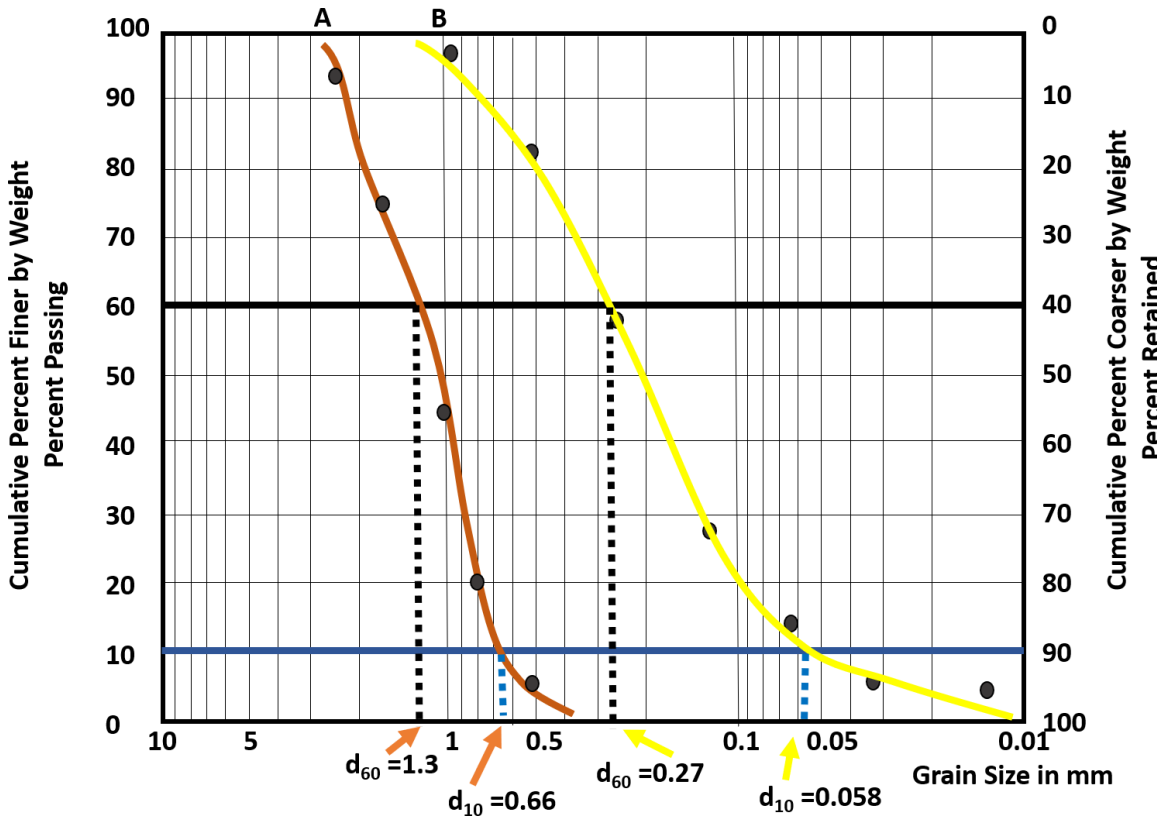


- a) By inspection of the graphs, which sample is likely to have the highest hydraulic conductivity? Why?

The text in section 4 of this book and material presented in Box 4 that describes empirical equations used to estimate K , reveal that K is directly proportional to the mean, median, effective or mean grain size (Equation Box 2-1) as defined in the discussion of grain size distribution analyses. For the data presented in the Figure above, each of these values is the largest in Sample A, coarse sand, as represented by the red line on the figure. The coarse sand would have the highest K value.

- b) Compute the uniformity coefficient for each sample. Compare and contrast the results. Do the coefficients appear to support your observations in part a?

The uniformity coefficient is defined in Box 2 of this book. The uniformity coefficient is equal to the diameter for cumulative 60% by weight finer-than (d_{60}) divided by the diameter for cumulative 10% by weight finer-than (d_{10}). The diameters are read from the graph as shown below.



$$\text{Uniformity Coefficient} = d_{60}/d_{10}$$

Uniformity Coefficient for the coarse sand: $1.3\text{mm}/0.66\text{mm} = 1.96$

Uniformity Coefficient for the fine sand: $0.27\text{mm}/0.058\text{mm} = 4.6$

Yes, these coefficients support the observation that the K would be highest for the Sample A with the larger grain sizes and the lower uniformity coefficient (1 = totally uniform sample). The slope of Sample A is closer to a vertical line which means it is more uniform than Sample B which has a gentler slope.

c) Using the Hazen approximation and Slichter method, estimate K in cm/s.

Computing first using Hazen and then Slichter:

First by Hazen:

The Hazen approximation equation is presented in Equation Box 4-9 in Box 4 of this book.

$$K = \frac{C d_{10}^2}{\text{cm s}}$$

where:

K = estimated hydraulic conductivity in centimeters per second

d_{10} = effective grain size in centimeters (d_{10} finer-than, d_{90} retained)

C = dimensionless coefficient defined as follows:

Material	C
Very fine sand, poorly sorted	40-80
Fine sand with appreciable fines	40-80
Medium sand, well sorted	80-120
Coarse sand, poorly sorted	80-120
Coarse sand, well sorted, clean	120-150

For Sample A, the coarse sand, the d_{10} in cm is $0.66 \text{ mm} \times 1 \text{ cm}/10\text{mm} = 0.066 \text{ cm}$.

The value of C is based on a qualitative description and as the sample is considered fairly uniform, uniformity coefficient of 1.96, is represented by a range of Hazen values of 120 to 150, coarse sand well sorted.

$$K = 120 (0.066 \text{ cm})^2/(\text{cm s}) = 0.52 \text{ cm/s} \text{ and } K = 150 ((0.066\text{cm})^2/(\text{cm s}) = 0.65 \text{ cm/s}$$

Using the Hazen method, the range of K values for Sample A are 0.52 cm/s to 0.65 cm/s

For Sample B, the fine sand, the d_{10} is $0.058 \text{ mm} \times 1 \text{ cm}/10 \text{ mm} = 0.0058 \text{ cm}$

The uniformity coefficient for the fine sand shows it is not very uniform so the Hazen coefficients for the are 40 to 80, fine sand with appreciable fines.

$$K = 40 (0.0058)^2/(\text{cm s}) = 0.001 \text{ cm/s, and } K = 80(0.0058)^2/(\text{cm s}) = 0.003 \text{ cm/s}$$

Using the Hazen method, the range of K values for Sample B is 0.001cm/s to 0.003 cm/s.

Next, estimates of K using the Slichter Method using Equation Box 4-8 in Box 4 of this book.

$$K = 10.22 \frac{\text{gram}}{\text{cm}^2 \text{s}^2} \frac{d^2}{\mu C_S}$$

where:

K = estimated hydraulic conductivity in centimeters per second

d = mean grain diameter in centimeters

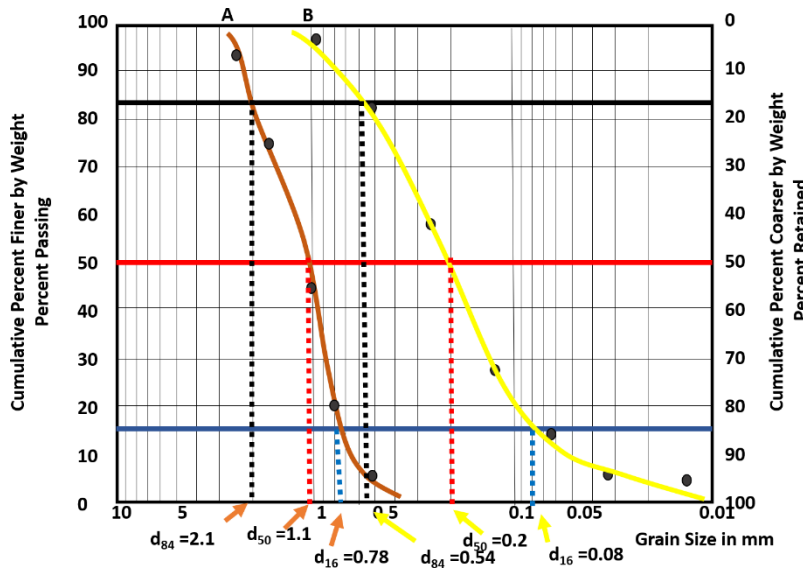
μ = dynamic viscosity at a given temperature in gram/cm s

C_S = a constant for a given porosity based on the following non-linear relationship: ($n=26\% C_S=84.3$; $n=36\% C_S=28.8$; $n=47\% C_S=11.8$)

To compute the mean grain diameter Equation Box 2-7 found in Box 2 of this book must be applied.

$$\text{Mean phi size} = \left(\frac{\phi_{16} + \phi_{50} + \phi_{84}}{3} \right)$$

The d_{16} , d_{50} and d_{84} are taken from the grain size distribution curve (in mm) for both samples. Then they are converted to Phi units (dimensionless) = $\ln(x)/\ln(2)$ where x is the d_{16} , d_{50} and d_{84} values.



Sample A $d_{84} = 2.1$ mm, $d_{50} = 1.1$ mm, $d_{16} = 0.78$ mm

Phi units $\phi_{84} \ln(2.1)/\ln(2) = 1.07$, $\phi_{50} \ln(1.1)/\ln(2) = 0.14$, $\phi_{16} \ln(0.78)/\ln(2) = -0.36$

Mean grain diameter = $(1.07 + 0.14 + (-0.36))/3 = 0.28$ phi units, needs to be converted back to mm:

Using $\phi \ln(2) = \ln(x)$ and $\ln(x) = \text{value}$, $x = e^{\text{value}}$

$0.28 (\ln 2) = 0.19 = \ln(x)$ and $x = e^{0.19} = 1.21$ mm

Change mean grain diameter of A to cm, 1.2 mm \times 1 cm/ 10 mm = 0.121 cm

Sample B $d_{84} = 0.54$ mm, $d_{50} = 0.2$ mm, $d_{16} = 0.08$ mm

Phi units $\phi_{84} \frac{\ln(0.54)}{\ln(2)} = -0.89$, $\phi_{50} \frac{\ln(0.2)}{\ln(2)} = -2.32$, $\phi_{16} \ln(0.08)/\ln(2) = -3.64$

Mean grain diameter = $(-0.89 - 2.32 - 3.64)/3 = -2.28$, convert back to mm

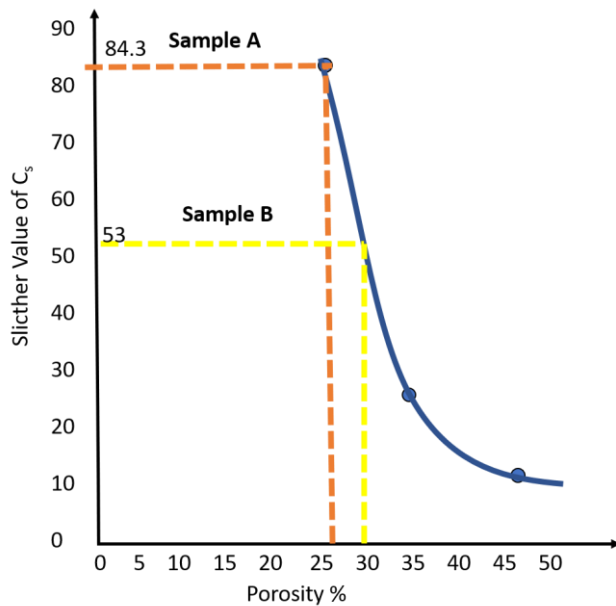
Using $\phi \ln(2) = \ln(x)$ and $\ln(x) = \text{value}$, $x = e^{\text{value}}$

$-2.28 (\ln 2) = -1.58 = \ln(x)$ and $x = e^{-1.58} = 0.2$ mm

Change mean grain diameter of B to cm, 0.2 mm (1 cm / 10 mm) = 0.02 cm

K by Slichter method:

First, determine the coefficient based on the porosity relationship defined by Slichter by plotting porosity values on the graph of Figure Box 4-5 in Box 4 of this book.



Sample A: $n = 0.26$ $C_s = 84.3$, this porosity happens to match the original data Slichter provided.

Sample B: $n = 0.30$ $C_s = 53$, from the graph.

The water temperature is 15°C so the dynamic viscosity needed for the calculation can be determined from Figure 28 of this book. The value is 1.20 millipascal-second = 0.012 gram/(cm s).

The K values are:

Sample A

$$K = (10.22 \text{ gram}/(\text{cm}^2\text{s}^2)) (0.12\text{cm})^2 / ((0.012\text{gram}/(\text{cm s})) (84.3)) = 0.14 \text{ cm/s}$$

Sample B

$$K = (10.22 \text{ gram}/(\text{cm}^2\text{s}^2)) (0.02\text{cm})^2 / ((0.012\text{gram}/(\text{cm s})) (53)) = 0.006 \text{ cm/s}$$

Vukovic and Soro (1992) noted the graph relating C_s and porosity can be represented by $1/n^{3.287}$ (with an error +/- 5%). They also proposed that the mean grain size be replaced by the effective grain size (d_{10} finer than). With a porosity of 26% for sample A, C_s would equal 83.7, and C_s for sample B with a porosity of 30% would be 52.3. Effective grain sizes are 0.07 cm for Sample A and 0.006 cm for sample B. Given these values of C_s , K values are as follows:

Sample A

$$K = (10.22 \text{ gram}/(\text{cm}^2\text{s}^2)) (0.07\text{cm})^2 / ((0.012 \text{ gram}/(\text{cm s})) (83.7)) = 0.05 \text{ cm/s}$$

Sample B

$$K = (10.22 \text{ gram}/(\text{cm}^2\text{s}^2)) (0.006\text{cm})^2 / ((0.012 \text{ gram}/(\text{cm s})) (52.3)) = 0.0006 \text{ cm/s}$$

Vukovic and Soro (1992) modifications to Slichter resulted in lower K values for Sample A and Sample B because the mean grain size values were significantly larger than the effective grain sizes.

d) Are the K values computed in part 6c characteristic of sands? Do both methods produce similar values? Why or why not?

The computed K values for both methods are characteristic of the coarse and fine sands as indicated on Figure 32 of this book. From that figure, sand ranges from 1×10^{-6} cm/s to 1 cm/s. The values for sample A fall in the upper range and the values for Sample B fall in the middle of the range of K values.

The values derived from both methods are of a similar order of magnitude, Sample A on the order of 10^{-1} cm/s and sample B on the order of 10^{-3} cm/s. The two methods generate similar values with Hazen's method yielding higher coarse sand values and lower fine sand values than the empirical equation proposed by Slichter. When the d_{10} was used instead of the mean gain size in the Slichter method K values were lower than Hazen by 100 %. It is unclear why the Hazen and original Slichter methods did not produce values that were more similar. They both approached developing the empirical equations focusing on the grain size distribution and then developed coefficients that brought laboratory K values in line with their choice of distribution parameters and other factors such as sorting and porosity. In doing so, equations did not produce identical hydraulic conductivity values. However, this is expected as they use different approaches. The values are within the same order of magnitude which is sufficient. It is suggested the modification of using the d_{10} instead of the mean grain size in the Slichter method should not be used. When using the methods to characterize K , the average of Hazen values could be used for each sample (0.6 cm/s for A and 0.002 cm/s for B), the range of the calculated values could be reported as the lowest and highest value of K for each sample computed by both methods (0.14 to 0.65 cm/s for Sample A and 0.001 to 0.006 cm/s for Sample B).

[Return to Exercise 6↑](#)

[Return to where text links to Exercise 6↑](#)

Solution to Exercise 7

Storage in confined aquifers relies on squeezing water in and out of the saturated skeleton. Explain the effects on the effective stress and pore water pressure when water is pumped into a confined aquifer and the water level in tightly cased wells penetrating the aquifer rises 1 m.

The increase in head during the injection of water in a confined aquifer causes an increase in pore water pressure that results in a slight lifting/separation of the grains comprising the aquifer skeleton thus decreasing the stress between grains and slightly increasing the porosity.

[Return to Exercise 7↑](#)

[Return to where text links to Exercise 7↑](#)

Solution to Exercise 8

Show that the units of S_s are 1/L.

Using Equation 45 in this book

$$S_s = \rho g (\alpha + n_e \beta)$$

where:

S_s = specific storage (1/L)

α = compressibility of the aquifer solid structure ($T^2 L/M$)

n_e = effective porosity (dimensionless)

β = compressibility of water ($T^2 L/M$)

checking units:

$$S_s : \frac{M}{L^3} \frac{L}{T^2} \left(\frac{T^2 L}{M} + \frac{L^3}{L^3} \frac{T^2 L}{M} \right)$$

$$S_s : \frac{M}{L^{23}} \frac{L}{T^2} \left(\frac{T^2 L}{M} + \frac{L^3}{L^3} \frac{T^2 L}{M} \right)$$

$$S_s : \frac{M}{L^2 T^2} \left(\frac{T^2 L}{M} \right)$$

$$S_s : \frac{M}{L^{12} T^2} \left(\frac{T^2 L}{M} \right)$$

$$S_s : \frac{1}{L}$$

[Return to Exercise 8 ↑](#)

[Return to where text links to Exercise 8 ↑](#)

Solution to Exercise 9

A confined aquifer underlies a 10 km^2 area. The average water level in a number of wells penetrating the confined system rose 2.5 m from April through June. An overlying unconfined aquifer showed an average water table rise of 2.5 m over the same period of time.

Assume the storativity, S , for the confined system is 3.6×10^{-5} , and specific yield, S_y , is 0.12 for the unconfined system. How much water (in m^3) recharged each aquifer based on the responses of each potentiometric surface?

Unconfined aquifer

Applying Equation 48 in this book to compute the volume of water recharged:

$$\text{Volume of Unconfined Water for a change in head} = S_y A \Delta h$$

$$\text{Unconfined Volume} = 0.12 \cdot 10 \text{ km}^2 \frac{1,000,000 \text{ m}^2}{1 \text{ km}^2} \cdot 2.5 \text{ m} = 3 \times 10^6 \text{ m}^3$$

Confined aquifer

Applying Equation 50 in this book to compute the volume of water recharged:

$$\text{Volume of Confined Water for a change in head} = S A \Delta h$$

$$\text{Confined Volume} = 3.6 \times 10^{-5} \cdot 10 \text{ km}^2 \frac{1,000,000 \text{ m}^2}{1 \text{ km}^2} \cdot 2.5 \text{ m} = 900 \text{ m}^3$$

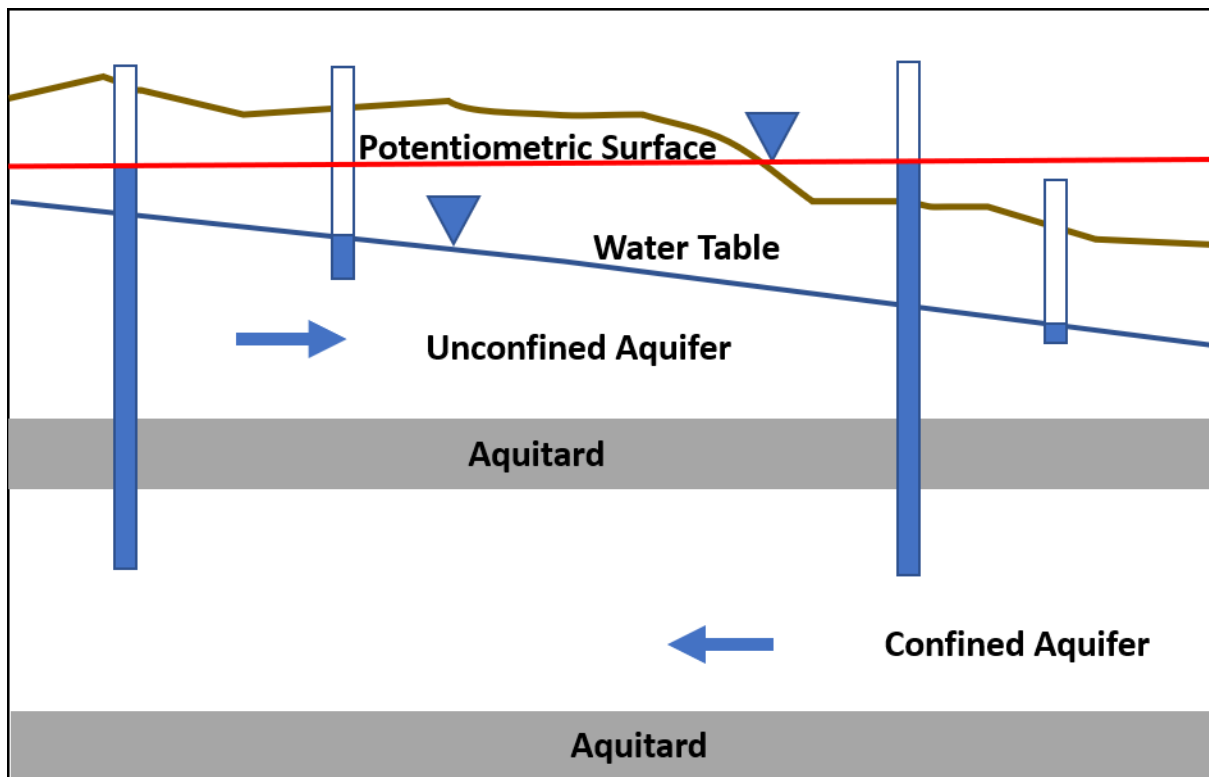
The unconfined aquifer received 3,333 times as much water as the confined aquifer.

[Return to Exercise 9 ↑](#)

[Return to where text links to Exercise 9 ↑](#)

Solution to Exercise 10

Draw and clearly label a cross section of a water table aquifer overlying a confined aquifer. Label the confining units as aquitards. Place two observation wells in each aquifer and show the water level in each of the wells so that groundwater flow is from the left to the right for the water table aquifer and from the right to the left for the confined aquifer. The illustration should suggest that leakage from the confined aquifer is upward into the unconfined aquifer. Show the corresponding water table and potentiometric surface positions.



This diagram meets the criteria set out in the problem. The flow in the unconfined aquifer is left to right and right to left in the confined system. The water table and potentiometric surface are labelled. The potentiometric surface is drawn higher than the water table suggesting the potential for upward flow of water from the confined aquifer to the unconfined system.

[Return to Exercise 10 ↑](#)

[Return to where text links to Exercise 10 ↑](#)

Solution to Exercise 11

A regional unconfined sand aquifer was developed during 1990. As a result of the extraction of water the water table dropped about 40 m over a 1 square km area. If the porosity, n , is 34% and the specific retention, S_r , is 12%, how much water (m^3) was withdrawn from the impacted area? How might this volume differ if the aquifer were a 100 m thick confined sand with water at a temperature of 8°C?

Calculate the volume by using Equation 48 of this book.

$$\text{Volume of Unconfined Water Drained} = S_y A \Delta h$$

where:

Volume = volume drained from an unconfined aquifer over an area, A , for a water table elevation change of Δh (L^3)

S_y = specific yield (dimensionless)

A = area over which the water table changes (L^2)

Δh = change in water table elevation (L)

S_y can be determined as $n_e - S_r$ as shown by Equation 13 of this book.

$$n_e = S_y + S_r$$

$$\text{Volume of Unconfined Water Drained} = (0.34 - 0.12) 1000\text{m} 1000\text{m} 40\text{m}$$

$$\text{Volume from Unconfined Aquifer} = 8,800,000 \text{ m}^3 = 8.8 \text{ million m}^3$$

To estimate the volume of water drained from a 100-meter-thick confined sand aquifer occupying an area of 1 square kilometer, Equation 50 of this book is applied.

First the confined storativity needs to be calculated by using Equation 49 of this book. The specific storage is calculated first (Equation 45 of this book). This requires an estimate of the aquifer compressibility from Table 4 and a density from Figure 28.

$$S_s = \rho g (\alpha + n_e \beta)$$

where:

S_s = specific storage ($1/\text{L}$)

α = compressibility of the aquifer solid structure ($\text{T}^2\text{L/M}$)

n_e = effective porosity (dimensionless)

β = compressibility of water ($\text{T}^2\text{L/M}$)

Using the compressibility value of $1 \times 10^{-8} \frac{\text{m}^2}{\text{kg m s}^2}$ obtained for sand and a density of $1000 \frac{\text{kg}}{\text{m}^3}$ for 8°C water, S_s is calculated as follows.

$$S_s = \left(1000 \frac{\text{kg}}{\text{m}^3}\right) \left(9.8 \frac{\text{m}}{\text{s}^2}\right) \left(1 \times 10^{-8} \frac{\text{m}^2}{\text{kg m s}^2} + (0.34) \left(4.4 \times 10^{-10} \frac{\text{m}^2}{\text{kg m s}^2}\right)\right)$$

$$S_s = \frac{1 \times 10^{-4}}{\text{m}}$$

Equation 49 of this book is used to determine storativity:

$$S_{\text{confined}} = S_s b = \left(\frac{1 \times 10^{-4}}{\text{m}}\right) 40\text{m} = 4 \times 10^{-3}$$

Equation 50 of this book determines the volume.

$$\text{Volume of Confined Water Drained} = SA\Delta h$$

$$\text{Volume of confined Water Drained} = 4 \times 10^{-3} \text{ } 1000\text{m } 1000\text{m } 40\text{m}$$

$$\text{Volume from Confined Aquifer} = 160,000\text{m}^3$$

[Return to Exercise 11](#) ↑

[Return to where text links to Exercise 11](#) ↑

Solution to Exercise 12

Write the governing equation that describes two-dimensional (x and y), steady-state flow in a confined anisotropic and homogenous aquifer.

This can be generated using Equation 68 in this book.

$$S_s \frac{\partial h}{\partial t} = K_x \frac{\partial^2 h}{\partial x^2} + K_y \frac{\partial^2 h}{\partial y^2} + K_z \frac{\partial^2 h}{\partial z^2}$$

This equation describes three-dimensional flow in a confined aquifer under transient, anisotropic and homogenous conditions. To generate the equation for steady state in two dimensions, set the left-hand side to zero and eliminate the z term.

$$0 = K_x \frac{\partial^2 h}{\partial x^2} + K_y \frac{\partial^2 h}{\partial y^2}$$

[Return to Exercise 12](#) ↑

[Return to where text links to Exercise 12](#) ↑

Solution to Exercise 13

What conditions does the following governing equation represent? Explain the features of the terms of the equation that indicate each condition.

$$S_s \frac{\partial h}{\partial t} = \frac{\partial}{\partial x} \left(K_x \frac{\partial h}{\partial x} \right) + \frac{\partial}{\partial y} \left(K_y \frac{\partial h}{\partial y} \right) + \frac{\partial}{\partial z} \left(K_z \frac{\partial h}{\partial z} \right)$$

This is Equation 67 of this book. It represents transient, confined, groundwater flow where conditions are anisotropic and heterogeneous. The K values are within the differential on the right-hand side of the equation signifying they are variables and can be different values everywhere in the domain (x, y, z) , thus the equation is applicable to a heterogeneous and anisotropic system. The left-hand side has a time derivative and thus, this equation represents transient conditions, that is, the heads change with time and water can go into, or come out of, storage. If the left-hand side was set to 0, the equation would represent steady state conditions. If the equation represented unconfined conditions, there would be an h inside the derivative, and S_y would be used instead of S_s as follows (as shown in Equation 74 of this book):

$$S_y \frac{\partial h}{\partial t} = \frac{\partial}{\partial x} K_x \left(h \frac{\partial h}{\partial x} \right) + \frac{\partial}{\partial y} K_y \left(h \frac{\partial h}{\partial y} \right)$$

[Return to Exercise 13 ↑](#)

[Return to where text links to Exercise 13 ↑](#)

Solution to Exercise 14

Ten wells are located in a valley setting. Glacial material underlies the land surface and a confined sandstone aquifer underlies the region. All wells shown in the accompanying diagram tap the confined aquifer. DATA: All water levels (WL) are measured depths below the top of casing (TOC) elevation. TD is the total well depth below land surface. The head measurement is at the bottom of each well.

Well A TD 150 m, TOC 1105 m, WL 57 m **Well B** TD 160 m, TOC 1100 m, WL 39 m

Well C TD 170 m, TOC 1108 m, WL 76 m **Well D** TD 150 m, TOC 1100 m, WL 59 m

Well E TD 180 m, TOC 1098 m, WL 67 m **Well F** TD 160 m, TOC 1090 m, WL 57 m

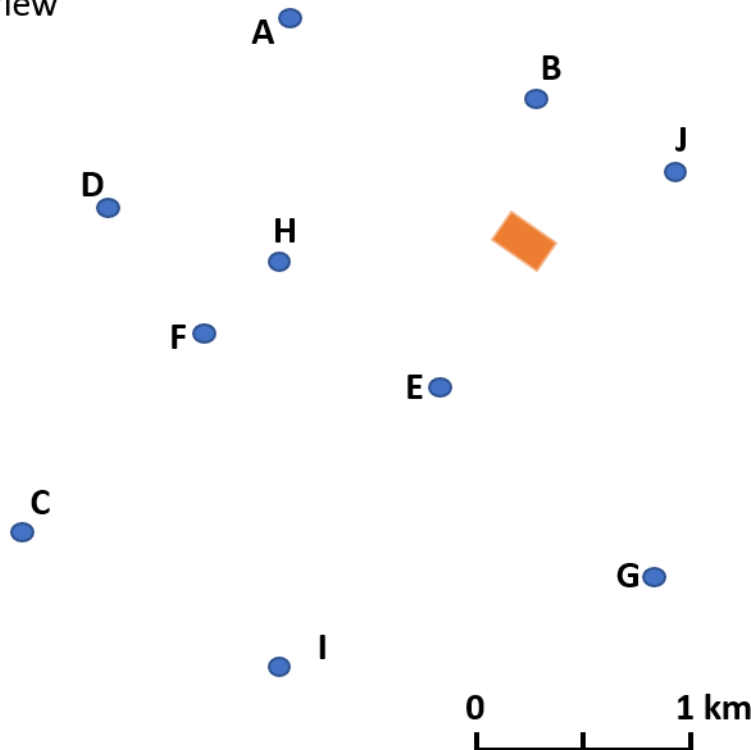
Well G TD 180 m, TOC 1080 m, WL 53 m **Well H** TD 170 m, TOC 1079 m, WL 41 m

Well I TD 180 m, TOC 1070 m, WL 50 m **Well J** TD 170 m, TOC 1100 m, WL 41 m

a) Create a potentiometric surface map view.

It is best to copy this map view figure of the confined aquifer well locations, plot the head values, contour the head values to create equipotential lines, and draw flow lines perpendicular to the equipotential lines. The heads at each well are computed by taking the measuring point elevation, TOC and subtracting the depth to water (WL). This head value is then plotted at the mapped location of well (x,y). The total well depth information is not used in the head calculation. As the head is the elevation of the water level in the well. The value of having the TD would be to confirm that the well is monitoring the confined sandstone aquifer.

Map View



Calculate head values and plot on map:

Well A TOC 1105 m - WL 57 m = 1048 m **Well B** TOC 1100 m - WL 39 m = 1061 m

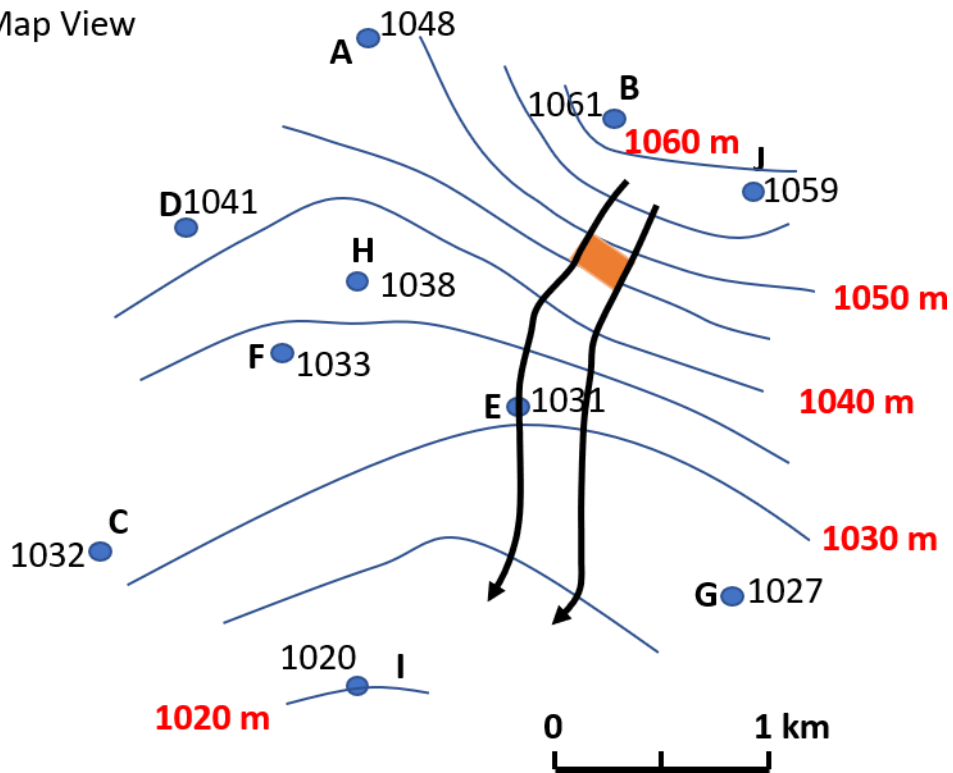
Well C TOC 1108 m - WL 76 m = 1032 m **Well D** TOC 1100 m - WL 59 m = 1041 m

Well E TOC 1098 m - WL 67 m = 1031 m **Well F** TOC 1090 m - WL 57 m = 1033 m

Well G TOC 1080 m - WL 53 m = 1027 m **Well H** TOC 1079 m - WL 41 m = 1038 m

Well I TOC 1070 m - WL 50 m = 1020 m **Well J** TOC 1100 m - WL 41 m = 1059 m

Map View



- b) If the confined aquifer water at the orange rectangle became contaminated with dissolved nitrate from downward leakage of water in the overlying unconfined aquifer, would any other monitoring wells become contaminated under steady state flow conditions? Construct equipotential lines and flow lines to support your answer.

The position of the equipotential lines will be slightly different depending on whether they are hand drawn (and these will differ between individuals) or a computer code is applied. The lines shown here were drawn by hand by estimating their positions between data points by approximate linear interpolation. The flow lines encompassing the orange contaminated groundwater area show flow would be to the southwest-south. In this diagram well E would be impacted. Depending on your results, E may or may not be in the direct flow path.

[Return to Exercise 14 ↑](#)

[Return to where text links to Exercise 14 ↑](#)

Solution to Exercise 15

A map view of a heterogeneous and isotropic field site containing a complex confined aquifer system is presented in the accompanying figure. If a contaminant is released at A and each zone of hydraulic conductivity is isotropic and homogeneous:

- a) Map the flowline from A to the row of houses. Would wells at any of the houses be impacted?

A copy of the base map is made and drawn on below. To determine if any of the houses (1-5) would be impacted by the flow from A, a flow line crossing equipotential lines at right angles (isotropic and homogeneous) is constructed from A to the north border of the zone with the lower K . At the point of intersection, a black line bisector is constructed at right angles to the boundary and the angle the flow line makes with the boundary is measured (with a protractor). As the flow will be refracted into the lower K zone the tangent law needs to be applied, Equation 91 of this book. Figure 71 illustrates the application of this principle.

$$\frac{K_1}{K_2} = \frac{\tan \theta_1}{\tan \theta_2}$$

For this problem, the flowline from A makes an angle of 40° with the boundary. With the given hydraulic conductivity values the refraction angle of the flow line is computed.

$$\tan 40^\circ / \tan \theta_2 = 10 \text{ m/d} / 1 \text{ m/d}$$

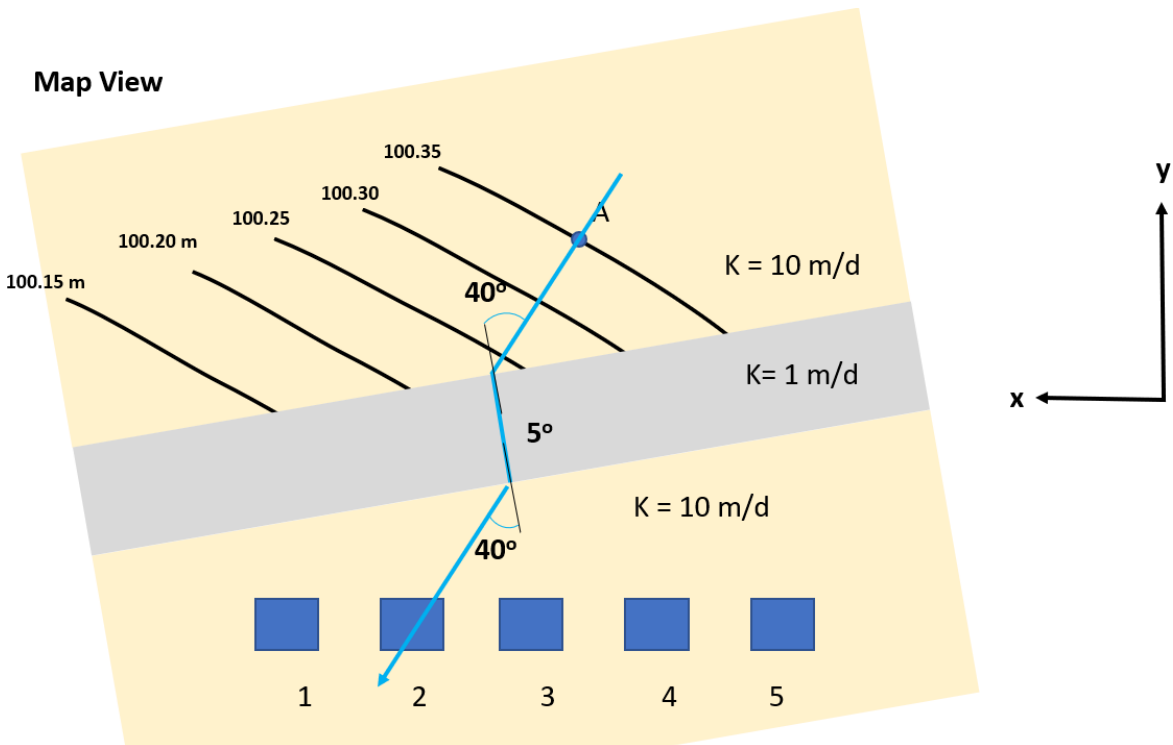
$$\text{Re-arranging } \tan \theta_2 = \tan 40^\circ / (10 \text{ m/d} / 1 \text{ m/d}) = 0.084$$

$$\arctan 0.084 = 4.8^\circ \text{ or about } 5^\circ$$

A 5° angle is constructed that represents the flow path through the low K zone.

Where the flow line intersects the southern boundary, a perpendicular bisector is constructed and since the K in the third zone is the same as the first zone, 10 m/d , the flow refracts at an angle of 40° .

Results show that the well at house 2 would be impacted by the contamination that entered the aquifer at A.

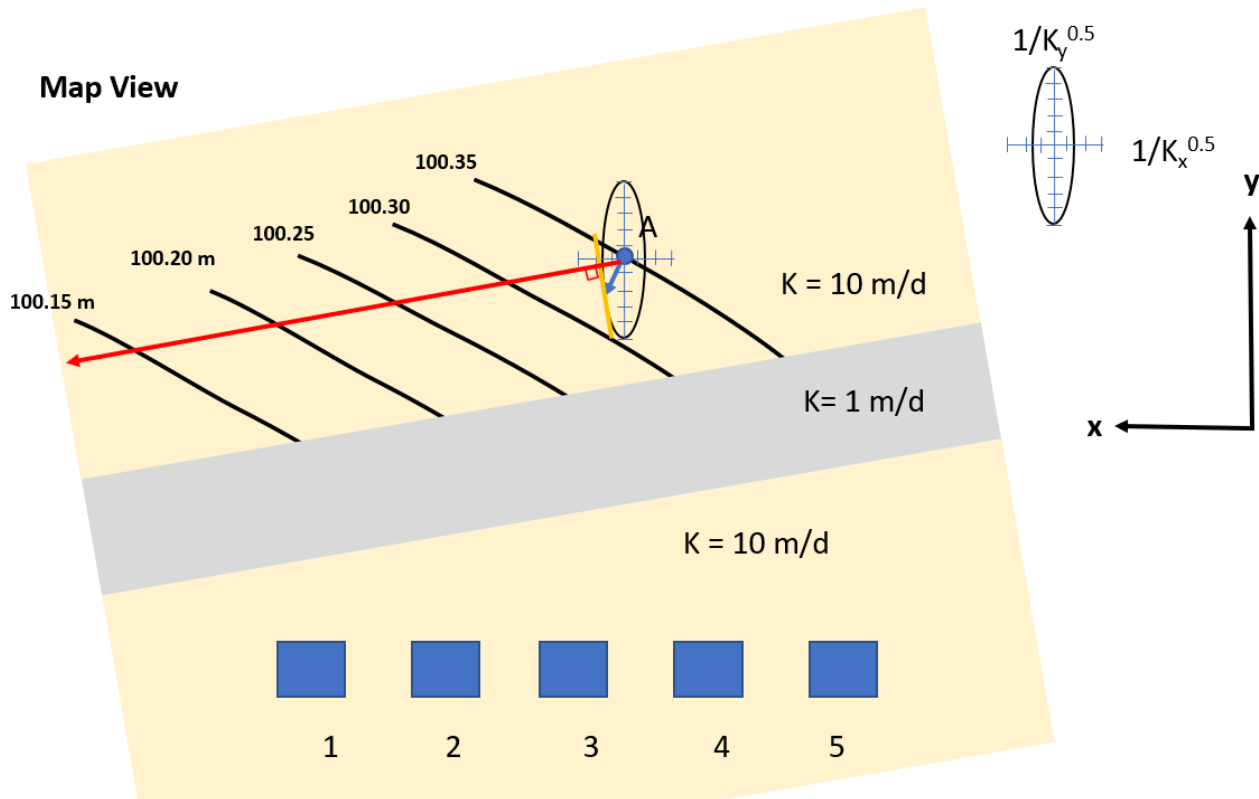


b) Now assume that only the northern portion of the aquifer is anisotropic $K_x = 10 \text{ m/d}$ and $K_y = 1 \text{ m/d}$. Starting at A construct the anisotropic flow path and show which, if any, of the houses (blue rectangles) will be affected by this new flow path. Present your construction and show how you determined the flow path in the northern portion of the aquifer.

This part of the problem asks that if A is located in an anisotropic groundwater system, which house might be impacted by the flow from A. The anisotropy of the area where A is found is $K_x = 10 \text{ m/d}$ and $K_y = 1 \text{ m/d}$. The flow line from A can be constructed using the inverse hydraulic conductivity ellipse method illustrated in Figure 69 of this book.

An inverse hydraulic conductivity ellipse is created by using a piece graph paper and plotting an ellipse with an x axis of $1/K_x^{0.5}$ and y axis equal to $1/K_y^{0.5}$. The ellipse size can be any size; however, it is kept at a manageable size for the base map presented with this problem. An example is presented on the solution below. Following the instructions in Figure 69 and keeping the axis parallel to x and y of the base map, the ellipse is placed on location A and a flow line for the anisotropic conditions is plotted (red arrow).

The anisotropy causes the flow to be deflected in the K_x direction. In this problem the flow from A does not reach the houses south of the low K zone.



[Return to Exercise 15↑](#)

[Return to where text links to Exercise 15↑](#)

Solution to Exercise 16

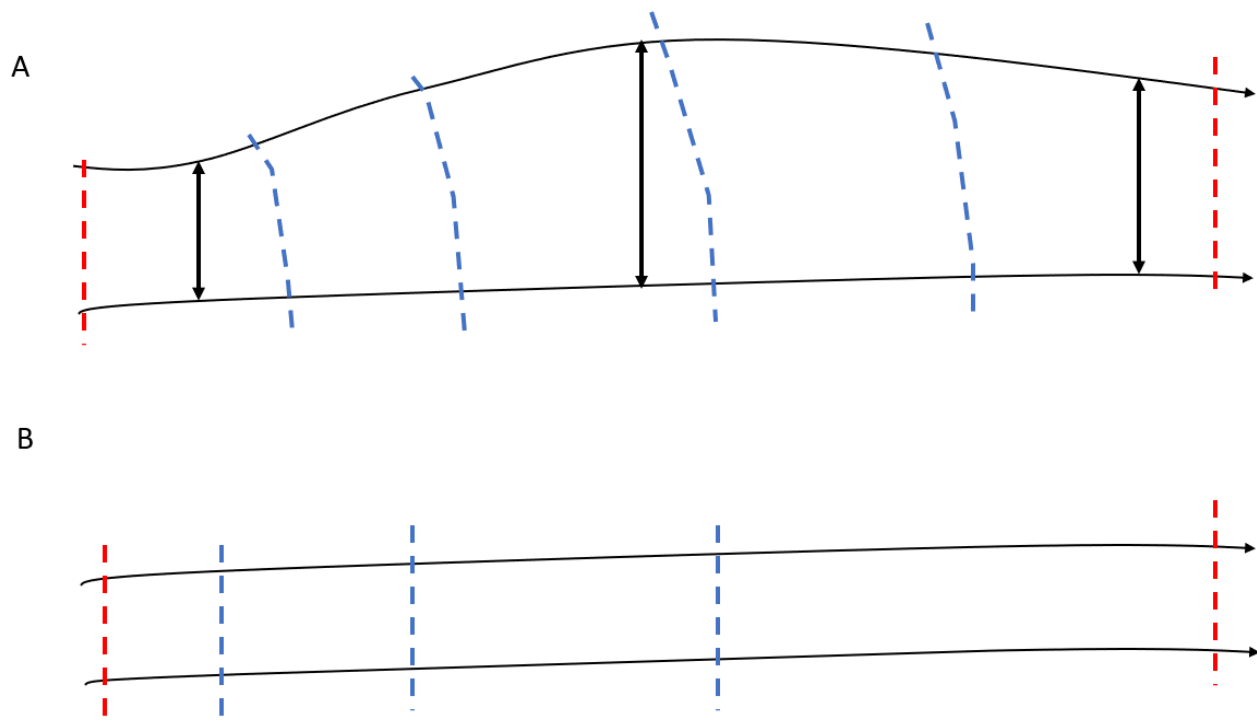
In the accompanying figure flow lines (black lines) form two flow tubes, A and B. If conditions are isotropic and homogeneous and flow is at steady state, create equipotential lines under the following conditions.

a) For A, assume the aquifer thickness and hydraulic conductivities are constant.

The volumetric flow rate in flow tube A must be constant, so the increasing distance between the flow lines (indicated by the black arrows) in a system where the aquifer thickness and hydraulic conductivity is constant indicates the gradient needs to decrease (equipotential lines space further apart).

b) For B, assume the thickness of the aquifer increases from left to right while all other conditions remain constant.

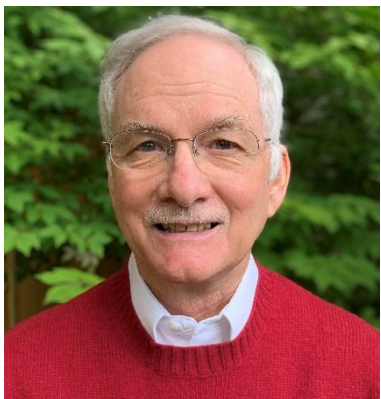
The volumetric flow rate in flow tube B must be constant, if the thickness of the aquifer is increasing from left to right, the flow area is increasing to the right. As a result, the gradients must decrease to the right, requiring larger distance between equipotential lines.



[Return to Exercise 16](#) ↑

[Return to where text links to Exercise 16](#) ↑

About the Authors



William W. Woessner is a University of Montana System Emeritus Regents' Professor of Hydrogeology at the University of Montana. He taught introductory and graduate courses in the hydrogeological sciences; is the Past Acting Director of the Center for Riverine Science and Stream Re-naturalization, and President of Woessner Hydrologic. With over 40 years of experience he has mentored over 60 graduate students, many of whom have founded or work for environmental consulting firms;

consulted for local, state and federal agencies, corporations, and non-profits applying field and modeling approaches to solve groundwater development and management issues including production well design and installation, and water use; propose resolutions to groundwater contamination events, and identify how surface water-groundwater interactions effect ecological systems. Dr. Woessner is the coauthor of two editions of "Applied Groundwater Modeling: Simulation of Flow and Advective Transport"; a 2011 Fulbright Scholar-NAWI Austria; is a Fellow of the Geological Society of America, the Birdsall Dreiss Lecturer in 2005, and the 2020 O. E. Meinzer Awardee; a Fellow and Life Member of the National Groundwater Association (NGWA) and was awarded the John Hem Excellence in Science and Engineering Award in 2008.



Eileen Poeter is an Emeritus Professor of Geological Engineering at Colorado School of Mines, where she taught groundwater courses and advised more than 40 graduate students who worked with her on groundwater system investigations and modeling research projects. She is also Past Director of the Integrated Groundwater Modeling Center; and retired President of Poeter Engineering. With 40 years of experience modeling groundwater systems, she has consulted to attorneys, industries, engineering companies, government agencies, research labs, and citizen

groups on groundwater modeling projects for: aquifer storage and recovery; slurry wall performance; drainage at proposed nuclear power plant facilities; regional groundwater management, large-scale regional pumping, dam seepage, contaminant migration, impacts of dewatering, and stream-aquifer interaction. Dr. Poeter is an author of groundwater modeling software including evaluation of model sensitivity, assessment of data needs, model calibration, selection and ranking of models, and evaluation of predictive uncertainty. She was the National Groundwater Association (NGWA) Darcy Lecturer in 2006 and received their M. King Hubbert award in 2017 as well as being an NGWA Fellow and Life Member.

Please consider signing up to the Groundwater Project mailing list and stay informed about new book releases, events and ways to participate in the Groundwater Project. When you sign up to our email list it helps us build a global groundwater community. [Sign-up ↗](#).



Modifications from original release

General changes:

A number of minor typographical errors were corrected such as deletion of extra blank spaces.

Occurrences of “elemental” were changed to “elementary.”

Some figure captions with sub parts a) b), and so on, were adjusted with respect to punctuation and wording to be consistent with current GW-Project formatting. These include the following Figures: 3, 5, 6, 7, 8, 9, 11, 12, 13, 15, 17, 18, 19, 20, 29, 30, 33, 34, 54, 67, 69, 77, 80, 83, Box 4-1, Box 6-2.

A few figure captions had slightly different or more significant wording changes of their captions, including the following Figures: 4, 13, 21, 35, 48, 49, 51, 53, 69, 70, 89, Box 4-1, Box 5-1, Box 7-1.

Where units were “/sec” or “/day”, they were changed to “/s” and “/d”.

Units that were in italics were changed to not italics.

Equation variables that were not in italics were changed to italics.

References to (Woessner and Poeter, 2020, gw-project.org) were removed to be consistent with the latest GW-Project formatting. This citation was removed from the reference list, rendering the book one page shorter than the original release.

Where “media” was used in a singular sense it was changed to “medium.”

Where “e.g.” was not followed by a comma, a comma was added “e.g.,”.

Occurrences of “principle” were changed to “principal” where the usage of principal to mean “main” applied.

Occurrences of “plain” were changed to “plane” where the usage of “plain” meant a flat geometric surface.

Minor changes to formatting of reference list to be consistent with GW-Project formats.

Adjustments were made to the size of a few figures prevent captions from spanning a page break.

Table of Contents was updated to ensure page numbers are correct given these revisions.

Specific changes:

page i, ii, Removed small caps font.

page iii, Removed keywords.

page iii, Added link to Groundwater Project email sign-up.

page iii, Added citation information.

page iii, Changed spelling of Steven Moran to Stephen Moran.

page v-vii, Table of Contents updated.

page 7, Figure 4 caption, for V#, numbers were changed to subscripts.

page 14, Paragraph 2, line 2, "are" changed to "is."

page 15, Table 2. Title changed to "Total and Effective Porosity".

page 17, Middle of first paragraph. Changed "wheel barrow" to "wheelbarrow".

page 18, Figure 11 caption. Added ending period.

page 22, Figure 13 caption. Added ending period.

page 24, Section 3.7 heading. Capitalized "Porosity".

page 26, Line preceding Equation 14. Changed "a" to "as".

page 26, Definition of Δh below Equation 14. Added "where h_2 is head at a location beyond the location of h_1 in the direction of flow".

page 26, Added paragraph after Equation 14. "The negative sign is included in Equation 14 because the volumetric flow rate, Q , is positive in the direction of flow under a negative change in head (i.e., head decreases in the direction of flow)."

page 27, Second full sentence of first paragraph. Deleted words as shown by strikeouts: "This mathematical relationship ~~that~~ is now referred to as Darcy's Law (Equation 15)."

page 27, Definition of Δh below Equation 15. Added "as defined for Equation 14".

page 27, Definition of ΔL below Equation 15. Added "along the flow path".

page 28, Expression immediately above section heading Specific Discharge. Final units changed from m^3 to m^3/d .

page 28, Definition of q below Equation 17. Added "in the direction of flow".

page 29, Last sentence. Added "in the direction of flow".

page 30, Equation 18. Removed variable "i".

page 34, Caption Figure 21, first line, added "and isotropic".

page 34, Caption Figure 21, deleted the struck-out portion of the following text "the column. Multiple piezometers penetrate the column wall and water levels are represented in blue vertical lines above the top of the sand column."

page 37, First sentence of section 4.3. Added "As shown in Equation 16, ".

page 37, First sentence of section 4.3. Changed "to" to "and".

page 37, First sentence of section 4.3. Changed "over" to "divided by".

page 37, First sentence of section 4.3. Changed $-dh/dL$ to dh/dL .

page 37, Definition of dL below Equation 21. Changed dL to dL .

page 37, Paragraph following Equation 21. Reworded as follows: "Given that the hydraulic gradient is computed by subtracting the head, h_1 , at the origin from the head, h_2 , at a distance ΔL from the origin in the direction of flow, and then dividing by the distance ΔL , the negative sign in Equation 21 provides a positive value of volumetric flow rate from high to low hydraulic head. In the vertical column shown in Figure 19, the value of head h_2 at L_2 is subtracted from h_1 at L_1 . This results in a negative gradient, $\Delta h/\Delta L$. That is, flow proceeds in the down gradient direction. Using this convention, flow is away from h_1 and toward h_2 . With the difference in head being a lower head value minus a higher head value, the gradient is negative (Equation 22)."

page 37, Equation 22. Removed negative signs from the first two terms.

page 37, Paragraph following Equation 22. Reworded to: "Hydraulic gradient can also be represented in three dimensions when flow is not aligned with a coordinate axis, x , y , or z (Equation 23), so there is a component of flow in each axis direction as shown in Equation 23. In this case, in order to determine the direction of flow, each hydraulic gradient component is calculated with h_2 being located at a larger coordinate position than h_1 ."

page 37, Equation 23. Removed negative signs and changed δ 's to ∂ 's.

page 37, First line after Equation 23. Changed δ 's to ∂ 's and removed negative sign.

page 37, In the definition of i after Equation 24. Removed negative signs.

page 38, First sentence, changed "over" to "divided by".

C

page 38, First sentence of second paragraph, changed “hydraulic gradient” to “head”.

page 39, Middle of last paragraph. Reworded to: “The magnitude of the vertical gradient is computed by comparing the absolute value of the head difference between the piezometers in the direction of flow, $\Delta h = |h_B - h_A|$, over the absolute value of the vertical distance separating their measurement locations, $\Delta L = |Z_B - Z_A|$. ”

page 40, Figure 26 caption. Specified the absolute value of the head and distance difference. Reversed order of length calculation $Z_A - Z_B$ to $Z_B - Z_A$ so as to be consistent with the calculation of head difference. Changed last sentence to say: “In this example, the potential for ground water flow is from the higher to lower head, in this case it is downward from A to B”.

page 42, Parentheses added around LT in the dimensions for dynamic viscosity after Equation 29, (M/(LT)).

page 51, Before the last sentence of Section 5.2, added information about “An Analysis and Evaluation of Pumping Test Data” by Kruseman and de Ridder (1994) and a link to download a pdf of the book.

page 52, Last sentence of first paragraph of section 5.4 was changed from “Hydraulic conductivity is a vector and when aligned with the principle coordinate axes, it is represented as K_x , K_y and K_z .” to “In the general case, hydraulic conductivity varies with direction, and when aligned with the principal coordinate axes, it is represented as K_x , K_y and K_z .”

page 54, Last paragraph, reference to (Freeze and Cherry, 1979) was expanded to (Freeze and Cherry, 1979, Chapter 2).

page 55, Caption Figure 35, changed “ θ to the x,z coordinates” to “ θ to the x coordinate.

page 56, Changed: “depositional process producing a fairly uniform set of conditions” to “a fairly uniform set of depositional and post-depositional conditions”

page 59, Equation 40, changed upper limit from “ $I = N$ ” to “ $i = N$ ”.

page 60, First line of second paragraph of section 5.6. Removed “s” to make “values” singular.

page 67, For clarification, replaced third and fourth sentence of first paragraph of section 6.3. Deleted “~~Pressure head of a confined aquifer is in excess of hydrostatic pressure because the recharge source is elevated, and that source of energy is transferred to the flowing groundwater in the aquifer. The confining bed constrains the excess pressure because the water leaks slowly through aquitards.~~” and replaced with “Groundwater recharge entering the aquifer typically occurs at an outcrop area where hydraulic heads are higher than the elevation of the confined portion of the groundwater system as shown

D

in Figure 46. When water flows into and through the confined aquifer, heads exceed the top elevation of the fully saturated confined aquifer zone. The overlying and underlying confining units constrain water from leaking out of the aquifer and direct flow parallel to the aquifer boundaries.”

page 70, last sentence of caption to Figure 48, added “saturated” to “so saturated thickness decreases”.

page 72, Equation 46. Changed first term on right of equal sign by changing subscript Y of S_Y to lower case y, S_y .

page 72, Equation 46. Changed last term on right of equal sign from b to b_{average} .

page 77, Parentheses added around L^2T in the dimensions for Mass Flux after Equation 52 and Equation 54, ($M/(L^2T)$).

page 78, Definition of Mass Flow after Equation 56 changed from “volume of water passing through a unit area per unit time (M/L^2T)” to (mass of water passing into, or out of, an REV per unit time (M/T)).

page 78, Figure 52, a few occurrences of Δx were not italics and were changed to italics.

page 79, changed definition of Inward Flow of Mass after Equation 57 from “volume of water flowing into the elementary volume per unit time (M/ L^2T)” to “mass of water flowing into the elementary volume per unit time (M/T)”.

page 82, Last sentence of first paragraph of section 7.3. Removed negative signs in front of dh/dx and dh/dL .

page 83, Figure 55. Removed negative signs in front of dh/dx and dh/dL .

page 83, Figure 55 caption. Removed negative signs front of dh/dx and dh/dL .

page 83, equation 76, changed $S_y \frac{\partial h}{\partial t} = \frac{K}{2} \left(\frac{\partial h^2}{\partial x^2} + \frac{\partial h^2}{\partial y^2} \right)$ to $S_y \frac{\partial h}{\partial t} = \frac{K}{2} \left(\frac{\partial^2 h^2}{\partial x^2} + \frac{\partial^2 h^2}{\partial y^2} \right)$

page 84, First word of second paragraph changed from “Where” to “Whereas”.

page 91, Definition of units for C_1 and C_2 after Equation 83. Changed units for C_1 and C_2 to L and L^2 respectively.

page 93, Third to last sentence. Removed comma after Equation 67.

page 95, Last sentence of Section 7.5, changed “impacted” to “impact”.

page 102, Last paragraph, replaced with: “The flow directions in anisotropic settings are dependent on the magnitude of the component hydraulic conductivities illustrated by

using an inverse hydraulic-conductivity tensor ellipse (Figure 69). Once $-grad h$ is identified for a set of equipotential lines and the inverse hydraulic-conductivity tensor ellipse is constructed with axes of $1/K_{max}^{0.5}$ and $1/K_{min}^{0.5}$, the anisotropic flow direction at a given location can be determined by graphical construction (Liakopoulos, 1965). The hydraulic-conductivity tensor ellipse described in Section 5.4 (Figures 34 and 35) is used to illustrate the directional nature of K whereas the inverse hydraulic-conductivity tensor ellipse is used to determine groundwater flow directions. The hydraulic-conductivity tensor ellipse described in Section 5.4 (Figures 34 and 35) is used to illustrate the directional nature of K where the inverse hydraulic-conductivity tensor ellipse is used to determine groundwater flow directions.”

page 103, The wording within Figure 69 was adjusted to clarify that this is an inverse hydraulic-conductivity tensor ellipse.

page 103, Wording of the caption of Figure 69 was changed to clarify that this is an inverse hydraulic-conductivity tensor ellipse that is aligned with the direction of maximum and minimum K on the map and cross section.

page 104, The wording within Figure 70 was adjusted to clarify that this is an inverse hydraulic-conductivity tensor ellipse.

page 104, Wording of the caption of Figure 70 was changed to clarify that this is an inverse hydraulic-conductivity tensor ellipse.

page 114, Figure 80, repositioned “d)” to more clearly indicated the proper part of the figure.

page 114, Figure 80 caption, part d. Removed “with a light gray base”.

page 133, Reference for Cohen and Cherry, 2020. Changed to “Conceptual and Visual Understanding of Hydraulic Head and Groundwater Flow, The Groundwater Project. The Groundwater Project, Guelph, Ontario, Canada, <https://gw-project.org/books/conceptual-and-visual-understanding-of-hydraulic-head-and-groundwater-flow/>.”

page 136, Added reference to Kruseman and de Ridder.

page 136, Reference for Poeter and Hsieh 2020. Changed to “Graphical Construction of Groundwater Flow Nets. The Groundwater Project Guelph, Ontario, Canada, <https://gw-project.org/books/graphical-construction-of-groundwater-flow-nets/>.”

page 139, Figure Box 1-1, formatted the 3's after cm to be superscripts.

page 142, Third line above Equation Box 2-6. Changed phi to lower case.

page 146, Equation Box 3-2 removed “/” from last term on right.

page 146, Paragraph following Equation Box 3-2, changed “Divide the force in Equation Box 3-3” to “Divide the force in Equation Box 3-2”.

page 149, Definition of terms following Equation Box 3-9, F_{wds} changed to F_wDL

page 151, Box 4, The last two sentences of the first paragraph were move to follow Figure Box 4-1. Two sentences were added between the last two sentences to include information about “An Analysis and Evaluation of Pumping Test Data” by Kruseman and de Ridder (1994) and a link to download a pdf of the book. The last sentence was modified to start with “The material in this Box” rather than “This material”.

page 153, Fifth line from bottom of page. Added negative signs to the calculated gradients “-0.36, -0.34, and -0.44”.

page 153, Fourth line from bottom of page. Added negative sign to $K = Q/(A_i)$ to $K = -Q/(A_i)$.

page 156, in parameter definitions following Equation Box 4-3, removed extra “(“ in definition of units for A_{sample} .

page 158, added (n) to definition of C_s .

page 158, “ $1/n^{3.287}$ ” changed to “ $1/n^{3.287}$ ”.

page 162, Two sentences were added before the last sentence of the last paragraph of Box 4 to include information about “An Analysis and Evaluation of Pumping Test Data” by Kruseman and de Ridder (1994) and a link to download a pdf of the book. The last sentence was modified to start with “Another” rather than “A”.

page 163, Second sentence of Box 5, changed “over a horizontal distance “ L_x ” to “ ΔL_x ”.

page 163, Third line of first paragraph of Box 5. Removed negative sign from $\Delta h/\Delta L_x$.

page 163, Figure Box 5-1 caption. Removed negative sign from $\Delta h/\Delta L_x$.

page 163, Figure Box 5-1 caption. Changed “were d is the flow” to “were Q is the flow”.

page 164, First line, changed “ L_x ” to “ ΔL_x ”.

page 164, Last paragraph, changed “ L_z ” to “ ΔL_z ”.

page 164, Third line of last paragraph. Removed negative sign from $\Delta h/\Delta L_x$.

page 169, Definition of terms for Equation Box6-1, changed “ d_y ” to “ dy ”.

page 170, Equation Box 6-4) changed from a first derivative “ $\frac{1}{2} \frac{dh^2}{dx^2} = -\frac{W}{K}$ ” to a second derivative, “ $\frac{1}{2} \frac{d^2h^2}{dx^2} = -\frac{W}{K}$ ”.

page 170, Definition of terms for Equation Box 6-5, changed from:

C_1, C_{2x} = constants of integration (dimensionless)

to:

C_1, C_2 = constants of integration (L and L², respectively)

page 170, Definition of terms for Equation Box 6-5, changed from:

x = area of the tube is 0.7854 d_{tube}^2 (L²)

to:

x = distance from the origin (L)

page 174, Fifth line of first paragraph of Box 8 changed “ $Q_2 = Q_2$ ” to “ $Q_1 = Q_2$ ”.

page 174, First paragraph of Box 8, removed “the” from “in the Region 2”

page 175, Removed repeated definition of “ Q_n ” from the parameter list at the top of the page.

page 175, Line above Equation Box 8-2, changed “ $Q_2 = Q_2$ ” to “ $Q_1 = Q_2$ ”.

page 179, Solution to exercise 1f, third equation from the bottom of the page, the denominator was changed from 10 to 100.

page 179, Bottom of the page, the numerator was changed from 0.51 to 5.1.

page 183, Midway down the page, the phrase “If the aquifer were a 100-meter-thick confined sand” had a sentence added before it as follows: “The specific storage can be calculated by using Equation 45 of this book.”

page 186, Parentheses added around LT in the dimensions for dynamic viscosity in solution to exercise 5b, (M/(LT)).

page 186, Second line of solution to exercise 5c, commas on either side of K were removed.

page 188, Solution for exercise 6b figure: numbers after “d’s” were adjusted to be subscripts.

page 189, Midway down page, cm units were added for d in the calculation of K.

page 190, Solution for exercise 6c figure: numbers after “d’s” were adjusted to be subscripts.

page 191, Midway down page, “(“ was added before 10.22 in the calculation of K for sample B.

page 192, The word “that” was changed to “than” as shown here “were lower ~~that~~^{than} Hazen”.

page 195, First line of second paragraph of solution to exercise 9, subscript was added to specific yield symbol, changed “specific yield, S” to “specific yield, S_y ”.

page 198, Unnecessary second to the last sentence of solution to exercise 12 was deleted because transmissivity is not clearly part of the expression presented. “~~It is confined because the transmissivity of the aquifer does not vary with head.~~”

page 202, Solution to exercise 12, some tangent symbols had the first letter as an upper case and these were changed to lower case.

page 206, Last line of Woessner biography. Second to last line changed “award” to “awarded”

page 207, Added link to Groundwater Project email sign-up.

Changes from Version 2 to Version 3

Version 2: December 29, 2020, Version 3: October 17, 2024

Page numbers refer to the Version 2 PDF.

General changes:

Now each book section begins on a new page

Links to Exercises were added throughout the body of the book

Updated Table of Contents

Links were made from the end of sections in the text to appropriate exercises. In order for the links to increase sequentially from Exercise 1 to Exercise 16 as they are mentioned throughout the book, the order of the Exercises was adjusted, resulting in the following changes:

Previous Exercise Number	New Number
3	4
4	11

10	3
11	12
12	13
13	10

Page breaks were added to start an exercise on a new page if the entire exercise did not fit on the page where it was introduced

Page breaks were added to start an exercise solution on a new page if the entire exercise did not fit on the page where it was introduced

Specific changes:

page ii, changed version number and date

page ii, added page with message regarding support of The Groundwater Project

page iii, updated copyright page information, added doi, updated number of pages

page 2, end of Section 1, added citation to a glossary of hydrogeology

page 25, added Section 3.8 with links to exercises 1 and 2

page 30, end of Section 4.1, added citation to a book about groundwater velocity

page 36, end of Section 4.2, added citation to a book about variable density groundwater flow

page 45, last paragraph, added citation to a book that introduces fluid mechanics to groundwater scientists

page 47, end of section 4.6, added link to exercise 3

page 50, Section 5.2, first paragraph, added citation to a book that describes field-based methods for determining aquifer properties

page 57, Figure 38 caption, deleted d from juxtaposed

page 62, end of Section 5.6, added citation to books about fractures, structural geology, and karst aquifers

page 62, added Section 5.7 with links to Exercises 4, 5, and 6

page 63, second to last paragraph, added citation to a book about large aquifer systems

page 67, end of Section 6.3, added citation to a book about the history and hydraulics of flowing wells

page 73, end of first paragraph, added citation to a book about storage in confined aquifers

page 74, added Section 6.5 with links to Exercises 7, 8, 9, 10, and 11

page 74, end of first paragraph of Section 7, added citation to a book that introduces fluid mechanics to groundwater scientists

page 92, end of first paragraph, added citations to books about using the numerical groundwater flow modeling code, MODFLOW, and about developing geologic frameworks for groundwater models

page 94, added Section 7.6 with links to Exercises 12 and 13

page 123, added Section 8.6 with links to Exercises 14, 15, and 16

page 125, Exercise Section, because links to exercises were added to the body of the text, a few exercises were renumbered to match their order of appearance in the text. These include:

Previous Exercise Number	New Number
3	4
4	11
10	3
11	12
12	13
13	10

If the text within the exercise referred to the exercise number, that was removed

page 125,

Exercise 10 of version 2 replaced Exercise 3 in version 3;

Exercise 3 of version 2 became Exercise 4 in version 3;

Exercise 4 of version 2 became Exercise 11 in version 3

page 127,

Exercise 10 of version 2 replace Exercise 3 of version 2 in version 3;

Exercise 10 of version 2 was replaced by the Exercise 13 of version 2 in version 3

page 128, Exercise 11 of version 2 was replaced by the Exercise 4 of version 2 in version 3

page 128, a task was added to Exercise 11 (previously Exercise 4) as delineated in the last 2 sentences of Exercise 11

page 128,

Exercise 12 of version 2 was replaced by the Exercise 13 of version 2 in version 3;

Exercise 13 of version 2 was replaced by the Exercise 10 of version 2 in version 3

page 132, added reference to Aydin and others (2023)

page 132, added reference to Brandenburg (2020)

page 132, added link for Cormican reference

page 132, added link for Davis reference

page 133, added reference to Devlin (2020)

page 133, added reference to Fernandes (2023)

page 134, added reference to Jiang (2024)

page 135, added reference to Klammler (2023)

page 135, added reference to Kuniansky and others (2022)

L

page 135, added reference to Marinelli (2024)

page 135, added link for Meerschaert and others (2013)

page 135, added reference to Sharp (2023)

page 136, added reference to Van der Gun (2022)

page 136, added reference to Wang (2020)

page 136, added reference to Winston (2023)

page 136, added reference to Woessner and others (2023)

page 149 and onward, in footer, added missing final g in gw-project.org

page 169, end of Box 6, revised the link for downloading a spreadsheet to explore the flow system to a link for a more robust, online, interactive tool for exploring the flow system

page 175, Exercise Solutions Section, because links to exercises were added to the body of the text, a few exercises were renumbered to match their order of appearance in the text. The associated exercise solution numbering was changed accordingly. These include:

Previous Exercise Solution Number	New Number
3	4
4	11
10	3
11	12
12	13
13	10

If the text within the exercise solution referred to the exercise number, that was removed

page 180,

Exercise Solution 10 of version 2 replaced Exercise Solution 3 of version 2 in version 3;

Exercise Solution 3 of version 2 became Exercise Solution 4 of version 3

page 181,

M

Exercise Solution 4 of version 2 was replaced by Exercise Solution 11 of version 2 in version 3

page 194,

Exercise Solution 10 of version 2 became Exercise Solution 3 in version 3;

Exercise Solution 10 was replaced by the Exercise Solution 13 of version 2 in version 3

page 195, Exercise Solution 11 of version 2 was replaced by the Exercise Solution 4 of version 2 in version 3

page 195, Exercise Solution 11 (previously Exercise Solution 4), first paragraph,

S_y was corrected to S_r ;

edits were made between the calculation of S_r and S_s . Tao provide the solution for the new task that was added to Exercise Solution 11, which was previously Exercise Solution 4

page 196, Exercise Solution 12 of version 2 was replaced by Exercise Solution 13 of version 2 in version 3

page 197, Exercise Solution 13 of version 2 was replaced by Exercise Solution 10 of version 2 in version 3

page 204, titles were deleted from authors names as per current Groundwater Project format convention

Changes from Version 3 to Version 4

Version 3: October 17, 2024, Version 4: December 21, 2024

Page numbers refer to the Version 3 PDF.

Specific changes:

page ii, changed version number and date

page 105, corrected 102 to 100 in caption of Figure 66

N